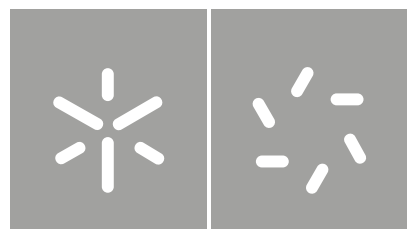


Universidade do Minho
Escola de Ciências

Mariana Gazire Lemos

Estudo geoambiental de resíduos de mineração de ouro em contexto de economia circular (Minas Gerais e Goiás, Brasil)

Mariana Gazire Lemos | Estudo geoambiental de resíduos de mineração de ouro em contexto de economia circular (Minas Gerais e Goiás, Brasil)



Universidade do Minho
Escola de Ciências

Mariana Gazire Lemos

**Estudo geoambiental de resíduos de
mineração de ouro em contexto de
economia circular (Minas Gerais e Goiás,
Brasil)**

Tese de doutoramento
Doutoramento em Geologia - Geoconservação, Geologia
Ambiental e Recursos Geológicos

Trabalho efetuado sob orientação da
Professora Doutora Teresa Maria F. Valente
Professora Doutora Amélia Paula M. Dias Reis
Professora Doutora Rita Maria F. da Fonseca

DIREITOS DE AUTOR E CONDIÇÕES DE UTILIZAÇÃO DO TRABALHO POR TERCEIROS

Este é um trabalho académico que pode ser utilizado por terceiros desde que respeitadas as regras e boas práticas internacionalmente aceites, no que concerne aos direitos de autor e direitos conexos.

Assim, o presente trabalho pode ser utilizado nos termos previstos na licença [abaixo](#) indicada.

Caso o utilizador necessite de permissão para poder fazer um uso do trabalho em condições não previstas no licenciamento indicado, deverá contactar o autor, através do Repositórium da Universidade do Minho.

Licença concedida aos utilizadores deste trabalho



Atribuição
CC BY

<https://creativecommons.org/licenses/by/4.0/>

"Você não pode esperar construir um mundo melhor sem melhorar os indivíduos. Para esse fim, cada um de nós deve trabalhar para o seu próprio aperfeiçoamento e, ao mesmo tempo, compartilhar uma responsabilidade geral por toda a humanidade."

Marie Curie (1867-1934)

Este trabalho está redigido em português do Brasil.

Agradecimentos

Trilhar este caminho só foi possível com o apoio, energia e força de várias pessoas, a quem dedico especialmente este projeto de vida.

As minhas orientadoras Prof^{as}. Dr^{as}. Teresa Maria Valente, Paula Reis e Rita Fonseca pela oportunidade, apoio na elaboração deste trabalho e pelo suporte no pouco tempo que lhe coube, pelas suas correções e incentivos.

Este trabalho foi co-financiado por fundos nacionais através da FCT - Fundação para a Ciência e a Tecnologia, I.P., no âmbito dos projectos Ref^{as}s UIDB/04683/2020 e UIDP/04683/2020.

Agradeço a todos os professores por me proporcionar o conhecimento não apenas racional, mas a manifestação do caráter e afetividade da educação no processo de formação profissional, por tanto que se dedicaram a mim, não somente por terem me ensinado, mas por terem me feito aprender. A palavra mestre, nunca fará justiça aos professores dedicados aos quais sem nominar terão os meus eternos agradecimentos.

A empresa AngloGold Ashanti, Universidade Federal de Minas Gerais e Universidade do Minho pelo suporte financeiro e laboratorial. Em especial quero agradecer aos meus amigos mais queridos, José Augusto Dumont, José Gregorio Filho e Marcus Magalhães, por apoio intelectual e acompanhamento de todo trabalho. Eles sempre estiveram presentes com palavras de encorajamento e força. Vocês também fazem parte da minha jornada durante este tempo de minha vida.

Aos colegas de doutoramento, Vanessa Soares, Thais Canesin, Fernanda Guabiroba, Antonio Roberto Silva, Paulo Lack e João Paulo Pantaleão pelo suporte em diferentes etapas desse trabalho e compartilhamentos das aflições, ideias e suporte.

À querida, Giovana Rebelo, agradeço o apoio e motivação incondicional que ajudou a tornar este trabalho uma válida e agradável experiência de aprendizagem. Estou grata por todo apoio.

A minha família, pelo amor, incentivo e apoio incondicional, em especial, meu marido Apolo Pedrosa Bhering e meu filho Nuno Lemos Bhering. A eles dedico este trabalho!

À Antonio Wilson Romano, pelos incentivos iniciais na minha carreira e por seu exemplo.

A todos que direta ou indiretamente fizeram parte de minha formação, o meu muito obrigado.

DECLARAÇÃO DE INTEGRIDADE

Declaro ter atuado com integridade na elaboração do presente trabalho académico e confirmo que não recorri à prática de plágio nem a qualquer forma de utilização indevida ou falsificação de informações ou resultados em nenhuma das etapas conducente à sua elaboração.

Mais declaro que conheço e que respeitei o Código de Conduta Ética da Universidade do Minho.

RESUMO

Estudo geoambiental de resíduos de mineração de ouro em contexto de economia circular (Minas Gerais e Goiás, Brasil)

Desde meados do século XIX, minérios de ouro, hospedados principalmente em sulfetos, são processados em plantas metalúrgicas localizadas em Minas Gerais e Goiás, Brasil. Os rejeitos gerados foram acumulados ao longo dos anos em barragens de rejeitos ou em pilhas. Esses materiais representam rejeitos de circuitos antigos, bem como de plantas ainda em produção.

Os resultados obtidos foram divididos em cinco fases principais: (i) descrição dos resultados da amostragem e monitorização da fase sólida e líquida; (ii) análise analítica e laboratorial com avaliação geoquímica e mineralógica; (iii) modelagem 3D para dimensionamento da quantidade e distribuição dos principais elementos das estruturas, realizada utilizando krigagem ordinária com variogramas unidimensionais para rejeito sólidos e inverso do quadrado da distância para a fase líquida quando aplicável; (iv) realização de ensaios metalúrgicos para avaliação da valorização dos resíduos para potencial de recuperação de Au, Sb, As e minerais gangas; e (v) um estudo de caso visando demonstrar possíveis receitas e viabilidade econômica do tratamento dos resíduos em questão para o depósito de Cocoruto, localizado na cidade de Nova Lima, Brasil.

A caracterização realizada detectou resíduos de granulometria muito fina contendo sulfetos e óxidos. Os resíduos apresentam altos graus de concentração de Au hospedados em diferentes minerais, além de S, Fe, Zn, Pb, Sb, Si e As. Os resultados indicaram a ocorrência de zonas de enriquecimento de Au e permitiram revelar os depósitos de rejeitos mais atraentes em termos de teor de Au. Testes metalúrgicos mostraram recuperação de 70% de Au e sugeriram outros potenciais de reaproveitamento dos resíduos, como agregados para o setor de construção civil e recuperação de outros metais.

Por fim, considerando o potencial econômico de Au presente em uma estrutura de rejeitos de mina inativa, para todos os valores de onça e uma produção anual de 400 toneladas, todos os cenários se mostram rentáveis, embora outros riscos e cenários devam ser avaliados mais detalhadamente.

Outros ensaios metalúrgicos indicaram que elementos tóxicos como Sb e As poderiam ser efetivamente reutilizados na forma de vidro. A geração de outros produtos a partir de técnicas

de limpeza a seco não foi eficaz, mas ainda assim foi promissora, uma vez que houve enriquecimento de elementos com Au, Fe, Al e K em frações específicas.

Palavras-chaves: Economia circular; Rejeitos de mineração; Recuperação de Au; Reuso e reprocessamento.

ABSTRACT

Geoenvironmental study of gold mining tailings in a circular economy context (Minas Gerais and Goiás, Brazil)

Since the 19th century, gold ores, primarily hosted in sulfides, have been processed in metallurgical plants in Minas Gerais and Goiás, Brazil. Over time, the resulting tailings have accumulated in tailings dams or piles, representing waste from both old and currently active circuits.

The obtained results can be divided into five main phases: (i) sampling and monitoring of the solid and liquid phases; (ii) analytical and laboratory analysis, including geochemical and mineralogical evaluations; (iii) 3D modeling to assess the quantity and distribution of key elements in the structures using ordinary kriging and inverse distance weighting; (iv) metallurgical tests to evaluate the recovery potential of Au, Sb, As, and gangue minerals from the waste; and (v) a case study focusing on the revenue and economic feasibility of treating the waste from the Cocoruto deposit in Nova Lima, Brazil.

Characterization of the tailings revealed fine-grained residues containing sulfides and oxides, with high levels of Au associated with different minerals. The samples also contained S, Fe, Zn, Pb, Sc, Si, and As. The results identified zones of Au enrichment and highlighted the most promising tailings deposits in terms of Au content. Metallurgical tests demonstrated a 70% Au recovery rate and suggested other potential reuse options for the waste, such as utilizing it as aggregates in the construction sector and recovering other metals.

Considering the economic potential of the Au present in these inactive mine tailings, various variables were analyzed, including cut-off and tonnage grades for each scenario and the net present value (NPV). From a financial perspective, all scenarios showed profitability, although further assessment of risks and additional scenarios is necessary.

Other metallurgical tests indicated the effective reuse of toxic elements such as Sb and As in the form of glass. Dry cleaning techniques did not yield effective results in generating other products but showed promise due to the enrichment of elements such as Au, Fe, Al, and K in specific fractions.

This study highlights the importance of an integrated characterization approach within the circular economy framework and emphasizes the value of tailings in the mineral sector's production chain.

Keywords: Circular economy; Mining tailings; Au recovery; Reuse and Reprocessing

ÍNDICE

1. Introdução	1
1.1. Enquadramento	2
1.2. Histórico da mineração de Ouro no Brasil.....	4
1.2.1. Geração de rejeitos na mineração de Au e seu impactos	6
1.3. Gestão de Resíduos de Mineração no Brasil	7
1.4. A visão de reuso de rejeitos no Brasil.....	9
1.5. Oportunidades do tema de tese e objetivos	11
1.6. Planificação da tese	12
2. Economia circular e mineração.....	14
2.1. Conceito da Economia Circular.....	15
2.2. O enquadramento da Economia Circular na mineração	18
2.3. Histórico do reuso no setor mineral.....	20
2.4. Casos de Sucesso do reuso na mineração de Au.....	21
3. Descrição da área de estudo.....	22
3.1. Depósitos e Barragens localizados em Minas Gerais	23
3.1.1. Barragem e Pilha de rejeitados de Santa Barbara	24
3.1.2. Depósitos e Pilhas de rejeitados de Nova Lima e Sabará	27
3.1.2.1. Depósitos e barragens de Isolamento, Bicalho e Mina Velha	30
3.1.2.2. Depósitos e barragens de Queiroz e Cuiabá	30
3.2. Barragem de Rejeitados localizados em Goiás.....	31
4. Metodologia	34
4.1. Amostragem	36

4.2. Ensaios Laboratoriais	40
4.2.1. Água de Porosidade	40
4.2.2. Resíduo Sólido	40
4.2.2.1. Análise Química	40
4.2.2.2. Granulometria a laser	41
4.2.2.3. Mineralogia.....	41
4.2.2.4. Microscopia Ótica	41
4.2.2.5. Difração de Raios X.....	41
4.2.2.6. Microscopia eletrônica por varredura.....	42
4.3. Modelamento 3D e Análises estatísticas.....	42
4.3.1. Análise Estatística.....	42
4.3.2. Modelamento 3D	43
4.4. Avaliação do Potencial de Valorização	46
4.4.1. Composição de Amostras para teste	46
4.4.2. Ensaios Metalúrgicos para Extração do Au	47
4.5. Valorização dos Resíduos – Outras Oportunidades	49
4.5.1. Recuperação e estabilização de arsênio e antimônio	49
4.5.2. Recuperação de minerais de ganga	51
4.6. Cenário Função Benefício	52
5. Resultados e discussões	54
5.1. Resultados Estruturas Localizadas na Região do Quadrilátero Ferrífero	55
5.1.1. Resíduos sólidos - caracterização de amostras sólidas	56
<i>Mineralogical and Geochemical Characterization of Gold Mining Tailings and Their Potential to Generate Acid Mine Drainage (Minas Gerais, Brazil)</i>	58

<i>Characterization of Arsenical Mud from Effluent Treatment of Au Concentration Plants, Minas Gerais – Brazil.....</i>	76
5.1.2. Distribuição dos elementos químicos e modelamento 3D	83
<i>Geochemistry and mineralogy of auriferous tailings deposits and their potential for reuse in Nova Lima Region, Brazil.....</i>	100
5.1.3. O estudo de reuso e reprocessamento.....	124
<i>Adding Value to Mine Waste through Recovery Au, Sb, and As: The Case of Auriferous Tailings in the Iron Quadrangle, Brazil.....</i>	125
5.1.4. Qualidade, distribuição química e potencial reuso para águas de porosidade	152
<i>Recovery of metals in mining tailing waters - Hydrochemistry and elements distribution in gold metallurgical treatment tailings dams.....</i>	153
5.1.5. Pre feasibility para o reprocessamento do Au	175
<i>Sensitivity analysis and pre-feasibility of reprocessing Au from a tailings dam in the Iron Quadrangle - The case of Cocoruto Dam, Nova Lima, Minas Gerais</i>	176
5.2. Estruturas Localizadas na Região de Goiás.....	186
<i>Geoenvironmental Characterization of Gold Mine Tailings from Minas Gerais and Goiás, Brazil</i>	187
5.3. Os impactos socioeconômicos e potencial dos rejeitos estudados	194
6. Considerações finais	196
Referências bibliográficas	201
Anexos	214

LISTA DE ABREVIATURAS E SIGLAS

Termos gerais

ACP análise de componentes principais

CaO calcário

CIP *carbon in pulp*

CN cianetação

DRMI Drenagem ácida de mina

EC economia circular

ESG *Environmental, Social and Governance*

FFB formações ferríferas bandadas

IDW *Inverse Distance Weighting* (inverso do quadrado da distância)

Kt mil toneladas

MMt milhões de toneladas

MM m³ milhões de metros cúbicos

Moz milhões de onças **NaCN** cianeto

NPV *net present value*

ODS objetivos de desenvolvimento sustentável

PSD *particle size distribution* (distribuição do tamanho de partículas)

QF Quadrilátero Ferrífero

ROM *run-of-mine*

SGRV Supergrupo Rio das Velhas

TSF *tailings store facilities*

Grupos de elementos

PGE *platinum group elements* (elementos do grupo da platina)

REE *rare earth elements* (elementos de terras raras)

Métodos analíticos

DRX difração de raios X

EBSD *electron backscatter diffraction* (difração elétrons retro-espalhamento)

EDS *energy-dispersive X-ray spectroscopy* (espectroscopia de raios X por dispersão em energia)

ICP-MS *inductively coupled plasma mass spectrometry* (espectrometria de massas com plasma indutivamente acoplado)

LA-ICP-MS *laser ablation inductively coupled plasma mass spectrometry* (ablação a laser acoplado a espectrômetro de massa com plasma indutivamente)

SEM *scanning electron microscopy* (microscopia eletrônica de varredura)

SPT sondagem a percussão

TOF-SIMS *time-of-flight secondary ion mass spectrometry* (espectrometria de massa de íons secundários por tempo de voo)

FRX fluorescência de raios X

Instituições e normativas

ABNT / NBR Associação Brasileira de Normas Técnicas / Norma Técnica Brasileira

AGA AngloGold Ashanti

CONAMA Conselho Nacional do Meio Ambiente

FEAM Fundação Estadual do Meio Ambiente

IBRAM Instituto Brasileiro de Mineração

IMWA *International Mine Water Association*

IPEA Instituto de Pesquisa Econômica Aplicada

PNRS Política Nacional de Resíduos Sólidos

SGS *Société Générale de Surveillance*

SINIR Sistema Nacional de Informações sobre a Gestão dos Resíduos Sólidos

SINISA Sistema Nacional de Informações em Saneamento Básico

UNDP *United Nations Development Programme*

ÍNDICE DE FIGURAS

1. Introdução

Figura 1.1. Localização das principais barragens de rejeitados da exploração de Au no Brasil (FEAM, 2022), com destaque para pontos em preto para as áreas em estudo.	2
Figura 1.2. Os 17 objetivos de desenvolvimento sustentáveis e o papel da mineração (adaptado de UNDP, 2022).	4
Figura 1.3. Localização das barragens de rejeito do Au no Brasil (em preto), com foco na área de estudo (em vermelho).	7

2. Economia circular e mineração

Figura 2.1. Diagrama de Borboleta (Ellen MacArthur Foundation, 2023)	17
Figura 2.2. Áreas chaves para integração e aplicação dos conceitos EC no setor mineral (adpatado de Tayebi-Khorami et al., 2019).	19

3. Descrição da área de estudo

Figura 3.1. Mapa do Quadrilátero Ferrífero (modificado de Alkmin & Marshak, 1998; Porto, 2008; Ruchkys et al., 2015).....	24
Figura 3.2. a) Localização e contexto geológico da região de Santa Barbara, b) Barragem Santa Barbara e c) Pilha de rejeitos Santa Barbara.....	25
Figura 3.3. a) Localização das amostras coletadas no primeiro ano da barragem de rejeitados e b) plano de coleta das amostras das pilhas de rejeitados.....	26
Figura 3.4. Localização áreas em estudo de Nova Lima.....	28
Figura 3.5. Localização área em estudo de Sabará.	29
Figura 3.6. a) Fluxograma de extração de Au desativado e b) atual.....	31
Figura 3.7. a) Localização da área de estudo em Goiás, b) mapa geológica da região de Crixás e c) Barragem de rejeitados de Crixás.....	32
Figura 3.8. Fluxograma de extração de Au de Crixás.	33

4. Metodologia

Figura 4.1. Metodologia aplicada ao estudo dos resíduos mineiros.	35
--	----

Figura 4.2. Imagens das amostras coletadas e programadas das áreas de estudo. a) Bicalho (leapfrog), b) Isolamento (leapfrog), c) Calcinados (leapfrog), d) Cocoruto (leapfrog), e) Mina Velha (leapfrog), f) Barragem de Santa Barbara (leapfrog), g) Pilha Santa.....	38
Figura 4.3. Imagens das coletas efetuadas nas áreas de estudo. a) Calcinados, b, f) Mina Velha, c) Isolamento, d,e) Coleta Cocoruto, h) Barragem Santa Barbara, i) Barragem Goiás, f, g) Etapa de amostragem dos testemunhos da sondagem.	39
Figura 4.4. Etapa de estimativa do modelo de teores das estruturas. A) Avaliação do banco de dados, b) Retirada dos valores outliers (<i>capping</i>), c) Construção do variograma, d) Validação e e) Obtenção do modelo.....	45
Figura 4.5. Etapa de definição da área a ser modelada	46
Figura 4.6. Exemplo de escolha das compostas de amostras para testes metalúrgicos para recuperação de Au – Caso de Cocoruto.	47
Figura 4.7. Fluxograma de trabalho para obtenção da recuperação de Au em laboratório escala de bancada para as amostras em estudo.....	49
Figura 4.8. Potencial de extração de Sb e As em forno rotativo.....	50
Figura 4.9. GlassLock™ (modificado de Dundee Sustainable Technologies, 2006; AGA, 2016) ..	51
Figura 4.10. Fluxograma de teste para a geração de três potenciais produtos geradores de insumos nas indústrias civil, de fertilizantes e outras.....	52
Figura 4.11. Etapas de processo para definição da função benefício de um empreendimento. .	52

5. Resultados e discussões

5.1. Resíduos sólidos - Caracterização de Amostras Sólidas

Mineralogical and Geochemical Characterization of Gold Mining Tailings and Their Potential to Generate Acid Mine Drainage (Minas Gerais, Brazil)

Figura 5.1 (Figure 1). Location of the study area and Iron Quadrangle map (a) [43,44]; (b,c) Images of the Cocoruto Dam sampled area (SIRGAS2000—10-09-2019).....	60
Figura 5.2 (Figure 2). Old and ongoing workflow of Nova Lima’s plant (a,b). Old circuit sources of Cocoruto Dam. (c) Ongoing workflow [46]. The yellow stars represent sampling points.	61
Figura 5.3 (Figure 3). Basic statistics and comparison of major element (%log) for the two sets of tailings samples.	64

Figura 5.4 (Figure 4). Basic statistics and comparison of trace element (mg/kg log) for the two sets of tailings samples.....	64
Figura 5.5 (Figure 5). Size distribution (Krumbein phi scale) of solid tailings.....	65
Figura 5.6 (Figure 6). False Images (a) sulfides associated with iron oxide and Au particles—CoT, (b) quartz, carbonates and Fe oxides particles—CoT, (c,d) Fe oxides associated with Au, silicates and Fe oxides with As, Ni, Co, Al, Zn, Pb—CaT samples. Photomicrographs taken under reflected light and uncrossed nico (e) hematite (Ht) from CaT samples and (f) Au associated with pyrite (Py)—CoT samples.	67
Figura 5.7 (Figure 7). Results of Modified Acid-Base Accounting (MABA) tests (a) global and (b) for CoT, by sampling depth. ..	68
Figura 5.8 (Figure 8). Relationship between the results of the MABA and Net Acid Generation (NAG) pH tests (NAF: region of non-acid-forming samples; PAF: region of potentially acid-forming samples.	69
Figura 5.9 (Figure 9). Comparison of the average levels of metals, metalloids, fluorides and pH in SPLP leaching extracts. VMP Al = 0.2 mg/L; VMP Sb = NA; VMP As = 0.05 mg/L; VMP Ba = 1.0 mg/L; VMP Ca = NA; VMP Pb = 0.05 mg/L; VMP Co = NA; VMP Cu = 1.0 mg/L; VMP Cr = 0.05 mg/L; VMP Fe = 0.3 mg/L; VMP P = NA; VMP Fluorides = NA; VMP Mg = NA; VMP Mn = 0.1 mg/L; VMP Ni = 0.1 mg/L. NA—Not applied for recreation use.	70
<p style="text-align: center;"><i>Characterization of Arsenical Mud from Effluent Treatment of Au Concentration Plants, Minas Gerais – Brazil</i></p>	
Figura 5.10 (Figure 1) Study area: a. iron quadrangle map location (modified from Ruchkys U.A 2007) and Nova Lima location and b. Nova Lima Metallurgic plant (SIRGAS2000 – 10-09-2019).	77
Figura 5.11 (Figure 2) On-going workflow of Nova Lima’s plant. The yellow stars represent sampling points in Arsenic effluent treatment (modified from Moura 2015).....	77
Figura 5.12 (Figure 3) Backscattered electron image of Sulfo Arsenical Compounds in arsenical mud. a) CSA, b) Reflected light image of porous hematite, c) total sample, d) and e) false image of total samples (pink, purple and blue – Gypsum (pink/purple) and CSA (Blue)).	81
Figura 5.13 (Figure 4) Transformation path of As sources along Nova Lima Au metallurgical plant until neoformation of arsenic mud.	81

5.2. Distribuição dos elementos químicos e modelamento 3D

Geoenvironmental Study of Gold Mining Tailings in a Circular Economy Context: Santa Barbara, Minas Gerais, Brazil

Figura 5.14 (Fig. 1) a Location of study area; b Iron Quadrangle map (modified from Alkmin & Marshak, 1998; Ruchkys et al. 2013; Porto 2008); and c sampled area (SIRGAS2000 – 14–06–2019).....	87
Figura 5.15 (Fig. 2) a Operational unit and tailings dam. b Panoramic image (bird's eye view) of residual water tailings.	89
Figura 5.16 (Fig. 3) Size distribution (Krumbein phi scale) of solid tailings from the Santa Barbara tailings dam.	90
Figura 5.17 (Fig. 4) Spatial distribution of As, Au, S and Sb by sampling depth and area.	92
Figura 5.18 (Fig. 5) Matrix plot of Pearson of Au, S, As, Fe, Cu and Sb mean values by area and depth.....	93
Figura 5.19 (Fig. 6) SEM-SE images and respective EDS spectra of Fe species and sulfides.....	95
Figura 5.20 (Fig. 7) SEM-SE images and respective EDS spectra of Au species and false image of Au associations (below right).	96

Geochemistry and mineralogy of auriferous tailings deposits and their potential for reuse in Nova Lima Region, Brazil

Figura 5.21 (Figure 1). Location of the QF (a), Nova Lima Region and the location in the QF (b), and the illustration location of the tailings deposit 1 to deposit 5. Google earth Pro V 7.3.6.9345 (64-bit). Image date 6/22/2022 19° 59' 05.66" S and 43° 50' 49.070" W. The dams and mine dumps in this region are located between the cities of Nova Lima and Raposos, 25 km from its capital, Belo Horizonte, Minas Gerais, Brazil (c).	102
Figura 5.22 (Figure 2). Schematic flowchart of the process that fed the Au extraction dams 4—old circuit (a—red line) and 5—current circuit (b—blue line) of the Nova Lima Metallurgical Plant.....	104
Figura 5.23 (Figure 3). Methodology applied to study tailings from deposits 1 to 5. (a) Step of defining the collection methodology for each deposit, (b) sampling of deposits and survey of the exact position of each sampled point, (c) stage of collecting information on the about	

chemistry and mineralogy of the samples, (d) assembly of a database containing survey and characteristics of each sample, (e) 3D modelling and geostatistical analysis of information obtained from sampling, (f) composition of samples after 3D modeling for metallurgical tests e, (g) study of the potential extraction of Au and reuse of the tailings in its entirety.	105
Figura 5.24 (Figure 4). (a) False color electron images of Au-bearing particles (yellow and black arrows): Deposit 1— Gold enclosed in pyrrhotite (black), chlorite (green), arsenopyrite (blue) and quartz (gray). Deposit 2: Free and enclosed gold particles in ankerite (purple), chlorite, quartz, and pyrite (dark pink). Deposit 3: Relics of arsenopyrite and gold particles enclosed in iron oxide (red). Deposit 4: Free gold particles and associated in quartz, chlorite, and Deposit 5: Gold particles enclosed in iron oxide and silicates (pink and gray). (b) Microphotographs of coarse gold particles associations (reflected light and parallel Nicols) in arsenopyrite (deposit 1), pyrite (deposit 2), rock minerals as quartz, chlorite, muscovite (deposits 3 and 4) and Hematite (deposit 5).....	108
Figura 5.25 (Figure 5). Variables projections on the first factorial plane (PC1/PC2). This plane accounts for about 50% of the total explained variance of the dataset. The blue circles highlight the clusters obtained by the PCA analysis.....	112
Figura 5.26 (Figure 6). Spatial distribution of Au grades from 3D model by elevation and deposits 1 to 5.....	113
Figura 5.27 (Figure 7). Distribution of Au contents in the block from 3D model for deposits 1 to 5	114
Figura 5.28 (Fig S1). a. Collection points of structures 1 to 5 and b. Instrument images and collections in dry deposits (above) and dam (below).	117
Figura 5.29 (Fig S2). Workflow of Au Metallurgical Procedure 1 (a) and 2 (b)	118
Figura 5.30 (Fig S3). Topography limits of 3D modeled by areas 1 to 5	118
Figura 5.31 (Fig S4). EDS spectra of Fe oxides and Au phases containing elements such as Cu, Ni, Ag, As from deposit 5.	119
Figura 5.32 (Fig S5). Box plots for 19 elements-based on dataset collected.....	120

5.3. O estudo de reuso e reprocessamento

Adding Value to Mine Waste through Recovery Au, Sb, and As: The Case of Auriferous Tailings in the Iron Quadrangle, Brazil

Figura 5.33 (Figure 1). (a) Location of the studied sites within the IQ, as shown in the modified schematic map from [32]. Dams and tailing piles in (b) Nova Lima (MV, ISO, and BIC) and (c) Santa Barbara (CDS1, CDS2), along with the sampling locations (black dots).	128
Figura 5.34 (Figure 2). Waste generation flowchart for (a) CDS1, (b) CDS2, and Queiroz plant—(c) CO (Cocoruto) and (d) CA (Calcine) samples. Sample locations are marked with a yellow star. Modified from [33,34].	129
Figura 5.35 (Figure 3). Particle size distribution of waste samples.....	134
Figura 5.36 (Figure 4). Electronic microscopy images of two phases of CA samples. (a) Hematite with As, Pb, S, Cu, and Zn, and (b) Jarosite with Sb.	136
Figura 5.37 (Figure 5). False color electron images and microphotographs (reflected light and parallel Nicols) illustrate the presence of Au-bearing particles (indicated by yellow and black/white arrows) and Fe Hydroxide. Mineral abbreviations follow [51]. (a) BIC—enclosed Au particles in Quartz (gray) and Arsenopyrite. (b) CDS1—Au particles enclosed in rock minerals (Quartz and Muscovite) and Fe Hydroxide. (c) CDS2—Free Au particles and Muscovite (dark green) along with Arsenopyrite. (d) CO—Au particles enclosed in Pyrite (orange) and Arsenopyrite (blue). (e) MV—fine Au particles enclosed in Fe Hydroxide (red). (f) ISO—Au particles enclosed in Arsenopyrite and rock minerals (Chlorite—light green). (g) CA—free Au particles and Au particles within porous Hematite (brown).....	138
Figura 5.38 (Figure 6). Dendrogram (generated using complete linkage and Euclidean distance), which illustrates the grouping of tailings samples for the purpose of guiding reuse tests. Group 1: BIC and CDS1 samples. Group 3: CO and MV samples. The remaining groups (2, 4, and 5) did not exhibit sufficient similarity within the 100% to 70% range and therefore were not grouped.	139
Figura 5.39 (Figure 7). Glass formed from GlassRock™ methodology demonstrates the possibility of As and Sb recovery and its use as an industrial product.....	141
Figura 5.40 (Figure S1). Au extraction potential in (a) Calcination + Leaching, (b) Direct Leaching and (c) Flotation+Calcination+Leaching, modified from [34].	143
Figura 5.41 (Figure S2). Sb and As extraction potential in (a) rotative klin and (b) GlassLock™, modified from [11, 35].	144
Figura 5.42 (Figure S3). Test flowchart for generation of three potential input-generating products in the civil, fertilizer and other industries.	144

Figura 5.43 (Figure S4). Gold department chart by structure complementing Figure 5 of this study.	146
Figura 5.44 (Figure S5). Image of tested samples in the selective grinding test, pneumatic and triboelectrostatic separation from (a) Group 4 and (b) Group 5.	148
5.4. Qualidade, distribuição química e potencial reuso para águas de porosidade		
<i>Recovery of metals in mining tailing waters - Hydrochemistry and elements distribution in gold metallurgical treatment tailings dams</i>		
Figura 5.45 (Figure 1). Location of the study areas in Minas Gerais State, near Belo Horizonte, Brazil: (a) Nova Lima (NL) dams and deposits; and (b) Santa Barbara (SB) dams and deposits. In both, the sample's locations are highlighted in white.	155
Figura 5.46 (Figure 2). Workflow of methodological approach.	156
Figura 5.47 (Figure 3). Projection of the samples for the three dams according to the Ficklin Diagram.	159
Figura 5.48 (Figure 4). 3D distribution of the concentrations of the main elements contained in the water of the three dams. (a) Calcinados, (b) Cocoruto and (c) CDS2.	162
Figura 5.49 (Figure 5). Enrichment ratio of the liquid to solid fraction (Ef) in each tailing dam: Calcinados (a), Cocoruto (b) and CDS2 (c).	164
Figura 5.50 (Figure S1). (a) Location of sample points in plan and depth for each structure: (b) Calcinados, (c) Cocoruto, and (d) Santa Barbara.	167
Figura 5.51 (Figure S2). Correlogram matrix of physicochemical variables of groundwater by structure: (a) Calcinados, (b) Cocoruto, and (c) CDS2.	168
Figura 5.52 (Figure S3). Distribuition of elements by depth in struture: (a) Calcinados, (b) Cocoruto, and (c) Santa Barbara.	169
5.5. Pre feasibility para o reprocessamento do Au		
<i>Sensitivity analysis and pre-feasibility of reprocessing Au from a tailings dam in the Iron Quadrangle - The case of Cocoruto Dam, Nova Lima, Minas Gerais</i>		
Figura 5.53 (Figure 1). Co dam setting. (a) Location of Nova Lima city in Minas Gerais state. (b) Co dam, near Queiroz plant. (c) Pit designed for CoCal scenario. (d) Pit designed for CoL20 scenario. (e) Pit designed for CoL74 scenario.	178

Figura 5.54 (Figure 2). Cut-of Grade versus tonnage for each considered scenario.	180
Figura 5.55 (Figure 3). Results of the generated pits for each scenario: CoCal, CoL20, and CoL74.	182
Figura 5.56 (Figure 4). Results and mine life for each scenario, considering the base scenario for CoCal (65 kt), CoL20 (400 kt) and CoL74 (400 kt), as well as variations for CoCal (400 kt), CoL20 (800 kt and 1000 kt) and CoL74 (800 kt).	182
Figura 5.57 (Figure 5). Results and mine life for each scenario considering different ounce values.	183

5.6. Resultados Estruturas Localizadas na Região de Goiás

Geoenvironmental Characterization of Gold Mine Tailings from Minas Gerais and Goiás, Brazil

Figura 5.58 (Figure 1) Location of the main Au dams in Brazil (source: FEAM – State Foundation for the Environment) – Highlight for black dots for the study regions.	188
Figura 5.59 (Figure 2) Box plot graphs demonstrating the variation and differentiation between the tailings of structures 1 to 8 studied for Au (mg/kg), S (%), As (%), Fe (%), Cu (%), Sb (%), and C (%) – Y (Logarithmic scale).....	189
Figura 5.60 (Figure 3) 3D PCA graphics showing the grouping of chemical results from structures 1 to 8 studied for Au (mg/ kg), S (%), As (%), Fe (%), Cu (%), Sb (%), and C (%) – Y (Logarithmic scale).....	190
Figura 5.61 (Figure 4) Electronic image in false color of minerals and Au association of the tailings deposits 1 to 8.	192

5.7. Os impactos socioeconômicos e potencial dos rejeitos estudados

Figura 5.62. Etapas para busca da valorização de resíduos de mineração: uma macroproposta para a indústria da mineração.....	195
--	-----

ÍNDICE DE TABELAS

1. Introdução

Tabela 1.1. As três categorias de minerais estratégicos para o Brasil e suas representações
(adaptado de Castro et al., 2022).....9

3. Descrição da área de estudo

Tabela 3.1. Depósitos, formas de recuperação do Au e estimativas de tonelagem e teor.....30

4. Metodologia

Tabela 4.1. Método de Amostragem por Depósito de Resíduo.36

5. Resultados e discussões

5.1. Resíduos sólidos - Caracterização de Amostras Sólidas

Mineralogical and Geochemical Characterization of Gold Mining Tailings and Their Potential to Generate Acid Mine Drainage (Minas Gerais, Brazil)

Tabela 5.1 (Table 1). Statistical summary of the major and trace elements. CoT—old circuit; CaT—ongoing circuit; N—number of samples.....63

Tabela 5.2 (Table 2). Mineralogical Composition of CaT and CoT..66

Tabela 5.3 (Table 3). VMP—maximum allowed values From Brazilian Law—CONAMA [54].....69

Characterization of Arsenical Mud from Effluent Treatment of Au Concentration Plants, Minas Gerais – Brazil

Tabela 5.4 (Table 1). Average water pH and concentration of major and trace elements - Solid and Water samples N – number of samples.78

Tabela 5.5 (Table 2). Mineralogy of Solid samples (average values) N – number of samples.78

5.2. Distribuição dos elementos químicos e modelamento 3D

Geoenvironmental Study of Gold Mining Tailings in a Circular Economy Context: Santa Barbara, Minas Gerais, Brazil

Tabela 5.6 (Table 1). Statistical summary of effluent water physical– chemical parameters and dissolved EC electrical conductivity SD – Standard deviation.....	89
Tabela 5.7 (Table 2). Summary statistics of Au, S, As, Fe, Sb and Cu by Depth and Sampled Area.	91
Tabela 5.8 (Table 3). Estimated tonnage and element mean of contents for Au, As, Cu, Sb and S in Santa Barbara tailings dam.....	93
Tabela 5.9 (Table 4). Mineralogical composition of santa barbara solid tailings.	94
Tabela 5.10 (Table 5). Batch tests results of Sb, As and Au recovery.	96
 <i>Geochemistry and mineralogy of auriferous tailings deposits and their potential for reuse in Nova Lima Region, Brazil</i>	
Tabela 5.11 (Table 1). Forms of Au extraction, mass estimates and concentrations of Au, As, and S for deposits 1, 2, and 3 (modified from ⁵³).....	103
Tabela 5.12 (Table 2). Means values of the modal mineralogy of the deposits 1 (**N = 130), 2 (N = 207), 3 (N = 400), 4 (N = 229) and 5 (N = 193). *Au particles accounting; **N number of samples.....	107
Tabela 5.13 (Table 3). Statistical summary of chemical variables of tails deposits 1 to 5. LOD bellow detection limit.....	109
Tabela 5.14 (Table 4). Estimation resources of Au for deposit 1 to 5.....	114
Tabela 5.15 (Table 5). Summary of results of metallurgical tests for reuse of Au.....	115
Tabela 5.16 (Table S1). Sampling Method by Tailings Deposit	117
Tabela 5.17 (Table S2). Summary of the main potential uses of the studied samples.....	120

5.3. O estudo de reuso e reprocessamento

Adding Value to Mine Waste through Recovery Au, Sb, and As: The Case of Auriferous Tailings in the Iron Quadrangle, Brazil

Tabela 5.18 (Table 1). Statistical summary of potential value elements for the structures' tailings samples.....	132
Tabela 5.19 (Table 2). Mineralogy of Au tailing samples from the IQ. Analyses are a result of the combination of SEM, optical microscopy, and XRD.	135

Tabela 5.20 (Table 3). Mineralogy (in two size fractions) by tailing structures. Mineral abbreviations after [51].....	136
Tabela 5.21 (Table 4). Potential recovery of metals, metalloids, and other products based on chemical, textural, and mineralogical characteristics.	139
Tabela 5.22 (Table 5). Summary of metallurgical tests results for Au reuse in each Group of tailing samples. Modified from [38].	140
Tabela 5.23 (Table 6). Summary of metallurgical tests results for Sb and As recovery for Groups 2 and 5.	140
Tabela 5.24 (Table 7). Summary of size separation results of Groups 4 and 5.	141
(Tabela 5.25 (Table S1). Statistical summary of major elements for the structures' tailings samples.....	145
Tabela 5.26 (Table S2). Statistical summary of trace elements for the structures' tailings samples.	145
Tabela 5.27 (Table S3). Mineralogical composition by XRD of < 2 mm fraction. Mineral abbreviations after [51].....	146
Tabela 5.28 (Table S4). Parameters of each group's centroids, which defined grouping by observations.	147

5.4. Qualidade, distribuição química e potencial reuso para águas de porosidade

Recovery of metals in mining tailing waters - Hydrochemistry and elements distribution in gold metallurgical treatment tailings dams

Tabela 5.29 (Table 1). Statistical summary of chemical variables of wastewater from CO, CA, and CDS2 tailing deposits.	157
Tabela 5.30 (Table 2). Correlation between the collected parameters for the three dams using Pearson Coefficient. Medium to strongest correlations are highlighted in blue ($r^2 > 0.25$).	158
Tabela 5.31 (Table 3). Recovery results of Au and other metals after contact with nanofiber containing URU (adapted from [57] and [58]).	166
Tabela 5.32 (Table S1). Mineralogy of the solid fraction of the Calcinados, Cocoruto and CDS2 tailings dams – Adapted from Lemos et al. (2023).....	170
Tabela 5.33 (Table S2). Statistical summary of the chemistry of the solid fractions of the Calcinados, Cocoruto and CDS2 tailings dams – Adapted from Lemos et al. (2023)	171

5.5. Pre feasibility para o reprocessamento do Au

Sensitivity analysis and pre-feasibility of reprocessing Au from a tailings dam in the Iron Quadrangle - The case of Cocoruto Dam, Nova Lima, Minas Gerais

Tabela 5.34 (Table 1). Summary of metallurgical test results for Au reuse in CO samples (after Lemos et al., 2023a) 180

Tabela 5.35 (Table 2). Summary statistics of the global resources in the CO dam (after Lemos et al., 2023a). 181

Tabela 5.36 (Table 3). Parameters of the reference case for valuation based on the benefit function 181

Tabela 5.37 (Table 4). Variation in annual production for each considered scenario 181

5.6. Resultados Estruturas Localizadas na Região de Goiás

Geoenvironmental Characterization of Gold Mine Tailings from Minas Gerais and Goiás, Brazil

Tabela 5.38 (Table 1). Information about the studied areas, collection methods, depth, number of samples and type of analysis. PSD – Particle size distribution; AAS - Atomic absorption spectroscopy; ICP (MS) – Inductively coupled plasma mass spectrometry. 189

Tabela 5.39 (Table 2). Mineralogy of tailings deposits 1 to 8 obtained by FEI microscopy analysis. 191

5.7. Os impactos socioeconômicos e potencial dos rejeitos estudados

Tabela 5.40. Resumo do Mapeamento potencial de reuso dos resíduos estudados por Região. 194

ÍNDICE DE EQUAÇÕES

5. Resultados e discussões

5.4. Qualidade, distribuição química e potencial reuso para águas de porosidade

Recovery of metals in mining tailing waters - Hydrochemistry and elements distribution in gold metallurgical treatment tailings dams

Equação 1. Cálculo do fator de enriquecimento.....	157
Equação 2. Origem de S a partir de sulfatos e sulfetos	164
Equação 3. Fórmula de associação de Au e Cl em meios aquosos	165
Equação 4. Influência de CN residual em sistemas com Au, para diferentes situações com alto pH	165

Capítulo 1

Introdução

1. Introdução

Os aspectos de natureza ambiental, bem como o potencial de valorização de resíduos mineiros, estão entre os temas de investigação mais relevantes e atuais, principalmente num contexto de mineração sustentável e economia circular (EC). O setor dos minerais metálicos, em especial o dedicado à exploração de metais nobres como o ouro (Au), caracteriza-se pela produção de grandes quantidades de resíduos com características muito diversas consoante a natureza dos depósitos, os processos de beneficiamento/tratamento metalúrgico e as estruturas de acumulação destes resíduos. O Brasil é um país mineiro e com forte tradição na exploração de ouro, pelo que o presente trabalho se foca neste âmbito territorial, mais concretamente no estado de Minas Gerais. Neste contexto, o presente trabalho centra-se na caracterização destes rejeitados de mineração de ouro, incluindo os resíduos sólidos e água das barragens. Os vários processos de caracterização geoquímica e mineralógica são orientados para a avaliação dos efeitos no meio ambiente e a possibilidades de valorização, mediante reaproveitamento ou extração de metais uteis.

1.1. Enquadramento

O Brasil é um país que tem forte relação com a mineração, sendo que atualmente esse setor representa entre 3 a 5% do PIB. Essa proximidade é notada desde o final do século XVII, no início do primeiro ciclo do Au (Fernandes et al., 2023). Em meados do século XVIII, o Brasil chegou a produzir aproximadamente a metade do Au mundial, atraindo a imigração de cerca de 400.000 portugueses. As principais regiões que retratam tal fato localizam-se em Minas Gerais e Goiás (Figura 1.1).



Figura 1.1. Localização das principais barragens de rejeitados da exploração de Au no Brasil (FEAM, 2022), com destaque para pontos em preto para as áreas em estudo.

Atualmente este setor movimenta outros através do suprimento da matérias-primas, de que são exemplo as indústrias da construção civil, automobilística, aeroespacial entre outras (Lottermoser, 2007). Muito embora a sua importância seja relevante e estratégica para a economia, a geração de resíduos é significativa. As principais infraestruturas de deposição destes resíduos são as barragens e depósitos (pilhas) de rejeitados conhecidos mundialmente como *tailings store facilities* (TSF), da bibliografia anglo-saxônica. No entanto, estas estruturas podem constituir depósitos minerais com teores e características físicas distintas do minério explorado (Araya et al., 2021). As barragens e depósitos de rejeitados procedentes da beneficiação de minérios e/ou de processos metalúrgicos do Au, constituem infraestruturas de acumulação de resíduos com duas potenciais valências: foco de impacte ambiental e eventuais fontes de novas matérias-primas.

Com a evolução e mudanças de mercado e tecnologia, estes resíduos podem assim proporcionar uma alternativa à exploração primária. Por outro lado, são foco de impacte ambiental devido às substâncias tóxicas que comportam (Acheampong et al., 2010), e que podem ser mobilizadas pela evolução geoquímica em contexto supergénico. Ou seja, o potencial económico do enorme volume de resíduos gerados pela mineração e processamento de minérios e os elevados impactes ambientais e riscos para a saúde humana (caso de numerosos desastres ambientais, ocorridos no Brasil nos últimos anos) são duas valências que se enquadram nas linhas atuais de investigação e sustentam a inovação, interesse e oportunidade do presente trabalho.

Em adição a tais fatos, a mineração, e concretamente no Brasil as minerações de Au, é um tema fundamental a considerar no âmbito das contribuições para aplicação dos 17 objetivos de desenvolvimento sustentável (ODS) da Agenda 2030 (ONU, 2023):

Mineração e os 17 ODSs: Prioridades Indicativas

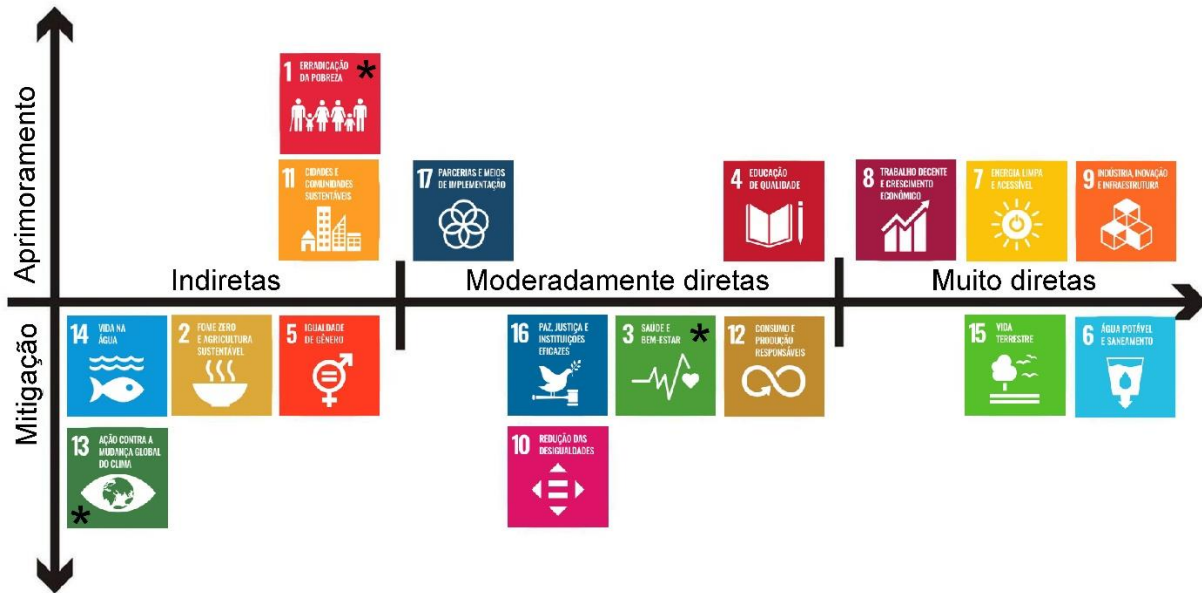


Figura 1.2. Os 17 objetivos de desenvolvimento sustentável e o papel da mineração (adaptado de UNDP, 2022).

Na Figura 1.2. são apresentados os principais objetivos com impactos que variam de direta a indiretamente e divididos em ações que são mitigadoras e aprimoradoras no setor da mineração. É nas iniciativas muito diretas, que este estudo se enquadra, sem prejuízo da visão global desta Agenda visando a gestão sustentável dos recursos geológicos: (i) iniciativa 7-energia limpa e acessível; (ii) iniciativa 8 - trabalho decente e crescimento econômico; e (iii) iniciativa 9 – indústria inovação e infraestrutura. Além disso, as iniciativas 6 – Água limpa e saneamento e vida terrestre também são forte objetivos relacionados a esta tese.

1.2. Histórico da mineração de Ouro no Brasil

A história da exploração de Au no Brasil remonta ao período colonial, quando os colonizadores portugueses descobriram grandes depósitos de Au em território brasileiro. A exploração de Au foi um dos principais motivos para a colonização do país pelos portugueses e desempenhou um papel importante na formação econômica e social do Brasil (Priore & Venâncio, 2001).

O primeiro grande episódio da exploração de Au no Brasil ocorreu no final do século XVII, na região que hoje é conhecida como Minas Gerais (Rios, 2018). As primeiras descobertas ocorreram em Minas Velhas (atual cidade de Ouro Preto) e rapidamente se espalharam para

outras áreas da região. Essa descoberta desencadeou uma verdadeira corrida do Au, atraindo milhares de pessoas de várias partes do Brasil e do mundo.

As minas de Au foram exploradas por meio do sistema de lavras, onde os mineradores independentes trabalhavam em busca do minério. No entanto, a Coroa Portuguesa impôs uma série de impostos e regulamentações para controlar a exploração e garantir sua parte dos lucros. O mais famoso deles foi o "quinto", que consistia na cobrança de 20% de todo o Au extraído (Priore & Venâncio., 2001).

A descoberta de Au também teve um impacto significativo no sistema escravista do Brasil. Com a necessidade de mão de obra nas minas, os proprietários de terras começaram a comprar mais escravos africanos para trabalhar nas minas de Au, resultando em um aumento considerável no tráfico de escravos.

Durante o período conhecido como "Ciclo do Ouro", que durou aproximadamente de meados do século XVIII até o início do século XIX, a exploração de Au em Minas Gerais atingiu seu auge. O Au extraído financiou a construção de igrejas, palácios e outras obras arquitetônicas, além de sustentar a economia colonial.

No entanto, com o esgotamento dos depósitos de Au de fácil acesso, a produção começou a declinar. Além disso, as medidas restritivas impostas pela Coroa Portuguesa levaram ao descontentamento dos mineiros e contribuíram para o movimento pela independência do Brasil.

Após a independência do país em 1822, a exploração de Au continuou em outras regiões do Brasil, como Goiás, Mato Grosso e Bahia. No entanto, a mineração de Au perdeu gradativamente sua importância econômica diante do desenvolvimento de outras atividades, como a produção de café, a industrialização e a exploração de outros minerais.

Atualmente, a mineração de Au no Brasil ainda é uma atividade significativa, com grandes empresas e cooperativas mineradoras explorando depósitos em várias regiões do país. As reservas mináveis de Au do Brasil somam quase duas mil toneladas (Silva et al., 2004; Rodrigues et al., 2022).

O Brasil é um dos maiores produtores de Au do mundo, com a produção concentrada principalmente nos estados de Minas Gerais, Pará e Goiás. Portanto, a exploração de Au continua sendo uma parte importante da economia brasileira, embora agora seja conduzida dentro de um quadro regulatório mais abrangente e mesmo restritivo no sentido de acautelar as preocupações com a sustentabilidade ambiental.

1.2.1. Geração de rejeitos na mineração de Au e seu impactos

A mineração de Au no Brasil gera uma quantidade significativa de resíduos. Esses resíduos são produzidos durante várias etapas do processo de extração e beneficiamento do Au e podem apresentar riscos ambientais e para a saúde humana, se não forem devidamente gerenciados. Apenas no Brasil são gerados cerca de 600 milhões de toneladas de rejeitos anualmente, e prevê-se que esse número deve chegar a quase 1 bilhão de toneladas até 2030 (ANM, 2023).

Um dos principais tipos de resíduos gerados na mineração de Au é o rejeito de barragem, que consiste em uma mistura de água, sedimentos e substâncias químicas utilizadas no processo de extração, como cianeto. Esses rejeitos eram depositados em barragens de contenção, também conhecidas como barragens de rejeitos.

A ruptura ou vazamento de barragens de rejeitos de mineração pode ter consequências devastadoras para o meio ambiente e para as comunidades próximas. Dois exemplos trágicos disso ocorreram em 2015 e 2019, quando as barragens de rejeitos da empresa Samarco em Mariana (Minas Gerais) e da Vale em Brumadinho se romperam, liberando uma enorme quantidade de rejeitos que contaminaram rios, causaram destruição de ecossistemas e resultaram em perdas humanas.

Além de lidar com estes riscos, a mineração de Au também gera outros tipos de resíduos, como pilhas de estéril (rochas sem valor econômico), escórias (resíduos da fundição do Au) e efluentes líquidos contaminados. Esses resíduos podem conter substâncias perigosas, tais como metais tóxicos e outros poluentes que podem contaminar o solo, a água, afetar a qualidade do ar ou mesmo provocar a degradação generalizada do ecossistema envolvente.

Para lidar com os resíduos da mineração de Au, é necessário um adequado gerenciamento e controle ambiental. O Brasil possui legislação específica que estabelece diretrizes e normas para a gestão de resíduos de mineração, incluindo a obrigatoriedade de licenciamento ambiental, monitoramento dos impactos ambientais e adoção de medidas de prevenção e mitigação. Na Figura 1.3, mostra-se a distribuição de barragem de resíduos de Au no Brasil, das quais 70% localizam-se nas áreas estudadas nesta tese:



Figura 1.3. Localização das barragens de rejeito do Au no Brasil (em preto), com foco na área de estudo (em vermelho).

Nos últimos anos tem havido um aumento da preocupação, traduzida também em termos de fiscalização em relação à gestão dos resíduos de mineração no Brasil, buscando-se evitar acidentes como o de Mariana. As empresas mineradoras estão sendo compelidas a adotar tecnologias mais seguras, investir em infraestrutura de contenção das barragens e em reabilitação ambiental, além de serem responsabilizadas por danos ambientais e sociais causados por suas operações.

A conscientização sobre os impactos ambientais da mineração de Au e a necessidade de uma abordagem sustentável têm levado a um maior envolvimento de diversos atores, incluindo órgãos governamentais, empresas, organizações não governamentais e a sociedade civil, na busca por soluções que garantam a minimização dos resíduos, a preservação dos recursos naturais e a segurança das populações.

1.3. Gestão de Resíduos de Mineração no Brasil

O gerenciamento de resíduos é um aspecto fundamental para se alcançar a almejada sustentabilidade ambiental. Com isso, surge a necessidade de se gerir de forma eficaz a geração, manuseio e a disposição final deste tipo de material. Ou seja, a gestão dos resíduos deve ser vista

na perspectiva global do ciclo de vida de todo o projeto, desde os recursos na mina até ao destino final dos resíduos.

Neste contexto, com o advento da implantação da Política Nacional de Resíduos Sólidos (PNRS) por meio da publicação da Lei nº 12.305, de 2 de agosto de 2010, no Brasil, buscou-se estabelecer diretrizes relativas ao gerenciamento de resíduos sólidos, apresentando princípios, objetivos e instrumentos orientadores com relação à prática de hábitos sustentáveis de consumo, de reutilização, reciclagem e reaproveitamento dos resíduos sólidos gerados, bem como a destinação ambientalmente adequada dos resíduos gerados.

Dentre os instrumentos previstos no artigo 8º da Lei nº 12.305/2020 incluem-se os planos de resíduos sólidos, os inventários e o sistema declaratório anual de resíduos sólidos, o Sistema Nacional de Informações sobre a Sistema Nacional de Informações sobre a Gestão dos Resíduos Sólidos (SINIR) e o Sistema Nacional de Informações em Saneamento Básico (SINISA). De forma igual, no setor mineiro, no Brasil, a gestão de resíduos de mineração é regulamentada por diversas leis e normas ambientais. Alguns dos principais documentos legais relacionadas ao tema são as seguintes:

1. Código de Mineração (Decreto-lei nº 227/1967): Estabelece as normas gerais para a atividade de mineração no país, incluindo disposições sobre a gestão de resíduos e rejeitos.
2. Política Nacional do Meio Ambiente (Lei nº 6.938/1981): Define os princípios e diretrizes gerais para a proteção e preservação do meio ambiente no Brasil, incluindo a gestão adequada de resíduos.
3. Lei de Crimes Ambientais (Lei nº 9.605/1998): Estabelece as penalidades e sanções para condutas lesivas ao meio ambiente, incluindo disposições sobre o descarte inadequado de resíduos e rejeitos.
4. Política Nacional de Resíduos Sólidos (Lei nº 12.305/2010): Estabelece diretrizes para a gestão integrada e o gerenciamento adequado de resíduos sólidos no país, incluindo os resíduos provenientes da mineração.
5. Resolução Conama nº 237/1997: Define os procedimentos para o licenciamento ambiental de atividades modificadoras do meio ambiente, incluindo a mineração, e estabelece os critérios e padrões para a disposição de rejeitos de mineração.

6. Resolução Conama nº 357/2005: Estabelece os padrões de qualidade e critérios para o enquadramento dos corpos de água, incluindo aqueles afetados pelos rejeitos de mineração.
7. Norma ABNT NBR 13028/2017: Estabelece diretrizes para o gerenciamento de áreas de disposição de rejeitos de mineração, incluindo critérios técnicos e operacionais para o planejamento, implantação e monitoramento dessas áreas.

Além das leis e normas federais, também podem existir legislações estaduais e municipais que estabelecem requisitos adicionais para a gestão de resíduos de mineração, de acordo com as particularidades de cada região.

É importante ressaltar que, em decorrência de desastres ambientais como o ocorrido em Mariana em 2015, houve um aumento da pressão por regulamentações mais rígidas e na fiscalização das atividades de mineração, visando evitar impactos negativos e garantir a segurança ambiental. Apesar disto, o tema reprocessamento e reuso é, ainda, pouco explorada no país. No entanto, embora de forma tímida, começa a ser discutido a nível nacional, à semelhança do que se passa internacionalmente como é exemplo as orientações como as da União Europeia (e.g., *Critical Raw Materials Resilience: Charting a Path Towards Greater Security and Sustainability – European Commission*).

1.4. A visão de reuso de rejeitos no Brasil

O Brasil também dispõe de uma trajetória de políticas sobre minerais estratégicos que orientam a produção segundo três segmentos: i) minerais que o país apresenta vantagem competitiva; ii) minerais cuja demanda tem sido crescente ou sobre a qual necessita importar; e iii) minerais que o país detém reservas e são considerados portadores de desenvolvimento econômico no futuro (Brasil, 2011). O Au está descrito como um dos elementos essenciais para o país, tal como apresentado na Tabela 1.1.

Tabela 1.1. As três categorias de minerais estratégicos para o Brasil e suas representações (adaptado de Castro et al., 2022).

Bens minerais que o país depende de seu suprimento para setores econômicos vitais			
Enxofre	Fosfato	Potássio	Molibdênio
Bens minerais importantes por sua aplicação em produtos e processos de alta tecnologia			
Cobalto	Cobre	Estanho	Grafita

Metais do Grupo da Platina	Lítio	Nióbio	Níquel
Silício	Tálio	Tântalo	Terras raras
Titânio	Tungstênio	Urânio	Vanádio
Bens minerais que o país detém vantagens competitivas e essenciais para a economia			
Alumínio	Cobre	Ferro	Grafita
Ouro	Manganês	Nióbio	Urânio

Embora o Brasil tenha uma posição de destaque como produtor de bens minerais, o país apresenta grande dependência por fontes externas para quatro minerais/elementos estratégicos que estão associados com fertilizantes agroindustriais e indústria química: fosfato, potássio, enxofre e molibdênio. A produção interna não consegue suprir a demanda ocasionando uma dependência de importação de aproximadamente 81% de todo o consumo interno (Junior, 2020). A guerra entre Rússia e Ucrânia a partir de fevereiro de 2022 acendeu um alerta global o que já acarretou elevação dos preços no mercado internacional e redução da oferta (Castro et al., 2022). Além disso, os efeitos da pandemia de COVID 19 também acarretou diversas alertas no setor de suprimento mineral no país.

Na cadeia de produção do Au, além deste ser vital para sustentação da economia mineral do país, é comum a ocorrência de elementos categorizados como vitais associados às mineralizações de Au, como é o caso do enxofre (Castro et al., 2022).

Apesar do tema ser ainda inicial no Brasil, o contexto é de grande importância e alguns casos de reutilização já aplicados na indústria são exemplificados por Rodrigues et al. (2022):

1. Programa areia sustentável: produção de areia a partir de resíduos de minério de Ferro;
2. Utilização de lama para pavimentação de estradas vicinais: Matéria prima composta pelo rejeito ultrafino de ferro e utilizada para pavimentação de estradas vicinais;
3. Recuperação de Nióbio (Nb) proveniente da escória em bloco e do rejeito de areia *shell* do desenformamento, através da implantação do processo de jigagem: FeNb recuperado através da transformação de antigos resíduos do processo em produto;
4. Zincal: Corretivo de acidez de solo para fins agrícolas a partir de rejeitos da metalurgia do Zn.

Outros projetos são também apresentados por Rodrigues et al. (2022) como em andamento e ainda não aplicáveis. Além disso, é importante destacar que apesar de contribuírem para o país na linha da sustentabilidade, poucos destes minerais são diretamente relacionados com a classificação de vital ou essencial para economia.

Portanto, constata-se que ainda existem muitas oportunidades neste contexto de reutilização, com interesse não só para o país, mas também para o mundo.

1.5. Oportunidades do tema de tese e objetivos

O ambiente mineiro pode ser encarado sob diversas perspectivas e em especial, no Brasil, a disposição de rejeitos é um problema e presente, mas simultaneamente pode ser uma oportunidade.

É neste contexto, de regiões tradicionais com vasta história de acumulação de rejeitos de Au, que esta tese é desenvolvida. O trabalho realizado foi suportado por inúmeras disciplinas, de modo a contextualizar a geologia das regiões, assegurara a caracterização dos rejeitados e encaminhar os resultados no sentido do modelo econômico de cenários de reprocessamento destes resíduos.

O trabalho tem como objetivo geral estudar os resíduos, entendidos no sentido lato do termo, visando distintos aspectos: (i) obtenção das suas propriedades gerais, ii) caracterização e avaliação ambiental das águas residuais e sólidos provenientes do lançamento de rejeitados das barragens e depósitos, iii) avaliar o potencial de aproveitamento económico de metais e minerais ganga associados.

Abaixo são expostos os objetivos específicos estabelecidos para concretizar o plano deste trabalho:

1. Analisar o banco de dados com informação disponível (bases de dados cartográficos, fotogeológicos) sobre as propriedades dos resíduos, etapas processuais que os originam e natureza dos depósitos e materiais explorados;
2. Estabelecer o referencial histórico e enquadrar o tema da deposição de resíduos em barragens de rejeitados no território em estudo do ponto de vista jurídico, técnico e ambiental, tendo em consideração normas brasileiras e internacionais;
3. Estabelecer um plano de monitorização, com estações de amostragem na água e nas barragens, avaliando o seu potencial contaminante e como ativo mineiro;
4. Characterizar os resíduos quanto a aspectos de natureza físico-química e mineralógica;

5. Relacionar os metais e compostos químicos, possíveis contaminantes, disponíveis nos rejeitados e mobilidade em meio aquático;
6. Aplicar técnicas de alta resolução para avaliar a reatividade, perigosidade e capacidade de retenção de contaminantes ou elementos críticos;
7. Investigar o potencial de valorização dos resíduos, no sentido da sua reintrodução na cadeia de valor e trazer para discussão sua integração com as listas de risco de supressão da união europeia e Brasil.

Devido aos impactos da pandemia e consequentes dificuldades de acesso e trabalho analítico, nas amostras localizadas em Goiás, a avaliação focou-se no potencial reuso da extração de ouro em detrimento de outras aplicações. Mas, mesmo com tais limitações, abordam-se neste estudo outras possibilidades de valorização.

1.6. Planificação da tese

O trabalho é dividido em seis capítulos, incluindo este primeiro de introdução, no qual se apresenta uma abordagem prévia e genérica ao tema. O enquadramento do tema, principalmente no cenário brasileiro, e sua relação com aplicações reais foram aqui abordados. A história do Au no Brasil e seus impactantes foram também demonstrados, com ênfase na abrangência da acumulação de resíduos nos estados de Minas Gerais e Goiás. Além disso, justificou-se o motivo deste desenvolvimento, bem como os objetivos para cumprimento desta tese.

No capítulo 2, economia circular e mineração, discutem-se conceitos relacionados com esta perspectiva e faz-se o seu enquadramento a nível internacional e brasileiro. Para além disto, identificam-se casos de estudo que demonstram a relevância e atualidade deste tópico.

No capítulo 3 são descritas as áreas de estudo – com a localização geográfica, os enquadramentos geológico e climático. São também apresentados aspectos relacionados com a história e atividade mineira, assim como fluxogramas metalúrgicos de empreendimentos encontrados nas regiões e geradores destes resíduos e seus impactantes ambientais.

A metodologia deste trabalho apresenta-se no capítulo 4, englobando as técnicas de amostragem e analíticas para a caracterização de resíduos e ensaios de recuperação de elementos como Au, As e Sb. Acresce aqui a descrição dos métodos de análise estatística, que também serviram de base para técnicas de análise econômica.

O capítulo 5 trata dos resultados e sua discussão. Os resultados da caracterização das fases solidas e líquidas das estruturas mineiras se relacionam e demonstram potenciais de geração de produtos, além do próprio Au. Os potenciais foram mapeados e quantificados gerando modelos geoestatísticos e mapas de potencial reuso para cada estrutura estudada. Em caso base foram obtidos modelos económicos em diferentes cenários.

A maioria dos resultados foram sujeitos a publicação, pelo que os respetivos artigos, indexados em bases de dados internacionais e/ou resumos alargados de conferências, são compilados neste capítulo.

No capítulo 6 são apresentadas as conclusões obtidas na tese, bem como oportunidades de estudos futuros. Por fim, são apresentadas as referências utilizadas.

Capítulo 2

Economia circular e mineração

2. Economia circular e mineração

O sistema de EC agregou diversos conceitos criados no último século, como: design regenerativo, economia de performance, capital natural, *cradle to cradle* – do berço ao berço, ecologia industrial, biomimética, *blue economy* e biologia sintética, tudo isto no sentido de desenvolver um modelo estrutural para a regeneração da sociedade (Araujo et al., 2017).

A EC segue uma utilização racional dos recursos. Com o uso em cascata dos materiais, eles permanecem o maior tempo possível na economia. Após um produto chegar ao fim de seu ciclo para o primeiro consumidor, ele pode ser compartilhado e ter sua utilização ampliada. Posteriormente ao esgotamento de reuso do artefato, ele pode ser material de *upcycling* (reaproveitamento), reformado, remanufaturado e, como última etapa, reciclado. As alternativas de reciclagem atuais operam sobre bens de consumo que não foram projetados com esta intenção. A EC parte da proposta de desconstruir o conceito de resíduo com a evolução de projetos e sistemas que privilegiam materiais naturais que possam ser totalmente recuperados.

A seguir, serão discutidos os conceitos mais atuais, seu enquadramento na mineração e bem como casos de sucesso na mineração de Au.

2.1. Conceito da Economia Circular

Segundo a *Ellen MacArthur Foundation* (2023), o conceito da EC é baseado em três princípios, orientados pelo design: (i) eliminar resíduos e poluição, (ii) circular produtos e materiais e (iii) regenerar a natureza.

O diagrama sistêmico da EC (Figura 2.1), conhecido como “diagrama de borboleta”, ilustra o fluxo contínuo de materiais em EC. O objetivo geral da economia circular, como representado neste diagrama, é criar um sistema em que nada é desperdiçado. Em vez de um modelo linear tradicional de "extrair, produzir, descartar", a economia circular busca criar um ciclo fechado de produção e consumo. Isso beneficia não apenas o meio ambiente, mas também a economia, pois busca maximizar o valor dos recursos e minimizar o desperdício. São dois ciclos principais – o técnico e o biológico e são detalhados a seguir:

1. Biosfera & Materiais Renováveis:

- No lado esquerdo, o diagrama representa o fluxo de materiais biológicos. Esses materiais são projetados para retornar à biosfera e, idealmente, regenerá-la.

- O diagrama inicia com o Gerenciamento do Fluxo de Renováveis, onde materiais como plantas são cultivados ou coletados.
- Esses materiais podem ser transformados em Insumos Bioquímicos, que têm várias aplicações.
- O processo de Digestão Anaeróbica pode ser usado para produzir biogás, uma fonte renovável de energia.
- As setas indicam que os resíduos retornam à biosfera, seja diretamente ou após serem usados como energia.

2. Materiais Finitos:

- No lado direito, o diagrama trata dos materiais técnicos, que são finitos. Estes são materiais que não são projetados para retornar à biosfera.
- Começa com o Gerenciamento de Estoque, garantindo que os materiais sejam usados de maneira eficiente e sustentável.
- Depois, segue para a Manufatura de Peças e Produtos. Posteriormente, esses produtos são fornecidos a Provedores de Serviço e, finalmente, aos Consumidores e Usuários.
- Há várias etapas posteriores ao uso inicial: Compartilhar, Manter/Prolongar, Reutilizar/Redistribuir, Reformar/Reproduzir e Reciclar. Estas etapas garantem que os produtos e materiais sejam reutilizados ao máximo antes de serem descartados.

3. Cascatas: Este conceito representa a ideia de que um produto pode ter múltiplas vidas em diferentes funções.

4. Minimizar Vazamentos Sistemáticos e Externalidades Negativas: O objetivo da economia circular é manter os materiais em circulação pelo máximo de tempo possível, evitando o desperdício e minimizando impactos negativos no meio ambiente.

5. Coleta: Ambos os lados do diagrama apresentam a coleta, seja de resíduos biológicos ou materiais técnicos, para reintroduzi-los no ciclo.

Diversos países sabem da importância e estão progressivamente implantando os conceitos. A PNRS, lei implantada no Brasil em 2010, visa garantir a responsabilidade compartilhada pelo ciclo de vida dos produtos, a operação reversa e o acordo setorial. Assim, todos os agentes do ciclo produtivo, os consumidores e os serviços públicos devem minimizar o volume de resíduos

sólidos gerados e adotar práticas que assegurem que os produtos sejam reintegrados ao ciclo produtivo.

Em países como a China, a EC faz parte da Lei de Promoção da Produção Limpa, promulgada em 2002. Medidas como rotulagem ecológica de produtos, difusão de informações sobre questões ambientais na mídia e cursos oferecidos pelas instituições de ensino são importantes para familiarizar a sociedade com a EC.

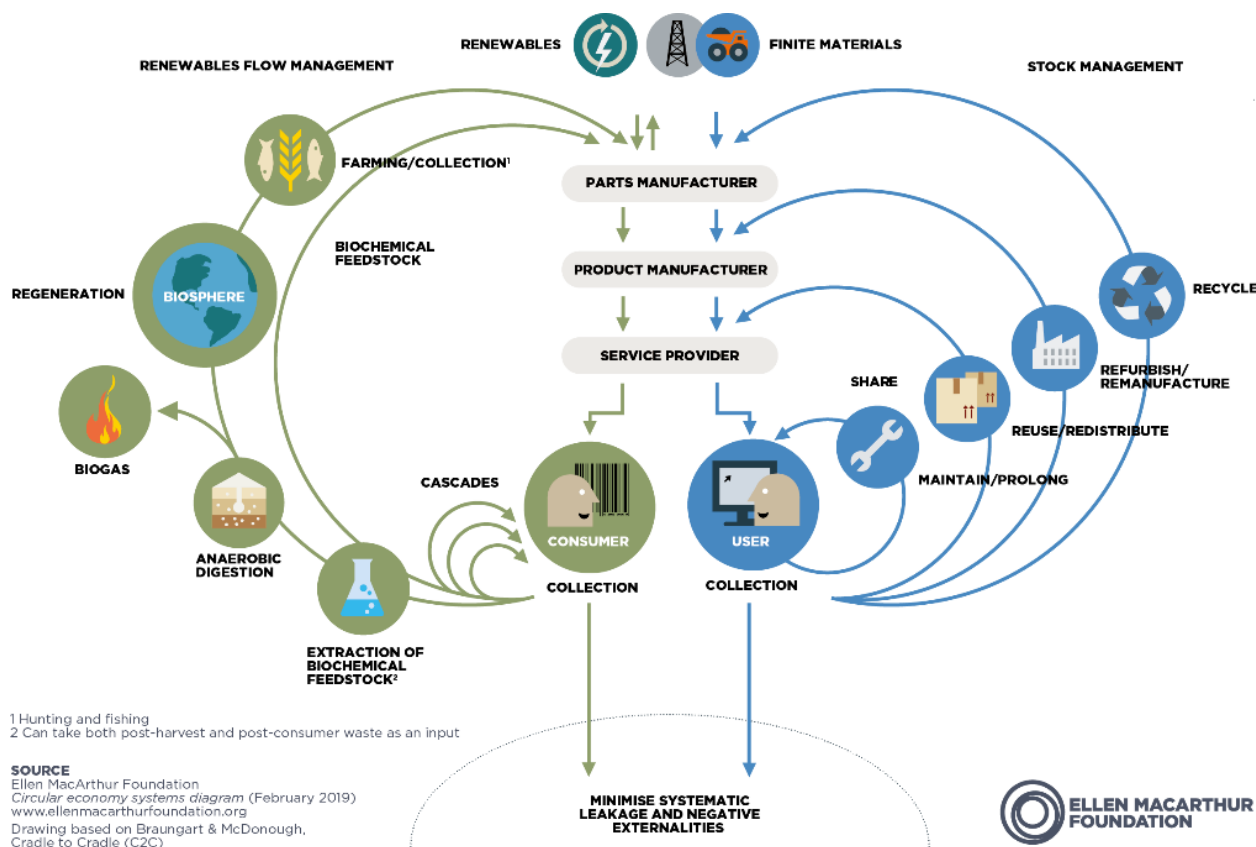


Figura 2.1. Diagrama de Borboleta (Ellen MacArthur Foundation, 2023).

Diferentemente do Brasil, no resto do mundo há sinais importantes de que a ideia de transição para a EC e suas práticas regenerativas está avançando de forma veloz.

O Parlamento Europeu aprovou, recentemente, uma classificação baseada em seis objetivos, que visa orientar investimentos públicos nos países do bloco que precisam atingir metas já estabelecidas nos acordos do clima, nas diretrizes contra a poluição de rios, mares e nos compromissos internacionais em relação aos resíduos.

Neste cenário, para que a EC seja implantada, o surgimento de um “consumidor circular” é fundamental.

2.2. O enquadramento da Economia Circular na mineração

Além dessa realidade e de uma abordagem de modelo econômico linear, os últimos rompimentos de barragens de rejeitos Mariana e Brumadinho-Minas Gerais (respectivamente, novembro de 2015 e janeiro de 2019), chamaram a atenção para os problemas do setor da mineração e aumentaram a dificuldade de obtenção de licenças ambientais e locais adequados para disposição de rejeitos. Consequentemente, a indústria de mineração enfrenta crescentes desafios econômicos, sociais e ambientais. A necessidade de garantir a mineração sustentável em conformidade com os marcos legais ambientais está levando o setor a um novo paradigma.

O componente-chave da EC é estender a vida útil de matérias-primas, como descrito acima, que já foram extraídas da litosfera (Gaustad et al., 2017) em uma perspectiva restaurativa que minimiza riscos sistêmicos por meio da gestão de inventários finitos e fluxos renováveis de recursos (Ellen MacArthur Foundation, 2023; Araújo et al., 2017). Além disso, de acordo com a mais recente lista europeia de risco de fornecimento de elementos químicos (Comissão da União Europeia, 2023), elementos de terras raras (REE), antimônio (Sb), germânio (Ge), bismuto (Bi), bem como arsênio (As), elementos do grupo da platina (PGE) e cobalto (Co) estão potencialmente sujeitos a altos níveis de risco de interrupção do fornecimento. Além disso, a água é uma questão-chave em todas as etapas do ciclo da mineração. Nesse contexto, Tayebi-Khorami et al. (2019) sugerem cinco áreas principais de integração dentro do setor de mineração: dimensões sociais, aspectos geoambientais, especificações geometalúrgicas, direcionadores econômicos e implicações legais (Figura 2.2).

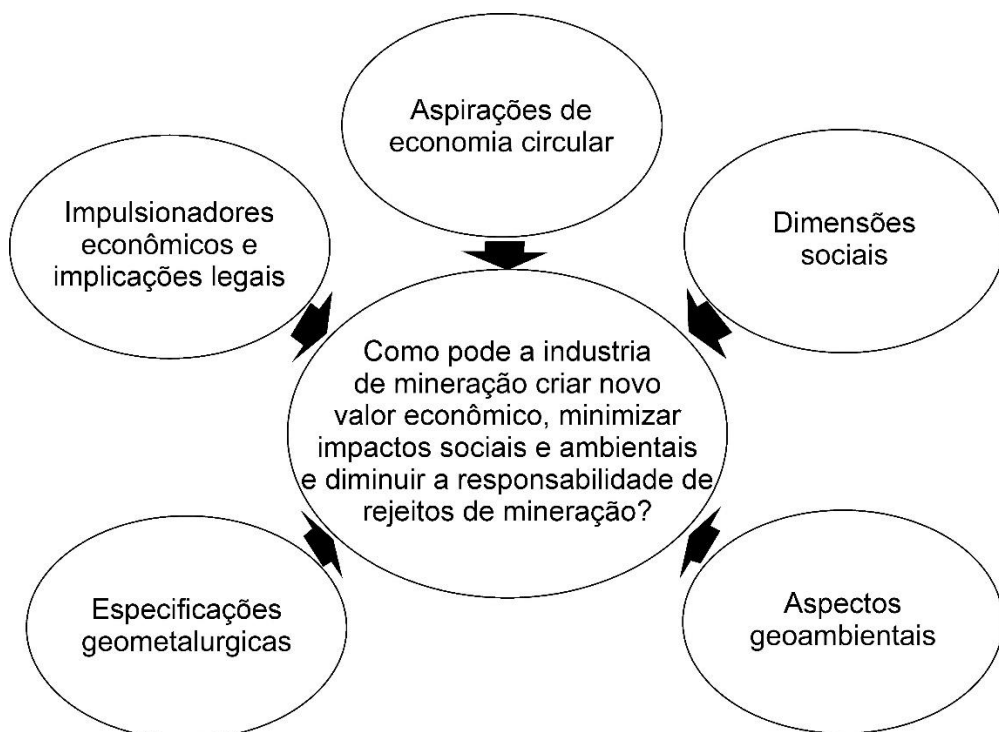


Figura 2.2. Áreas chaves para integração e aplicação dos conceitos EC no setor mineral (adaptado de Tayebi-Khorami et al., 2019).

Continua a ser necessária investigação e desenvolvimento consideráveis para identificar soluções eficazes em cada um destes domínios-chave. Existem várias maneiras amplas de fazer isso no contexto da mineração, incluindo a valorização de resíduos, em que os resíduos formados durante o processo de extração de metais são transformados em produto. Também envolve o processamento de resíduos, como águas residuais, resíduos de solventes, resíduos sólidos, gases de exaustão e cinzas (Singh et al., 2020; Spooren et al., 2020).

Alinhado ao conceito definido pela *Ellen MacArthur Foundation*, onde EC é alinhado aos princípios do design, o reuso e o reprocessamento de rejeitos são abordagens possíveis, mas requerem esforços metodológicos apoiados em técnicas geoquímicas e mineralógicas robustas para a necessária caracterização. Estes incluem difração de raios X (DRX) e fluorescência de raios X (FRX) em associação com mineralogia eletrônica quantitativa (Pires et al., 2019) para a caracterização mineralógica, quantificação automática de fases minerais, espectrometria de massa de íons secundários por tempo de voo (TOF-SIMS), espectrometria de massa com plasma indutivamente acoplado por ablação a laser (LA-ICP-MS) e difração de elétrons retroespelhados (EBSD) (por exemplo, Martin et al., 1997; Silva et al., 2004; Shi et al., 2009; Parbhakar-Fox, 2016; Novhe et al., 2018; Guanira et al., 2020; Gomes et al., 2022).

2.3. Histórico do reuso no setor mineral

Há muitos exemplos de estudos de caso e implementações para recuperação de metais e metaloides presentes em resíduos de mineração. Um exemplo de desenvolvimento atual, a vitrificação permitiu a recuperação de contaminantes como As e Sb (US9981295B2 - Dundee Sustainable Technologies Inc., 2016) e foi implementada em minas de Au em pesquisadores na África do Sul, Canadá e Brasil estão tentando usar essa tecnologia em minas de Au. Tecnologias baseadas em sensores podem ser úteis em resíduos grosseiros e estoques antigos para reprocessar e recuperar estanho, tungstênio e Au (Von Ketelhodt, 2009; Manoucheri et al., 2016; Robben et al., 2020). Altinkaya et al. (2019) sugeriram novas abordagens para recuperar metais traço de rejeitos de flotação de sulfeto em soluções de cloreto cúprico; as recuperações de Ni, Zn, Co, Fe e Au excederam 58%. O pré-tratamento de rejeitos cianetados por ustulação e seu efeito na recuperação abrangente seguida de metais valiosos foram investigados em Bailong et al. (2013). Os resultados indicam que a taxa de lixiviação do Au atinge 46,14% e que a suscetibilidade magnética do ferro é de até 86,27%. Além disso, há oportunidades para extrair metais preciosos e outras substâncias críticas como Ag, Pt, In, Ge W,, Zn, Pb e Sb através de rotas metalúrgicas comuns, usando remoagem, flotação, ustulação, lixiviação, biolixiviação, etc. (por exemplo, Dehghani et al., 2009; Chen et al., 2014; Martin et al., 2015; Falagán, 2017). Biossorventes e nanofibras podem ser uma forma de recuperar metais como, Pb e Cd de águas efluentes (Sang et al., 2008; Bailong et al., 2013), e metais preciosos também podem ser recuperados das águas de minas e lixiviados. Outras abordagens, como a flotação iônica, sugerem boa recuperação para (Jafari et al., 2017). A remediação de drenagem ácida de mina (DMRI) tem custos elevados, mas pode representar uma fonte de metais, como mostrado por Skoronski et al. (2017), por meio da recuperação de contaminantes de Al e Fe em formas utilizáveis, e mostra novas formas para minimizar o custo do tratamento de água (Ryan et al., 2017; Akinwekomi et al., 2020). O trabalho de Antunes et al (2010), Hedin (2003), Valente et al. (2016) e Silva et al. (2019) indicam o potencial de recuperação de ocre-precipitados do tratamento passivo da DMRI, para uso como pigmentos e no setor cerâmico. Grande et al. (2013) apresentaram um sistema para neutralizar a DMRI e recuperar sua carga metálica, utilizando energia obtida de fontes renováveis. Assim, a neutralização e o tratamento poderiam servir ao propósito de reduzir passivos ambientais ao mesmo tempo em que geram renda, de acordo com o paradigma da EC (Valente et al., 2016).

2.4. Casos de Sucesso do reuso na mineração de Au

O potencial de recuperação de Au de vários tipos de rejeitos tem sido extensivamente investigado por todo mundo, como demonstra o estado-da-arte apresentado no ponto anterior.

Os testes de flotação e cianetação são os principais métodos empregados para reprocessar tal material, às vezes envolvendo etapas adicionais, como remoagem, ustulação e cianetação de concentrados de flotação. Em certos estudos (Dehghani et al., 2009), dissolução e recuperação de Au as taxas variaram de 87,8% a 98,4% nos rejeitos de Au contendo sulfeto. Avanços tecnológicos no processamento mineral, juntamente com as formas dos minerais que contém Au encontrado em rejeitos, oferecem oportunidades para o desenvolvimento de rotas de valorização da Au presente nestes resíduos (Cairncross & Tadie, 2022).

O reprocessamento de rejeitos de minas de Au tem se mostrado economicamente viável e benéfico, particularmente quando integrado em instalações existentes para compensar a escassez de minério bruto e perdas operacionais (Cairncross & Tadie, 2022). Algumas plantas atualmente incorporam o reprocessamento de rejeitos de Au em suas cadeias de produção, como a estação de retratamento de rejeitos de Elikhulu (África Austral), que processa 1,2 Mt de rejeitos históricos por ano a partir de três barragens de lodo existentes (PanAfrican Resources, 2018) e Mina de Paracatu (Brasil) na qual 10 milhões de toneladas de rejeitos de hidrometalurgia contendo 1 mg Au/kg são reprocessados (Monte et al., 2020). Além disso, elementos perigosos para a saúde, que ocorrem paralelamente ao Au, também pode possuir valor industrial (Lalancette et al., 2015; Parviainen et al., 2020). Além disso, pesquisas de ponta indicam que os minerais de ganga encontrados nos rejeitos têm potencial significativo para aplicação na área civil construção civil e até mesmo como fertilizantes, dependendo de propriedades como granulometria e composição química (Swaroop et al., 2013; Mapinduzi et al., 2016; Sanchez-Pena, 2018; Ince, 2019; Yao et al., 2019).

O trabalho apresentado por Soares (2022), utilizou águas dessas barragens, caracterizadas nos itens acima, e teve como objetivo recuperar Au(III),(II), Ni(II) e outros metais utilizando nanofibras de *Bixa orellana Linnaeus* (URU), planta típica brasileira com propriedades quelantes. A recuperação de Au atingiu valores acima de 70%.

Capítulo 3

Descrição da área de estudo

3. Descrição da Área de Estudo

O estudo foi dedicado a duas importantes Províncias Auríferas. Os primeiros estudos e mais detalhados foram desenvolvidos em TSF da região do Quadrilátero Ferrífero (QF), nomeadamente nas cidades de Nova Lima e Santa Barbara no estado de Minas Gerais. O segundo grupo de amostras estudadas é referente a estruturas de rejeitos localizadas na cidade de Crixás, no estado de Goiás.

Assim, serão aqui descritos os aspectos geológicos, geográficos, históricos e os fluxos de geração de resíduos destas duas regiões.

3.1. Depósitos e Barragens localizados em Minas Gerais

As áreas de estudos estão no QF, uma província metalogenética que hospeda grandes depósitos de Au e ferro, além de gemas e minerais industriais (Porto, 2008). O QF representa uma das unidades geotectônicas mais importantes com rochas e evolução geológica das idades Arqueana e Proterozóica (Almeida, 1967). Três domínios tectonoestratigráficos principais compõem a província QF: terrenos granito-gnáissicos, uma sequência do tipo cinturão xistos verdes(Supergrupo Rio das Velhas - SGRV) e uma sequência supracrustal de rochas sedimentares químicas e clásticas (Supergrupo Minas). O *Greenstone Belt* do Rio das Velhas, em grande parte localizado no Estado de Minas Gerais (Figura 3.1), é o distrito de Au mais importante do Brasil, com uma estimativa de 4,5% (936 t) das reservas mundiais de minério (Goldfarb et al., 2001; Lobato et al., 2001). De baixo para cima, compreende rochas vulcânicas maficas toleíticas e komatiitos, formações ferríferas bandadas do tipo Algoma, xistos e filitos metavulcanoclásticos e sequências clásticas terrestres, todas metamorfoseadas em fácies xisto verde a anfibolito (Figura 3.1, Almeida, 1976; Schorscherida, 1976; Schorscherida, 1978). Os corpos mineralizados, hospedados em rochas arqueanas, são estruturalmente associados e controlados por alteração hidrotermal.

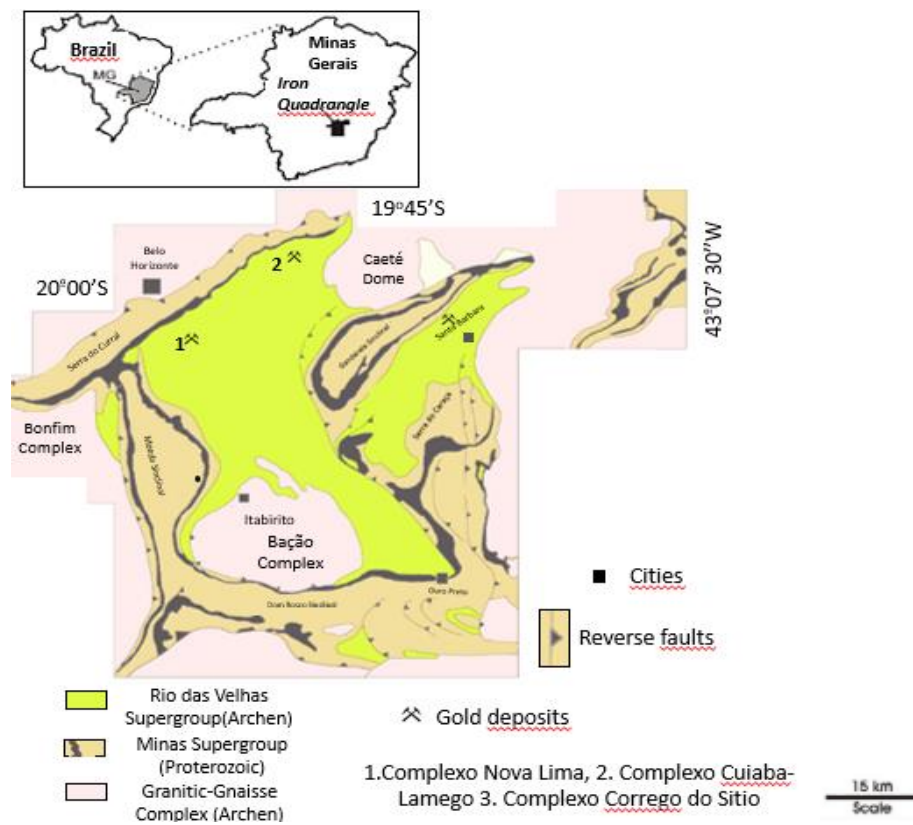


Figura 3.1. Mapa do Quadrilátero Ferrífero (modificado de Alkmin & Marshak, 1998; Porto, 2008; Ruchkys et al., 2015).

3.1.1. Barragem e Pilha de rejeitados de Santa Barbara

A barragem e pilhas de rejeitados de Santa Bárbara estão localizadas na parte norte do QF, em Santa Bárbara, Minas Gerais, a 110 km de Belo Horizonte (Figura 3.2.a). Resíduos de minas subterrâneas de usinas metalúrgicas de Au foram depositados nesta estrutura desde 1986.

Santa Bárbara tem um clima tropical com invernos secos e verões úmidos. O mês mais quente é fevereiro, com temperatura média de 27 °C, e o mais frio, julho, com 13,6 °C. A precipitação média anual é de 1897 mm, sendo maior no verão (IBGE, 2019).

A barragem e pilhas de rejeitados de Santa Bárbara estão inseridas no contexto geológico da unidade Córrego do Sítio (Baltazar, 1998). A unidade Córrego do Sítio é um turbidito metamorfizado em uma sequência alternada de metagrauvaca e filitos, englobando diques e peitoris metamáficos. A zona de minério encontra-se na descontinuidade estratigráfica entre as rochas metassedimentares e metamáficas. O Au está associado à arsenopirita e à pirita, que se disseminam em rochas metapelíticas e veios de quartzo-carbonato. A mineralização inclui vários estágios de cristalização: (1) pirita e pirrotita, (2) arsenopirita, pirrotita e pirita fina, (3) arsenopirita com pirrotita e sulfossais em veios de quartzo, e (4) pirita difusa (David, 2006; Porto,

2008) Os sulfossais são representados principalmente por bertiierita. Nas zonas mineralizadas, quando intemperizadas, o Au está associado a reliquitos de sulfossais, silicatos e óxidos.

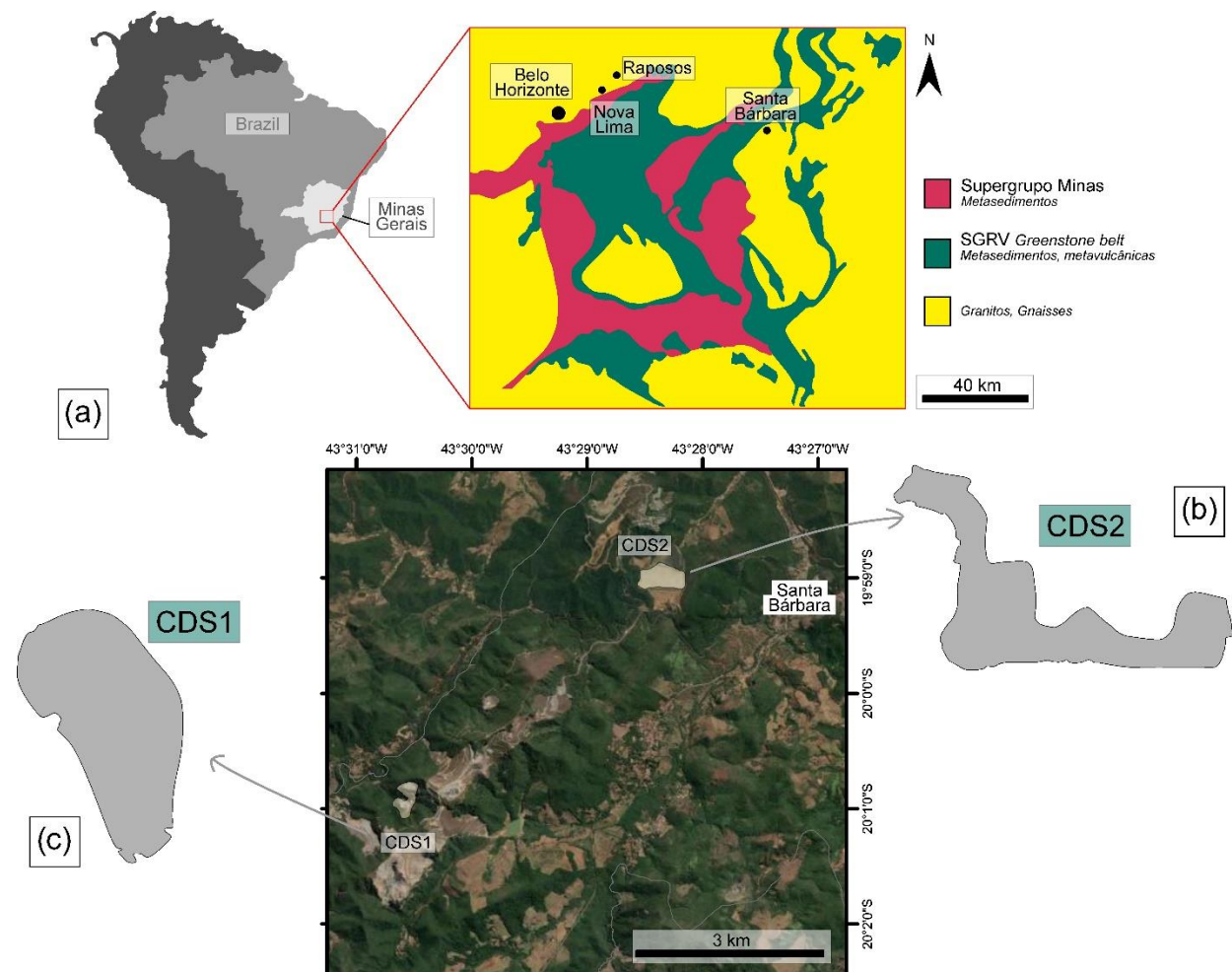


Figura 3.2. a) Localização e contexto geológico da região de Santa Barbara, b) Barragem Santa Barbara e c) Pilha de rejeitos Santa Barbara.

As fontes de rejeitados destas estruturas possuem diferentes proveniências: a) a pilha de rejeitados derivados da planta de eiras de lixiviação (*heap leach*) alimentada pelo minério explorado em lavras a céu aberto e oxidado (Figura 3.3.a) e b) as barragens de rejeitados representadas por resíduos de uma planta de flotação e lixiviação, provenientes de minérios fresco da lavra subterrânea (Figura 3.3.b).

O minério oxidado é extraído em cavas a céu aberto e alimenta a planta de beneficiamento *heap leaching*. O material é primeiramente britado (1), aglomerado com cimento (2) para formação de pilhas (3). Em seguida, é inserido cianeto e o Au é lixiviado em pilhas (4). A solução é encaminhada para eluição (5), eletrólise (6) e fundição (7). A recuperação de Au é variável dependendo dos tipos de minérios, mas em média alcança valores iguais a 70% (Figura 3.3,

Magalhães, 2022). As pilhas são mobilizadas após tempo padrão da cianetação para uma área próxima da planta e são monitoradas para avaliação de formação de drenagem ácida e demais parâmetros ambientais conforme diretrizes do CONAMA (2005). O teor médio do Au estimado nestes resíduos é de 0.5 g/t com massa estimada de 60 mil toneladas.

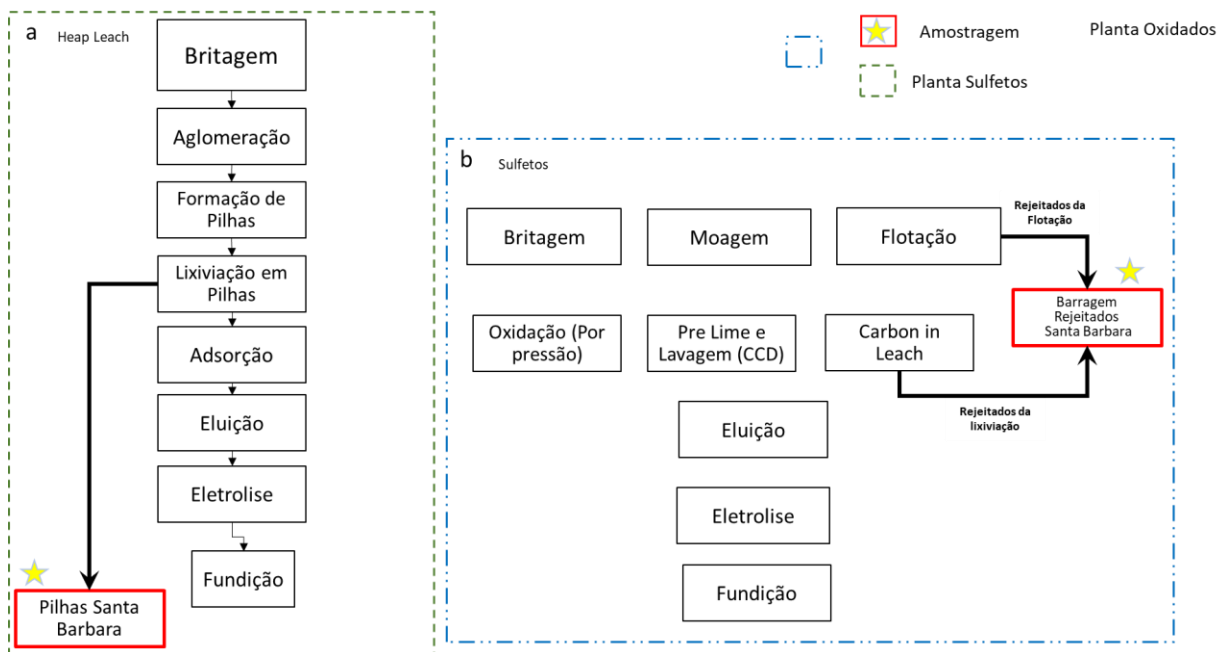


Figura 3.3. a) Localização das amostras coletadas no primeiro ano da barragem de rejeitados e b) plano de coleta das amostras das pilhas de rejeitados.

O minério extraído da mina subterrânea alimenta a planta metalúrgica sulfetada, onde passa por: (1) britagem, (2) moagem, (3) separação gravimétrica, (4) flotação de sulfeto, (5) oxidação por pressão em autoclave e (6) lixiviação. Atualmente, apenas 25% da massa *run-of-mine* (ROM – 1 milhão de toneladas/ano) é utilizada para recuperação de Au, com variações relacionadas ao tipo de minério tratado (Figura 3.3, Lemos et al., 2020), resultando em diferentes volumes e teores de Au nos rejeitados depositados e empilhados. A água do processo metalúrgico é reaproveitada sem tratamento, porém, os efluentes que são descartados na drenagem regional são previamente tratados. A barragem de rejeitados de Santa Bárbara foi construída usando um método de linha central e se espalha por uma área de 25 km² (Figura 3.2). Água e rejeitados sólidos das operações de flotação e lixiviação são depositados nesta estrutura com capacidade de 5 milhões de m³ de rejeitados com teor de Au de 0.5 g/t (AGA, 2018). Após a tragédia de Brumadinho, apenas rejeitados da última etapa são coletados na barragem, já que rejeitos da flotação passam agora para um processo de pilha a seco. No entanto, de 1986 a 2019,

a barragem recebeu volumes consideráveis de rejeitados de mina, sugerindo potencial considerável para estudos de reutilização.

3.1.2. Depósitos e Pilhas de rejeitados de Nova Lima e Sabará

As minas da região de Nova Lima são depósitos minerais de Au orogênico, bem como outros presentes no QF, entre os quais se citam Cuiabá, Morro Velho, Raposos, São Bento e Juca Vieira, diretamente relacionados à evolução do *greenstone belt* Rio das Velhas (ca. 2.75 Ga) e suas formações ferríferas bandadas (FFB) do tipo Algoma (Lobato et al., 2001; Martins et al., 2016). A principal hospedeira da mineralização é uma FFB, sulfetada. A presença de pirita (\pm arsenical) associada à arsenopirita indica mineralização em Au. Além disso, o Au também ocorre associado a veios de quartzo, com minérios pouco a totalmente refratários.

Além desta estrutura de Santa Barbara, em um mesmo contexto geológico, também se realizaram estudos em barragem de rejeitados e pilhas na cidade de Nova Lima e Sabará (Figuras 3.4 e 3.5). Na cidade, localizam-se barragens não ativas e ativas, bem como depósito de rejeitados explorados desde o século antepassado. De 1834 até à data atual foram depositados resíduos de minas da região e estimam-se 107 toneladas de Au nestes depósitos (AGA, 2018). As principais estruturas são:

1. Depósitos de rejeitados Isolamento;
2. Barragem não ativa da Mina de Bicalho;
3. Depósitos da Planta de Mina Velha;
4. Barragens ativas e não ativas da planta metalúrgica de Queiroz;
5. Barragem de Cuiabá.

DESCRIÇÃO DA ÁREA DE ESTUDO

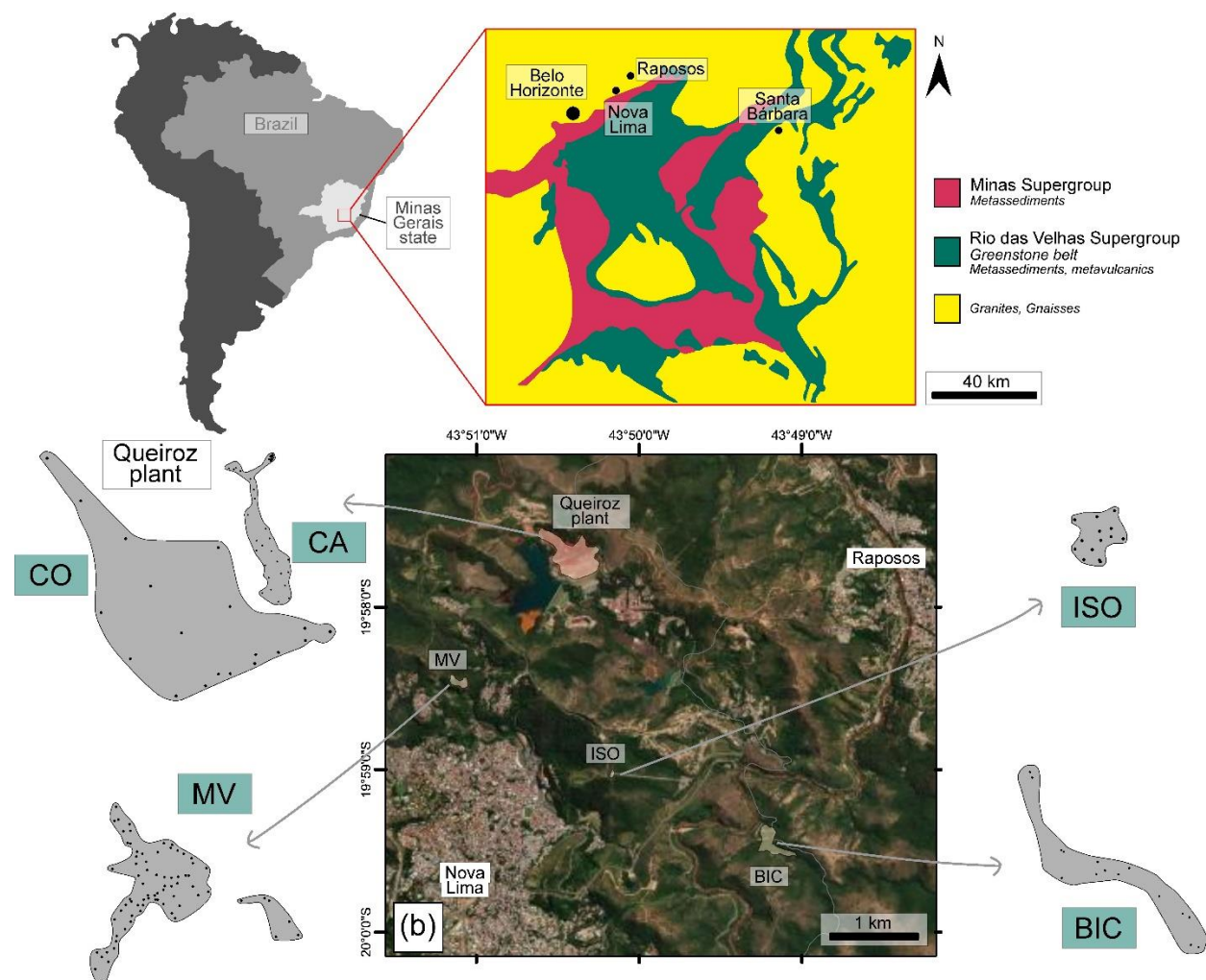


Figura 3.4. Localização áreas em estudo de Nova Lima.

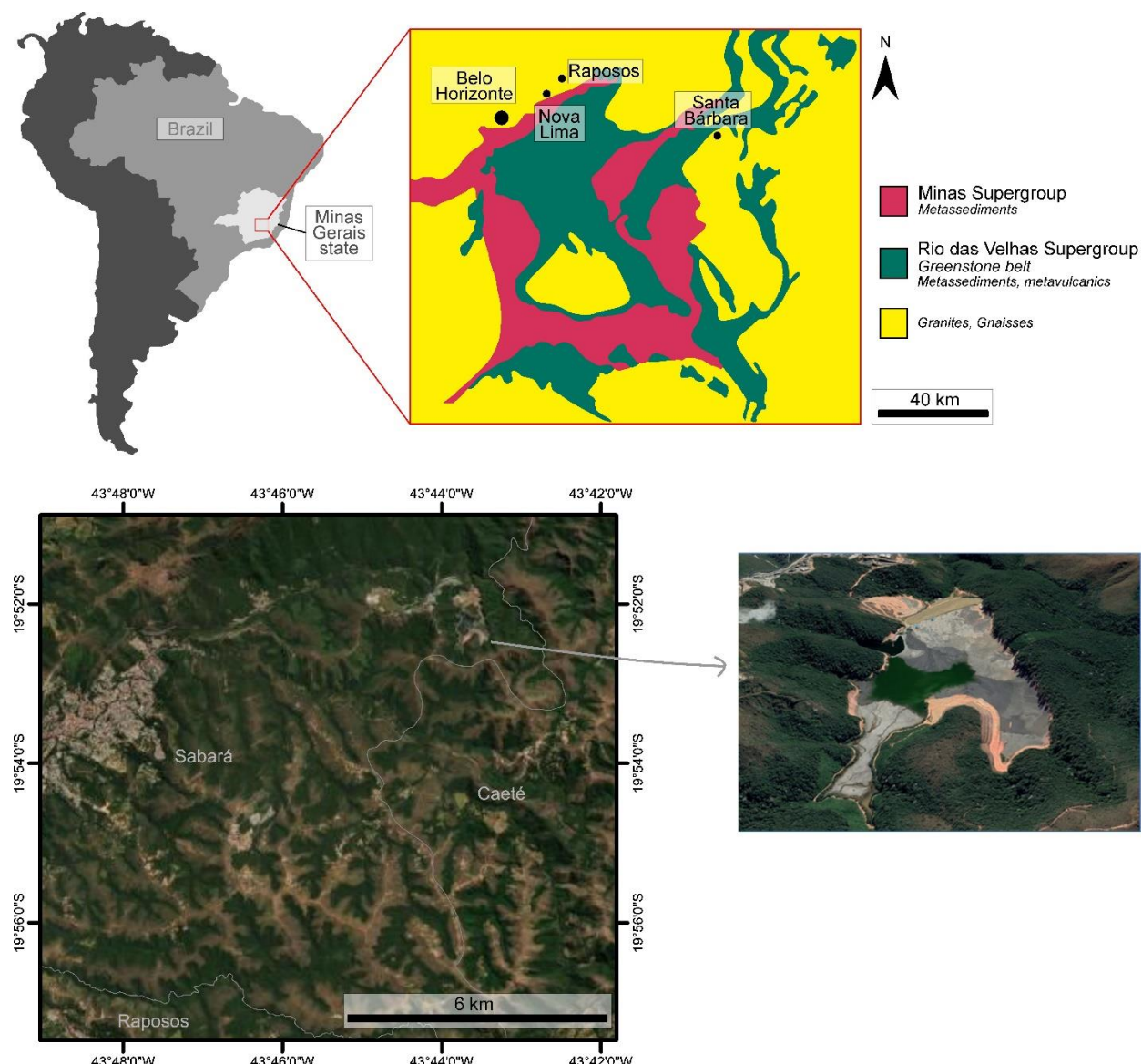


Figura 3.5. Localização área em estudo de Sabará.

As barragens e depósitos de rejeitados desta região localizam-se na parte norte do QF, entre as cidades de Nova Lima e Raposos, além da cidade de Sabará, Minas Gerais, a 25 km de sua capital, Belo Horizonte (Figuras 3.4 e 3.5). A região possui clima quente e temperado, segundo a classificação Koppen (clima subtropical úmido). A precipitação média ronda os 1390 mm anuais, sendo o mês de Agosto o mais seco e o mês de Dezembro o de maior pluviosidade, quando apresenta uma média de 302 mm. Sua temperatura média é de 23,3°C, sendo janeiro o mês mais quente do ano e a menor temperatura anual é junho, com temperatura média de 17,6°C (IBGE, 2019).

3.1.2.1. Depósitos e barragens de Isolamento, Bicalho e Mina Velha

Os depósitos de Isolamento, Bicalho e Mina Velha receberam diversos tipos de rejeitados de plantas antigas de Au da região. Estima-se que rejeitados de plantas do século passado estejam aqui dispostos, representando processos de extração do Au antes da utilização de cianeto. Portanto, descrever o processo de extração com exatidão torna-se difícil (AGA, 2019). Na Tabela 3.1 são descritos historicamente os processos de beneficiamento, bem como, a recuperação de Au.

No depósito da Mina Velha (primeira planta em operação na cidade de Nova Lima), foram depositados rejeitados provenientes de recuperação gravimétrica (50% de recuperação de Au) e rejeitados dos processos de lixiviação por cianeto e precipitação por Zn. Os depósitos de Bicalho e Isolamento são representados por rejeitados beneficiados em gravimetria, flotação, lixiviação por cianeto e precipitação utilizando Zn (Tabela 3.1).

Tabela 3.1. Depósitos, formas de recuperação do Au e estimativas de tonelagem e teor.

Depósito	Ano	Recuperação de Au (%)	Método de extração	Toneladas (t)	Teor Au (mg/kg)	Teor As (mg/kg)	Teor S (%)
Mina Velha	1834-1930	50-80	Apenas gravidade e gravidade + CN + precipitação de Zn	315 000	4,06	8,87	6,61
Bicalho	1960-1980	93	Gravidade + flotação + CN + precipitação de Zn	240 500	1,83	3,7	7,63
Isolamento	1930-1945	90	Gravidade + flotação + CN + precipitação de Zn	500 000	4,93	8,07	9,06

3.1.2.2. Depósitos e barragens de Queiroz e Cuiabá

A planta de Queiroz trata minérios de Au sulfetados há mais de trinta anos. Os materiais tratados na fábrica foram subdivididos em dois circuitos distintos. O circuito de Raposos (Figura 3.6.a), planta que tratava minério de sulfeto não refratário (pirita, pirrotita e arsenopirita subordinada) oriundo principalmente das minas de Raposos. O circuito atingiu 90% de recuperação de Au e foi dividido em moagem, concentração de gravidade, lixiviação convencional e CIP (*carbon in pulp*), eluição e eletrorrecuperação. Esta parte da planta foi

desativada em 1998 com o encerramento da mina subterrânea de Raposos (Moura, 2005; AGA, 2016).

O circuito Cuiabá (Figura 3.6.b) trata minério refratário (Au encerrado principalmente em pirita) com 92% de recuperação de Au e foi dividido em moagem, concentração de gravidade, flotação de sulfeto, torra, neutralização, lixiviação calcinada, CIP, eluição e eletrodeposição (Moura, 2005). Atualmente, na planta de Queiroz, o material é tratado desde a etapa de calcinação (Figura 3.6), já que as etapas anteriores são realizadas diretamente na planta localizada na mina Cuiabá em Sabará, próxima a Nova Lima, Minas Gerais. Os rejeitados dos circuitos de flotação de Raposos e Cuiabá foram depositados em uma barragem, já desativada, batizada de Cocoruto (Figura 3.6). O rejeito do circuito atual (calcinada e lixiviação) está disponível em uma barragem conhecida como “Calcinada” e os rejeitados atuais da flotação em outra barragem denominada Cuiaba (Figura 3.6).

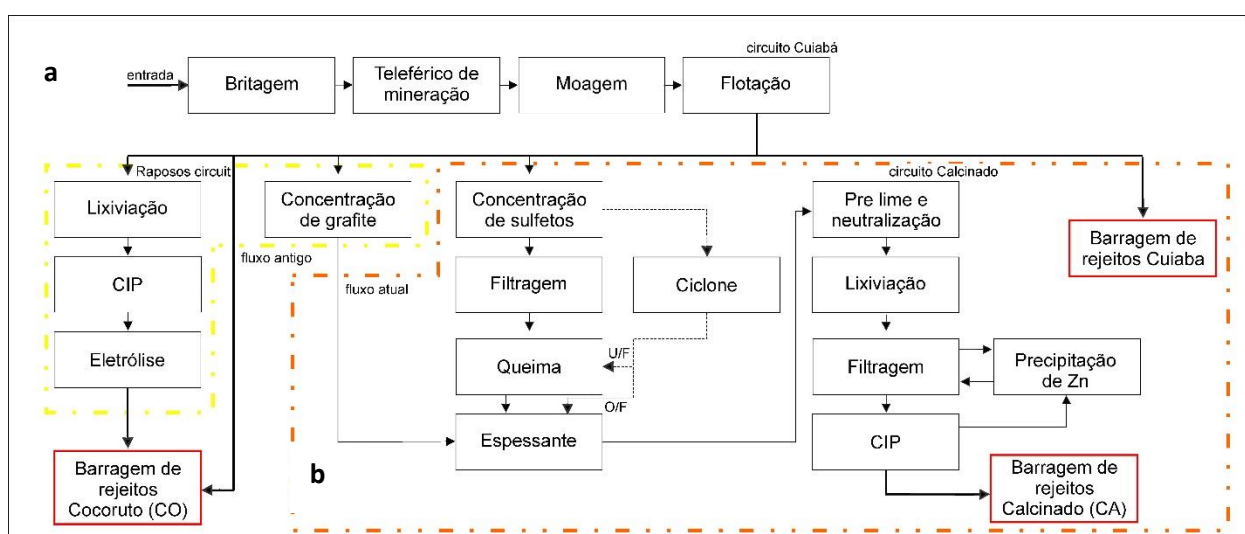


Figura 3.6. a) Fluxograma de extração de Au desativado e b) atual.

As estruturas são do tipo *downstream*, monitoradas e declaradas seguras de acordo com a agência nacional de mineração (ANM, 2023).

3.2. Barragem de Rejeitados localizados em Goiás

A Barragem de Crixás localiza-se a noroeste do estado de Goiás, na cidade de Crixás. Este distrito aurífero, contém a sexta maior reserva de minério de Au do Brasil e é o único depósito na região central (Castoldi, 2015).

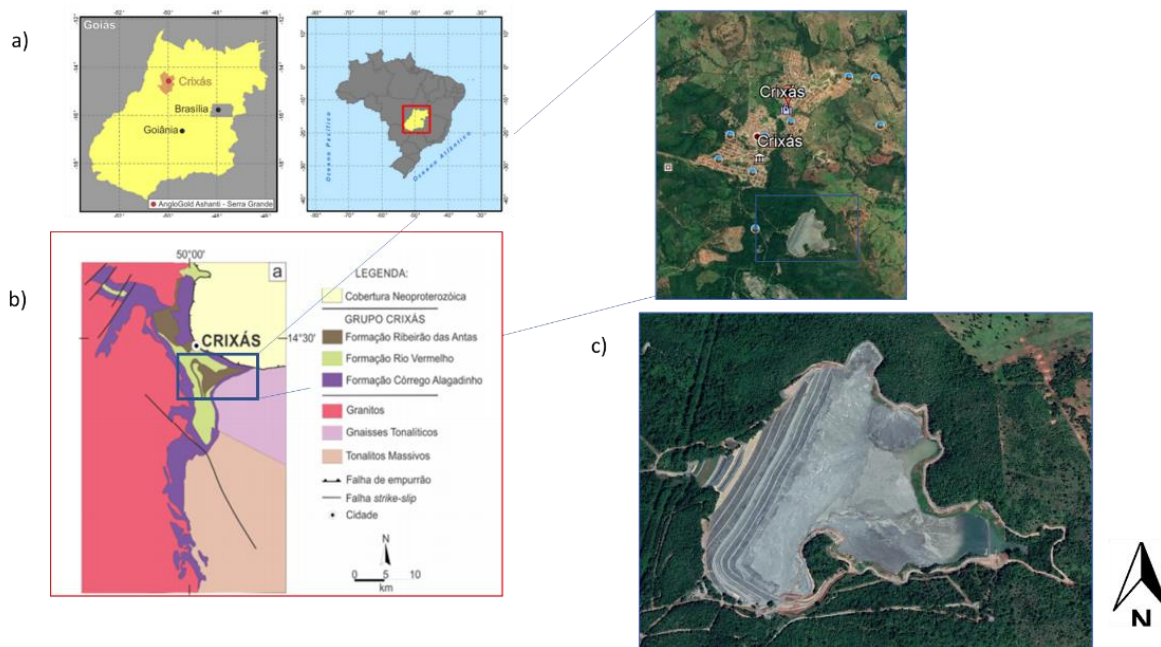


Figura 3.7. a) Localização da área de estudo em Goiás, b) mapa geológico da região de Crixás e c) Barragem de rejeitados de Crixás.

A mina de Crixás (Figura 3.7.) é atualmente lavrada em minas subterrâneas hospedadas no *greenstone belt* de Crixás. Este caracteriza-se por uma sequência vulcâno-sedimentar e com três tipos de mineralização principais: sulfeto maciço (arsenopirita e pirita), Au em veios de quartzo e sulfetos disseminados (Jost & Fortes, 2001; Castoldi, 2015).

A atividade da mina iniciou-se em 1989. O minério sulfetado é britado, moído, classificado gravimetricamente, lixiviado com cianeto em tanques e precipitado com Zn (Leite, 2016). Portanto, a produção final de Au é proveniente de dois circuitos paralelos: precipitado e densitário. Ambos são destinados a fundição (Figura 3.8). Atualmente, as recuperações da extração de Au atingem 95%. O rejeito deste processo, é depositado em uma barragem *upstream* com capacidade de 16m³ de material com teor médio de Au igual a 0.3 g/t.

Em Crixás, durante o ano inteiro, o clima é quente. Ao longo do ano, em geral a temperatura varia entre 17 °C e 37 °C e raramente é inferior a 15 °C ou superior a 40 °C (IBGE, 2019). De acordo com a classificação Köppen-Geiger, tem-se um clima de savana, com pluviosidade média anual de 1677 mm.

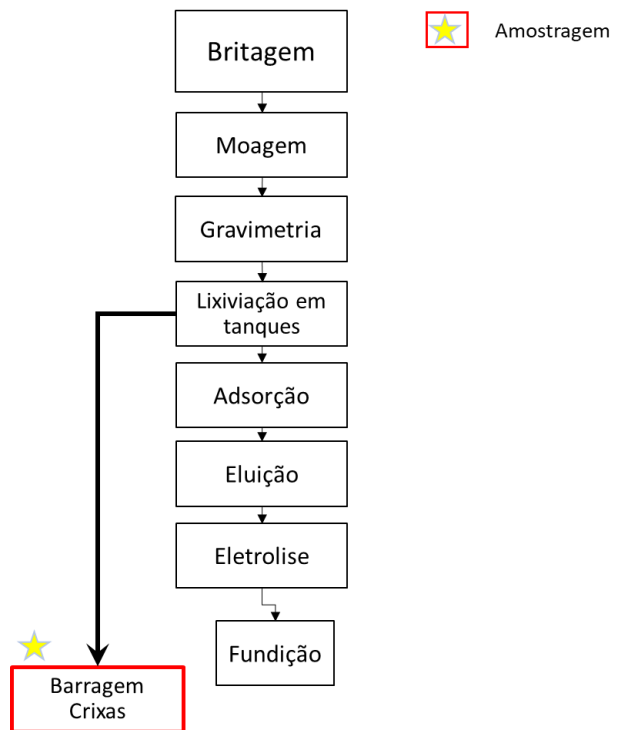


Figura 3.8. Fluxograma de extração de Au de Crixás.

Capítulo 4

Metodologia

4. Metodologia

Neste capítulo apresentam-se os principais métodos e técnicas que suportam a amostragem e os procedimentos para obtenção e tratamento de resultados. Depois, em cada publicação resultante do presente trabalho (artigos do capítulo 5), descreve-se a metodologia específica.

No fluxograma da Figura 4.1. descrevem-se as principais etapas da abordagem metodológica geral.

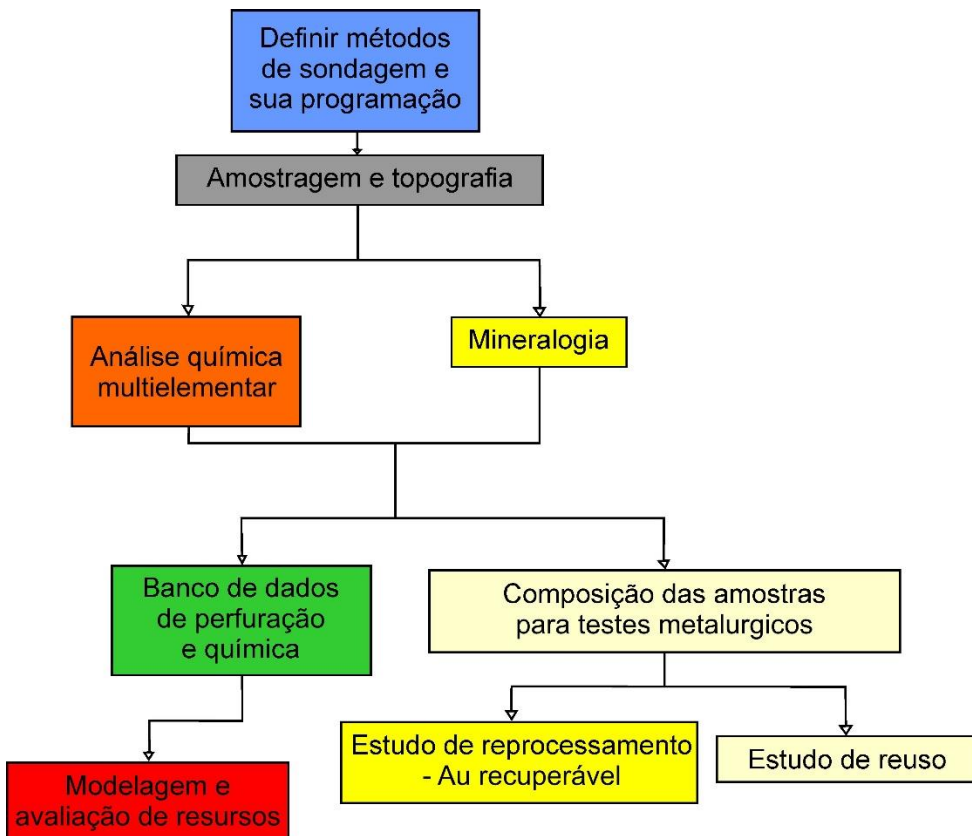


Figura 4.1. Metodologia aplicada ao estudo dos resíduos mineiros.

De uma maneira geral, as etapas de trabalho consistiram em:

- Definição da metodologia de recolha de amostras em cada depósito;
- Amostragem dos depósitos e levantamento da posição exacta de cada ponto amostrado de fase líquidas e sólidas;
- Caracterização física, geoquímica e mineralógica das amostras líquidas e sólidas;
- Montagem de uma base de dados contendo o levantamento e as características de cada amostra;
- Modelação 3D e análise geoestatística das informações obtidas por amostragem;

- f) Composição das amostras após modelagem 3D para ensaios metalúrgicos e;
- g) Estudo do potencial de extração de Au e reaproveitamento dos rejeitos em sua totalidade.

Para além destas etapas gerais, definiu-se o modelo econômico e realizou-se o estudo da viabilidade do reprocessamento do Au para um caso de estudo (Cocoruto).

No caso das barragens de Goiás, apenas foram realizadas as etapas c, d, f e g.

4.1. Amostragem

A campanha de amostragem foi realizada no inverno e início da primavera (Maio a setembro de 2020), época em que as condições climáticas variam muito. Normalmente, durante estes meses é comum alternar entre períodos secos e pouco úmidos, com temperaturas entre 15°C e 25°C (IBGE, 2019). A amostragem foi dependente do tipo de depósito e abrangeu métodos de sondagem por percussão, *direct push* e trado. Esta foi realizada até um máximo de 20 m, totalizando 2342 metros amostrados. Na Tabela 4.1. são expostos os métodos e profundidades médias de acordo com cada depósito de resíduos. A malha de sondagem variou de acordo com a estrutura amostrada. Em média, a distância entre os furos foi de 10 a 50 metros (Figura 4.2).

Tabela 4.1. Método de Amostragem por Depósito de Resíduo.

Estrutura	Tipo	Metros sondagem (m)	Trado (m)	Recuperação (%)	Total (m)
CDS2	<i>direct push</i>	105	178.4	95.91	283.4
CDS1	Retro	179		86.67	179
Isolamento	Mista	257	13.4	67.00	270.02
Bicalho	SPT	112	8	54.86	119.75
Mina Velha	<i>direct push</i>	307		91.83	307.08
Cocoruto	<i>direct push</i>	251	34.7	95.15	285.7
Calcinados	<i>direct push</i>	226	11.5	88.99	237
MSG	Mista	660		42.17	660
		2096	246		2342

As amostras foram coletadas a cada metro avançado (Figura 4.3), já que ocorreram intervalos não recuperados. Além do resíduo sólido, a água de porosidade das estruturas onde os rejeitados são armazenados em polpa, também foi coletada. Neste caso representam duas barragens da planta de Queiroz (Calcinados e Corouto) e uma da planta de Santa Barbara (CDS2). As amostras em polpas foram pesadas e encaminhas para laboratório, as quais foram filtradas a vácuo. As partes sólidas e líquidas foram enviadas para análise, cujo métodos serão discutidos no item a seguir. Para barragem de Crixás foi considerada apenas a parte sólida dos testemunhos de sondagem coletados, além de uma malha maior em relação às demais. O contexto pandémico determinou restrições de acesso ao local ocasionando menor número de amostras. .

Todas as amostras foram imediatamente lacradas e refrigeradas até a análise. O material adicional foi transferido para sacos de polipropileno e congelados até a análise. Amostras refrigeradas e congeladas foram embaladas e enviadas ao laboratório químico para análise.

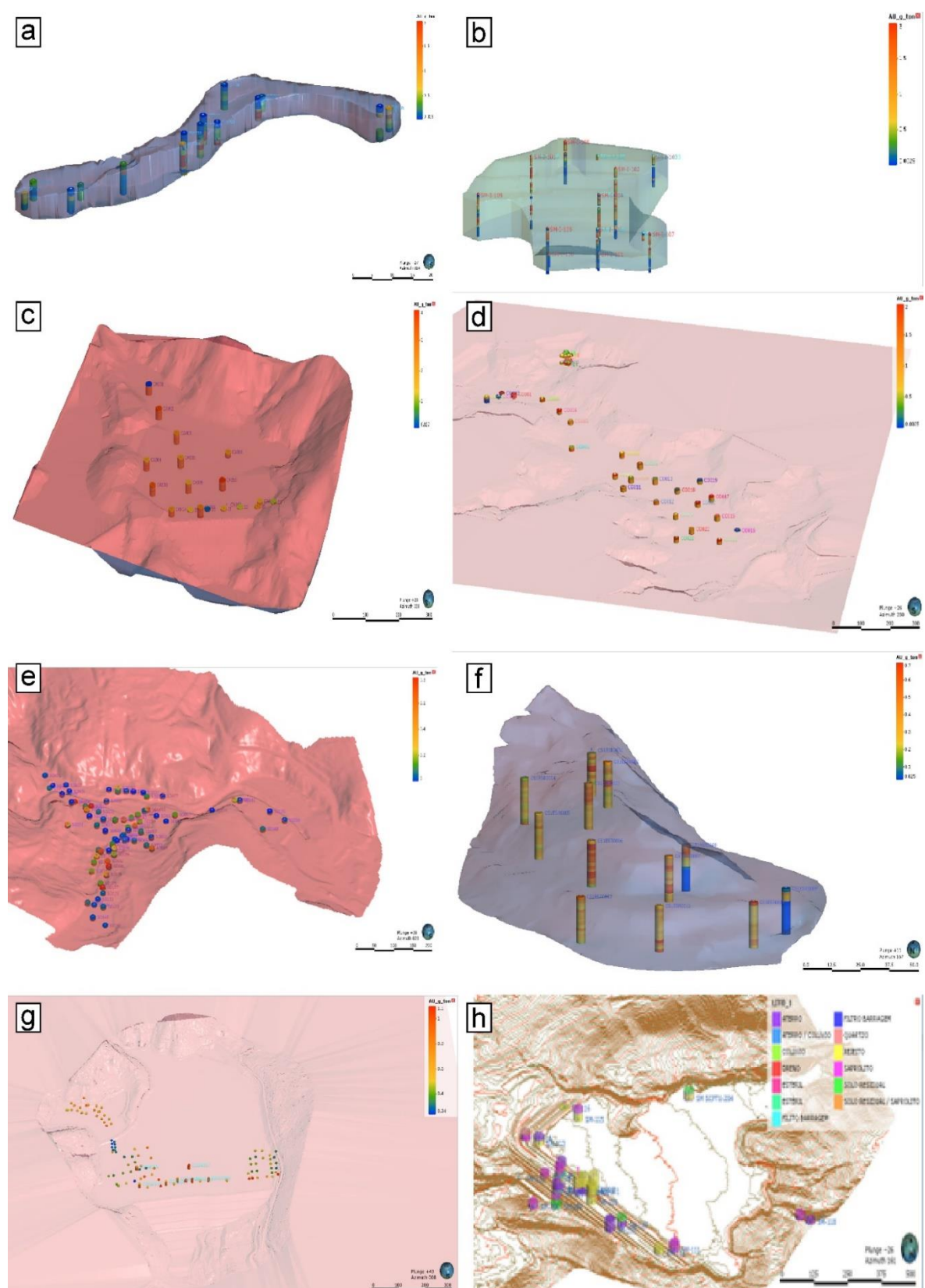


Figura 4.2. Imagens das amostras coletadas e programadas das áreas de estudo. a) Bicalho (leapfrog), b) Isolamento (leapfrog), c) Calcinados (leapfrog), d) Cocoruto (leapfrog), e) Mina Velha (leapfrog), f) Barragem de Santa Barbara (leapfrog), g) Pilha Santa.

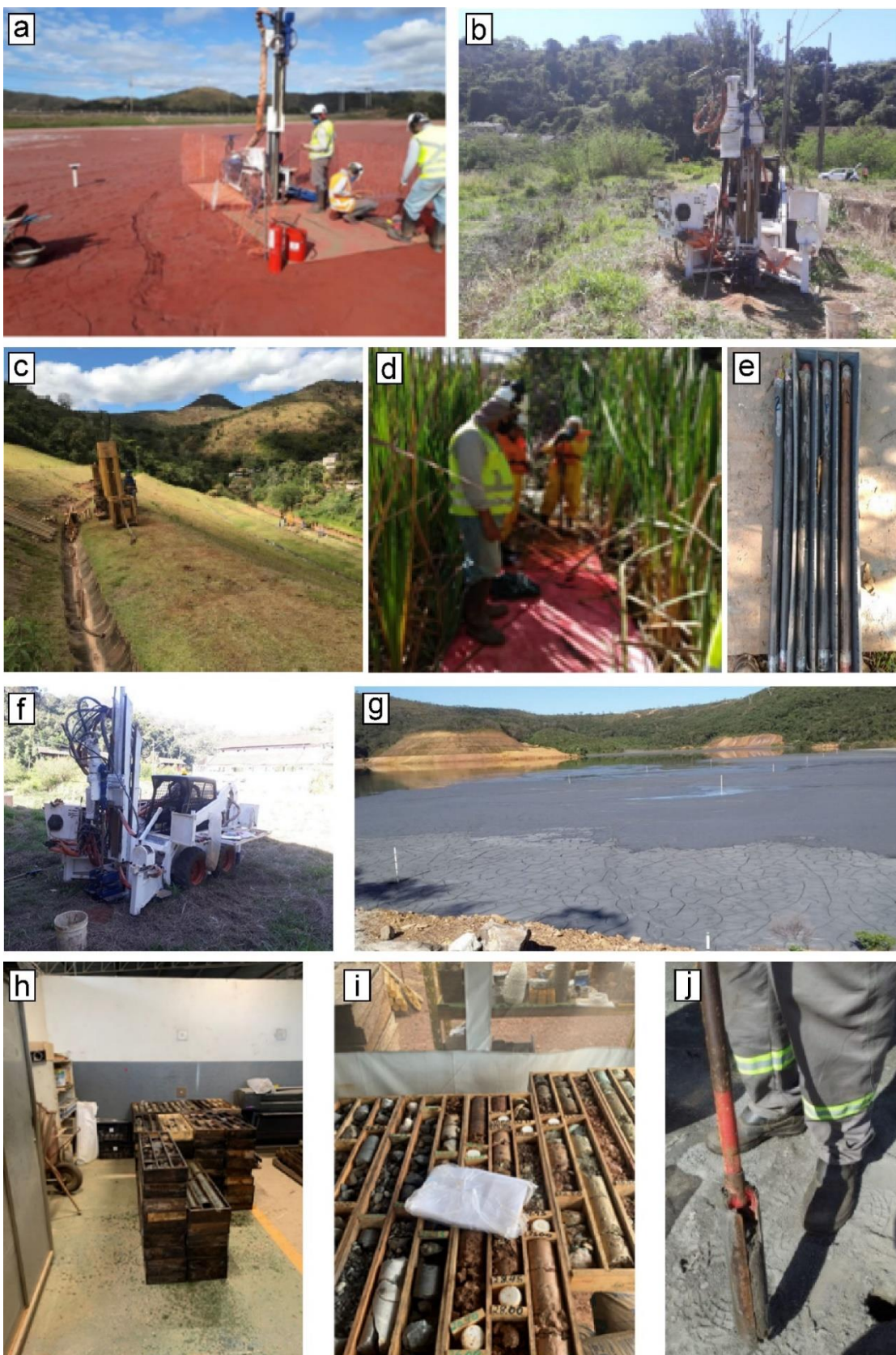


Figura 4.3. Imagens das coletas efetuadas nas áreas de estudo. a) Calcinados, b, f) Mina Velha, c) Isolamento, d,e) Coleta Cocoruto, h,j) Barragem Santa Barbara, i) Barragem Goiás, f, g) Etapa de amostragem dos testemunhos da sondagem.

As densidades das amostras foram obtidas daquelas com 100% de recuperação dentro do cilindro amostrador de volume conhecido. Após a ponderação, a densidade foi calculada e adicionada ao banco de dados (Blake & Hartge, 1986).

4.2. Ensaios Laboratoriais

4.2.1. Água de Porosidade

Os ensaios dedicados às águas e porosidade realizaram-se para amostras colhidas em estruturas do tipo barragem, especificamente: Calcinados, Cocoruto e CDS2.

Durante a etapa de sondagem, as amostras foram filtradas a vácuo e posteriormente em filtro 0.20 µm para obtenção dos teores totais dos elementos Au, Cd, Hg, Mn, Zn, Pb, Fe, Cu, Ni, As, Sb e sulfato. Para análise de metais e metalóides, aliquotas de 50-100 mL foram armazenadas em frascos de polipropileno, acidificadas a pH<2 e mantidas a temperaturas < 5 °C até ao momento da análise.

Em laboratório, parâmetros como o pH e condutividade elétrica foram obtidos utilizando metodologias do *Standard Methods of Water and WasteWater Wastewater* (APHA, 2005).

O cianeto *Wad* (CN *Wad*) é um grupo de espécies de cianeto que são definidas operacionalmente e liberam cianeto livre quando refluído sob condições fracamente ácidas (pH 4.5-6). Esses parâmetros também são definidos nos Métodos Padrão de Água e Efluentes. Elementos como Au, As, Fe, Cd, Sb, Mn, Ni, Pb, Zn, Hg foram analisados por espectrometria de massas com plasma indutivamente acoplado (ICP-MS) para ambas as frações (solida e líquida).

4.2.2. Resíduo Sólido

4.2.2.1. Análise Química

A composição química foi adquirida por espectrometria de massa de plasma indutivamente acoplado (ICP-MS, PerkinElmer SCIEX, Waltham, Massachusetts, EUA - limite de detecção 0,001 mg/kg) após digestão ácida (ácido nítrico, peróxido de hidrogênio e ácido clorídrico) no laboratório da AGA e *Société Générale de Surveillance* (SGS) no Brasil. Foram analisados 24 elementos.

As análises de Au foram realizadas por espectroscopia de absorção atômica (AAS, Varian, Palo Alto, Califórnia, EUA - limite de detecção de 0,05 mg/kg), usando o método *fireassay*.

Os teores de S e C foram obtidos via infravermelho (LECO, St Joseph, Michigan, EUA, limite detecção de 0.01%). Para garantir a qualidade e exatidão das análises, réplicas, brancos e materiais de referência padrão (Si81 da Rocklabs) foram incluídos.

4.2.2.2. *Granulometria a laser*

A distribuição granulométrica (PSD) foi obtida utilizando-se o equipamento MasterSizer 3000 (Malvern Instruments Ltd., Worcestershire, UK). Os resultados da PSD foram categorizados em seguintes gamas: <2 µm para a fração lama, 2–20 µm para o silte fino, 20–63 µm para o silte grosso e 63–2000 µm para a fração areia.

4.2.2.3. *Mineralogia*

Amostras compostas para alimentar os ensaios de reuso e reaproveitamento foram submetidas a um estudo mineralógico empregando várias tecnologias, incluindo microscopia óptica, difração de raios X (DRX) e microscopia eletrônica de varredura (SEM), realizados na Universidade Federal de Minas Gerais (Belo Horizonte, Brasil) e na Universidade do Minho (Braga, Portugal).

4.2.2.4. *Microscopia Ótica*

Microscopia Óptica de Luz Polarizada é o ponto de partida para praticamente todos os demais métodos analíticos. Seções e lâminas delgadas polidas foram analisados usando um microscópio óptico Leica DM 4500 P LED um conjunto de lentes para ampliação das imagens e uma parte mecânica para sustentar o sistema óptico e realizar a focalização, fornecendo ampliações de 50 a 500 vezes, com resolução de cerca de 1 µm. Foram avaliadas 50 lâmina polidas em total para todas as estruturas.

4.2.2.5. *Difração de Raios X*

A composição mineralógica foi determinada usando análise de DRX com um difratômetro X'pert Pro-MPD (Philips PW 1710, APD), usando radiação CuK α , e equipado com fenda de divergência automática e monocromador de grafite. Os difratogramas foram obtidos a partir da fração em pó <2 mm, cobrindo uma faixa de 3 a 65° 2θ com um tamanho de passo de 2θ de 0,02° e um tempo de contagem de 1,25 s, conforme procedimento descrito por Whittig & Allardice (1986).

A semi-quantificação da mineralogia presente fez-se usando a intensidade dos picos diagnósticos, como por exemplo para o quartzo (3.34 Å); mica (10 Å); Feldspato- K (3.24 Å); plagioclásio (3.18-3.20 Å); goetita (4.18-4.20 Å) e minerais de argila (4.43-4.49 Å).

4.2.2.6. *Microscopia eletrônica por varredura*

A mineralogia das amostras foi obtida por microscopia eletrônica de varredura (*Scanning Electron Microscopy – SEM-FEI quanta 200*) acoplada a um espectrômetro de energia dispersiva (EDS) e software analisador de liberação mineral (MLA-FEI). Para a produção do banco de dados dos equipamentos de MLA, as principais fases foram analisadas utilizando-se uma microssonda Jeol JXA 8900RL WDS/EDX. Os espectros obtidos por varredura por comprimento de onda (WDS) entraram no software MLA para calibração e posterior análise automatizada. Durante a análise automatizada dos dados obtidos, dois modos foram utilizados: mapeamento de raios X baseado em grãos (GXMAP) para coletar informações modais e liberação de fase esparsa (SPLDZ) para coletar informações relacionadas aos minerais portadores de Au55.

O software Dataview v 3.1.4.686 foi utilizado para processar os dados de MLA, pois permite analisar dados mineralógicos quantitativos obtidos através do software de medição de MLA. Os dados de pixel são combinados com a composição química e densidade dos minerais identificados, permitindo várias análises como a mineralogia modal (Fandrich et al., 2007).

4.3. Modelamento 3D e Análises estatísticas

4.3.1. Análise Estatística

A análise de componentes principais (ACP) foi realizada em 19 variáveis geoquímicas para amostras de sólidos para identificar as associações dos elementos. A ACP é uma técnica estatística amplamente utilizada para reduzir a dimensionalidade do conjunto de dados, diminuindo o número de variáveis por meio da transformação de variáveis altamente correlacionadas num conjunto menor de variáveis não correlacionadas, os componentes principais explicando a variabilidade dos dados com o menor número de componentes principais. As variáveis transformadas, referentes aos componentes principais, são uma função linear daquelas do conjunto de dados original (Jolliffe & Cadima, 2016; Reis et al., 2018; González-Díaz et al., 2022). Todas as análises foram realizadas no software logastm-Reflex-64.v7.2.1.

Em complemento à ACP, foi realizada uma análise estatística multivariada utilizando o método de agrupamento, combinando ligação completa e distância euclidiana (Hastie et al.,

2009). Parâmetros físico-químicos das amostras foram empregados para esta análise, gerando um dendrograma. Quatro parâmetros principais foram identificados para a análise dos grupos observados: (1) Avaliação da mineralogia principal e seu agrupamento com base no potencial de reutilização; (2) identificação de contaminantes com alto nível de risco crítico e contaminação; (3) análise do tamanho das partículas; e (4) avaliação do conteúdo de Au. Essa análise permitiu uma abordagem mais direcionada na seleção de amostras para testes laboratoriais com base em seu potencial de reutilização. Esta análise foi realizada utilizando o Minitab Statistical Software versão 21.1.0.

4.3.2. Modelamento 3D

Uma vez preenchido o banco de dados, foram aplicadas ferramentas geoestatísticas para analisar a distribuição dos elementos de interesse econômico e dos contaminantes.

Para amostras de sólidos, foram utilizados modelos de blocos 3D com célula de discretização de $5\text{ m} \times 5\text{ m} \times 1\text{ m}$ (Wilson et al., 2021; González-Díaz et al., 2022; Soto et al., 2022). A análise compreendeu a avaliação dos erros amostrais, nomeadamente eficiência de recuperação da amostra, remoção de outliers para evitar a superestimação dos modelos (*capping*), resumo estatístico, estimação e validação (Figura 4.4). A topografia dos depósitos foi utilizada para definir os limites da área a ser modelada. Os dados topográficos utilizados para a modelagem 3D foram obtidos usando o método da estação total. A posição inicial (0 m de profundidade) de todas as amostras também foi obtida por este método. O uso da topografia de superfície na modelagem é importante, pois influencia os cálculos do volume de material depositado ou empilhado, além de ser uma ferramenta necessária para a estabilidade física em operações futuras (Parviainen et al., 2020; González-Díaz et al., 2022).

Os volumes foram definidos pelo limite topográfico e pela densidade das amostras (ver item 4.1.Amostragem). Os dados de densidade foram interpolados por krigagem em blocos, e cada bloco apresentou seu valor de densidade. Dessa forma, foi possível calcular o volume do modelo. O método foi utilizado para todos os depósitos de rejeitos.

Todos os dados foram processados usando o *software* Leapfrog v2021.1 e Datamine Studio RM.

Para definir os padrões espaciais de variação das concentrações de Au nos depósitos de rejeitos, foram obtidos mapas geoquímicos através de krigagem ordinária (Journel, 1986; Reis et al., 2009; Ansah-sam et al., 2015; Tripodi et al., 2019; González-Díaz et al., 2022) para os volumes

previamente definidos. A identificação de padrões espaciais de Au foi fundamental para identificar áreas de alto teor. O variograma omnidirecional calculado para as variáveis geoquímicas foi utilizado para obter os modelos de variabilidade espacial (Reis et al., 2009). O uso de variogramas com elipsóide omnidirecional deve-se à incerteza existente na localização das fontes de alimentação nas barragens e depósitos de rejeitos. Com base no modelo de continuidade espacial foi possível obter a distribuição espacial das concentrações de Au para cada área.

Para as águas de porosidade, obtiveram-se modelos de blocos 3D com tamanho de célula de discretização de 30 m × 30 m × 5 m (Rostami et al., 2019; Wilson et al., 2021; Lemos et al., 2023). Ao contrário do modelo com sólidos, nesta etapa os blocos são maiores devido à malha amostrada e o suporte amostrado. Foi utilizada uma ferramenta estatística denominada *Inverse Distance Weighting* (IDW), que é um dos métodos de interpolação amplamente utilizados na gestão de recursos hídricos (Wilson et al., 2021). A estimativa é baseada em locais conhecidos próximos, e os pesos atribuídos aos pontos de interpolação são inversamente proporcionais à sua distância do ponto de interpolação. Portanto, pontos mais próximos do ponto de interpolação têm pesos maiores do que pontos distantes, e vice-versa (Dehghani et al., 2009; Wilson et al., 2021). Nas áreas de estudo, um quinto peso de potência foi usado para limitar a influência de uma amostra em uma região distante e refinar a estimativa (Acosta et al., 2009).

Portanto, o processo de avaliação (Figura 4.4) englobou uma estatística descritiva (etapa descrita acima) que também incluiu avaliação das densidades e recuperação das amostras obtidas em campo, retirada de outliers para evitar sobreestimação dos modelos (*capping*), interpolação por krigagem ordinária (utilizado variograma omnidirecional) e validação. Também se assumiu utilizar a topografia limitante pela área amostradas tanto em elevação vertical como horizontal (Figura 4.5).

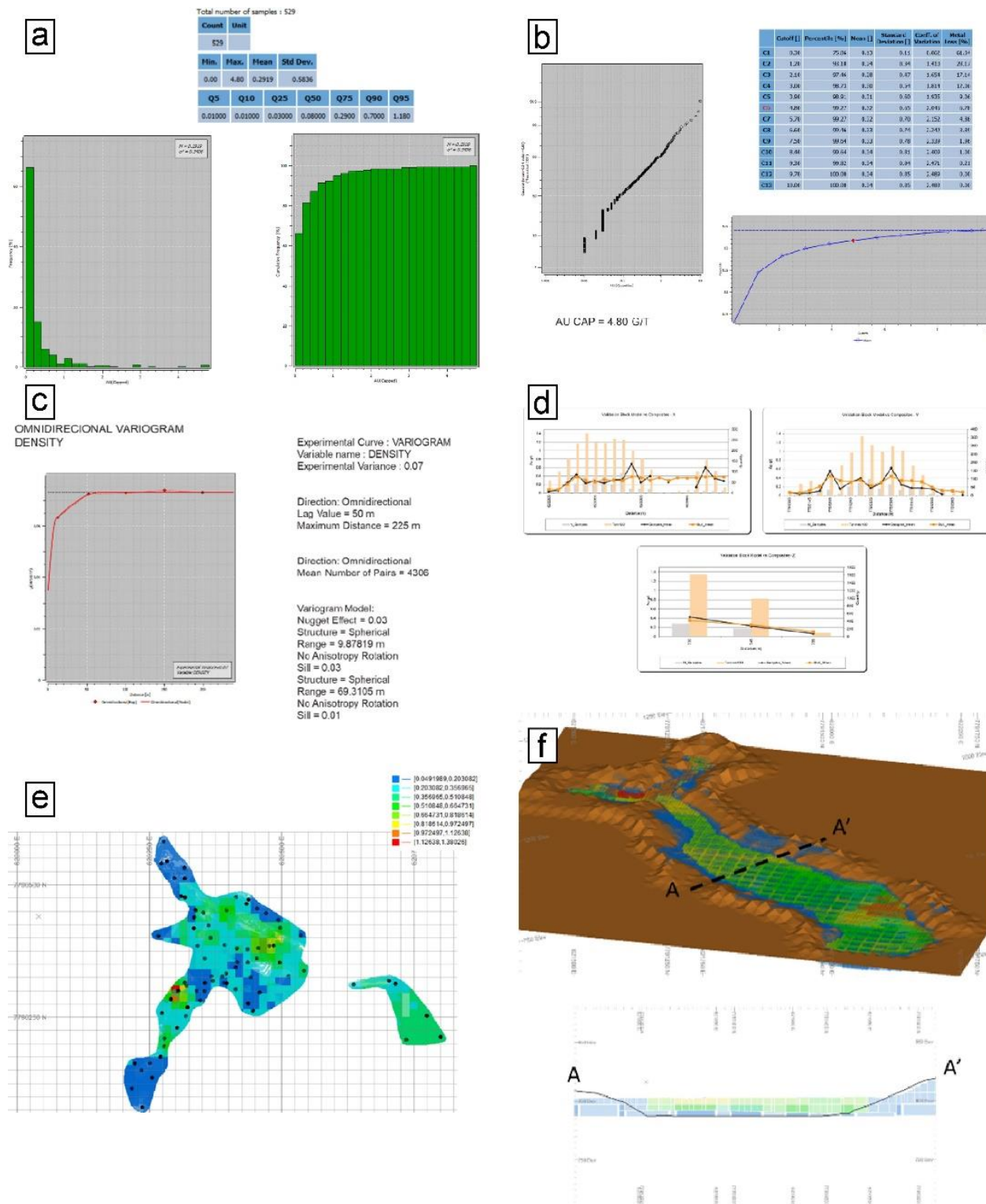


Figura 4.4. Etapa de estimativa do modelo de teores das estruturas. a) Avaliação do banco de dados, b) Retirada dos valores outliers (capping), c) Construção do variograma, d) Validação e e) Obtenção do modelo.

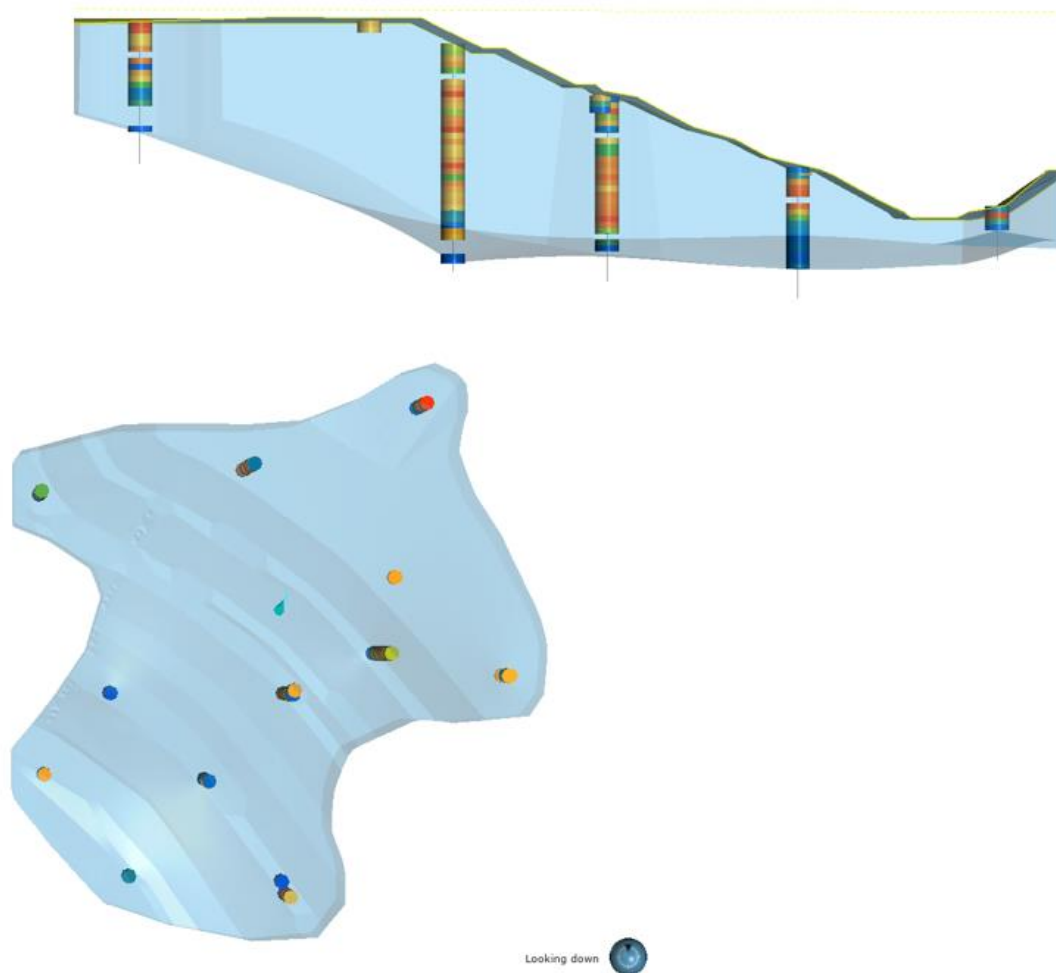


Figura 4.5. Etapa de definição da área a ser modelada.

4.4. Avaliação do Potencial de Valorização

Após a etapa de caracterização e modelamento, as amostras foram encaminhadas para estudo do potencial de valorização. Nesta etapa foram englobadas avaliações de reuso dos resíduos com âmbito no aproveitamento do Au e no reaproveitamento do resíduo como outras oportunidades.

4.4.1. Composição de Amostras para teste

Para os ensaios acima, foram levantadas amostras compostas de cada estrutura e baseadas na distribuição dos teores de Au vertical e horizontal da etapa de modelamento. Na Figura 4.6. exemplifica-se a definição das amostras compostas para os testes.

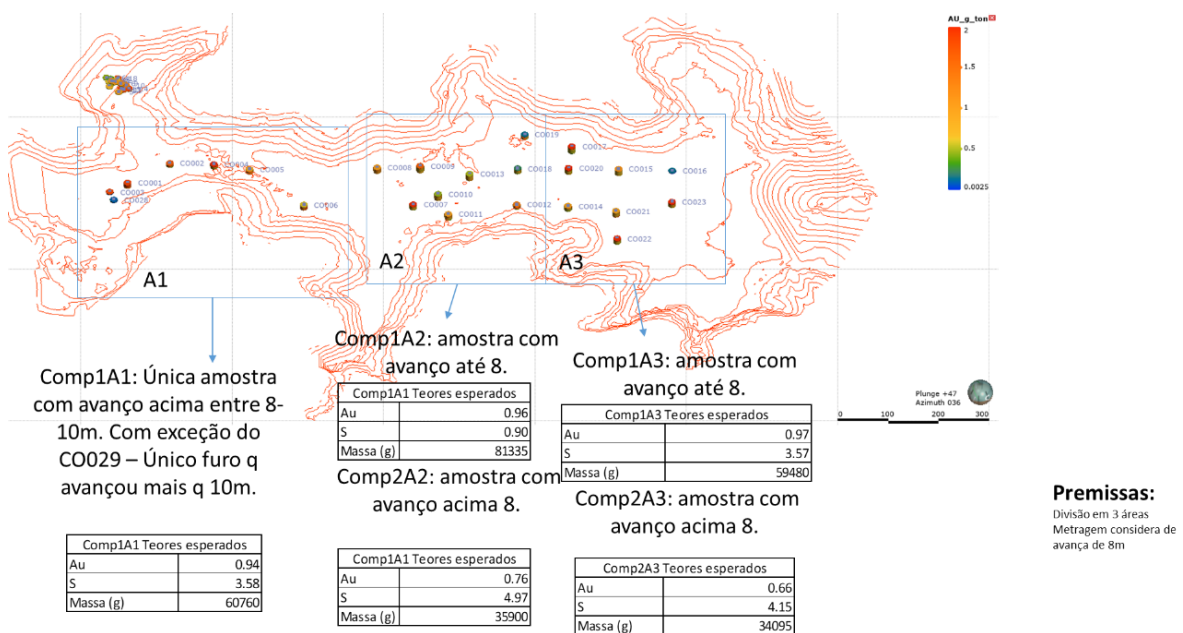


Figura 4.6. Exemplo de escolha das compostas de amostras para testes metalúrgicos para recuperação de Au.

4.4.2. Ensaios Metalúrgicos para Extração do Au

A partir da caracterização geoquímica e mineralógica, analisou-se o potencial de extração do Au para as amostras das estruturas caracterizadas. Portanto, foi proposto a análise de seis cenários de extração baseados nas características levantadas nos itens anteriores.

As amostras foram moídas para um tamanho de partícula de 74 µm e 20 µm, com 80% das partículas dentro desta faixa, após uma análise de liberação por tamanho para sulfetos e partículas de Au. A etapa de calcinação foi desconsiderada e as amostras foram diretamente submetidas à lixiviação (Figura 4.7). Para a extração de Au, os testes em garrafa foram realizados usando uma solução de lixiviação contendo 2000 mg/kg de cianeto (NaCN) e 4000 mg/kg de calcário (CaO), com uma relação sólido/líquido de 50%. Para as amostras de Crixás, foram executados os cenários 3 e 4, mas com 80% das partículas passantes em 106 µm.

Especificamente projetada para as características do resíduo na área de CDS2 (Figura 4.7), a amostra foi submetida à moagem até o tamanho de partícula de 74 µm usando um moinho de bolas, seguido de pré-concentração via flotação. Esta etapa de flotação envolveu duas fases (mais áspera e limpa), com a adição de 150 mg/kg de CuSO₄ para ativação de partículas, 30 mg/kg de coletores (xantato e difosfato de sódio – INT214) e 60 mg/kg de agente espumante mibcol. Este último também foi adicionado durante a etapa de fresagem. O concentrado resultante foi calcinado em mufla a 700°C para facilitar o acesso ao Au incluído nas partículas de sulfeto e,

posteriormente, lixiviado em um frasco com uma relação sólido/líquido de 50%, usando uma solução de lixiviação contendo 2000 mg/kg de NaCN e 4000 mg/kg de CaO. Os rejeitos mais rugosos e limpos foram combinados e submetidos à lixiviação nas mesmas condições do concentrado.

Os cenários 1 e 2 são configurados com etapa de calcinação em mufla a 700 °C. Para a extração de Au, o material calcinado foi colocado em frascos contendo solução com 40% de sólidos, contendo 2000 mg/kg de NaCN e 6000 mg/kg de CaO. O processo de extração ocorreu ao longo de 24 h, dividido em duas etapas com período de pré-ventilação de 2 h. Os resíduos desta etapa serão submetidos a testes para recuperação de As e Sb e novos produtos.

Na Figura 4.7. são especificados todos os cenários avaliados para recuperação do Au. Verifica-se que alguns cenários são específicos de alguns depósitos de rejeitados, devido características distintas de cada estrutura, como já explicados nos itens acima. Todos os ensaios foram realizados em escala de laboratório e englobam as etapas de moagem, lixiviação, flotação e calcinação. Os *setups* foram realizados conforme ilustra a Figura 4.7.

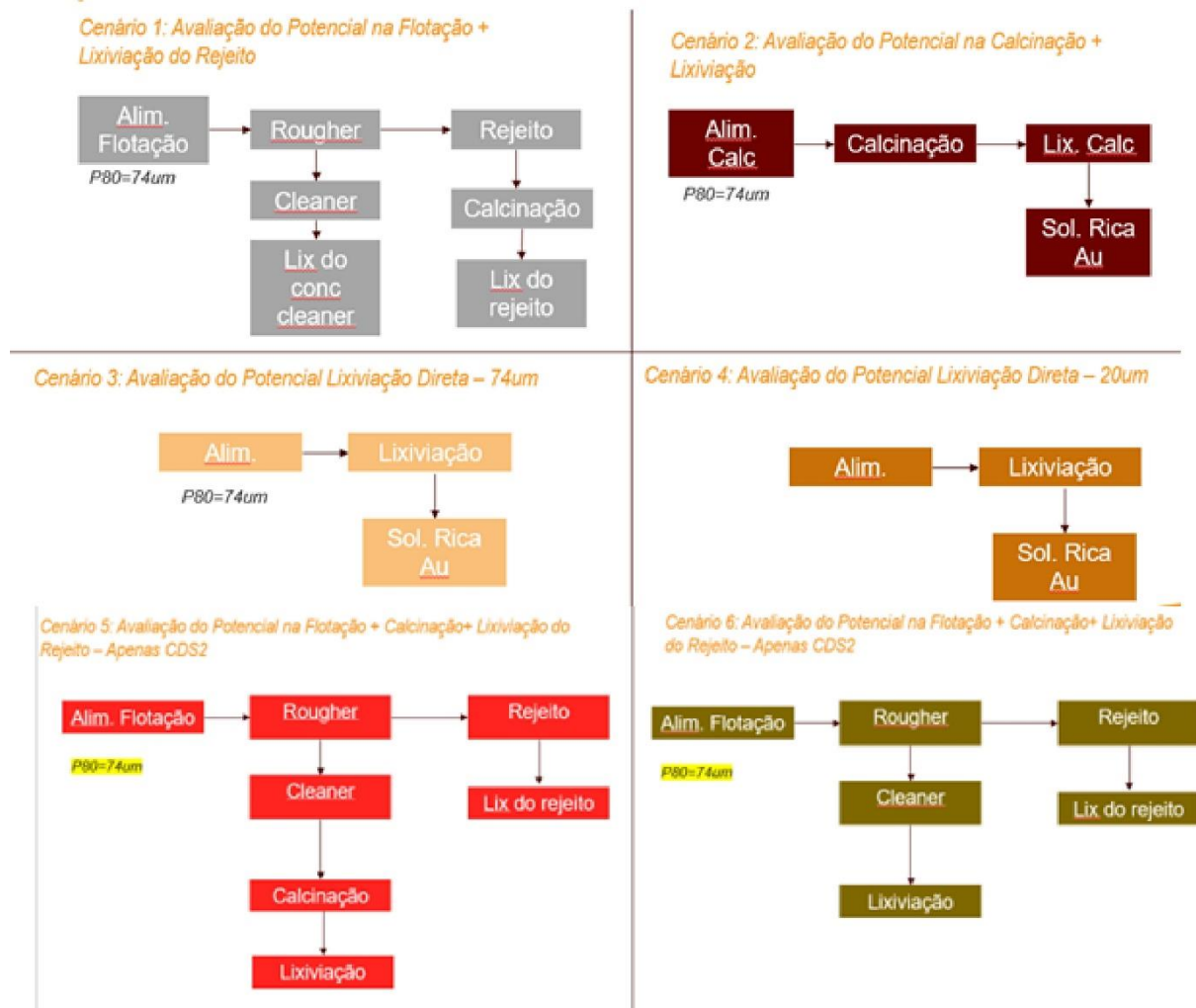


Figura 4.7. Fluxograma de trabalho para obtenção da recuperação de Au em laboratório escala de bancada para as amostras em estudo.

4.5. Valorização dos Resíduos – Outras Oportunidades

Os rejeitos obtidos na extração de Au, foram encaminhados para estudo do potencial reuso de As, Sb e produtos destinados à construção civil e entre outros.

4.5.1. Recuperação e estabilização de arsênio e antimônio

O objetivo do teste foi recuperar Sb e As termicamente, volatilizando-os e coletando-os a jusante como subprodutos óxidos. As amostras de resíduos foram submetidas a dois ensaios em klin de quartzo rotativo e horizontal, com temperatura final de 850°C, com duração de 6 h, e mistura gasosa de 20% de CO e 80% de N₂. O segundo teste foi realizado em duas fases, atingindo temperatura final de 930°C, com duração de 16 h, com 3% de O₂ e 97% de N₂ (Figura 4.8.).

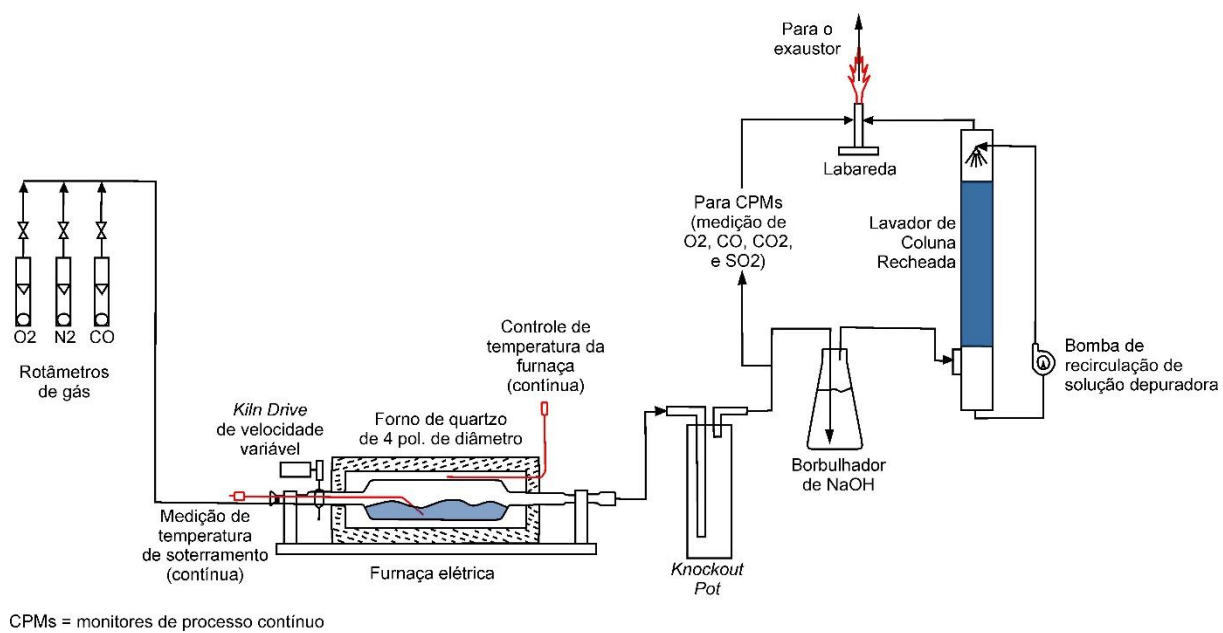


Figura 4.8. Potencial de extração de Sb e As em forno rotativo.

Outro experimento foi feito em um separador magnético úmido de alta intensidade (WHIMS). Na literatura, são descritos alguns casos de sucesso da aplicação dessa metodologia em rejeitos para recuperação de ferro, cobre e chumbo (Guest et al., 1988; Rao et al., 2016). O teste ocorreu em cinco etapas para reproduzir um concentrado de Sb de alto grau. Uma amostra de 200 g dos rejeitos sólidos foi processada usando uma unidade Eriez L4 WHIMS. Os rejeitos de cada separação foram reprocessados em intensidades magnéticas sucessivamente maiores (1.500–10.100 G).

Em relação à amostra com potencial de estabilização e reutilização, seguiu-se o protocolo delineado no processo de patente DST-s GlassLock™ (Lalancette et al., 2015). Esse processo envolveu a mistura das amostras de rejeito com sílica, hematita e carbonato de sódio, seguida de submissão a um forno em temperaturas variando de 1000°C a 1200°C e pressão atmosférica por duas horas. Este tratamento resultou em um produto de vidro contendo formas estáveis de óxidos, incluindo As e Sb (Figura 4.9.).

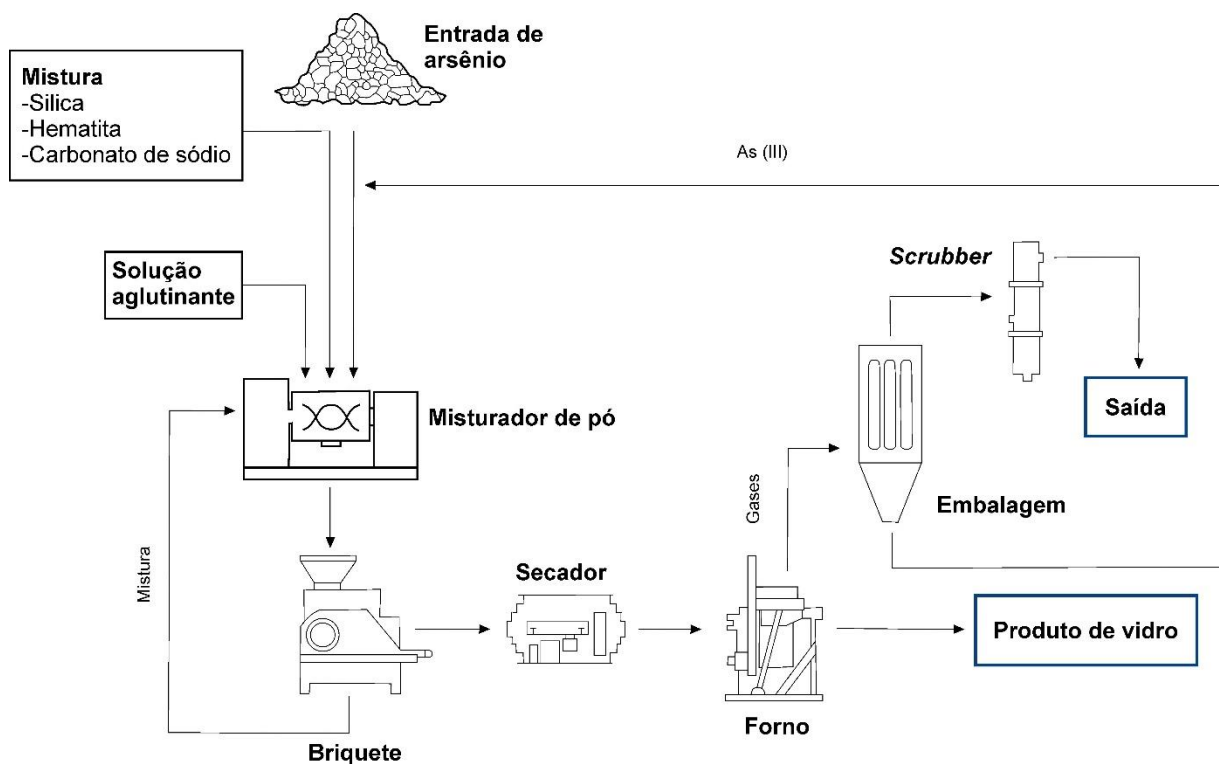


Figura 4.9. GlassLock™ (modificado de Dundee Sustainable Technologies, 2006; AGA, 2016)

4.5.2. Recuperação de minerais de ganga

A utilização da separação triboelectrostática tem demonstrado resultados promissores na produção de subprodutos a partir de rejeitos de Au (Cho et al., 2012). Além disso, as técnicas de moagem seletiva e concentração pneumática também são consideradas favoráveis para esse tipo de material, por serem processos de limpeza a seco com mínimos impactos ambientais (Ferguson, 2010). O objetivo da moagem seletiva e da separação pneumática é pulverizar minerais com dureza inferior a cinco na escala de Mohs e separar a fração menor que 8 µm para concentração. Assim, esses métodos permitem a geração de múltiplos produtos a partir de uma única fonte (Jordan et al., 1980; Emrullahoglu et al., 1993; Yang et al., 2022).

Portanto, após priorização das amostras, o método escolhido para avaliar o potencial de geração de produtos alternativos envolveu: (1) moagem em moinho pendular com gás quente a 450°C; (2) separação pneumática em três frações granulométricas (fina, menor que 8 µm; intermediária, 30–8 µm; e grosseira, maior que 30 µm); e (3) concentração triboelectrostática da fração fina (Figura 4.10). A separação por triboelectricidade refere-se à eletrificação de materiais devido ao contato e fricção entre eles. Quando dois materiais diferentes são postos em contato e depois separados, eles se carregam eletricamente. Um material se torna positivamente carregado,

enquanto o outro se torna negativamente carregado. As partículas carregadas são então atraídas para um eletrodo de carga oposta, permitindo a separação do material.

Consequentemente, três produtos potenciais foram gerados e analisados para investigar seu potencial de uso em indústrias civis e como fertilizantes, entre outras aplicações.

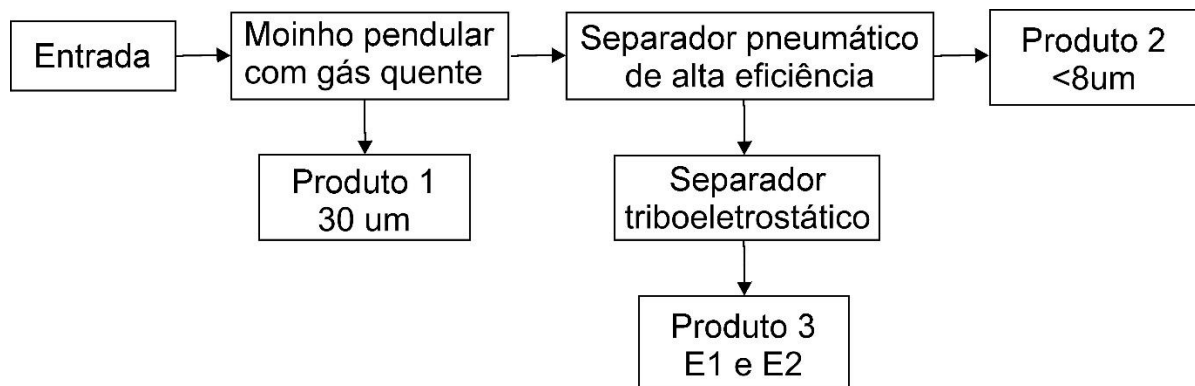


Figura 4.10. Fluxograma de teste para a geração de três potenciais produtos geradores de insumos nas indústrias civil, de fertilizantes e outras.

4.6. Cenário Função Benefício

Qualquer projeto tem uma variedade de atividades e processos envolvidos na produção com a intenção de reduzir custos e ao mesmo tempo agregar valor ao produto, gerando um benefício ou lucro (Changanane, 2017). Os principais elementos que formam a função benefício na atividade de reaproveitamento são identificados em receitas e custos. Os vários fatores que afetam os parâmetros da função benefício são detalhados na Figura 4.11.

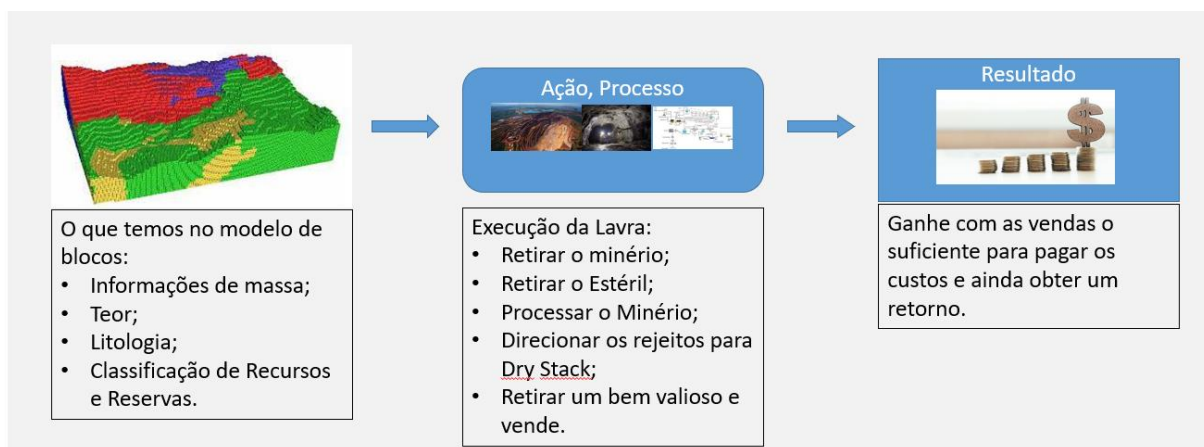


Figura 4.11. Etapas de processo para definição da função benefício de um empreendimento.

Neste contexto, descrevem-se aqui os fatores econômicos relacionados nos itens descritos acima fazendo uma análise de todos os aspectos envolvidos na determinação da função benefício do reaproveitamento dos resíduos, dado o conceito de planejamento que, segundo Costa (1979) citado por Curi (2014), é a progressão envolvendo a previsão dos meios necessários para a realização das operações e determinação dos custos inerentes a estas operações para reuso e reaproveitamento.

Para entendimento do possível retorno econômico dos resíduos estudado fez-se este exercício para o depósito de Cocoruto. Para o cálculo do NPV do projeto, foi aplicado a todos os cenários desenvolvidos a taxa de desconto de 8% anual. Para todos os cenários foi utilizado o ângulo geral de talude de 20º ou seja 36.4% (o ângulo de 11.31º ou 20% não gerou cava). Para a análise da sensibilidade usou-se três valores de dólar para a onças de Au extraídas. As cavas são otimizados para cada cenário usando o algoritmo de Lerchs-Grossmann (Lerchs & Grossmann, 1965). Posteriormente, foi realizada a otimização dos desenhos das cavas para cada cenário (CoL74, CoL20 e CoCal). A análise de sensibilidade foi conduzida considerando diferentes preços de Au de US\$ 1300, US\$ 1500 e US\$ 1700, bem como o tempo de mineração para cada cenário. Todos os estudos foram realizados utilizando o *software* Deswik Suite v5.1.

Capítulo 5

Resultados e discussões

5. Resultados e discussões

Apresentam-se neste capítulo os resultados obtidos. Compilam-se os dados referentes à região estudada – Quadrilátero Ferrífero (Estruturas de Nova Lima e Santa Barbara), cujas estruturas passaram por todo o fluxo de trabalho e, especificamente com foco na extração de Au, as estruturas de Crixás.

As áreas de estudo, Quadrilátero Ferrífero e Crixás, são ricas em história e potencial metalúrgico, tornando-as extremamente relevantes para investigações sobre a valorização dos resíduos gerados. Apresentam semelhanças por estarem em contextos geológico e metalúrgicos semelhantes, mas particularidades são descritas e inumeradas nas publicações a serem apresentadas a seguir.

Em relação as amostras estudadas no QF, os resultados foram alvo de publicação em revistas e atas de conferências indexadas em base de dados internacionais. Nestes casos optou-se por apresentar, como parte integrante do presente capítulo, o respetivo trabalho na forma original de publicação no (item 5.1).

Por sua vez, os resultados correspondentes à área de Crixás são apresentados no item 5.2.

Por fim, no item 5.3 discutem-se e avaliam-se as mais-valias socioambientais associadas ao trabalho realizado, nomeadamente os ganhos esperados na sequência dos potenciais formas de valorização dos resíduos identificadas.

Em síntese, o corpo deste capítulo é constituído principalmente por trabalhos, na sua maioria já publicados e dois em processo de revisão, terminando com uma proposta de modelo visando a valorização de resíduos de mineração.

5.1. Resultados Estruturas Localizadas na Região do Quadrilátero Ferrífero

Os resultados obtidos no contexto global para as barragens e depósitos localizados no QF, são apresentados tal como foram publicados. Para melhor compreensão, faz-se aqui um enquadramento sumário destes trabalhos, em português, evidenciando os seus objetivos e principais conclusões. O item está dividido em três temas principais, (i) caracterização, impactos ambientais, distribuição química e reuso dos resíduos sólidos, (ii) avaliação da qualidade das águas com seu potencial de reuso e (iii) por fim uma avaliação da viabilidade do reprocessamento de Au em um estudo de caso.

5.1.1. Resíduos sólidos - caracterização de amostras sólidas

O estudo do reuso de rejeitos de mineração é importante para promover a sustentabilidade ambiental, a conservação dos recursos naturais, a recuperação de materiais valiosos, a redução de passivos ambientais e o bem-estar das comunidades afetadas pela mineração. Considerando a tradição da região e sua relação com a mineração de Au, considera-se imperativo transformar os resíduos resultantes desta atividade histórica em recursos e, assim, contribuir para uma indústria de mineração mais responsável e sustentável associada a uma filosofia do tipo “*Environmental, Social and Governance*” (ESG).

Neste contexto, apresentam-se e discutem-se resultados de caracterização, seus impactos e potencial geração de drenagem ácida em duas barragens de rejeitos de Au localizadas em Nova Lima. No artigo intitulado *Mineralogical and Geochemical Characterization of Gold Mining Tailings and Their Potential to Generate Acid Mine Drainage (Minas Gerais, Brazil)* publicado na revista Minerals (<https://doi.org/10.3390/min11010039>) discute-se a necessidade de manejo e controle adequados das barragens de rejeitos, mesmo em ambientes de drenagem alcalina como o da barragem de Cocomoto. Além disso, mostra-se que um amplo conhecimento da dinâmica dos rejeitos em termos de geoquímica e mineralogia é fundamental para apoiar decisões de longo prazo sobre gerenciamento e disposição de resíduos. As características aqui abordadas dão ênfase ao contexto da EC e chamam a atenção para a responsabilidade socioambiental necessária para a gestão destes resíduos.

Adicionalmente aos resíduos sólidos acumulados, a lama arsenical, efluente do tratamento do minério de Au é também exposto em regiões próximas às barragens de Nova Lima. Portanto, com o objetivo de obter mais conhecimento sobre a diversidade de resíduos presentes na área de estudo, refere-se o trabalho apresentado no congresso da *International Mine Water Association (IMWA) congress 2021*. Dele consta uma caracterização robusta deste particular resíduo com intuído de gerar informações para a avaliação de rotas de reuso e estabilização de metais e metaloides como Fe e As. São identificados compostos neoformados durante o processo de beneficiamento do Au e as fontes destes contaminantes. Os compostos são em sua maioria sulfatos e óxidos contendo As, Fe, Ca, Al e carregam elementos fontes de toxicidade como o As. O trabalho *Characterization of Arsenical Mud from Effluent Treatment of Au Concentration Plants, Minas Gerais – Brazil*

(https://www.imwa.info/docs/imwa_2021/IMWA2021_Lemos_274.pdf) encontra-se na página 67.



Article

Mineralogical and Geochemical Characterization of Gold Mining Tailings and Their Potential to Generate Acid Mine Drainage (Minas Gerais, Brazil)

Mariana Lemos ^{1,2}, Teresa Valente ^{1,*}, Paula Marinho Reis ^{1,3}, Rita Fonseca ⁴, Itamar Delbem ⁵, Juliana Ventura ² and Marcus Magalhães ²



Citation: Lemos, M.; Valente, T.; Reis, P.M.; Fonseca, R.; Delbem, I.; Ventura, J.; Magalhães, M. Mineralogical and Geochemical Characterization of Gold Mining Tailings and Their Potential to Generate Acid Mine Drainage (Minas Gerais, Brazil).

Minerals 2021, 11, 39.

<https://doi.org/10.3390/min11010039>

Received: 5 December 2020

Accepted: 24 December 2020

Published: 31 December 2020

Publisher's Note: MDPI stays neutral with regard to jurisdictional claims in published maps and institutional affiliations.



Copyright: © 2020 by the authors. Licensee MDPI, Basel, Switzerland. This article is an open access article distributed under the terms and conditions of the Creative Commons Attribution (CC BY) license (<https://creativecommons.org/licenses/by/4.0/>).

¹ Institute of Earth Sciences, Pole of University of Universidade de Minho, Campus de Gualtar, Universidade do Minho, 4710-057 Braga, Portugal; id8548@alunos.uminho.pt or mglemos@anglogoldashanti.com.br (M.L.); pmarinho@dct.uminho.pt (P.M.R.)

² Anglogold Ashanti, Mining & Technical, COO International, Nova Lima 34000-000, Brazil; jdventura@AngloGoldAshanti.com.br (J.V.); mfmagalhaes@AngloGoldAshanti.com.br (M.M.)

³ GEOBIOTEC, Departamento de Geociências, Campus Universitário de Santiago, Universidade de Aveiro, 3810-193 Aveiro, Portugal

⁴ Institute of Earth Sciences, Pole of University of Évora, University of Évora, 7000-345 Évora, Portugal; rfonseca@uevora.pt

⁵ Microscopy Center, Universidade Federal de Minas Gerais, Belo Horizonte 31270-013, Brazil; ssgerais@microscopia.ufmg.br

* Correspondence: teresav@dct.uminho.pt

Abstract: For more than 30 years, sulfide gold ores were treated in metallurgical plants located in Nova Lima, Minas Gerais, Brazil, and accumulated in the Cocoruto tailings dam. Both flotation and leaching tailings from a deactivated circuit, as well as roasted and leaching tailings from an ongoing plant, were studied for their acid mine drainage potential and elements' mobility. Detailed characterization of both tailings types indicates the presence of fine-grain size material hosting substantial amounts of sulfides that exhibit distinct geochemical and mineralogical characteristics. The samples from the ongoing plant show high grades of Fe in the form of oxides, cyanide, and sulfates. Differently, samples from the old circuit have higher average concentrations of Al (0.88%), Ca (2.4%), Mg (0.96%), and Mn (0.17%), present as silicates and carbonates. These samples also show relics of preserved sulfides, such as pyrite and pyrrhotite. Concentrations of Zn, Cu, Au, and As are higher in the tailings of the ongoing circuit, while Cr and Hg stand out in the tailings of the deactivated circuit. Although the obtained results show that the sulfide wastes do not tend to generate acid mine drainage, leaching tests indicate the possibility of mobilization of toxic elements, namely As and Mn in the old circuit, and Sb, As, Fe, Ni, and Se in the tailings of the plant that still works. This work highlights the need for proper management and control of tailing dams even in alkaline drainage environments such as the one of the Cocoruto dam. Furthermore, strong knowledge of the tailings' dynamics in terms of geochemistry and mineralogy would be pivotal to support long-term decisions on wastes management and disposal.

Keywords: geochemistry and environmental mineralogy; tailings; mobility of toxic elements; acid mine drainage; Minas Gerais—Brazil

1. Introduction

Mining of metals throughout the world produces high volumes of wastes represented by different types of materials [1]. Although highly variable as a function of the characteristics of the ore deposit and the beneficiation processes, as an example [2] estimated around 50,000 Mt of wastes, with 33% of them in tailing dams. In plants for Au metallurgy, the ratio tailings/concentrate can achieve 200:1 [3]. In South Africa, one of the largest Au producing countries, [2] reported a production of 7.4×10^5 t of tailings from 1997 to 2006.

58

These waste materials are discharged in tailing dams and/or ditches in conditions that could be dangerous to the environment. Even though the tailings treatment and control processes use alkaline products [4], the main sources of Au are often associated with sulfides, such as pyrite (FeS_2), arsenopyrite (FeAsS), and pyrrhotite (Fe_{1-x}S). Deposition of these waste materials in subaerial storage facilities allows the oxidation of sulfides, which may promote the generation of acid mine drainage (AMD) [5–8] with the consequent mobilization of potentially toxic elements (PTE). Unregulated mining also deserves a special mention for its contribution to AMD pollution in regions with great influence of artisanal and small-scale mining operations [9,10].

In order to assure safe closure conditions, it is important to evaluate the AMD potential in the long term and understand the factors that may control the mobility of PTE. Several parameters, in addition to the presence of sulfides, can contribute to generation of AMD and contamination of the surrounding environment [11–15]. Tailings can have a wide variety of chemical and mineralogical compositions and can suffer geochemical evolution controlled not only by the original ore paragenesis, but also depending on the mineral processing techniques and weathering conditions [15]. Supergenetic evolution of the tailings results in a secondary paragenesis with high diversity of mineral phases, including soluble sulfates, oxides and iron oxyhydroxides, and arsenates, among others. These secondary minerals, occurring as efflorescences, crusts and other iron-rich precipitates, play important roles in the dynamics of the sulfide oxidation and in mobility of PTE in surface and groundwater [16–18]. Another important factor is the dimension of the tailing particles, as the relationship between size and exposure to weathering can directly influence the oxidation rate of sulfides [7,19].

In general, AMD develops when the neutralization capacity of carbonate minerals or alkaline reagents used in the mineral processing plants (as lime) is depleted due to ongoing sulfide-mineral oxidation. In addition to carbonates, or when they are absent, silicate minerals can provide some level of acid buffering [19–22]. Nevertheless, major and trace elements, such as Se and As can be leached from the tailing dams, contributing to the contamination of water bodies, even if the global geochemical balance is neutral or even alkaline [8]. Furthermore, [23] presents a review of the geochemistry of these elements, emphasizing their sources and mobility in naturally contaminated rocks, namely due to desorption from iron-rich minerals.

Once the production of AMD starts, it is very complex to stop the process. In addition, the remediation techniques based on passive or active processes [24,25] are often inefficient or expensive as they require long-term application of the treatment strategies. Moreover, as mentioned by [26], these classical approaches demand an adequate control and disposal of the resulted PTE-enriched sludge.

Thus, for the management and control of the tailings, it is crucial to assess the AMD potential as well as the mobility of toxic elements such as As, Ni or Se. In general, a good understanding of the environmental behavior of the tailings involves a set of procedures, including acid base accounting and leaching tests (e.g., batch, column and/or in situ) [3,14,15,27–35].

In this work, results of chemical, mineralogical and environmental evaluation of two different set of tailings from Au beneficiation are presented and discussed. The tailings represent different scenarios regarding mineralogy and geochemistry as well as mineral processing techniques and temporal evolution. Therefore, there are tailings from an old circuit (already deactivated) that are accumulated in an abandoned dam (Cocoruto dam) and tailings from an active plant, both located in Minas Gerais, Brazil. These two types represent distinctive beneficiation processes. The old circuit was a sulfide flotation plant and direct leaching. The ongoing circuit includes stages of calcination of sulfide concentrates and leaching.

The general objective is to compare the two types of tailings, using detailed geochemical and mineralogical characterization, namely for determining the AMD potential and the ability to mobilize PTE. This comparison intends to (i) understand the supergenetic evolution of different tailings and (ii) support

monitoring and identify possible opportunities for environmental improvements and management of both types of tailings.

2. Location and Characterization of the Study Area

The study area is in the Iron Quadrangle (QF), one of the most gold-producing regions in Brazil [36,37]. The gold world-class deposits are part of the Rio das Velhas Greenstone Belt, largely located in State of Minas Gerais (Figure 1a), with an estimated 4.5% of the world's ore reserves, almost half, about 936 tonnes [38–40]. The orebodies, hosted in Archaean rocks, are structurally associated and controlled by hydrothermal alteration. The mineralization is related to different typologies such as iron-banded formation, clastic and turbiditic metasedimentary rocks, and quartz veins enriched with sulfides, mainly pyrite, arsenopyrite, and pyrrhotite [38,40–42].

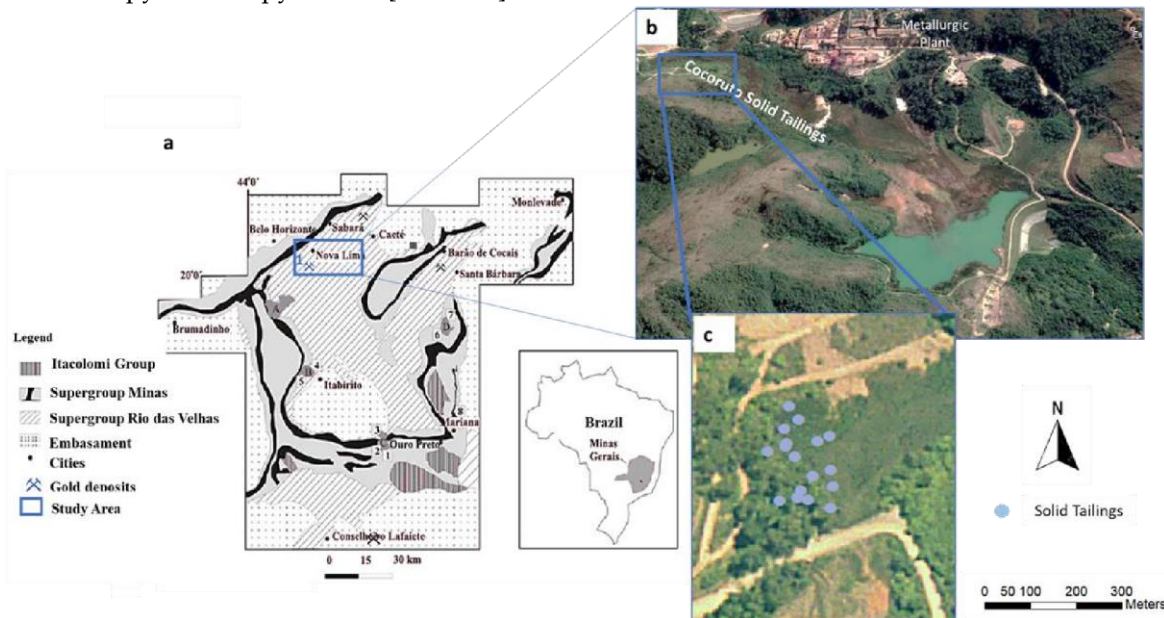


(Figura 5.1) **Figure 1.** Location of the study area and Iron Quadrangle map (a) [43,44]; (b,c) Images of the Cocoruto Dam sampled area (SIRGAS2000—10-09-2019).

These sulfide Au ores have been treated for over 30 years in metallurgic plants located in Nova Lima, in the northern part of the QF, Minas Gerais, 25 km away from its capital, Belo Horizonte (Figure 1a). The region has a warm and temperate climate, according to the Cfa classification (humid subtropical climate). The average rainfall is around 1390 mm per year, with the month of August being the driest and the month of December having the highest rainfall, with an average of 302 mm. The average temperature is 23.3 °C, with January the hottest month of the year while the lowest annual temperature is in June (average temperature of 17.6 °C) [45].

The circuits of the Nova Lima plant are and were fed by ores from the Raposos (Raposos circuits (Figure 2a)) and Cuiaba mines (Cuiaba circuit (Figure 2b) and ongoing roasted plant (Figure 2c)). The Raposos circuit (Figure 2a) is a plant that treated nonrefractory sulfide (pyrite, pyrrhotite and arsenopyrite) ore. The circuit reached 90% of Au recovery and was divided into grinding, gravity concentration, conventional leaching and CIP (carbon in leach), elution and electrorecovery. This part of the plant was deactivated in 1998 with the deactivation of the Raposos underground mining works, [46].

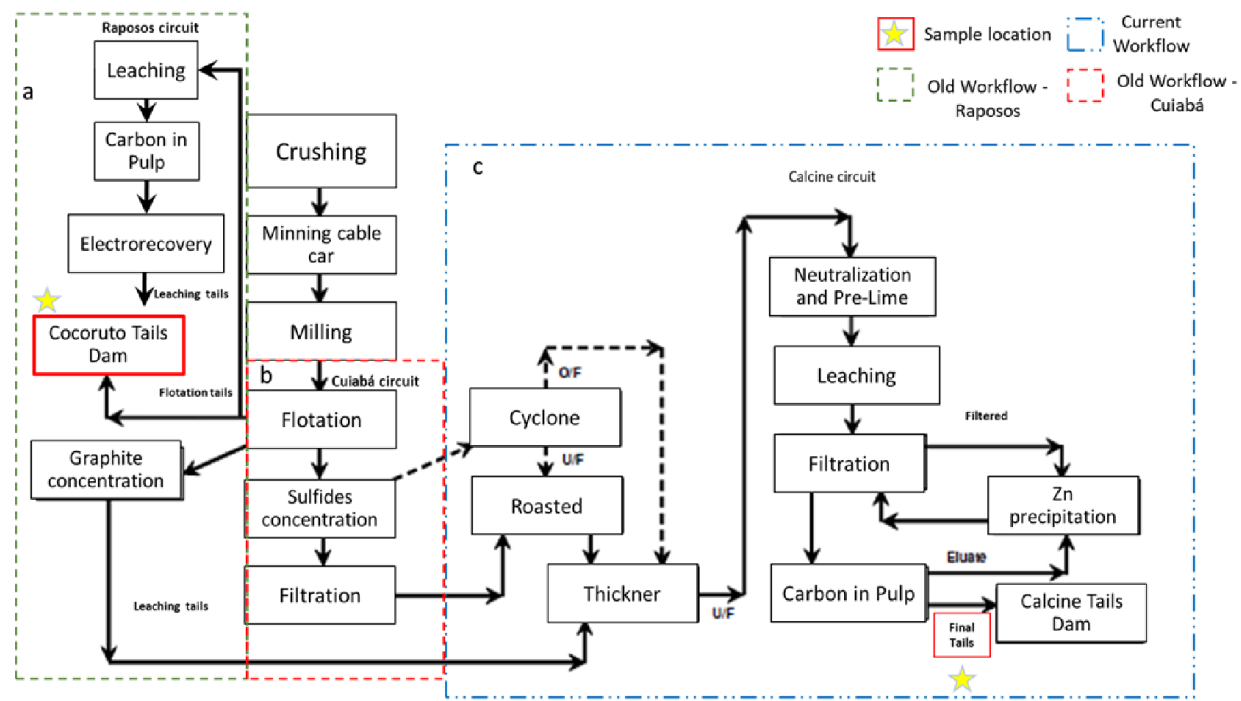


(Figura 5.2) **Figure 2.** Old and ongoing workflow of Nova Lima's plant (a,b). Old circuit sources of Cocoruto Dam. (c) Ongoing workflow [46]. The yellow stars represent sampling points.

The Cuiaba circuit (Figure 2b) treats refractory ore (mainly Au enclosed in pyrite) with 92% of Au recovery and was divided into grinding, gravity concentration, sulfide flotation, roasting, neutralization, calcined leaching, CIP, elution and electrodeposition [46]. Currently at the Nova Lima plant, the material is treated from the roasting stage (Figure 2c), as the previous steps are carried out directly at the plant located in the Cuiaba mine in Sabará, Minas Gerais. The tailings from the Raposo and the Cuiaba flotation circuits were deposited in a dam, already deactivated, named by Cocoruto (Figure 2a,b). The tailings from the ongoing circuit (roasting and leaching) are available in a dam known as calcined (Figure 2c).

Both structures are downstream type, monitored and declared safe according to the mining national agency [47]. In this study, the tailings samples representing the old circuits were collected directly at the Cocoruto dam, while the tailings from the ongoing circuit were collected directly at the calcined dam discharge. Therefore, the Nova Lima facility provides the opportunity to examine the potential environmental impact promoted by leaching and mobilization of PTE [48].

3. Materials and Methods

The sampling campaign was performed in the spring, a season (September 2019) in which weather conditions vary greatly. Typically, during this month it is common to alternate between dry and humid periods, with temperatures between 19 °C and 25 °C [45]. A total of 15 sites were selected in the Cocoruto dam (CoT samples) to represent the old circuit. Sampling, using percussion and auger methods, was performed at a maximum of 10 m. Another set of fresh tailings samples (CaT samples) was collected over 28 days in September 2019 during the production stage, representing a total of 40 samples from the active plant (Figure 2c). All samples were immediately sealed and refrigerated until analysis. Additional material was transferred to polypropylene bags and frozen until analysis. Refrigerated and frozen samples were packaged and shipped to the chemical laboratory for analysis.

The chemical composition was analyzed by inductively coupled plasma mass spectrometry (ICP-MS, PerkinElmer SCIEX, Waltham, MA, USA—detection limit 0.001 mg/kg) after acid digestion (nitric acid, hydrogen peroxide and hydrochloric acid) in accordance with Method 3050B published by the U.S. Environmental Protection Agency (USEPA) [49]. In addition, Au analyses were performed by atomic absorption spectroscopy (AAS, Varian, Palo Alto, CA, USA—detection limit 0.05 mg/kg), using the fire assay method. All metal solutions were prepared from concentrated stock solutions (Sigma Aldrich). High-purity water produced with a Millipore Milli-Q system was used throughout the analytical process. Quality assurance and quality control (QC/QA) procedures included duplicates, blanks and standard reference materials for ICP-MS. Certified Reference Materials Si81 (Rocklabs) for solid tails were selected to represent a wide range of total elemental concentrations. Results of blanks were always below detection limits. Values for precision (expressed as RSD %) were less than 5% for all elements.

The particle size distribution (PSD) was obtained by vibratory sieving between 212–38 µm. In addition to the geochemical and PSD data, polished sections were prepared in composed samples for mineralogical characterization. The mineralogical study was carried out through optical microscopy and scanning electron microscopy (SEM—Field Electron and Ion Company—FEI; Hillsboro, OR, USA) at the UFMG, Belo Horizonte. The samples were analyzed in an FEI electronic microscope, Quanta 600 FEG, high vacuum mode, coupled to the automated analyzer software (MLA—mode GXMAP and SPL-DZ) and the EDS Espirit Bruker (20 Kve) microanalysis system.

The evaluation of acid mine drainage potential consisted of the comparison of the Modified Acid-Base Accounting (MABA) and Net Acid Generation Test (NAG-test) [50,51]. The acid base accounting (ABA) test is conducted to assess the static potential of generating acidic drainage from a material. It was conducted in accordance with the MEND guide [50] and aims to determine the balance between acid production and consumption from the mineral components of a given sample. Acid production and consumption were measured, respectively, using the parameters acidity potential (AP) and neutralization potential (NP). The NAG-test was carried out in accordance with the MEND guide [51], in which hydrogen peroxide was used to oxidize an aliquot (2.5 g) of comminuted sample (<75 mm). Final pH values (NAG-pH), and electrical conductivity were noted, and the liquor, filtered, was titrated with NaOH solution to defined pH values (4.5 and 7.0) in order to obtain indications on the global amount of non-neutralized acidity, per sample weight. The results of the NAG and MABA tests are compared with each other, allowing a refinement of the interpretation of the latter, and a more improved classification (according to both criteria) regarding the sample's AMD potential [50,51]. In addition, leaching test derived (SPLP) was carried out in accordance with the USEPA 1312 method [52].

4. Results

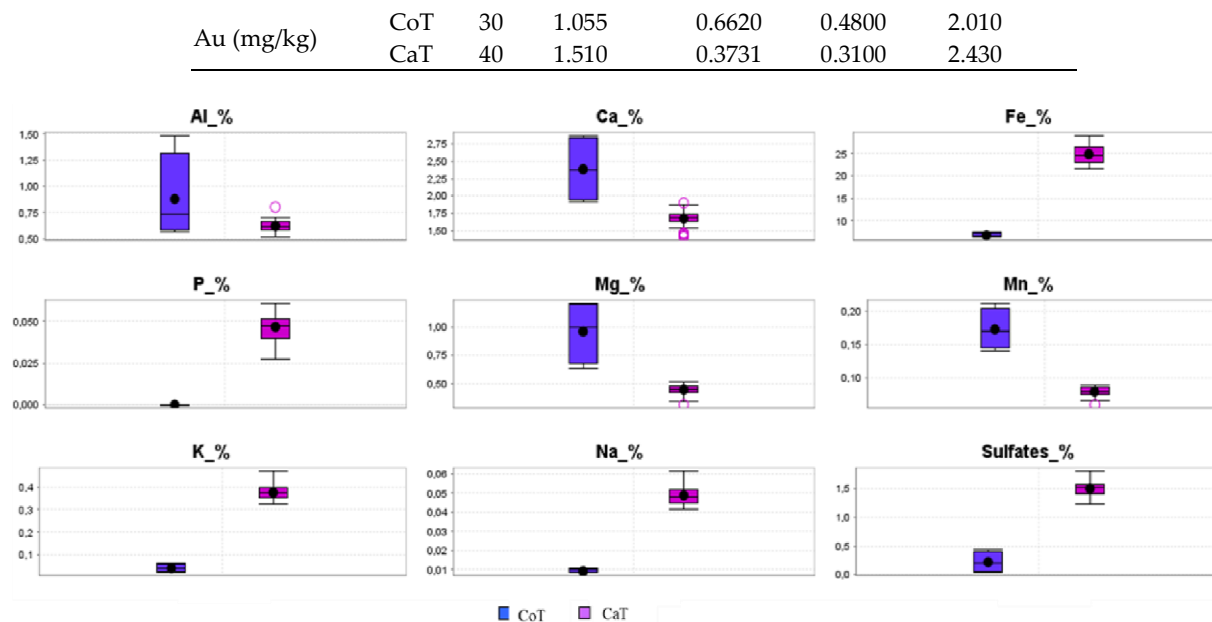
4.1. Chemical Composition

Table 1 and Figure 2 show the composition of the tailings. The elements were selected primarily based on the environmental relevance and inclusion in the Brazilian legal framework as well as potential economic interest. The samples from the ongoing process (CaT) comprise the following major elements, according to the decreasing order of their average concentration: Fe > Ca > Al > Mg > K > Mn, Na. The samples from the old Cocoruto dam (CoT) contain higher levels of Mn than CaT tailings: Fe > Ca > Mg > Al > Mn > K, Na (Table 1 and Figure 2). A relative depletion of the iron concentrations could be verified for the tailings deposited historically in the Cocoruto Dam. The elements Na and, especially K, on the other hand, had an enrichment of the order of 3× and 10×, respectively (Table 1 and Figure 3).

The average concentrations of sulfur and cyanide in the ongoing process samples were also an order of magnitude higher than that of the CoT samples (Figure 3). Based only on the sulfur contents, this result could suggest that the CaT samples may have greater acid generation potential, compared to the samples from the Cocoruto Dam.

(Tabela 5.1) **Table 1.** Statistical summary of the major and trace elements. CoT—old circuit; CaT—ongoing circuit; N—number of samples.

Element	Source	N	Average	Standard Deviation	Minimum	Maximum
Ag(mg/kg)	CoT	30	0.5000	0.0000	0.5000	0.5000
	CaT	40	3.260	0.5478	2.970	4.960
Al (%)	CoT	30	0.8790	0.4150	0.5670	1.4820
	CaT	40	0.622	0.0569	0.516	0.799
Sb (mg/kg)	CoT	30	0.5000	0.0000	0.5000	0.5000
	CaT	40	49.060	10.4800	29.600	70.300
As (mg/kg)	CoT	30	1799	171.2	1610	2018
	CaT	40	7905	878.0	3553	9275
Ba (mg/kg)	CoT	30	17.1500	7.3800	12.0000	28.1000
	CaT	40	23.427	2.4770	18.600	30.300
Cd (mg/kg)	CoT	30	2.9325	0.0670	2.8700	3.0000
	CaT	40	14.083	1.2010	11.000	17.000
Ca (%)	CoT	30	2.3850	0.4850	1.9190	2.8720
	CaT	40	1.672	0.1177	1.404	1.903
Pb (mg/kg)	CoT	30	21.1000	4.4800	15.9000	26.7000
	CaT	40	258.480	32.0600	215.000	343.000
Cyanide (mg/kg)	CoT	30	2.9850	1.2920	1.6200	4.2600
	CaT	40	51.890	21.1700	13.900	87.600
Co (mg/kg)	CoT	30	4.0000	0.0000	4.0000	4.0000
	CaT	40	116.330	11.7400	95.300	144.000
Cu (mg/kg)	CoT	30	78.0500	15.4100	56.6000	93.0000
	CaT	40	670.520	56.4700	583.000	824.000
Cr (mg/kg)	CoT	30	85.2000	20.5000	59.0000	109.0000
	CaT	40	35.020	8.4700	26.900	81.400
Fe (%)	CoT	30	6.7600	0.5520	6.3970	7.5660
	CaT	40	24.859	2.0270	21.557	28.974
P (%)	CoT	30	0.0002	0.0000	0.0002	0.0002
	CaT	40	0.047	0.0075	0.027	0.061
Mg (%)	CoT	30	0.9570	0.2720	0.6340	1.2040
	CaT	40	0.450	0.0424	0.317	0.520
Mn (%)	CoT	30	0.1728	0.0307	0.1396	0.2119
	CaT	40	0.079	0.0072	0.059	0.088
Hg (mg/kg)	CoT	30	0.0688	0.0338	0.0250	0.1000
	CaT	40	0.036	0.0274	0.025	0.160
Ni (mg/kg)	CoT	30	72.2000	15.2200	52.9000	90.1000
	CaT	40	392.630	51.7200	269.000	506.000
K (%)	CoT	30	0.0411	0.0178	0.0226	0.0644
	CaT	40	0.377	0.0310	0.326	0.471
Na (%)	CoT	30	0.0091	0.0010	0.0086	0.0106
	CaT	40	0.049	0.0050	0.041	0.062
Sulfates (%)	CoT	30	0.2175	0.1763	0.0400	0.4400
	CaT	40	1.505	0.1333	1.230	1.810
Zn (mg/kg)	CoT	30	170.5	38.3	136	0.5000
	CaT	40	2724	318.8	1941	1.430



(Figura 5.3) **Figure 3.** Basic statistics and comparison of major element (%log) for the two sets of tailings samples.

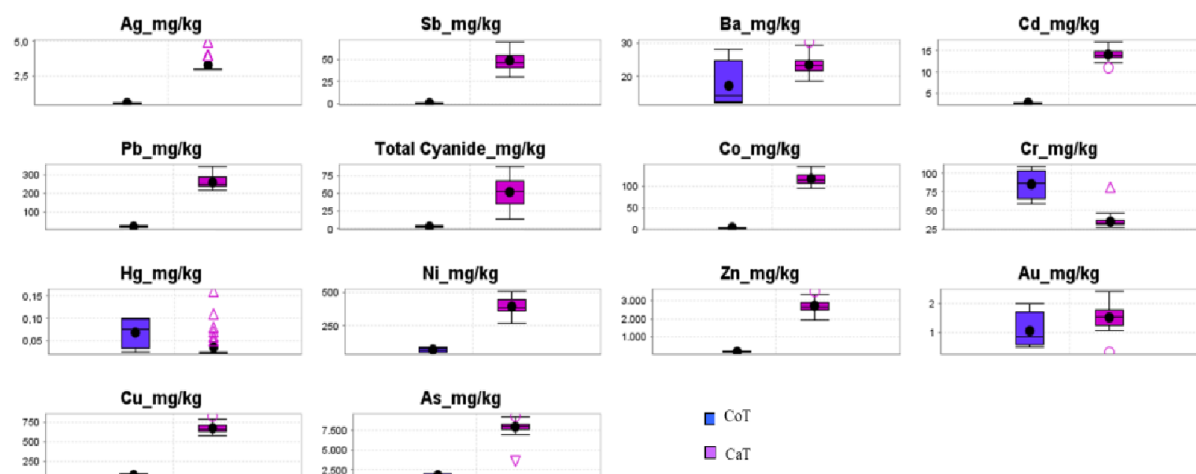


(Figura 5.4) **Figure 4.** Basic statistics and comparison of trace element (mg/kg log) for the two sets of tailings samples.

The trace elements with environmental interest [40] presented the following decreasing order of their average concentrations for CaT: (As > Zn) 10 mg/kg > (Cu > Ni > Pb > Co) 102 mg/kg > (Sb, Cr, Ba, Cd) 101 mg/kg and CoT (As) 103 mg/kg > (Zn) 102 mg/kg > (Cr > Cu > Ni > Pb > Hg) 101 mg/kg. The As followed by Zn remained as the main trace elements of environmental interest in the samples of tailings collected both in mineral processing and in the Cocoruto Dam (Table 1 and Figure 4). The element Hg was not detected in the CaT samples, but it had an average content of 21 mg/kg in the samples from the Cocoruto Dam.

4.2. Size Particle Distribution

In general, the grain size distribution (Figure 5) is similar to other dams that store tailings from Au exploitation [7,8,27,53]. The tailings presented 80% of their particles classified as silt-sized (Figure 5). The CoT samples are shown to have a thicker distribution than the ongoing process tailings (CaT). The difference can be explained by changes in the grinding process and different features of the ore sources

and their variability [30]. In addition, the samples that represent CoT originate from older circuits, which have low grinding efficiency when compared to the ongoing one (CaT).

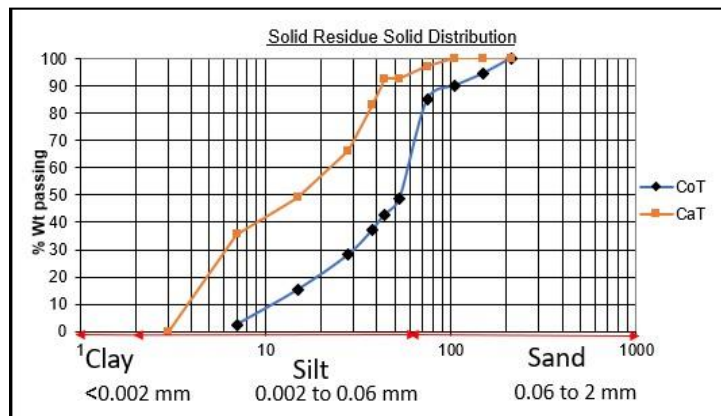


(Figura 5.5) **Figure 5.** Size distribution (Krumbein phi scale) of solid tailings.

4.3. Mineralogy

Table 2 shows the mineralogical composition of both tailings. The samples from the Cocoruto dam (old circuit) consist mainly of quartz, carbonates, iron oxides and phyllosilicates such as muscovite and chlorite (Figure 6). This is in accordance with higher Al, Ca and Mg concentrations. Sulfides are present, but they look well-preserved, mainly in the form of iron sulfides with sphalerite, covellite and arsenopyrite subordinated.

The samples from the ongoing process (CaT) are characterized by high concentrations of iron oxides, in addition to sulfates and silicates (mainly quartz). The high concentration of oxides justifies higher Fe contents than the samples of Cocoruto. Sulfides are reliquaries, associated with oxidized phases, and are rare. In Figure 6b, is identified, in false images, the presence of As, Cu, Ni, and Zn with oxidized phases, in addition to Fe. In both types of samples there are still fine Au grains. These particles are associated with iron oxides in the CaT and with sulfides in CoT samples. (Figure 6a–d). The optical microscopy images (Figure 6e–f) support these observations, showing the dominant hematite in CaT samples and the presence of Au in association with pyrite in CoT samples, respectively.

4.4. AMD Potential

The results of the MABA tests are presented graphically in Figure 7. Calcined samples collected in mineral processing showed relatively small variability in acidity (AP) and neutralization potentials (NP): In the first case, it ranged between 1.5 and 2.5 kg/CaCO₃ t and, in the second, it varied between 8.3 and 15.5 kg/CaCO₃ t. All these samples were classified as potentially non-acid-forming (PNA) by the MABA assay criterion, as they presented NP/AP ratio (NPR) > 2. The average NPR value for CaT corresponded to 6.1 kg/CaCO₃ t.

The tailings samples collected at the Cocoruto Dam showed relevant dispersion of acidity and neutralization potentials, in accordance with the mineralogical features. The AP values oscillated mainly in the range of 5–150 kg/CaCO₃ t. NP values between 44 to 123 kg/CaCO₃ t. This dispersion resulted in the following relative potentials for the generation of acid drainage, according to the MABA test criteria: Nonacid-forming samples (NPR > 2) represent 45%, samples in the uncertainty zone (NPR 1 to 2) are 50%, and samples acid-forming (NPR < 1) are 5%. Vertically, the samples in the uncertainty zone corresponded mainly to depths of 4.0 to 5.5 m and 8.0 to 11.5 m. The non-acid-forming samples occurred mainly between 0.0 and 1.5 m and from 6.0 to 7.5 m in depth (Figure 7b).

The NAG test (net acid generation) was another method used in order to compare with the results obtained by MABA, mainly because of the S grades. Figure 8 presents the graph NAGpH versus NPR, allowing to correlate the results of the MABA and NAG-tests, and to better refine the classification of acid generation potential of the samples under analysis. The results of the NAG test showed a pH value well above the limit of 4.5, indicating all samples as non-acid-forming, regardless of the result of the NPR. The pH fluctuated from 7.4 to 8.5 for samples from the Cocoruto Dam, and from 8.1 to 9.5 for process samples. These results indicate less potential for liquid acidity than previously indicated, only by the NPR (MABA) criterion. The summary of the assessment of the potential for acidity generation, based on the MABA and NAG, therefore, demonstrates that all process samples resulted in potentially non-acid forming (NAF). Only 45% of the samples collected at the Cocoruto Dam resulted in potentially non-acid forming, using the MABA criterion. However, this number was 100% using the NAG criterion.

(Tabela 5.2) Table 2. Mineralogical Composition of CaT and CoT..

Minerals	Chemical Formula	CaT (Wt%)	CoT (Wt%)
Quartz	SiO ₂	15.6	55.8
Feldspar Group Albite			
	NaAlSi ₃ O ₈	1.50	0.370
Anorthite	CaAl ₂ Si ₂ O ₈	0.053	0.01
K feldspar	KAlSi ₃ O ₈		0.390
Phyllosilicates Biotite			
	KMg _{2.5} Fe _{0.5} AlSi ₃ O ₁₀ (OH) _{1.75} F _{0.25}	1.00	0.16
Smectite	(Si,Al)(Mg,Fe)O(OH)NaH ₂ O.	1.80	0.13
Muscovite Group	KAl ₃ Si ₃ O ₁₀ (OH) _{1.9} F _{0.1}	11.0	5.56
Chlorite	(Mg,Fe) ₃ (Si,Al) ₄ O ₁₀ (OH) ₂ -(Mg,Fe) ₃ (OH) ₆	3.30	6.12
Oxides			
Iron			
Oxides/Hydroxides	Fe ₂ O ₃ /FeOOH	56.8	8.86
Rutile/Anathase	TiO ₂	0.599	0.49
Carbonates Ankerite			
	Ca(Fe,Mg,Mn)(CO ₃)	1.00	11.2
Siderite	FeCO ₃	-	7.25
Calcite	CaCO ₃	0.200	2.25
Sulfates			
Gypsum	CaSO ₄ ·2H ₂ O	7.00	0.030
Sulfides Pyrite			
	FeS ₂	0.002	0.500
Pyrrhotite	Fe _(1-x) S	0.004	0.790
Arsenopyrite	FeAsS	0.056	0.240
Gesdorffite	NiAsS	0.010	-
Covellite	CuS	0.100	0.070
Sphalerite	ZnS	-	0.010
Gold Minerals Native			
Gold	Au > 80%, Ag, Cu, Hg	(526)	(364)
Electrum	Au = 80%, Ag = 20%	(42)	(10)

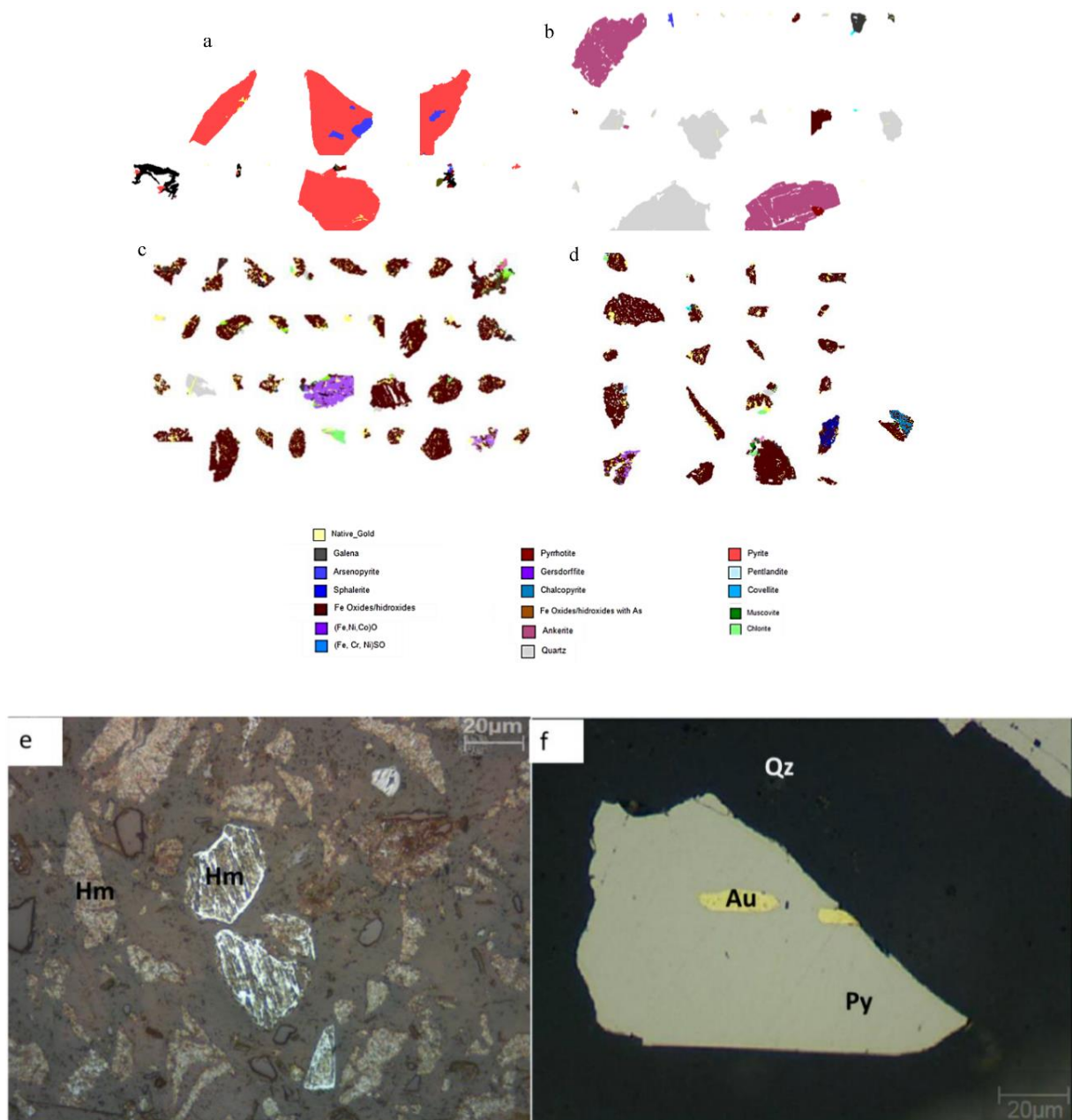


(Figura 5.6) **Figure 6.** False Images (a) sulfides associated with iron oxide and Au particles—CoT, (b) quartz, carbonates and Fe oxides particles—CoT, (c,d) Fe oxides associated with Au, silicates and Fe oxides with As, Ni, Co, Al, Zn, Pb—CaT samples. Photomicrographs taken under reflected light and uncrossed nico (e) hematite (Ht) from CaT samples and (f) Au associated with pyrite (Py)—CoT samples.

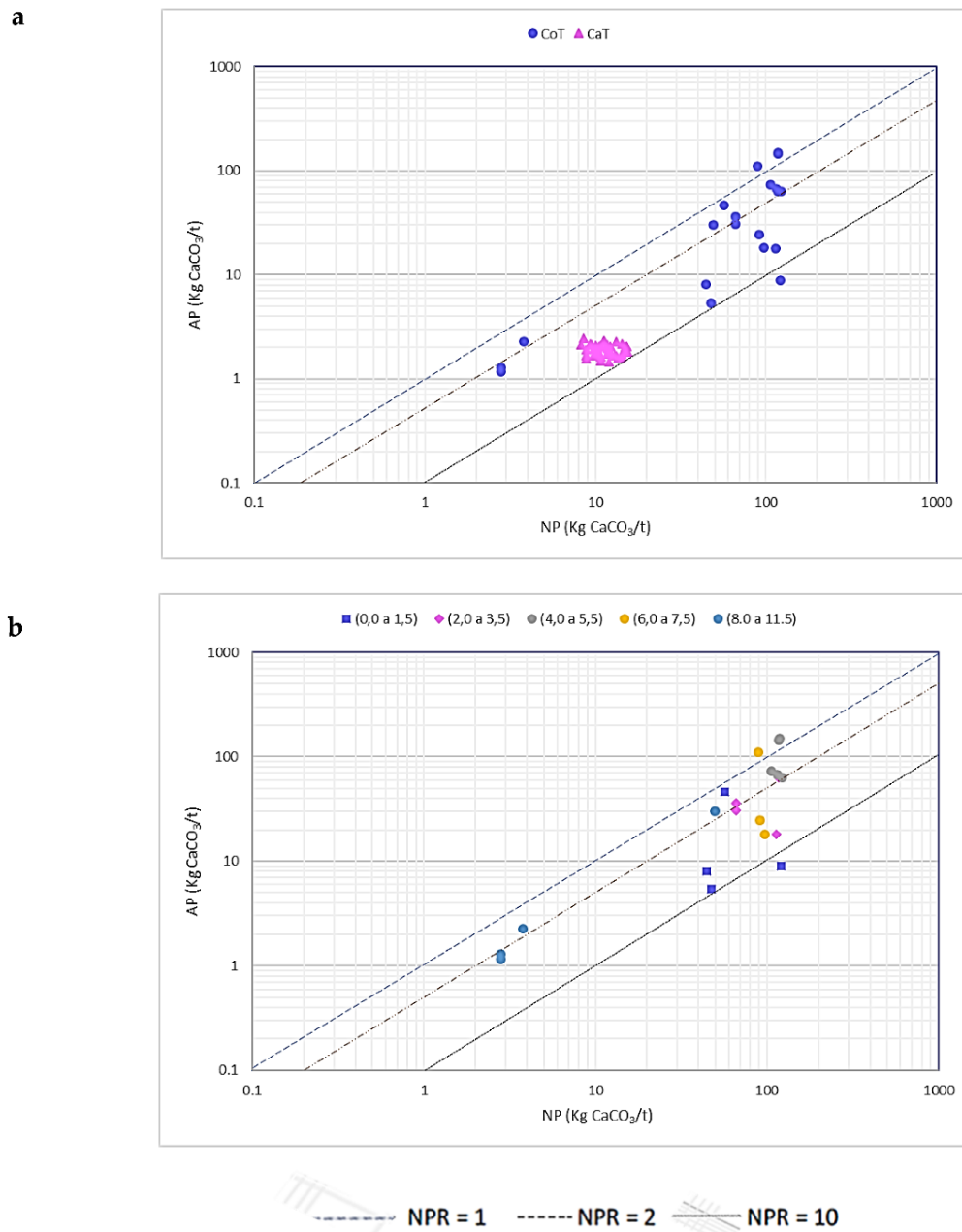


(Figura 5.7) **Figure 7.** Results of Modified Acid-Base Accounting (MABA) tests (a) global and (b) for CoT, by sampling depth.

4.5. SPLP Leaching

In addition to the tests already presented, the SPLP leaching test (USEPA 1312 method) was carried out in order to assess the potential for leaching toxic elements. Data from leaching tests can be used as indicators of potentially contaminating substances, even though the test conditions are very limited in view of the environmental geochemical conditions. A basic criterion used to assess the magnitude of the potential impact is the comparison with benchmarks in the context of the legal framework. The Brazilian law, through CONAMA Resolution 396/2008, was used as reference for the permitted limits of the following elements: Al, Sb, As, Ba, Be, Cd, Pb, Co, Cu, Cr, Fe, Mn, Hg, Ni, Ag and Zn. Since there is no definition for the predominant industrial use, recreation was defined as the predominant use.

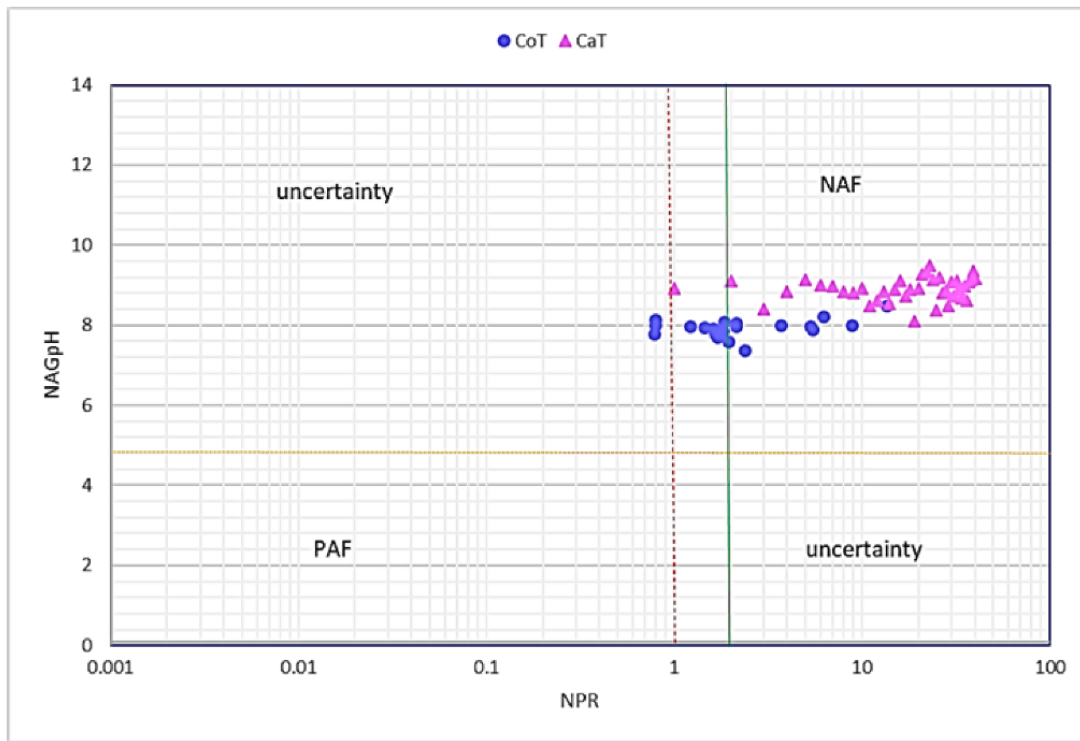


(Figura 5.8) **Figure 8.** Relationship between the results of the MABA and Net Acid Generation (NAG) pH tests (NAF: region of non-acid-forming samples; PAF: region of potentially acid-forming samples).

The elements Cd, Pb, Hg, and Zn were not detected in the leaching extracts (Table and Figure 9), with two exceptions: Pb equal to 0.02 mg/L, and Zn equal to 0.1 mg/L in a sample from the Cocoruto Dam. In the extracts of this dam, only the elements As and Mn showed concentrations above the respective legal reference (VMP) (i.e., 0.05 mg As/L, and 0.1 mg Mn/L). The average concentrations were around an order of magnitude higher than the VMP, in these cases (Figure 9).

(Tabela 5.3) **Table 3.** VMP—maximum allowed values From Brazilian Law—CONAMA [54].

Samples	Not Detected Elements	Parameters with Values Above VMP Conama 2005 Reference
CoT	Cd, Hg, Pb, Zn	As (VMP 0.05 mg/L) Mn (VMP 0.1 mg/L)
CaT	Cd, Hg, Pb, Zn	As (VMP 0.05 mg/L) Fe (VMP 0.3 mg/L) Ni (VMP 0.1 mg/L) Se (VMP 0.01 mg/L)

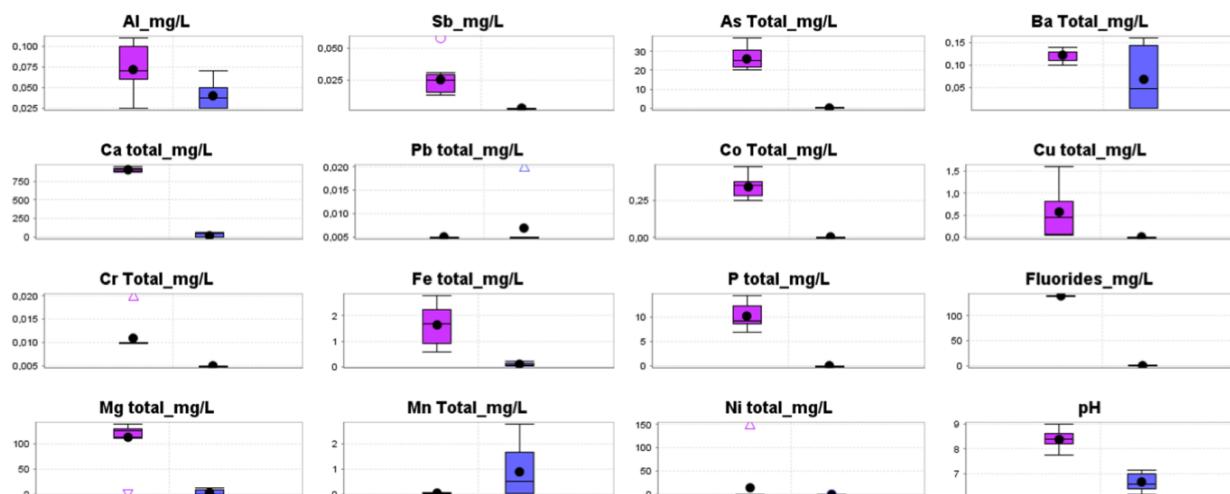


(Figura 5.9) **Figure 9.** Comparison of the average levels of metals, metalloids, fluorides and pH in SPLP leaching extracts. VMP Al = 0.2 mg/L; VMP Sb = NA; VMP As = 0.05 mg/L; VMP Ba = 1.0 mg/L; VMP Ca = NA; VMP Pb = 0.05 mg/L; VMP Co = NA; VMP Cu = 1.0 mg/L; VMP Cr = 0.05 mg/L; VMP Fe = 0.3 mg/L; VMP P = NA; VMP Fluorides = NA; VMP Mg = NA; VMP Mn = 0.1 mg/L; VMP Ni = 0.1 mg/L. NA—Not applied for recreation use.

On the other hand, in the calcined ongoing process the elements As, Fe, Ni, and Se showed values above the CONAMA references, in at least one of the leaching extracts.

5. Discussion

The differences in particle distribution could contribute to differentiate the two types of tailings regarding the speed and magnitude of AMD. It is known that the rate of oxidation of sulfides is directly related to the size of the particles and the availability of the surface for reaction [20,55]. The mineralogical characteristics confirmed the distinction between tailings that were subjected to different processes, in accordance with the geochemical signatures (Figure 1). Such geochemical and mineralogical diversity could result in different potentials for mobilizing pollutants in AMD. For example, the higher amounts of sulfides in the Cocomoto tailings (old circuit) could suggest higher potential for AMD generation. However, Figure 6 suggests that inhibition of the oxidative dissolution processes occurs, since the sulfide grains are preserved. Moreover, AMD generation could be controlled by the presence of carbonates due to the ore paragenesis and metallurgical ore treatment [7].

Neutralization conditions also occur in CaT samples due to the addition of lime.

The chemical and mineralogical study highlights the occurrence of high grades of Au in these two sets of tailings. In CoT samples, the concentration reaches 1.0 mg/kg with Au crystals associated with sulfides and rock minerals such as carbonates and silicates (Figure 6a,b). In the ongoing process, in CaT samples, the concentration reaches 1.70 mg/kg, with grains enclosed in iron oxides (Figure 6c). Both Au features portray limitations and problems in the beneficiation old and ongoing processes. However, this inefficiency of the mineral separation processes may represent an opportunity for creating profit through valorization of the mine wastes. The reuse of tailings is now an important research line, as discussed in [53,56–60]. Especially in view of the scenario experienced in Brazil after the mediatised disasters of the Mariana (2015) and Brumadinho (2019) dams [61–64], it is crucial to find sustainable solutions for the closure stage. Therefore, in the present cases, the obtained results suggest the possibility of transforming an environmental liability into an economic outcome.

The tests for prediction of AMD indicate that minimum pH is around 8, reaching a maximum of 9.6, reflecting the alkaline products used for extraction of Au with cyanide solutions. However, the levels of S

present in the forms of sulfate and sulfide, thin PSD, and the presence of toxic leachable elements above permitted limits do not rule out the generation of AMD in practice if the tailings are stored improperly. These results, in addition to geochemical and mineralogical features, imply that the samples from the Cocoruto Dam are not potentially acid-forming under the conditions in which they are disposed. The net potential for acidity generation is low. However, in the case of removal of these materials, they must be disposed properly, without long-term exposure (months/years).

Under pH conditions close to neutrality, a series of trace elements can remain solubilized [8], as verified for As, Fe, Ni, Mn and Se. This behavior was also observed by [23], specifically for As and Se leached out in underground rock excavation works. The Al for the sample of the CoT tailings was an exception. Thus, the generation of effluents with metals or metalloids does not require long periods of exposure of sulfide minerals [7]. The As stood out in SPLP leaching test, with an average concentration (26 mg As/L), 3× of magnitude above the permitted limits by the Brazilian law (VMP). This could be explained by the presence of arsenopyrite in CoT samples and iron oxide in CaT. For the other parameters mentioned, the averages values found were up to an order of magnitude higher than the corresponding VMP.

6. Conclusions

An integrated characterization of tailings from different mineral beneficiation processes was performed to evaluate the environmental risk of mobilizing pollutants from the mine drainage.

The tailings presented 80% of their particles classified as silt-sized. Sulfides are present in the samples from the historic Cocoruto dam, but they appear well-preserved. The tailings consist mainly of quartz (55.8%), carbonates (20.7%), iron oxides (8.86%), muscovite (5.56%) and chlorite (6.12%). Therefore, the potential acidity associated with sulfides could be neutralized by the dissolution of carbonates, such as calcite and silicates such as chlorite, besides the reagents used during the process. This fact contributes to make it a less dangerous waste when compared to the current one (CaT).

The tailings from the ongoing process (CaT) are characterized by high contents of iron oxides (56.8%), gypsum (7%) and silicates (mainly quartz—15.6%). In both types of tailings, the chemical composition allowed to identify elements with environmental relevance by their toxicity, namely Mn in the old tailings and As, Fe, and Ni in the more recent tailings. In addition to these elements of environmental concern, it should be noted the interesting values of Au (up to 2.4 mg/kg in the recent tailings), suggesting a potential for reuse during closures of dam facilities or tailings mass-rearrangement needs.

The geochemical tests, MABA and NAG, indicate that these tailings are not potentially acid-forming, under the conditions in which they are disposed. The net potential for acidity generation is low. However, the results of the SPLP leaching tests indicated a leaching potential for As and Mn in the Cocoruto Dam. Samples that are subject to calcination indicate leaching potential for other elements, namely Sb, As, Fe, Ni, and Se. It is of note that As concentrations in these samples were two orders of magnitude higher than the ones found in samples from Cocoruto Dam. Moreover, the concentrations of S present in the forms of sulfate and sulfide, together with thin PSD and the presence of leachable PTE above permitted limits by the Brazilian law are important issues of concern. In the case of tailings mobilization or inappropriate storage, the generation of AMD and contamination by PTE is likely to occur.

Author Contributions: Conceptualization, M.L., T.V., P.M.R. and R.F.; Data curation, M.L., T.V., I.D., J.V. and M.M.; Funding acquisition, M.L., T.V. and J.V.; Investigation, M.L., T.V., P.M.R., R.F., I.D., J.V. and M.M.; Resources, T.V. and J.V.; Supervision, T.V.; Visualization, M.L. and T.V.; Writing—original draft, M.L., T.V., P.M.R. and R.F. All authors have read and agreed to the published version of the manuscript.

Funding: This work was funded by FCT—Fundação para a Ciência e a Tecnologia through projects UIDB/04683/2020 e UIDP/04683/2020 and Nano-MINENV 029259 (PTDC/CTA-AMB/29259/2017, and by AngloGold Ashanti Brazil.

Institutional Review Board Statement: Not applicable.

Informed Consent Statement: Not applicable.

Data Availability Statement: Not applicable.

Acknowledgments: We thank our colleagues from ICT, microscopy center from Universidade Federal de Minas Gerais (CM-UFMG), and AngloGold Ashanti who provided insight and expertise that greatly assisted the research. The authors are grateful to the two anonymous reviewers and to the editor Dr Carlito Tabelin for their valuable contributions to improving the manuscript.

Conflicts of Interest: Authors declare no conflict of interest.

References

1. Mohapatra, D.; Kirpalani, D. Process effluents and mine tailings: Sources, effects and management and role of nanotechnology. *Nanotechnol. Environ. Eng.* **2017**, *2*, 1–12. [[CrossRef](#)]
2. Blight, G. Mine waste: A brief overview of origins, quantities, and methods of storage. In *Waste: A Handbook for Management*, 2nd ed.; Letcher, T., Vallero, D., Eds.; Academic Press: Cambridge, MA, USA, 2011; pp. 77–88.
3. Lottermoser, B. *Mine Wastes: Characterization, Treatment and Environmental Impacts*; Springer: New York, NY, USA, 2012; pp. 1–400. ISBN 978-3-662-05133-7.
4. Park, I.; Tabelin, C.B.; Jeon, S.; Li, X.; Seno, K.; Ito, M.; Hiroyoshi, N. A review of recent strategies for acid mine drainage prevention and mine tailings recycling. *Chemosphere* **2019**, *219*, 588–606. [[CrossRef](#)] [[PubMed](#)]
5. Blowes, D.W.; Jambor, J.L.; Hanton-Fong, C.J.; Lortie, L.; Gould, W.D. Geochemical, mineralogical and microbiological characterization of a sulphide-bearing carbonate-rich gold mine tailings impoundment, Joutel, Quebec. *Appl. Geochem.* **1998**, *13*, 687–705. [[CrossRef](#)]
6. Johnson, D.B. Chemical and microbiological characteristics of mineral spoils and drainage waters at abandoned coal and metal mines. *Water Air Soil Pollut.* **2003**, *3*, 47–66. [[CrossRef](#)]
7. Lindsay, M.B.; Condon, P.D.; Jambor, J.L.; Lear, K.G.; Blowes, D.W.; Ptacek, C.J. Mineralogical, geochemical, and microbial investigation of a sulfide-rich tailings deposit characterized by neutral drainage. *J. App. Geochem.* **2009**, *24*, 2212–2221. [[CrossRef](#)]
8. Bissacot, L.; Ciminelli, V.; Logsdon, M. Arsenic Mobility under a Neutral Mine Drainage Environment in a Gold-Mine Tailings Dam—In Agreeing on solutions for more sustainable mine water management. In Proceedings of the 10th International Conference on Acid Rock Drainage & IMWA Annual Conference (ICARD & IMWA-2005), Santiago, Chile, 21–24 April 2005; pp. 170–174.
9. Opiso, E.; Aseneiro, J.; Banda, M.; Tabelin, C.B. Solid-phase partitioning of mercury in artisanal gold mine tailings from selected key areas in Mindanao, Philippines, and its implications for mercury detoxification. *Waste Manag. Res.* **2018**, *36*, 269–276. [[CrossRef](#)] [[PubMed](#)]
10. Tabelin, C.B.; Silwamba, M.; Paglinawan, F.C.; Mondejar, A.J.S.; Duc, H.G.; Resabal, V.J.; Opiso, E.M.; Igarashi, T.; Tomiyama, S.; Ito, M.; et al. Solid-phase partitioning and release-retention mechanisms of copper, lead, zinc and arsenic in soils impacted by artisanal and small-scale gold mining (ASGM) activities. *Chemosphere* **2020**, *260*, 127574. [[CrossRef](#)]
11. Nordstrom, K. Mine Waters: Acidic to Circumneutral. *Elements* **2011**, *7*, 393–398. [[CrossRef](#)]
12. Nordstrom, D.K. Hydrogeochemical processes governing the origin, transport and fate of major and trace elements from mine wastes and mineralized rock to surface waters. *Appl. Geochem.* **2011**, *26*, 1777–1791. [[CrossRef](#)]
13. Smuda, J.; Dold, B.; Spangenberg, J.E.; Friese, K.; Kobek, M.R.; Bustos, C.A.; Pfeifer, H.R. Element cycling during the transition from alkaline to acidic environment in an active porphyry copper tailings impoundment, Chuquicamata, Chile. *J. Geochem. Explor.* **2014**, *140*, 23–40. [[CrossRef](#)]
14. Guseva, O.; Opitz, A.K.B.; Broadhurst, J.L.; Harrison, S.T.L.; Bradshaw, D.J.; Becker, M. Fe-Sulfide Liberation and Association as a Proxy for the Interpretation of Acid Rock Drainage (ARD) Test Results. In *Mine Water—Risk to Opportunity*; Wolkersdorfer, C.H., Sartz, L., Weber, A., Burgess, J., Tremblay, G., Eds.; Tshwane University of Technology: Pretoria, South Africa, 2018; pp. 345–351.

15. Wolkersdorfer, C.; Nordstrom, D.K.; Beckie, R.D.; Cicerone, D.S.; Elliot, T.; Edraki, M.; Valente, T.; França, S.C.A.; Kumar, P.; Oyarzún, R. Guidance for the Integrated Use of Hydrological, Geochemical, and Isotopic Tools in Mining Operations. *Mine Water Environ.* **2020**, *39*, 204–228. [[CrossRef](#)]
16. Tabelin, B.C.; Corpuz, R.D.; Igarashi, T.; Villacorte-Tabelin, M.; Alorro, R.D.; Yoo, K.; Raval, S.; Ito, M.; Hiroyoshi, N. Acid mine drainage formation and arsenic mobility under strongly acidic conditions: Importance of soluble phases, iron oxyhydroxides/oxides and nature of oxidation layer on pyrite. *J. Hazard. Mater.* **2020**, *399*, 122844. [[CrossRef](#)] [[PubMed](#)]
17. Tomiyama, S.; Igarashi, T.; Tabelin, C.B.; Tangviroon, P.; Li, H. Acid mine drainage sources and hydrogeochemistry at the Yatani mine, Yamagata, Japan: A geochemical and isotopic study. *J. Contam. Hydrol.* **2019**, *225*, 103502. [[CrossRef](#)] [[PubMed](#)]
18. Tomiyama, S.; Igarashi, T.; Tabelin, C.B.; Tangviroon, P.; Li, H. Modeling of the groundwater flow system in excavated areas of an abandoned mine. *J. Contam. Hydrol.* **2020**, *230*, 103617. [[CrossRef](#)]
19. Lapakko, K.A.; Engstrom, J.N.; Antonson, D.A. Effects of particle size on drainage quality from three lithologies. In Proceedings of the 7th International Conference on Acid Rock Drainage (ICARD), St. Louis, MO, USA, 26–30 March 2006; pp. 1026–1050.
20. Eary, L.; Williamson, M. Simulations of the neutralizing capacity of silicate rocks in acid mine drainage environments. *J. Am. Soc. Min. Reclam.* **2006**, *2*, 564–577. [[CrossRef](#)]
21. Blowes, D.W.; Ptacek, C.J.; Jurjovec, J. Mill tailings: Hydrogeology and geochemistry. In *Environmental Aspects of Mine Wastes*; Jambor, J.L., Ritchie, A.I.M., Eds.; Mineral Association of Canada, Short Course: Québec, QC, Canada, 2003; Volume 31, pp. 95–116.
22. Ritcey, G.M. Tailings Management in Gold Plants. *Hydrometallurgy* **2005**, *78*, 3–20. [[CrossRef](#)]
23. Tabelin, C.B.; Igarashi, T.; Villacorte-Tabelin, M.; Park, I.; Opiso, E.M.; Ito, M.; Hiroyoshi, N. Arsenic, selenium, boron, lead, cadmium, copper, and zinc in naturally contaminated rocks: A review of their sources, modes of enrichment, mechanisms of release, and mitigation strategies. *Sci. Total Environ.* **2018**, *645*, 1522–1553. [[CrossRef](#)]
24. Moodley, I.; Sheridan, C.M.; Kappelmeyer, U.; Akcil, A. Environmentally sustainable acid mine drainage remediation: Research developments with a focus on waste/by-products. *Miner. Eng.* **2018**, *126*, 207–220. [[CrossRef](#)]
25. Dutta, M.; Islam, N.; Rabha, S.; Narzary, B.; Bordoloi, M.; Saikia, D.; Silva, L.F.O.; Saikia, B.K. Acid mine drainage in an Indian high-sulfur coal mining area: Cytotoxicity assay and remediation study. *J. Hazard. Mater.* **2020**, *389*, 304–389. [[CrossRef](#)]
26. Igarashi, T.; Herrera, P.S.; Uchiyama, H.; Miyamae, H.; Iyatomi, N.; Hashimoto, K.; Tabelin, C.B. The two-step neutralization ferrite-formation process for sustainable acid mine drainage treatment: Removal of copper, zinc and arsenic, and the influence of coexisting ions on ferritization. *Sci. Total Environ.* **2020**, *715*, 136877. [[CrossRef](#)]
27. Nengovhela, A.C.; Yibas, B.; Ogola, J.S. Characterisation of gold tailings dams of the Witwatersrand Basin with reference to their acid mine drainage potential Johannesburg, South Africa. *Water* **2006**, *32*, 4–8. [[CrossRef](#)]
28. Valente, T.; Antunes, M.; Sequeira, B.M.A.; Prudêncio, M.I.; Marques, R.; Pamplona, J. Mineralogical attenuation for metallic remediation in a passive system for mine water treatment. *Environ. Earth Sci.* **2012**, *66*, 39–54. [[CrossRef](#)]
29. Valente, T.; Grande, J.A.; De La Torre, M.L. Extracting value resources from acid mine drainages and mine wastes in the Iberian Pyrite Belt. In Proceedings of the International Mine Water Association Symposium 2016—Mining Meets Water—Conflicts and Solutions, Leipzig, Germany, 11–15 July 2016; pp. 1339–1340.
30. Foli, G.; Gauw, S.K.Y. Modified acid-base accounting model validation and pH buffer trend characterization in mine drainage at the AngloGold-Ashanti Obuasi mine in Ghana, West Africa. *Environ. Earth Sci.* **2017**, *76*, 663–682. [[CrossRef](#)]
31. Becker, M.; Charikinya, E.; Ntlhabane, S.; Voigt, M.; Broadhurst, J.; Harrison, S.T.L.; Bradshaw, D. An Integrated Mineralogy-based Modelling Framework for the Simultaneous Assessment of Plant Operational Parameters with Acid Rock Drainage Potential of Tailings. In *Mine Water—Risk to Opportunity*; Wolkersdorfer, C.H., Sartz, L., Weber, A., Burgess, J., Tremblay, G., Eds.; Tshwane University of Technology: Pretoria, South Africa, 2018; Volume 1, pp. 309–315.
32. Borba, R.P.; Figueiredo, B.R.; Rawlins, B. Geochemical distribution of arsenic in waters, sediments and weathered gold mineralized rocks from Iron Quadrangle, Brazil. *Environ. Geol.* **2003**, *44*, 39–52. [[CrossRef](#)]

33. Tabelin, C.B.; Hashimoto, A.; Igarashi, T.; Yoneda, T. Leaching of boron, arsenic and selenium from sedimentary rocks: I. Effects of contact time, mixing speed and liquid-to-solid ratio. *Sci. Total Environ.* **2014**, *472*, 620–629. [[CrossRef](#)] [[PubMed](#)]
34. Tabelin, C.B.; Sasaki, R.; Igarashi, T.; Park, I.; Tamoto, S.; Arima, T.; Ito, M.; Hiroyoshi, N. Simultaneous leaching of arsenite, arsenate, selenite and selenate, and their migration in tunnel-excavated sedimentary rocks: I. Column experiments under intermittent and unsaturated flow. *Chemosphere* **2017**, *186*, 558–569. [[CrossRef](#)] [[PubMed](#)]
35. Tamoto, S.; Tabelin, C.B.; Igarashi, T.; Ito, M.; Hiroyoshi, N. Short and long term release mechanisms of arsenic, selenium and boron from a tunnel-excavated sedimentary rock under in situ conditions. *J. Contam. Hydrol.* **2015**, *175–176*, 60–71. [[CrossRef](#)]
36. Porto, C.G. A Mineralização Aurífera do Depósito Córrego do Sítio e Sua Relação Com o Enxame de Diques Metamáficos No Corpo CACHORRO BRAVO—Quadrilátero Ferrífero—Minas Gerais. Master's Thesis, Universidade Federal de Minas Gerais, Belo Horizonte, Spain, 2008; pp. 1–117. (In English).
37. Goldfarb, R.J.; Groves, D.; Gardoll, S. Orogenic gold and geologic time: A global synthesis. *Ore Geol. Rev.* **2001**, *18*, 1–75. [[CrossRef](#)]
38. Lobato, L.M.; Ribeiro-Rodrigues, L.C.; Vieira, F.W.R. Brazil's premier gold province. Part II: Geology and genesis of gold deposits in the Archean Rio das Velhas greenstone belt, Quadrilátero Ferrífero. *Miner. Depos.* **2001**, *36*, 249–277. [[CrossRef](#)]
39. IBRAM—Instituto Brasileiro de Mineração. Available online: <http://www.ibram.org.br/> (accessed on 20 September 2020).
40. Deschamps, E.; Ciminelli, V.S.T.; Lange, F.T. Soil and sediment geochemistry of the iron quadrangle, Brazil the case of arsenic. *J. Soils Sediments* **2002**, *2*, 216–222. [[CrossRef](#)]
41. Vieira, F.W.R.; Biasi, E.E.; Lisboa, L.H. Geology of and excursion to the Morro Velho and Cuiabá mines. In *Field and Mine Trip to Quadrilátero Ferrífero. Brazil Gold'91 Internat Symp on the Geology of Gold*; Fleischer, R., Grossi, S.J.H., Fuzuikawa, K., Ladeira, E.A., Eds.; Departamento Nacional de Produção Mineral (DNPM): Minas Gerais, Brazil, 1991; pp. 87–99.
42. Vitorino, A.L.A.; e Silva, R.C.F.; Lobato, L.M. Shear-zone-related gold mineralization in quartz-carbonate veins from metamafic rocks of the BIF-hosted world-class Cuiabá deposit, Rio das Velhas greenstone belt, Quadrilátero Ferrífero, Brazil: Vein classification and structural control. *Ore Geol. Rev.* **2020**, *127*, 103–789. [[CrossRef](#)]
43. Almeida, F.F.M. *Origem e Evolução da Plataforma Brasileira*; Departamento Nacional de Produção Mineral (DNPM): Rio de Janeiro, Brazil, 1967; pp. 1–36.
44. Alkmin, F.F.; Marshak, S. Transamazonian Orogeny in the Souther São Francisco Craton Region, Minas Gerais, Brazil: Evidence for Paleoproterozoic Collision and Collapse in the Quadrilátero Ferrífero. *Precambrian Res.* **1998**, *90*, 29–58. [[CrossRef](#)]
45. IBGE—Instituto Brasileiro de Geografia e Estatística. Available online: <https://www.ibge.gov.br/> (accessed on 30 September 2019).
46. Moura, W. Especiação de Cianeto para Redução do Consumo no Circuito de Lixiviação de Calcinado da Usina do Queiróz. Dissertação de Mestrado, Departamento de Engenharia Metalúrgica e de Minas – UFMG, Belo Horizonte, Brazil, 2005; pp. 1–138. (In English).
47. ANM—Agencia Nacional de Mineração. Available online: <https://www.gov.br/anm/pt-br> (accessed on 30 September 2019).
48. Ciminelli, V.S.T. Arsenic in mining: Sources and stability. In *One Century of the Discovery of Arsenicosis in Latin America (1914–2014), Proceedings of the 5th International Congress on Arsenic in the Environment*, Buenos Aires, Argentina, 2014; Taylor & Francis Group: London, UK, 2014; pp. 3–7.
49. USEPA—United States Environmental Protection Agency. *Test Methods for Evaluating Solid Waste—Physical/Chemical Methods (SW-846)*; USEPA: Washington, DC, USA, 1996.
50. MEND—The Mine Environment Neutral Drainage Program. *Coastech Research, Acid Rock Drainage Prediction Manual, MEND Project Report*; MEND: Ottawa, ON, Canada, 1991.
51. MEND—The Mine Environment Neutral Drainage Program. *Prediction Manual for Drainage Chemistry from Sulphidic Geologic Materials. MEND Report. 1.20.1*; MEND: Ottawa, ON, Canada, 2009.
52. USEPA—United States Environmental Protection Agency. *Acid Mine Drainage Prediction: Technical Document, US EPA, Office of Solid Waste Special Waste Branch, EPA530-R94-036, NTIS PB94-201829*; USEPA: Washington, DC, USA, 2018.

53. Oliveira, W.S.; Neves, M.F.; Brito, M.M.B.; Mesquita, R.M.M.; Costa, D.S. Uso da flotação para o aproveitamento de um rejeito fino de minério de ouro. In Proceedings of the XXVI Encontro Nacional de Tratamento de Minérios e Metalurgia Extrativa 2015, Poços de Caldas-MG, Brasil, 18–22 October 2015.
54. CONAMA (CONSELHO NACIONAL DE MEIO AMBIENTE). *Resolução nº 396, de 03 de abril de 2008. Dispõe Sobre a Classificação e Diretrizes Ambientais Para o Enquadramento das Águas Subterrâneas e dá Outras Providências*; CONAMA: Brasília, Brazil, 2008.
55. Erguler, G.K.; Erguler, Z.A.; Akcakoca, H.; Ucar, A. The effect of column dimensions and particle size on the results of kinetic column test used for acid mine drainage (AMD) prediction. *Miner. Eng.* **2014**, *55*, 18–29. [[CrossRef](#)]
56. Falagán, C.; Grail, B.M.; Johnson, D.B. New approaches for extracting and recovering metals from mine tailings. *Miner. Eng.* **2016**, *106*, 71–78. [[CrossRef](#)]
57. Li, H.; Ma, A.; Srinivasakannan, C.; Zhang, L.; Li, S.; Yin, S. Investigation on the recovery of gold and silver from cyanide tailings using chlorination roasting process. *J. Alloy. Comp.* **2018**, *763*, 241–249. [[CrossRef](#)]
58. Lu, H.; Qi, C.; Li, C.; Gan, D.; Du, Y.; Li, S. A light barricade for tailings recycling as cemented paste backfill. *J. Clean. Prod.* **2020**, *247*, 119388. [[CrossRef](#)]
59. Araya, N.; Kraslawski, A.; Cisternas, L.A. Towards mine tailings valorization: Recovery of critical materials from Chilean mine tailings. *J. Clean. Prod.* **2020**, *263*, 121555. [[CrossRef](#)]
60. Alcalde, J.; Kelm, U.; Vergara, D. Historical assessment of metal recovery potential from old mine tailings: A study case for porphyry copper tailings, Chile. *Miner Eng.* **2018**, *127*, 334–338. [[CrossRef](#)]
61. Girotto, L.; Espíndola, E.L.G.; Gebara, R.C.; Freitas, J.S. Acute and Chronic Effects on Tadpoles (*Lithobates catesbeianus*) Exposed to Mining Tailings from the Dam Rupture in Mariana, MG (Brazil). *Water Air Soil Pollut.* **2020**, *231*, 1–15. [[CrossRef](#)]
62. Aires, U.R.V.; Santos, B.S.M.; Coelho, C.D.; Silva, D.D.; Calijuri, M.L. Changes in land use and land cover as a result of the failure of a mining tailings dam in Mariana, MG, Brazil. *Land Use Policy* **2018**, *70*, 63–70. [[CrossRef](#)]
63. Thompson, F.; Oliveira, B.C.; Cordeiro, M.C.; Masi, B.P.; Rangel, T.P.; Paz, P.; Freitas, T.; Lopes, G.; Silva, B.S.; Cabral, A.S.; et al. Severe impacts of the Brumadinho dam failure (Minas Gerais, Brazil) on the water quality of the Paraopeba River. *Sci. Total Environ.* **2020**, *705*, 135914. [[CrossRef](#)] [[PubMed](#)]
64. Rotta, L.H.S.; Alcântara, E.; Park, E.; Negri, R.G.; Lin, Y.N.; Bernardo, N.; Mendes, T.S.G.; Filho, C.R.S. The 2019 Brumadinho tailings dam collapse: Possible cause and impacts of the worst human and environmental disaster in Brazil. *Int. J. Appl. Earth Obs. Geoinf.* **2020**, *90*, 102119. [[CrossRef](#)]

Characterization of Arsenical Mud from Effluent Treatment of Au Concentration Plants, Minas Gerais – Brazil

Mariana Lemos^{1,2}, Teresa Valente¹, Paula Marinho¹, Rita Fonseca³, José Gregório Filho², José Augusto Dumont², Juliana Ventura², Itamar Delben⁴

¹Institute of Earth Sciences, Pole of University of Minho, University of Minho, Campus de Gualtar, 4710-057 Braga, Portugal

²Anglogold Ashanti, Mining & Technical, COO International, 34000-000, Nova Lima, Brazil

³Institute of Earth Sciences, Pole of University of Évora, University of Évora, 7000 Évora, Portugal ⁴Microscopy Center, Universidade Federal de Minas Gerais, 31270-013, Belo Horizonte, Brazil

Abstract

The determination of the general properties of arsenical mud was carried out in effluent treatment plant of an Au metallurgical facility, located in Nova Lima, Minas Gerais, Brazil. This effluent, which comes from the calcination stage, is treated via Fe-coprecipitation / lime-neutralization and thus mud with high As concentration is generated. Instrumental methods were applied to investigate physical-chemical characteristics, such as pH, in addition to the forms of occurrence of As and its associations. The results indicated that the mud has an alkaline pH (≈ 8.5), particles with grain size below 20 μm , and As, Fe, S and Al concentrations above 5%. The element As is essentially associated with Fe, Ca, S, and Al, forming phases with wide compositional variation as major and minor constituents generically classified as “complex sulfates” and “compounds with S”. The obtained results could assist optimization of the treatment routes in the plant and even to consider the potential reuse of this arsenic mud as a potential valuable product.

Keywords: Geochemistry and Environmental Mineralogy, Tailings Dam, Arsenic

Introduction

Arsenic (As) is a common deleterious element in gold (Au) deposits (Jacob-Tatapu 2018). Materials with elevated As concentration are difficult to process without the associated environmental risks. Very few facilities in the world are capable of treating material containing high concentration of As. The main sources are sulfides such as arsenopyrite, commonly associated with Au. In the Au metallurgical beneficiation process, stages for treating toxic elements in effluents are essential and corroborate the environmental and social responsibilities of a sustainable mining sector. Due to limited alternatives, the As is often volatilized or left in tailings exposed to lixiviation and are generally arranged in small dams or pits (Deschamps *et al.* 2002; Procópio 2004; Pantuzzo *et al.* 2007a; Bissacot *et al.* 2015; Moura 2015). This fact, coupled with challenges in the mineral industry regarding the sustainability of its resources and the difficulties of obtaining new environmental licenses, made critical the need for detailed characterization studies in search of new alternatives and

improvements for disposal of residues rich in As (Lemos *et al.* 2021a).

The work was focused on arsenical muds generated from the effluent treatment of an Au concentration plant, located in Nova Lima, Minas Gerais (Fig 1). The ore that feeds the plant comes from mines, located within the Rio das Velhas Greenstone Belt in the Iron Quadrangle region and are mainly composed of sulfides such as pyrite, arsenopyrite, pyrrhotite and rare sulfides, like as gerdosfite, galena, sphalerite (Lobato *et al.* 2001; Moura 2015; Kresse *et al.* 2018).

These sulfides are concentrated by flotation, calcined, and subsequently leached to recover Au, as illustrated in Fig 2 (Moura 2015). The As, originating from the sulfide concentrated, is volatilized in the form of As trioxide in the roasting stage, absorbed in an aqueous phase in the gas washing towers and finally removed by coprecipitation processes with iron and neutralization with lime (Fig 2). The resulting solid waste (arsenic sludge or mud) is then disposed of in waterproofed ditches (dug into the surface of the land), located in the plant's area of influence (Pantuzzo *et al.* 2007b).

Pantuzzo 2017 refers the presence of As in the waste ditches essentially associated with Fe and to a lesser extent with Ca (probably Caarsenates), Al, or even Mn, and Zn, through coprecipitation / adsorption mechanisms. However, it is necessary to detail the sources of As in the waste generated in the plant.

Therefore, the main objective of the present work is the characterization of this current arsenical mud after the neutralization step, mainly the geochemical and mineralogical properties, and identification of the neoformed host phases of As.

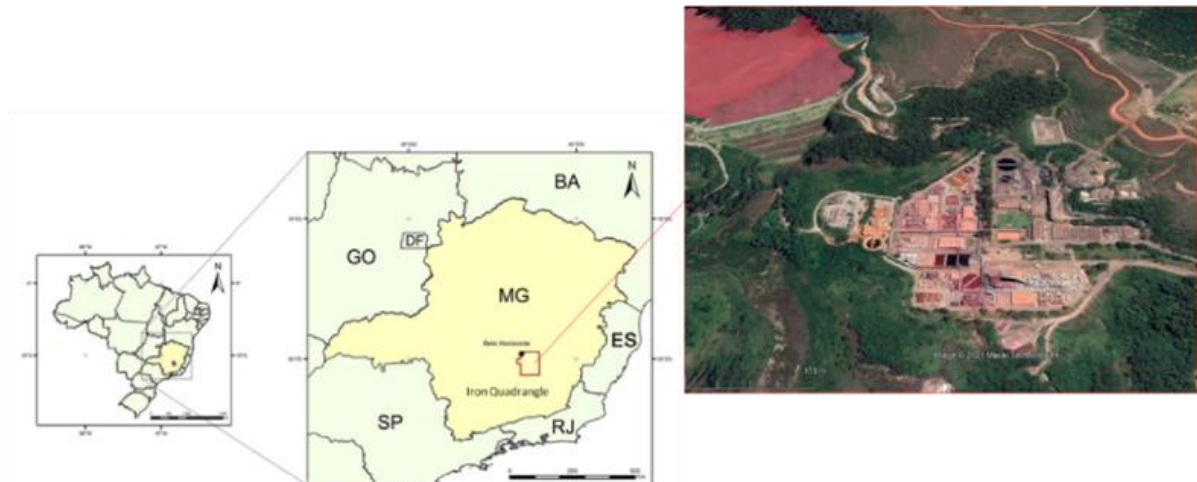


(Figura 5.10) **Figure 1** Study area: a. iron quadrangle map location (modified from Ruchkys U.A 2007) and Nova Lima location and b. Nova Lima Metallurgic plant (SIRGAS2000 – 10-09-2019).

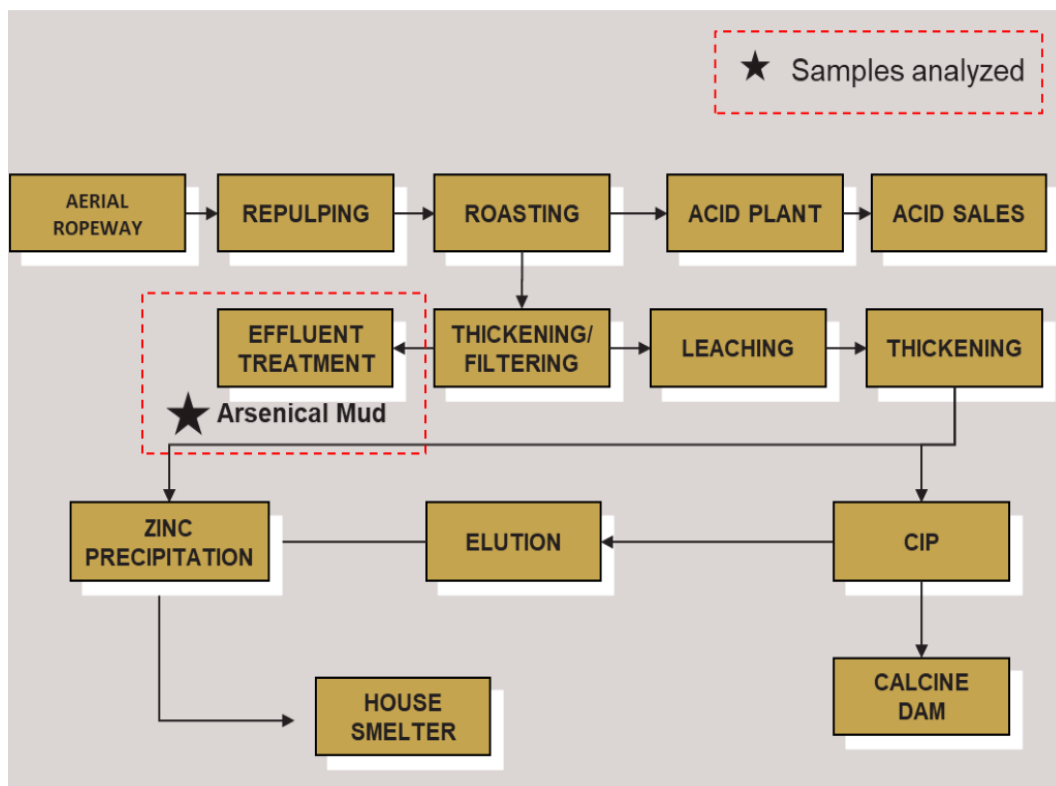


(Figura 5.11) **Figure 2** On-going workflow of Nova Lima's plant. The yellow stars represent sampling points in Arsenic effluent treatment (modified from Moura 2015).

Methods

The sampling campaign was performed over twenty-eight days in September 2019 during the production stage, representing a total of 40 samples after neutralization stage from the active plant (Fig 2). All samples were immediately sealed and refrigerated until analysis. Additional material was transferred to polypropylene bags and frozen until analysis. Refrigerated and frozen samples were packaged and shipped to the chemical laboratory for analysis.

Parameters such as pH of the effluent water samples were obtained using methodologies from the Standard Methods of Water and Wastewater (APHA 2005). Water

samples were filtered using a 0.45 µm filter (Sigma Aldrich) and subjected to chemical analysis by inductively coupled plasma mass spectrometry (ICP-MS) at Universidade Federal de Minas Gerais (UFMG) water analysis laboratory.

Chemical analysis of the solid tailings was performed by atomic absorption spectroscopy (AAS using AAS280 FS Varian). Infrared analysis (LECO) was used to obtain analytical S and C data.

The mineralogical study was carried out using polished sections analyzed by optical microscopy and scanning electron microscopy (SEM, Field Electron and Ion Company, FEI) at UFMG, Belo Horizonte.

(Tabela 5.4) **Table 1** Average water pH and concentration of major and trace elements - Solid and Water samples N – number of samples.

Physical parameters	Solid (N=40)	Residual Water (N=10)
	Average	Average
pH	-	8.5
Elements	%	mg/L
Fe	8.68	<2.50
As	3.58	5.31
S	13.30	436.39
Si	0.36	-
Ca	14.89	491,01
Al	1.50	<2.50
Mg	0.52	16.58
K	0.02	100.73
Zn	0.43	<0.1
C	0.10	-

(Tabela 5.5) **Table 2** Mineralogy of Solid samples (average values) N – number of samples.

Mineral/Composed	Solid (N=40)
	Average %
Hematite	1.13
Gypsum (Fe)	28.57
(CSA1 -3%As in composition)	38.36
(CSA2 -13%As in composition)	18.10
(CSA3 -5%As in composition)	11.68
Others	3.03

Results and Discussion

This section presents the general properties of the arsenic mud, which in general has particles of fine grain size (P80:15µm).

Geochemistry

The arsenical mud samples are mainly composed of Ca (14.5 - 17.2%), S (13.1 - 13.8%), Fe (6.8 - 8.7%), As (3.6 - 4.2%) and other elements in low concentrations (Tab. 1).

The water has low concentrations of Fe (<2.5 mg /L) and As (1.4 - 5.3 mg/L), which is consistent with the neutralization step in the beneficiation plant. For sulfur, the concentration of 1.0 g/L in the solution of the neutralization step is expected as the pH increases because of the lime addition. The consistency of this information is confirmed, therefore, by the concentration of Fe, As and S found in the solid phase already presented.

Mineralogy

The mineralogical study by SEM revealed the presence of Hematite, Gypsum, Sulfo Arsenical Compounds (CSA), Compounds with S and other elements (Ca, Al, Si, Mg and Fe), Al silicates, Ferrosaponite, Gibbsite and Fe / Al oxides. The types of arsenical sulfo compounds (CSA) were differentiated by their As amount, varying from 3 to 13% (Tab 2; Fig 3). In addition to As and S, they are made up of Fe, Al, Zn, Ca.

The arsenical mud consists essentially of "CSA 1" (38.36% by weight), and "Gypsum Fe" (28.57% by weight). The total percentage of all phases with S (sulfates, "Compounds with S" and "CSA") is 90.63% (Fig 3). Also noteworthy are the low amounts of "Hematite", which make up a total of 1.13% by weight in this sample, as well as quartz and other silicate phases classified as others.

The predominant presence of calcium and sulfur is consistent with the identification of gypsum indicated by electron microscopy (Fig. 3). On the other hand, the occurrence of Fe and As in relevant quantities is associated with the complex phases that contain variable concentrations of As.

The samples underwent several types of "attacks", from breaking the structure by calcination, followed by complementary chemical processes. This can result in complex phase transformations and, in addition, chemical dissolutions and substitutions in the crystalline structure. As a result, some phases have very complex micro-chemical and textural compositions. These phases with wide compositional variations and made up of several elements as major and minor constituents were generically classified as "Complex Sulfates", "CSA". The rate of this transformation should be directly related to the size of the particles and the availability of the surface for reaction.

In calcination, part of the Fe^{+2} released from the dissolution of the primary minerals (sulfides, oxides, silicates with Fe) is oxidized to Fe^{+3} and precipitated as hematite / oxides, which in turn, may have been attacked chemically generating skeletal and porous hematite, richer in contaminating elements (Fig 3b).

In addition, the breakdown of the structure by calcination may result in ion solubilization, such as Ca and Mg, of some silicates (and carbonates) originally present. Also, the leaching of elements by acidic attacks and the addition of lime and precipitating agents may have caused the precipitation of phases, such as gypsum and other sulfates, dissolution and ionic substitutions, partial to total, resulting in the formation of complex phases, with various constituent elements (e.g., Fe, S, Ca, Mg, Al, Si). Fig 4, therefore, illustrates the transformations of As minerals along the process of this metallurgical plant until the generation of the arsenical sludge.

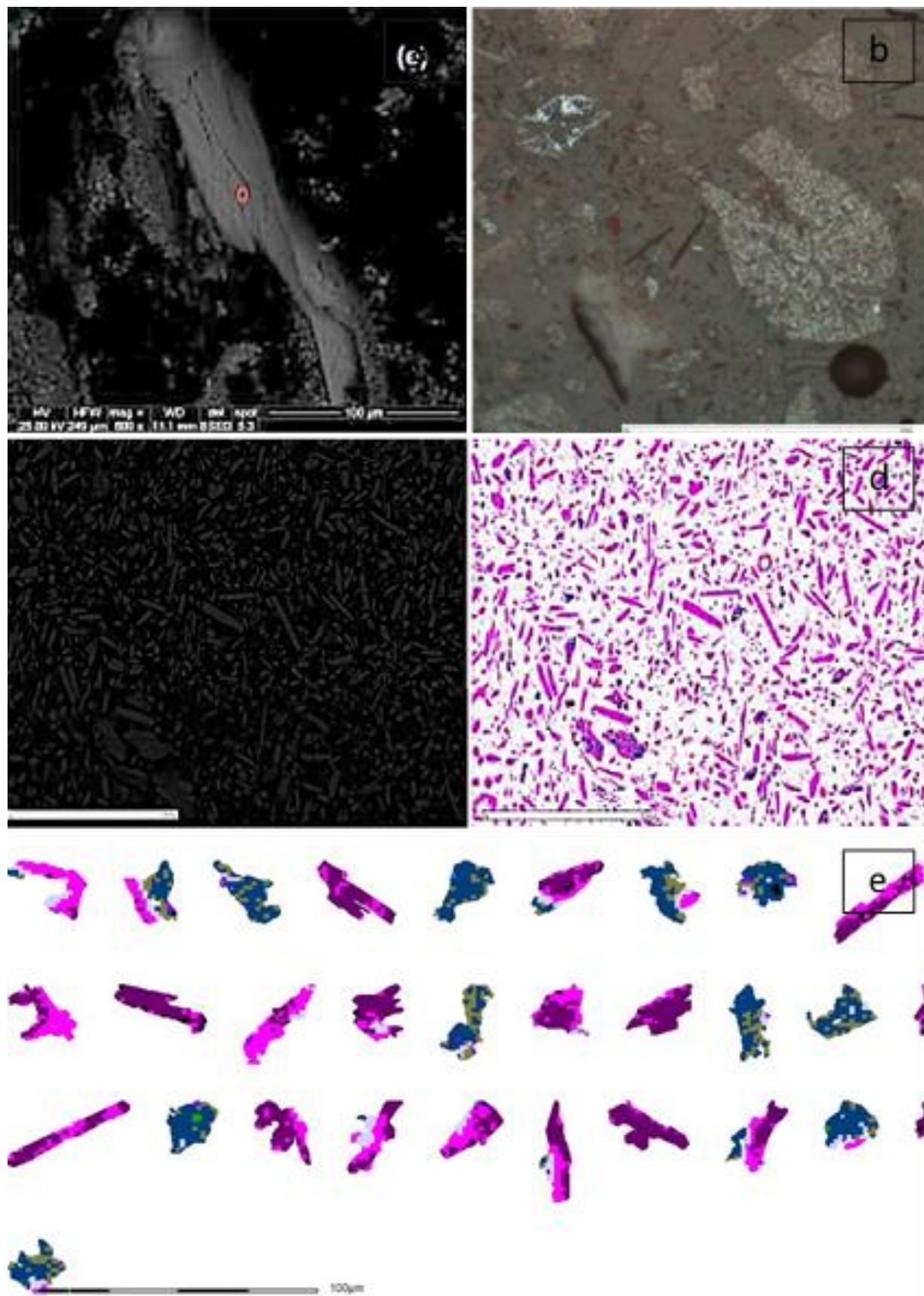


(Figura 5.12) **Figure 3** Backscattered electron image of Sulfo Arsenical Compounds in arsenical mud. a) CSA, b) Reflected light image of porous hematite, c) total sample, d) and e) false image of total samples (pink, purple and blue – Gypsum (pink/purple) and CSA (Blue).

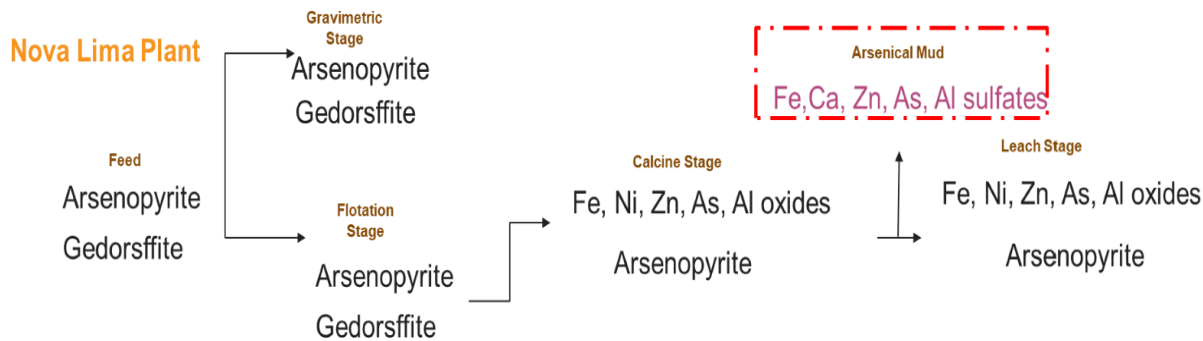


(Figura 5.13) **Figure 4** Transformation path of As sources along Nova Lima Au metallurgical plant until neoformation of arsenic mud.

Conclusions

Arsenical sludge is the product of the neutralization stage of the Au treatment of a plant located in Nova Lima, Brazil. An integrated characterization, including geochemistry and mineralogy was performed to evaluate the sources of As and their associations. The predominant presence of Ca and S is consistent with the identification of gypsum. On the other hand, the occurrence of Fe and As in high quantities is mainly associated with the complex phases with variation in the grades of As.

The arsenical mud is mainly composed by Ca (14.5 - 17.2%), S (13.1 - 13.8%), Fe (6.8 - 8.7%) and As (3.6 - 4.2%). It is noteworthy that the water has low concentrations of Fe (<2.5 mg/L) and As (1.4 - 5.3 mg/L), which is expected after the neutralization step. The samples analysed underwent several types of “attacks”, from

breaking the structure by calcination, followed by complementary chemical attacks. This resulted in complex phase transformations and, in addition, chemical dissolutions and substitutions in the crystalline structure. As a result, some phases have very complex microchemical and textural compositions. In the analyzed samples, these phases with wide compositional variations and made up of several elements as major and minor constituents were generically classified as “Complex Sulfates”, “CSA”.

From the results of this characterization study, it is possible to propose optimization in the current treatment routes and even propose new alternatives, in addition to initiatives in the reuse of these as a valuable product for As recovery.

Acknowledgements

We thank our colleagues from ICT, microscopy center from Universidade Federal de Minas Gerais (CM-UFGM), and Anglo Gold Ashanti who provided insight and expertise that greatly assisted the research. This work was funded by FCT—Fundação para a Ciência e a Tecnologia through projects UIDB/04683/2020 and UIDP/04683/2020 and Nano-MINENV 029259 (PTDC/CTA-AMB/29259/2017), and by AngloGold Ashanti Brazil.

References

- Bissacot L, Ciminelli V, Logsdon M (2015) Arsenic Mobility under a Neutral Mine Drainage Environment in a Gold-Mine Tailings Dam Deschamps E, Ciminelli VST, Lange FT, *et al* (2002) Soil and sediment geochemistry of the iron quadrangle, Brazil: The case of Arsenic. Journal of Soils and Sediments 2:216–222. <https://doi.org/10.1007/BF02991043>

- Jacob-Tatapu KJ (2018) Investigating the elevated arsenic concentrations in the Gold Ridge Tailings Storage Facility surface water. School of Civil Engineering
- Kresse C, Lobato LM, Hagemann SG, Figueiredo e Silva RC (2018) Sulfur isotope and metal variations in sulfides in the BIF-hosted orogenic Cuiabá gold deposit, Brazil: Implications for the hydrothermal fluid evolution. *Ore Geology Reviews* 98:1–27. <https://doi.org/10.1016/j.oregeorev.2018.05.012>
- Lemos MG, Valente T, Marinho-Reis AP, et al (2021a) Geoenvironmental Study of Gold Mining Tailings in a Circular Economy Context: Santa Barbara, Minas Gerais, Brazil. *Mine Water and the Environment* 40:257–269. <https://doi.org/10.1007/s10230-021-00754-6>
- Lemos MG, Valente T, Marinho-Reis AP, et al (2021b) Geoenvironmental Study of Gold Mining Tailings in a Circular Economy Context: Santa Barbara, Minas Gerais, Brazil. *Mine Water and the Environment* 40:257–269. <https://doi.org/10.1007/s10230-021-00754-6>
- Lindsay MBJ, Moncur MC, Bain JG, et al (2015) Geochemical and mineralogical aspects of sulfide mine tailings. *Applied Geochemistry* 57:157–177
- Lobato LM, Ribeiro-Rodrigues LC, Zucchetti M, et al (2001) Brazil's premier gold province. Part I: The tectonic, magmatic and structural setting of the Archean Rio das Velhas greenstones belts, Quadrilátero Ferrífero. *Mineralium Deposita* 36:228–248. <https://doi.org/10.1007/s001260100179>
- Moura (2015) Lixiviação Queiroz. Thesis
- Pantuzzo FL, Cimiclini VS, Braga frany (2007a) Especiação do arsênio em lamas arsenicais
- Procópio SO (2004) Caracterização de rejeito de mineração de ouro para avaliação de solubilização de metais pesados e arsênio e revegetação local (1) seção ix-poluição do solo e qualidade ambiental
- Ruchkys U.A (2007) Patrimônio Geológico e Geoconservação no Quadrilátero Ferrífero, Minas Gerais: Potencial para a Criação de um Geoparque da UNESCO. Universidade federal de minas gerais instituto de geociências programa de pós-graduação em geologia coorientação carlos schobbenhaus. Belo horizonte

5.1.2. Distribuição dos elementos químicos e modelamento 3D

A distribuição de elementos encontrados nas barragens de rejeito e suas formas de acumulação, são apresentadas e discutidas em dois artigos. O primeiro, além de demonstrar as formas de distribuição, passa também pelas principais características das águas e sólidos amostrados. São apresentados os primeiros resultados do potencial reprocessamento do Au e outros elementos como As e Sb. O artigo intitulado como *Geoenvironmental Study of Gold Mining Tailings in a Circular Economy Context: Santa Barbara, Minas Gerais, Brazil* (<https://doi.org/10.1007/s10230-021-00754-6>) foi publicado pela revista *Mine Waters and the Environment* da editora Springer.

A presença e o potencial reaproveitamento de Au é indiscutível para todos as TSF estudadas. Portanto, o artigo *Geochemistry and mineralogy of auriferous tailings deposits and their potential for reuse in Nova Lima Region, Brazil* (<https://doi.org/10.1038/s41598-023-31133-6>) foca-se no modelamento de Au e o potencial de seu processamento, estando publicado na revista *Scientific reports* da editora *Nature*.

TECHNICAL ARTICLE



Geoenvironmental Study of Gold Mining Tailings in a Circular Economy Context: Santa Barbara, Minas Gerais, Brazil

M. G. Lemos^{1,2} · T. Valente¹ · A. P. Marinho-Reis^{1,3} · R. Fonsceca⁴ · J. M. Dumont² · G. M. M. Ferreira² · I. D. Delbem⁵

M. G. Lemos mglemos@anglogoldashanti.com

¹ Institute of Earth Sciences, Pole of University of Minho, Campus of Gualtar, 4710-057 Braga, Portugal

² Anglogold Ashanti, Mining and Technical, COO International, Nova Lima 34000-000, Brazil

³ Geobiotec, Departamento de Geociências, Universidade de Aveiro, Campus Universitário de Santiago, 3810-193 Aveiro, Portugal

⁴ Institute of Earth Sciences, Pole of University of Évora, University of Évora, 7000 Évora, Portugal

⁵ Microscopy Center, Universidade Federal de Minas Gerais, Belo Horizonte 31270-013, Brazil

Received: 3 February 2020 / Accepted: 14 January 2021 / Published online: 31 January 2021

© Springer-Verlag GmbH Germany, part of Springer Nature 2021

Abstract

We characterized the tailings from the Santa Barbara tailings dam, which is located in Minas Gerais, southeastern Brazil, to: (i) identify its chemical, mineralogical, and metallurgical properties, and (ii) perform an environmental evaluation of the water at the surface of the tailings facility. The potential recovery of elements such as Sb, As, and Au was also considered for potential tailings reuse. The water was alkaline, with maximum pH values of ≈ 10 , and contained potentially toxic elements, such as Sb (up to 0.500 mg/L), As (up to 0.080 mg/L), and Cu (up to 20 mg/L). Gold enrichment areas were found in the tailings dam, with concentrations up to 0.5 g/t. Alignment exists among tailings management, demand for critical raw materials, and increased interest in the processing of low-grade ores and mining waste, which is important in the context of the circular economy. They suggest that valorisation of tailings, although challenging, can be achieved by economic recovery of the more valuable metals.

Keywords Geochemistry and environmental mineralogy · Tailings dam · Environmental risk assessment and characterization

Introduction

The amount of waste rock and tailings produced over a mine's life cycle depends, among other aspects, on the extraction process, the concentrations of valuable minerals, and the location of the deposit. The exact quantification of the produced waste is complex due to the diversity of operations and technologies used in extraction and beneficiation processes (Souza Junior et al. 2018). While variable, the volume of mine wastes is almost always high. Lottermoser (2007) estimates the ratio of tailings to concentrate is generally around 200:1. The total non-coal mine waste lying in dumps around the world was estimated in 1985 at 50,000 Mt; of this, 33% were tailings, 17% dump/heap leach wastes and mine water, and 50% surface and underground waste rock (1985 Report to Congress, after Wilmoth 2000 in Twardowska et al. 2004). According to Blight (2011), South Africa's gold mining industry produced 7.4×10^5 t of tailings from 1997 to 2006. In Brazil, it is estimated that 3.8 M oz. of gold can be found in old tailings dam(s) operated from 1834 to 1982.

In the traditional metal mining sector, waste rock dumps and tailings dams are among the infrastructures with the greatest environmental impact. Tailings are especially contaminated due to their fine particle size and comparatively high surface area, which sorb contaminants (HudsonEdwards et al. 2008) and can chemically change after deposition (Kossoff et al. 2014). The generation of tailings can have serious

negative repercussions for stakeholders and the global economy (Gaustad et al. 2017). Therefore, industrial water supply and contamination by potentially toxic elements are worldwide environmental problems in the mineral sector (Acheampong et al. 2010).

In Brazil, in addition to this reality and a linear economic model approach, the latest Mariana and Brumadinho-Minas Gerais tailings dam failures (respectively, Nov. 2015 and Jan. 2019), drew attention to the sector's problems and enhanced the difficulty of obtaining environmental permits and suitable places for tailings disposal. Consequently, the mining industry faces increasing economic, social, and environmental challenges. The need to ensure sustainable mining in compliance with legal environmental frameworks is leading the sector towards a new paradigm.

The key component of the circular economy is extending the useful life of raw materials that have already been extracted from the ecosphere (Gaustad et al. 2017) in a restorative perspective that minimizes systemic risks by managing finite inventories and renewable flows of resources (Araújo et al. 2017; Ellen Macarthur Foundation 2013). Besides this, according to the latest British supply risk list of chemical elements (British Geological Survey 2015), rare earth elements (REE), antimony (Sb), germanium (Ge), bismuth (Bi), as well as arsenic (As), platinum group elements (PGE), and cobalt (Co) are potentially subject to high levels of risk of supply disruption. In this context, Tayebi-Khorami et al. (2019) suggest five main areas of integration within the mining sector: social dimensions, geoenvironmental aspects, geometallurgy specifications, economic drivers, and legal implications. Considerable research and development are still necessary to identify effective solutions in each of these key areas. There are several broad ways to do this in the mining context, including residue valorisation, wherein the residues formed during the metal extraction process are valorized (i.e. transformed into a product with value). It also involves processing residues, such as wastewaters, waste solvents, solid residue, exhaust gasses, and ashes (Singh et al. 2020; Spooren et al. 2020). Reuse and reprocessing of tailings are possible approaches but require characterization efforts supported by robust geochemical and mineralogical techniques. These include x-ray diffraction (XRD) and x-ray fluorescence (XRF) in association with quantitative electronic mineralogy (Pires et al. 2019) for mineralogical characterization, automatic quantification of mineral phases, time-of-flight secondary ion mass spectrometry (TOF-SIMS), laser ablation inductively coupled plasma mass spectrometry (LA-ICP-MS), and electron backscatter diffraction (EBSD) (e.g. Guanira et al. 2020; Martin et al. 1997; Novhe et al. 2018; Parbhakar-Fox 2016; Shi et al. 2009; Silva et al. 2004).

Biosorbents and nanofibers may prove to be a way to recover metals such as Cu, Pb, and Cd from effluent water (Sang et al. 2008; Li et al. 2013), and precious metals can potentially be recovered from mine waters and leachates as well. Other approaches, such as ion flotation, suggest good recovery for Cu (Jafari et al. 2017). Acid mine drainage (AMD) remediation has high costs, but could represent a source of metals, as shown by Skoronski et al. (2017), through recovery of Al and Fe contaminants in usable forms, and show new forms to minimize the cost of water treatment (Akinwekomi et al. 2020, Ryan et al. 2017). The work of Antunes et al (2010); Hedin (2003); Silva et al. (2019); and Valente et al (2016) indicate the potential of recovering ochre-precipitates from passive AMD treatment, for use as pigments and in the ceramic sector. Also, Grande et al. (2013) presented a system to neutralize AMD and recover its metal load, using energy obtained from renewable sources. Thus, neutralization and treatment could serve the purpose of reducing environmental liabilities while generating income, in agreement with the circular economy paradigm (Valente et al. 2016).

There are many examples of case studies and implementations for recovering metals and metalloids from mining waste. An example of current development is vitrification of contaminants such as As and Sb (US9981295B2—Dundee Sustainable Technologies 2016), which has been implemented at gold mines in South Africa, Canada, and Brazil. Sensor-based technologies can be useful in coarse wastes and old stockpiles to reprocess and recover tin, tungsten, and gold (Manoucheri et al. 2016; Robben et al. 2020; Von Ketelhodt

2009). Altinkaya et al. (2019) suggested new approaches to recover trace metals from sulfide flotation tailings in cupric chloride solutions; recoveries of Cu, Ni, Zn, Co, Fe, and Au exceeded 58%. Pretreatment of cyanide tailings by magnetic roasting and its effect on the followed comprehensive recovery of valuable metals were investigated in Liu et al. (2013). The results indicate that the leaching rate of gold reaches 46.1% and that the magnetic susceptibility of iron is up to 86.3%. In addition, there are opportunities for extracting precious metals and other critical substances like Ag, Pt, In, Ge W, Cu, Zn, Pb, and Sb via common metallurgical routes, using regrinding, flotation, roasting, leaching, bioleaching, etc. (e.g. Chen et al. 2014; Dehghani 2009; Falagán 2017; Martin et al. 2015).

The present study applies the concept and goals of the circular economy to gold processing tailings in Santa Barbara, MG, Brazil. The main aims are to: (i) evaluate the quality of the surface effluent water; (ii) present an integrated physical, geochemical and mineralogical characterization of the solid tailings; and (iii) understand the chemical and grade distribution and potential for metallurgical extraction of various elements from the tailings dam. Overall, the study demonstrates the potential of recovering metals in a conceptually linear process, promoting a more sustainable Study Site.

The study area is in the Iron Quadrangle (QF), a metallogenic province that hosts large gold and iron deposits, in addition to industrial gems and minerals (Porto 2008). The QF represents one of the most important geotectonic unit with rocks and geological evolution of Archaean and Proterozoic ages (Almeida 1967). Three main tectono-stratigraphic domains compose the QF province: granite-gneissic terrains, a sequence of greenstone belt type (Rio das Velhas Supergroup—SGRV), and a supracrustal sequence of chemical and clastic sedimentary rocks (Minas Supergroup). The Rio das Velhas Greenstone Belt, largely located in the State of Minas Gerais (Fig. 1a), is the most important gold district in Brazil, with an estimated 4.5% (936 t) of the world's ore reserves (Goldfarb et al. 2001; Lobato et al. 2001b). From the bottom to the top, it comprises tholeiitic mafic volcanic rocks and komatiites, banded iron formations of the Algoma type, metavolcanoclastic schists and phyllites, and terrestrial clastic sequences, all metamorphosed into greenschist to amphibolite facies (Fig. 1b; Almeida 1976; Schorscher 1978). The mineralized bodies, hosted in Archaean rocks, are structurally associated and controlled by hydrothermal alteration.

The Santa Barbara tailings dam is located in the northern part of the QF, in Santa Bárbara, Minas Gerais, 110 km from Belo Horizonte (Fig. 1). Underground mine waste from gold metallurgical plants has been deposited in this structure (Fig. 1c) since 1986.

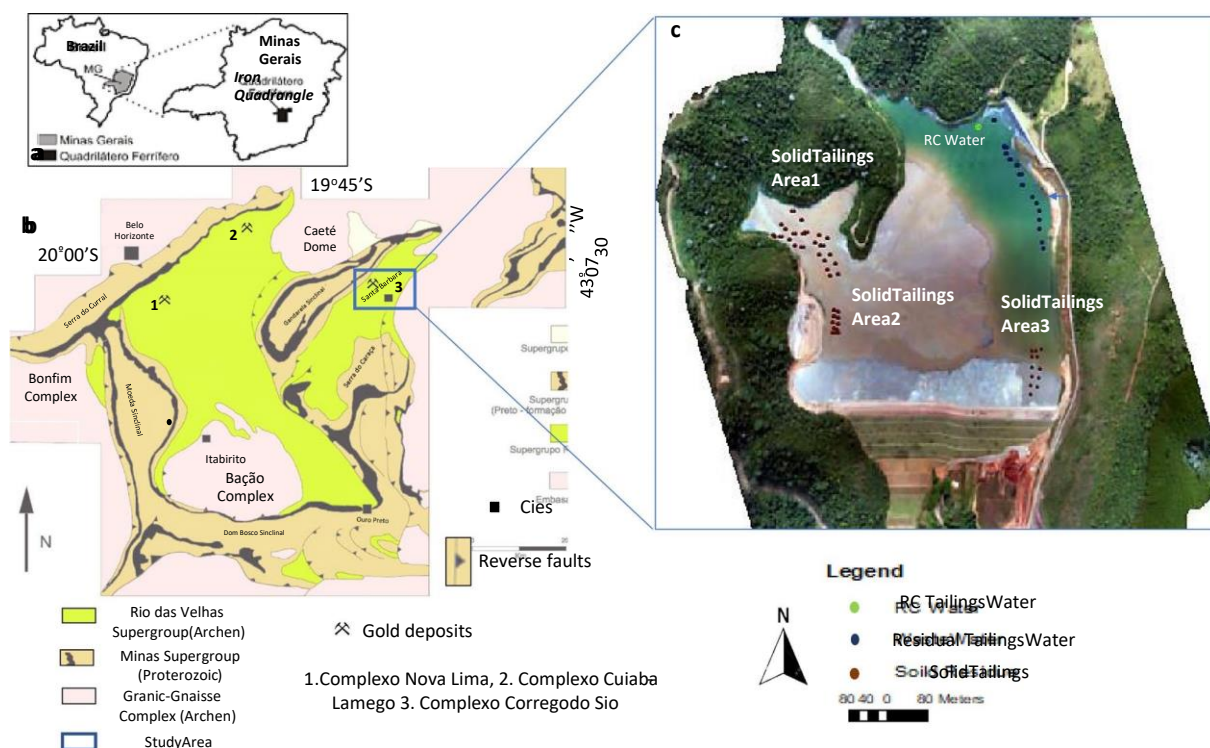


(Figura 5.14) **Fig. 1** a Location of study area; b Iron Quadrangle map (modified from Alkmin et al. 1998; Ruchkys et al. 2013; Porto 2008); and c sampled area (SIRGAS2000 – 14–06–2019).

Santa Barbara has a tropical climate with dry winters and humid summers. The hottest month is February, with an average temperature of 27 °C, and the coldest is July, with 13.6 °C. The average annual rainfall is 1897 mm, higher in the summer (IBGE 2019).

The Santa Barbara tailings dam lies within the geological context of the Córrego do Sítio unit (Baltazar 1998). The Córrego do Sítio unit is a metamorphosed turbidite in an alternating sequence of metagraywacke and phyllites, enclosing metamafic dikes and sills. The ore zone lies at the stratigraphic discontinuity between metasedimentary and metamafic rocks. The gold is associated with arsenopyrite and pyrite, which are disseminated in metapelitic rocks and quartz-carbonate veins. The mineralization includes several stages of crystallization: (1) pyrite and pyrrhotite, (2) arsenopyrite, pyrrhotite, and fine pyrite, (3) arsenopyrite with pyrrhotite and sulfosalts in quartz vein, and (4) pervasive pyrite (David 2006; Porto 2008). The sulfosalts are mainly represented by berthierite.

The mined ore feeds the metallurgical plant, where it undergoes: (1) crushing, (2) grinding, (3) gravimetric separation, (4) sulfide flotation, (5) pressure oxidation in an autoclave, and (6) leaching. Currently, only 25% of the run-of-mine (ROM) mass is used to recover gold, with variations related to the ore type treated (Lemos et al. 2019), resulting in different volumes and gold grades in the deposited tailings. Water from the metallurgical process is reused without treatment (RC—Fig. 2c).

The Santa Barbara tailings dam was built using a centerline method and spreads over a 25 km² area (Fig. 2). Water and solid tailings from the flotation and leaching operations are deposited in this structure with a capacity of 5MM m³ of tailings (AGA 2018). After the Brumadinho tragedy, only last-stage tailings are collected in the dam, since all flotation tails now pass to a dry stack process. However, from 1986 to 2019, the dam received considerable volumes of mine tailings, thus suggesting considerable potential for reuse studies.

Materials and Methods

Sampling occurred during the end of winter and early spring (from late August to late September 2019). In this season, the weather varied between dry and humid periods, with rainfall occurring in the late afternoon. Temperatures ranged from 19 to 25 °C (IBGE 2019). The water samples were collected in the flooded areas (total 14 sites—Fig. 1b) and from the catchment that stores the water tailings reused in the metallurgical plant (total of 10 water samples representing one month period, three times per week). The water was stored in polyethylene bottles and kept at a 4 °C until analysis. Samples for metal analysis were acidified with H NO₃ to avoid precipitation.

A total of 123 sediment samples were collected using an auger, drilling up to 2 m (Fig. 1b). The dam was divided into three regions that were dry and had safe access. The distance between the samples ranged from 13 to 20 m, depending on the sampling area.

In the laboratory, parameters such as pH, Eh, turbidity, and electrical conductivity of effluent water samples were obtained using methodologies from the Standard Methods of Water and Wastewater (APHA 2005). Water samples were filtered using a 0.45 µm filter (Sigma Aldrich) and subjected to chemical analysis for Fe, Al, S, As, Cu, Sb, and Au by inductively coupled plasma mass spectrometry (ICP-MS) at Universidade Federal de Minas Gerais (UFMG) water analysis laboratory.

Chemical analysis of the solid tailings was performed by atomic absorption spectroscopy (AAS using AAS280 FS Varian) to determine Cu, As, Sb, S, and Fe. Fire assaying was used to obtain analytical gold data from the tailings. The choice of these elements was based on ore mineralogy and concentrations during production monitoring.

All the reagents used were of analytical grade. All metal solutions were prepared from concentrated stock solutions (Sigma Aldrich). High-purity water (HPW) was produced with a Millipore Milli-Q Academic system, which was used throughout the analytical process. Each sample batch prepared for ICP-MS and AAS analysis included water samples, duplicates, blanks, and standard reference materials for quality assurance and quality control (QC/QA) procedures. The Certified Reference Materials Si81 (Rocklabs) for solid tails were selected to represent a wide range of total elemental concentrations. Results of method blanks were always below detection limits. Values for precision (expressed as RSD %) were typically less than 15% for all elements.

In addition to the geochemical data, polished sections were prepared for mineralogical characterization. The mineralogical study was carried out using optical microscopy and scanning electron microscopy (SEM, Field Electron and Ion Company, FEI) at UFMG, Belo Horizonte. The samples were analyzed in a FEI electronic microscope, Quanta 600 FEG, high vacuum mode, coupled to the automated analyzer software (MLA—mode GXMAP and SPL-DZ) and the EDS Espirit Bruker (20Kve) microanalysis system.

To evaluate the potential of recovering metals and metalloids such as Au, Sb, and As, three batch tests were conducted on samples composed of solid wastes representing the three areas (Fig. 1c). The first test was an attempt to recover Sb and As thermally (Dundee Sustainable Technologies 2016; Liu et al. 2013; Padilha et al. 2014) by volatilizing and collecting it downstream as an oxide byproduct. The goal was to volatilize the Sb in the kiln in an inert or reducing atmosphere, separating it from the gangue material, and then oxidize it as it exited the kiln body. The experiment was conducted in a rotary horizontal quartz kiln, in a single stage with a final temperature of 850 °C, for 350 min in an atmosphere of 20% CO and 80% N₂. The second test was conducted in two stages with a final temperature of 930 °C, 994 min, and an atmosphere of 3% O₂ and 97% N₂. Another experiment was made in a wet, high intensity magnetic separator (WHIMS) as some successful applications of this methodology for iron, copper, and lead recovery from tailings have been described (Guest et al. 1988; Rao et al. 2016). The test occurred in five stages to reproduce a high grades Sb concentrate. A 200 g sample of the solid tailings was processed using an Eriez L4 WHIMS unit. Tailings from each separation were reprocessed at successively higher magnetic intensities (1500–10,100 G). For Au recovery, well-established bottle roll tests were performed in an agitated cyanide leaching solution at a pH

of 11. Oxygen levels, alkalinity, acid consumption, and other parameters were monitored and strictly controlled.



(Figura 5.15) Fig. 2 a Operational unit and tailings dam. b Panoramic image (bird's eye view) of residual water tailings.

Results and Discussion

Surface Effluent Water

Table 1 presents the physical and chemical parameters of the water collected from the tailings dam's surface. Liquids samples from accumulated flooded areas (RP) were compared with samples taken over time from the point of return to the plant (RC – Fig. 2b). Mine waters are very often acidic due to the water–rock interaction processes involving sulfides, but neutral to alkaline waters are also common and may present high concentrations of metals and metalloids (Nordstrom 2011).

(Tabela 5.6) Table 1 Statistical summary of effluent water physical–chemical parameters and dissolved EC electrical conductivity
SD – Standard deviation

Physical Parameters	RC WasteWater (N = 10)				Residual WasteWater (N = 14)			
	Mean	Max	Min	Stdesv	Mean	Max	Min	Stdesv
Turbidity (NTU)	17.0	65.0	4.56	13.7	22.00	40.00	9.00	8.36
eC (um/cm)	2822	4058	2414	353	3390	5076	2077	770
pH	8.60	9.71	8.00	0.449	8.56	9.90	7.80	0.512
eH	234	264	214	14.8	250	288	215	23.6
Metals (mg/L)								
Au	< 0.05	< 0.05	< 0.05	0	0.136	0.17	0.07	0.022
Fe	0.264	0.315	0.22	0.034	0.208	1.96	0.04	0.206
Al	0.310	0.386	0.247	0.051	0.278	0.35	0.12	0.042
Cu	5.23	11.4	3.37	1.77	23.6	24.9	21.0	0.769
Sb	0.645	0.652	0.632	0.009	0.639	0.664	0.610	0.023
SO ₄	1683	1759	1570	75.6	1754	1914	1683	54.9
As	0.046	0.074	0.023	0.012	0.075	0.15	0.06	0.021

In the present study, the results (Table 1) indicate that water quality was controlled not only by the ore deposit geology, but especially by the processing conditions in the hydrometallurgical plant. Therefore, sulfate occurs in high concentrations (1683–1914 mg/L in RP), in accordance with the ore mineralogy

characterized by the presence of sulfides (pyrite, pyrrhotite, arsenopyrite). However, there are no AMD conditions as minimum pH is around 8, reaching a maximum of 10, reflecting the alkaline products used for extraction of gold with cyanide solutions. Therefore, as referred by Dold (2014), the general properties are typical of the operational phase of mining tailings, with an alkaline pH-Eh regime, and high concentrations of sulfate, metals (Cu), and metalloids mobilized from the primary minerals.

Climatic conditions control the evaporation/concentration and leaching/dilution cycle at tailings dams. Consequently, the difference between the residual and recirculated water may be due to these effects since the RC samples were collected over a two month period with rainfall; thus, the concentration changes could be due to dilution, in addition to these other parameters.

Comparing the two samples groups suggests a decrease in the mean values of some of the RC parameters, including sulfate, As (which decreased by \approx 40%), and especially Cu, which changed from 23.6 mg/L in RP to 5.23 mg/L in the recirculated water (a decrease of \approx 78%). The variability observed for Au in the RP was also noteworthy. Comparing the results, the Cu values were generally above the discharge limits in Brazil (CONAMA 2005). Therefore, this characteristic is another motivator for studying the effluent for reuse of metals.

Solid Tailings

Among physical properties, grain size is a key issue to consider, both for environmental implications and potential for economic recovery. Many properties, such as specific surface area, are dependent on particle size. Consequently, processes such as adsorption/desorption, dissolution rates, and the general reactivity of the tailings are controlled by grain size fractionation. Figure 3 shows the average particle size distribution of the Santa Barbara dam samples. Results indicate that 80% pass through a 40 μm sieve. Thus, similar to many other tailings storage facilities (e.g. Nengovhela et al. 2006), this profile is dominated by silt and clay sized particles.

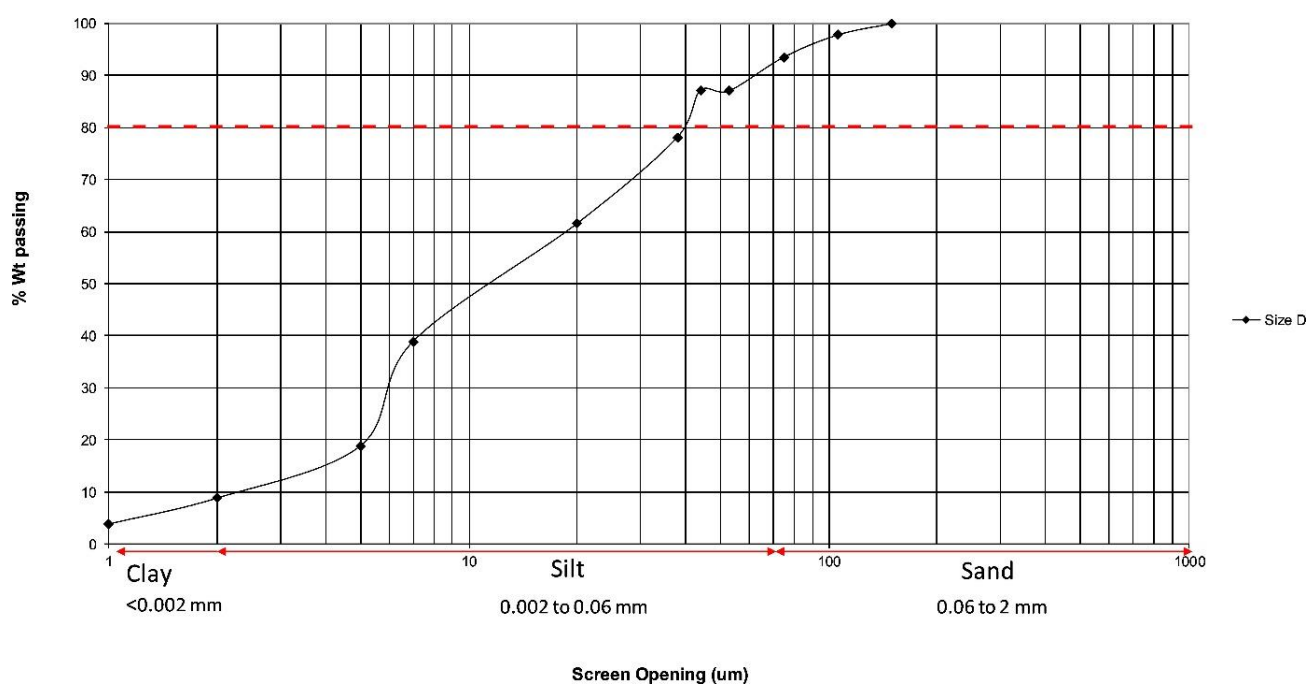


(Figura 5.16) Fig. 3 Size distribution (Krumbein phi scale) of solid tailings from the Santa Barbara tailings dam.

The chemical composition of the tailings is presented in Table 2 as a statistical summary for the sampled areas (Fig. 1c) and the two depths. In general, the Au mean grades were 0.505 g/t for the first sampled meter (S1m) and 0.684 g/t for the second sampled meter (S2m).

(Tabela 5.7) **Table 2** Summary statistics of Au, S, As, Fe, Sb and Cu by Depth and Sampled Area.

		Element	Depth (m)	Mean	StDev	Minimum	Maximum
Area 1 (N1m = 24 and N2m = 24)	Au g/t	1		0.619	0.119	0.470	0.910
		2		1.02	1.242	0.510	6.74
	S (%)	1		0.880	0.219	0.100	1.28
		2		0.925	0.127	0.750	1.21
	As (%)	1		0.065	0.072	0.001	0.170
		2		0.060	0.074	0.001	0.180
	Fe (%)	1		2.74	0.976	1.08	5.88
		2		2.87	0.897	1.74	4.90
	Sb (%)	1		0.189	0.258	0.002	0.808
		2		0.241	0.282	0.002	0.988
	Cu (%)	1		0.011	0.010	0.001	0.030
		2		0.009	0.009	0.001	0.040
Area 2 (N1m = 10 and N2m = 5)	Au g/t	1		0.316	0.098	0.250	0.590
		2		0.293	0.076	0.240	0.380
	S (%)	1		0.603	0.526	0.005	1.23
		2		0.957	0.074	0.900	1.04
	As (%)	1		0.156	0.029	0.100	0.190
		2		0.193	0.025	0.170	0.220
	Fe (%)	1		2.86	0.920	1.79	4.26
		2		3.20	1.73	1.71	5.09
	Sb (%)	1		0.197	0.053	0.090	0.270
		2		0.303	0.085	0.240	0.400
	Cu (%)	1		0.035	0.005	0.030	0.040
		2		0.040	0.000	0.040	0.040
Area 3 (N1m = 28 and N2m = 27)	Au g/t	1		0.474	0.173	0.290	1.20
		2		0.431	0.088	0.320	0.680
	S (%)	1		0.670	0.364	0.005	1.530
		2		0.805	0.256	0.005	1.130
	As (%)	1		0.013	0.011	0.001	0.050
		2		0.009	0.001	0.001	0.030
	Fe (%)	1		2.17	0.785	1.03	3.86
		2		2.34	0.975	1.03	4.25
	Sb (%)	1		0.120	0.236	0.002	0.830
		2		0.141	0.252	0.001	0.838
	Cu (%)	1		0.005	0.005	0.001	0.010
		2		0.005	0.005	0.001	0.010
Total (N1m = 62 and N2m = 61)	Au g/t	1		0.505	0.176	0.250	1.20
		2		0.684	0.875	0.240	6.74
	S (%)	1		0.741	0.361	0.005	1.53
		2		0.867	0.208	0.005	1.21
	As (%)	1		0.056	0.068	0.005	0.190
		2		0.042	0.067	0.005	0.220
	Fe (%)	1		2.50	0.923	1.03	5.88
		2		2.62	1.01	1.03	5.09

Sb (%)	1	0.159	0.226	0.002	0.830
	2	0.194	0.263	0.001	0.988
Cu (%)	1	0.012	0.013	0.001	0.040
	2	0.009	0.011	0.001	0.040

The mean concentrations of elements such as S, As Fe, Sb, and Cu are respectively 0.741%, 0.056%, 2.50%, 0.159%, and 0.012% for S1m and 0.860%, 0.042%, 2.62%, 0.194%, and 0.009% for S2m. The mean grades showed low variation by depth and a slight trend to increase in samples collected from the second meter (with some exceptions in Areas 2 and 3 – Fig. 4). Evaluating the grades by sampled region, Area 1 had the samples with the highest grades of Au, S, and Sb. The distributions by metals and metalloid by depth and area are illustrated in Fig. 4. The distribution can be associated to the variability of the metallurgic plant during the production process, spilling pulses, and migrating spilling points that caused local enrichment of individual phases like sulfides, as reported by others, e.g. Redwan et al. (2012). Besides this, after deposition, mine tailings could suffer geochemical and mineralogical evolution through weathering process. Therefore, these three assumptions together can explain the variations in content of samples collected from different areas and at different depths (Fig. 4).

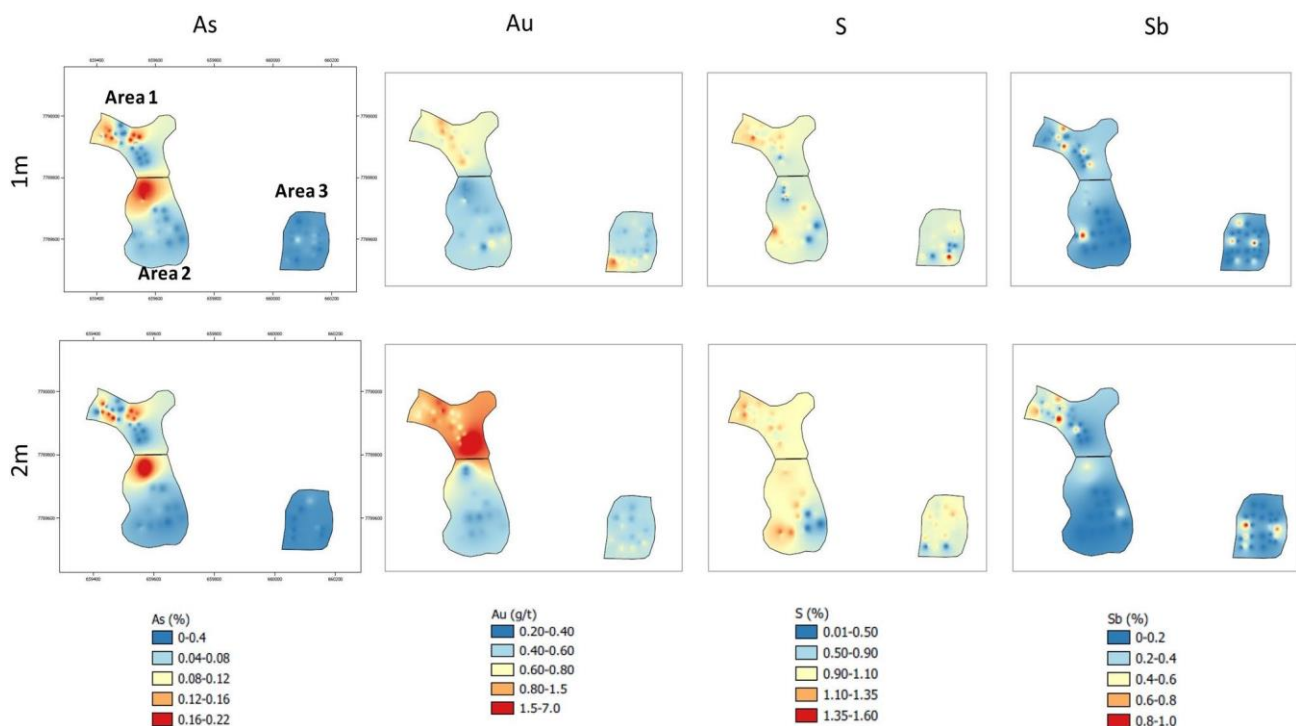


(Figura 5.17) Fig. 4 Spatial distribution of As, Au, S and Sb by sampling depth and area.

Figure 5 also shows a correlation trend expressed as a Pearson correlation between the elements analyzed. For Au, a positive and not very significant coefficient of 0.42 was found for S; however, there is a negative trend for the mean grades of Au and As. Arsenic, Sb, Cu, and Fe presented higher positive correlation trends (e.g. 0.84 for Sb with As and 0.96 Sb with Fe). Table 3 shows an estimate of tonnage and respective element mean of content for the total area of the storage facility, considering the density of the tailings and two sampling depths.

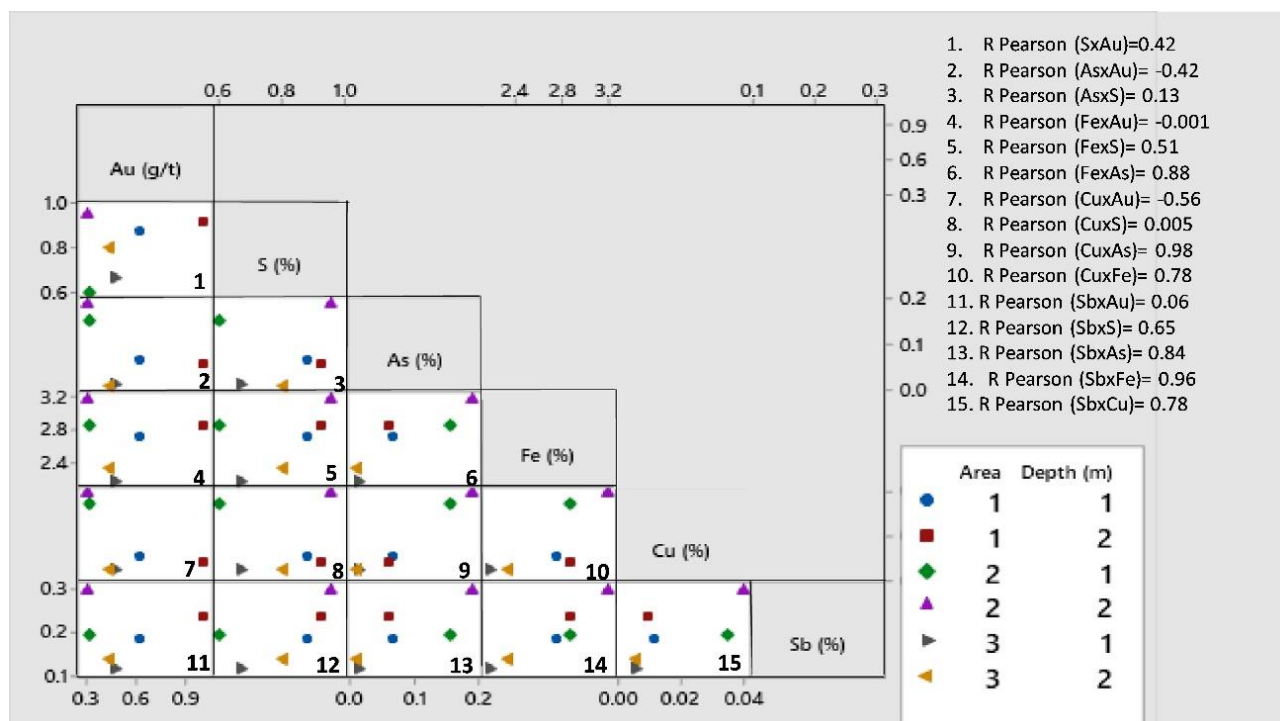


(Figura 5.18) Fig. 5 Matrix plot of Pearson of Au, S, As, Fe, Cu and Sb mean values by area and depth.

(Tabela 5.8) Table 3 Estimated tonnage and element mean of contents for Au, As, Cu, Sb and S in Santa Barbara tailings dam.

Element	Tonnes (kt) ^a	Grade	Element Content
Au (g/t)	853.5	0.504	13.83 ^b
S (%)		0.804	686 ^c
As (%)		0.049	41.82 ^c
Sb (%)		0.177	151 ^c

^a Kt = t*1000 for 2 m sampled ^b Koz ^c t*1000

Chemical and mineralogical characterization, using quantitative electronic approaches, are key tools for optimization of the extraction processes, in complex ores (e.g. Goodall et al. 2012) and in tailings storage facilities (Guanira et al. 2020). In the present study, the mineralogy of the tailings provides the knowledge needed to understand mineral associations, mineral liberation, and, consequently, to evaluate the potential for metal recovery.

Table 4 identifies the host minerals and how the elements of interest occur in the Santa Barbara dam. The mineralogy comprises inherited minerals like quartz, as antimony oxide and rarely in arsenopyrite. Jarosite was muscovite, biotite, and phases formed during process- the main host of Fe and S, instead of pyrite. Iron oxide/ ing stages, such as gypsum, jarosite, and Fe-antimoniate. hydroxide was also identified in the samples. The source These latter two are sources of Sb, as can be seen in Fig. 6. of Cu is chalcopyrite, but it was rarely detected.

RESULTADOS E DISCUSSÕES

Mine Water and the Environment (2021) 40:257–269

<https://doi.org/10.1007/s10230-021-00754-6>

(Tabela 5.9) **Table 4** Mineralogical composition of santa barbara solid tailings.

Minerals	Chemical Formula	Wt%	Distribution and association
Quartz	SiO ₂	35.6	Mainly liberated
Feldspar Group			Mainly liberated
Albite	NaAlSi ₃ O ₈	1.11	
Anorthite	CaAl ₂ Si ₂ O ₈	0.053	
K feldspar	KAlSi ₃ O ₈	1.27	
Sheet Silicates			
Biotite	KMg _{2.5} Fe _{2+0.5} AlSi ₃ O ₁₀ (OH) _{1.75} F _{0.25}	1.26	
Muscovite Group	KAl ₃ Si ₃ O ₁₀ (OH) _{1.9} F _{0.1}	29.0	Mainly liberated and associated with quartz and Fe species
Chlorite	(Mg,Fe) ₃ (Si,Al) ₄ O ₁₀ (OH) ₂ (Mg,Fe) ₃ (OH) ₆	5.01	
Oxides			Mainly liberated and associated with jarosite
Iron Oxides/Hydroxides	Fe ₂ O ₃ /FeOOH	0.378	
Rutile/Anathase	TiO ₂	0.599	
Fe antimoniate	FeSb(As)O	0.806	
Carbonates			
Ankerite	Ca(Fe,Mg,Mn)(CO ₃)O ₂	9.00	Mainly liberated
Siderite	FeCO ₃	7.20	
Calcite	CaCO ₃	5.40	
Sulphates			
Gypsum	CaSO ₄ 2H ₂ O	1.00	Mainly liberated
Jarosite (With Sb)	KFe(SO ₄) ₂ (OH) ₆ & (H ₃ O)Fe(SO ₄) ₂ (OH) ₆	2.00	
Arsenates			Enclosed in jarosite and silicates
Scorodite	FeAsO ₄ •2(H ₂ O)	0.049	
Sulphides			
Pyrite	Fe ₂ S ₂	0.080	Enclosed in jarosite and silicates
Pyrrhotite	Fe _{2+0.95} S	0.041	
Arsenopyrite	Fe ³⁺ AsS	0.056	
Berthierite	FeS ₂ S ₄	0.141	
Chalcopyrite	CuFe ₂ S ₂	0.028	
Sphalerite		0.009	
Gold Minerals			
Native Gold	Au > 80%, Ag, Cu	(158)*	
Electrum	Au = 80%, Ag = 20%	(6)*	With quartz, gypsum, sulphides and jarosite
Aurostibite	AuSb	(146)*	

*⁰ Number of gold mineral grains identified and characterized

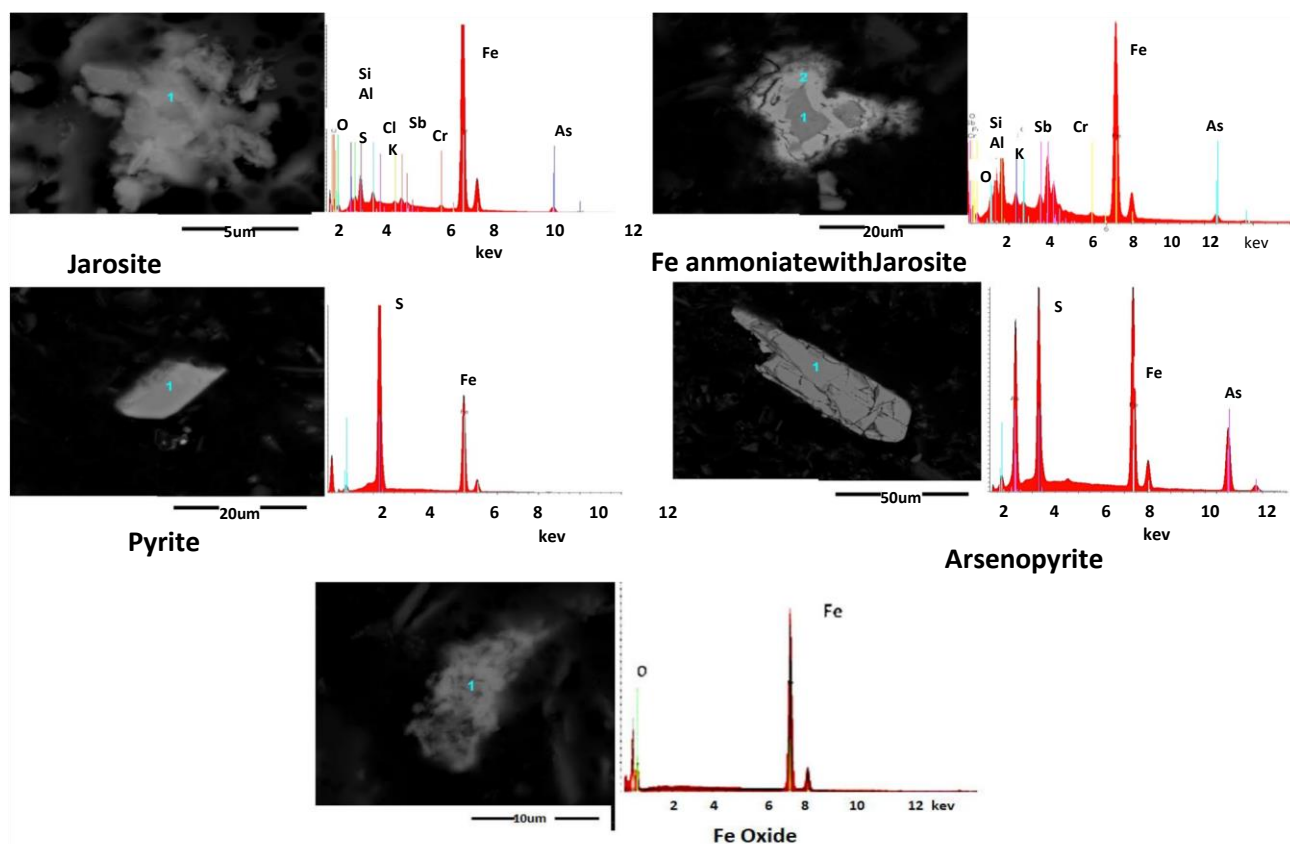


(Figura 5.19) Fig. 6 SEM-SE images and respective EDS spectra of Fe species and sulfides.

A special emphasis was given to the behavior of gold due to its economic value (Fig. 7). The following gold phases were detected: native gold, gold associated with Cu and Ag and aurostibite. Au particles were liberated and associated with jarosite and quartz, as illustrated by the false color image processed in multispectral linear arrays (MLA—right below in Fig. 7). The gold-containing phases are very thin, mostly less than 7 µm.

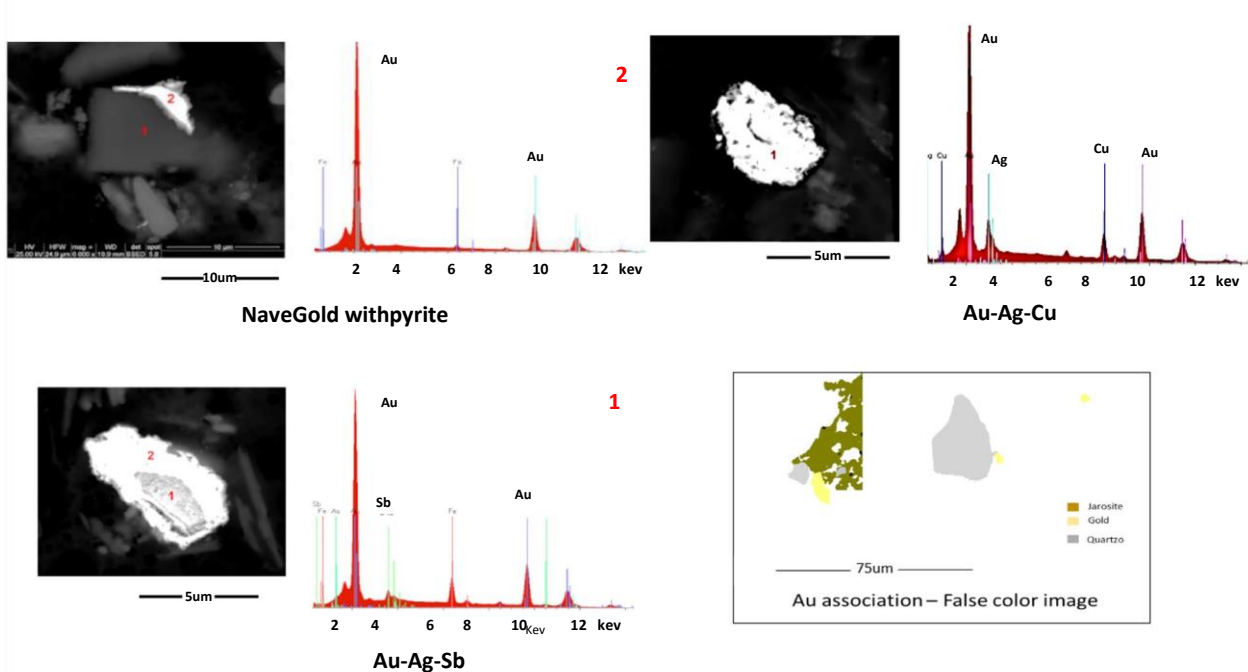


(Figura 5.20) **Fig. 7** SEM-SE images and respective EDS spectra of Au species and false image of Au associations (below right).

This mineralogical study provides additional information on and helps to understand the chemical behavior of the elements in the tailings dams. The correlations observed between the elements (Fig. 5) reflects their association with common mineralogical hosts. For example, Sb with Fe and Sb with As, with a correlation of 0.84 and 0.96 occur in common phases.

Most of these elements are in phases transformed in the oxidation by pressure stages and associated with sulfides not recovered in flotation. Jarosite, iron antimoniate, and even iron oxide are suggested to be the result of the oxidation and precipitation of these elements from sulfides, such as berthierite and arsenopyrite (Berezowsky et al. 1984). Residual gold and sulfides represent extraction inefficiencies during the beneficiation, which results in co-precipitation/ encapsulation of elements like Sb and As in phases such as jarosite.

Batch Test to Recover Sb, As, and Au from Solid Tailings

According to the forms of occurrences of the metals and metalloid of potential value, such as Au, Sb, and As (Figs. 4 and 5, and Table 4), batch tests were conducted on solid tailings to check the feasibility of recovery. The highest reported Sb and As volatilization occurred in a two-stage roast as shown, together with the conditions tested, in Table 5. Even though Sb and As were associated with magnetic phases, the WHIMS test showed very low recoveries. The same behavior was observed for gold, with an extraction rate of 10%.

(Tabela 5.10) **Table 5.** Batch tests results of Sb, As and Au recovery.

Experiment	Feed Grade Sb (%)	Overall recovery (%)				
			As (%)	Au (ppm)	Sb (%)	As (%)
WHIMS	0.2	0.05	—	—	3	6
1 stage klin roasting	0.2	0.05	—	—	4	6
2 stage klin roasting	0.2	0.05	—	—	19	7
Cyanide bottlerRoll	—	—	0.5	—	—	10

In a way, the results showed relatively low recovery rates, as expected due to the complexity demonstrated by the mineralogy and low content of these metals. However, the recoveries were obtained

from composite samples and not in the most optimistic scenarios, that is, when performing selective extraction of the enriched areas (Fig. 4).

Therefore, the results indicate a need for review of the current experiments for increasing efficiency. Moreover, even though these metals are present as complex phases and the tailings are very fine (Fig. 6), such evaluations should be performed to precisely assess the potential of tailings for reuse.

Only a slight increase of grades by depth (Table 2) was detected, and the results were promising regarding the possibility of metal recovery, especially considering similar and new studies. Moreover, in accordance with the element supply risk list (British Geological Survey 2015), Sb and As were ranked in the highest risk category, enhancing interest in their recovery. Therefore, the data obtained in Santa Bárbara justify an effort towards more detailed studies, covering the entire area and depth of the dam to accurately assess the recovery potential of these critical substances.

Conclusion

A gold process plant tailings dam was characterized for surface water and solids tailings up to 2 m deep. Information was obtained using integrated hydrochemical, geochemical, and mineralogical techniques. Moreover, it supported preliminary metallurgical testing and a more detailed view of the loss of Au, the main product of this operation. Mineralogical characterization demonstrated how metals and metalloids such as Sb, As, S, and Au occur in complex forms and detailed and innovative metallurgical tests must be performed. Therefore, and most importantly, the present study compiled a knowledge base that could support future decisions about the potential reuse of the tailings, while making clear how complex it would be.

The effluent water is alkaline, in accordance with the operation stage and the chemical products used in the treatment plant. The most important properties are the high concentrations of sulfate, Cu, As, and Sb, associated both with the mineralization and the process chemicals used for gold extraction. These results suggest the need for further research on metal recovery and improving the quality of the industrial water recirculated for the beneficiation process.

The characterization of the tailings solids confirms the need for reevaluation of the process routes already tested, in order to improve extraction efficiency. Also, the chemical and mineralogical compositions revealed the grades and occurrence modes of elements that are considered to be facing supply risk, such as Au, Sb, and As. Jarosite and Fe antimoniate are host phases.

Even considering that these metals occur in complex forms and the recovery of elements as Sb, As, and Au presented low rates in preliminary metallurgical tests, the results demonstrate the potential for reuse or refinement of the process for better use of the resource. Further efforts should be developed for an accurate calculation for the entire dam, which will allow more precise assessment of the recovery potential of enriched areas and to validate the aspirations in the context of a circular economy.

Acknowledgements This work was funded by the Fundação para a Ciência e a Tecnologia (FCT) through projects UIDB/04683/2020, UIDP/04683/2020, Nano-MINENV 029259 (PTDC/CTA-AMB/29259/2017), and by AngloGold Ashanti Brazil. We thank our colleagues from the ICT, microscopy center from Universidade Federal de Minas Gerais (CM-UFGM), and AngloGold Ashanti who provided insight and expertise that greatly assisted the research. The authors are also deeply grateful to Professor Rafael Rubio, the editorial staff, and the anonymous reviewers for their valuable comments and suggestions.

References

- Acheampong MA, Meulepas RJW, Lens PNL (2010) Removal of heavy metals and cyanide from gold mine wastewater. *J Chem Technol Biot* 85(5):590–619
- AGA (AngloGold Ashanti) (2018) AngloGold Ashanti recommendations. Internal LGU report. Unpubl
- Akinwekomi V, Maree JP, Masindi V, Zvinowanda C, Osman MS, Foteinis S, Mpenyana-Monyatsi L, Chatzisymeon E (2020) Beneficiation of acid mine drainage (AMD): a viable option for the synthesis of goethite, hematite, magnetite, and gypsum – gearing towards a circular economy concept. *Miner Eng*. <https://doi.org/10.1016/j.minen.2020.106204>

RESULTADOS E DISCUSSÕES

Mine Water and the Environment (2021) 40:257–269

<https://doi.org/10.1007/s10230-021-00754-6>

- Alkmin FF, Marshak S (1998) Transamazonian orogeny in the southern São Francisco craton region, Minas Gerais, Brazil: evidence for paleoproterozoic collision and collapse in the Quadrilátero Ferrífero. *Precambrian Res* 90(1–2). [https://doi.org/10.1016/S0301-9268\(98\)00032-1](https://doi.org/10.1016/S0301-9268(98)00032-1)
- Almeida FFM (1967) Origem e Evolução da plataforma brasileira. Rio de Janeiro, DNPM 241:36 ([in Portuguese])
- Almeida FFM (1976) Estruturas do Pré-Cambriano Inferior Brasileiro. Proc, 29º Congresso Brasileiro de Geologia, pp 201–202 [in Portuguese]
- Altinkaya P, Liipo J, Kolehmainen E, Haapalainen M, Leikola M, Lundström M (2019) Leaching of trace amounts of metals from flotation tailings in cupric chloride solutions. *Min Metall Explor* 36:335–342
- Antunes M, Fernandes R, Pinheiro A, Valente T, Nascimento S (2010). Potential of reuse and environmental behavior of ochre-precipitates from passive mine treatment. In: Wolkersdorfer C, Freund A (Eds), IMWA Proceedings, pp 205–208
- APHA - American Public Health Association (2005) Standard method for examination of water and wastewater, 21st edit. AWWA, WPCF, Washington DC
- Araújo TD, Queiroz AASL (2017) Economia Circular: um breve panorama da produção científica entre 2007 e 2017. Proc, XIX Encontro Internacional sobre Gestão Empresarial e Meio Ambiente (ENGEMA), p 1–17 [in Portuguese]
- Baltazar OF, Silva SL (1998) Mapa geológico integrado - texto explicativo em escala 1: 100.000. In: Projeto Rio das VelhasDNPM/ CPRM, Brasília [in Portuguese]
- Berezowsky RMG, Weir DR (1984) Pressure oxidation pretreatment of refractory gold. *Min Metall Explor* 1:1–4. <https://doi.org/10.1007/BF03402544>
- Blight G (2011) Mine waste: a brief overview of origins, quantities, and methods of storage. In: Vallero D (ed) Letcher T. Waste, A Handbook for Management. Cambridge Academic, pp 77–88
- British Geological Survey (2015) British Geological Survey risk list, British Geological Survey, England. https://www.bgs.ac.uk/minerals_risk_list.html
- Chen T, Lei C, Yan B, Xiao XM (2014) Metal recovery from the copper sulfide tailing with leaching and fractional precipitation technology. *Hydrometallurgy* 147–148:178–182
- CONAMA - Conselho Nacional do Meio Ambiente - CONAMA
- (2005) Resolução nº 430, de 13 de maio de 2001 Dispõe sobre as condições e padrões de lançamento de efluentes, complementa e altera a Resolução no 357 Environmetal Protection Authority of
- Brazil, Brasília [in Portuguese]
- David MEV (2006) Composição isotópica de Pb, Sr e Nd da mineralização de ouro do depósito Córrego do Sítio, Quadrilátero Ferrífero (MG): implicações na modelagem conceitual. Instituto de Geociências, Univ de São Paulo, MSc Diss ([in Portuguese])
- de Silva R, A, Secco MP, Lermen RT, Schneider IAH, Hidalgo GEN, Sampaio CH, (2019) Optimizing the selective precipitation of iron to produce yellow pigment from acid mine drainage. *Miner Eng* 135:111–117
- Dehghani A, Mostad-Rahimi M, Mojtabahedzadeh S, Gharibi K (2009) Recovery of gold from the Mouteh gold mine tailings dam. *J S Afr I Min Met* 109:417–421
- Dold B (2014) Evolution of acid mine drainage formation in sulphidic mine tailings. *Minerals* 4:621–641
- Dundee Sustainable Technologies (2006) Method for vitrification of arsenic and antimony. US9981295B2, <https://patents.google.com/patent/US9981295B2/en>
- Ellen Macarthur Foundation (2013) Towards the Circular Economy, Cowes, UK. <http://www.ellenmacarthurfoundation.org/business-reports>
- Falagán C, Grail BM, Johnson DB (2017) New approaches for extracting and recovering metals from mine tailings. *Miner Eng* 106:71–78
- Gaustad G, Krystofik M, Bustamante M, Badami K (2017) Circular economy strategies for mitigating critical material supply issues. *Resour Conserv Recycl*. <https://doi.org/10.1016/j.resconrec.2017.08.002>
- Goldfarb R (2001) Orogenic gold and geologic time: a global synthesis. *Ore Geol Rev* 18:1–75
- Goodall W, Butcher A (2012) The use of QEMSCAN in practical gold deportment studies. *Min Proc Ext Met* 121:199–204
- Grande JA, De La Torre ML, Andujar JM, Valente T, Santisteban M (2013) Definition of a clean energy system for decontamination of acid mine waters and recovering their metal load. *Miner Mag*. <https://doi.org/10.1180/minmag.2013.077.5.7>
- Guanira K, Valente TM, Ríos CA, Castellano OM, Salazare L, Lattanzi D, Jaimee P (2020) Methodological approach for mineralogical characterization of tailings from a Cu (Au, Ag) skarn type deposit using QEMSCAN (Quantitative Evaluation of Minerals by Scanning Electron Microscopy). *J Geochem Explor*. <https://doi.org/10.1016/j.gexplo.2019.106439>
- Guest RN, Svoboda J, Venter WJC (1998) The use of gravity and magnetic separation to recover copper and lead from Tsumeb flotation tailings. *J S Afr I Min Met* 88(6):21–26
- Heiden R (2003) Recovery of marketable iron oxide from mine drainage in the USA. *Land Reclamat* 11:93–97
- Hudson-Edwards KA, Macklin MG, Brewer PA, Dennis IA (2008) Assessment of Metal Mining-contaminated River Sediments in England and Wales. Environment Agency. <http://www.eugris.info/displaysourcesource.aspx?r=6681>
- IBGE (2019) Instituto Brasileiro de Geografia e Estatística. <https://www.ibge.gov.br/geociencias/informacoes-ambientais/climatologia.html>
- Jafari M, Abdollahzadeh A, Aghababaei F (2017) Copper ion recovery from mine water by ion flotation. *Mine Water Environ* 36:1–5. <https://doi.org/10.1007/s10230-016-0408-2>
- Kossoff D, Dubbin WE, Alfredsson M, Edwards SJ, Macklin MG, Hudson- Edwards KA (2014) Mine tailings dams: characteristics, failure, environmental impacts, and remediation. *Appl Geochem* 51(229):245
- Lemos MG, Magalhães MF, Souza TFQ, Pereira MS, Vieira MMS (2019) Geometallurgical analysis for increasing gold recovery – Santa Barbara, MG. *Proc World Gold* 2019:210–218

RESULTADOS E DISCUSSÕES

Mine Water and the Environment (2021) 40:257–269

<https://doi.org/10.1007/s10230-021-00754-6>

- Li X, Zhao C, Lu R, Xu X, Jia X (2013) Efficient adsorption of gold ions from aqueous systems with thioamide-group chelating nanofiber membranes. *Chem Eng J* 229:420–448
- Liu B, Zhang C, Li L, Wang Y (2013) Recovery of gold and iron from the cyanide tailings by magnetic roasting. *Rare Metal Mater Eng* 42(9):1805–1809
- Lobato LM, Ribeiro-Rodrigues LC, Vieira FWR (2001) Brazil's premier gold province. Part II: geology and genesis of gold deposits in the Archean Rio das Velhas greenstone belt. *Quadrilátero Ferrífero Miner Depos* 36:249–277
- Lottermoser B (2007) Mine wastes: characterization, treatment and environmental impacts. Springer, Berlin
- Manoucheri H, Mossler A, Gaul F (2016) Techno-economic aspect of ore sorting - is sorting a missing part in the mining industry - a case study at Sandvik's Mittersill tungsten mine. In: Proceedings of 28th International Mineral Processing Conference, ISBN: 978-1-926872-29-2
- Martin CJ, Al TA, Cabri LJ (1997) Surface analysis of particles in mine tailings by time-of-flight laser-ionization mass spectrometry (TOF-LIMS). *Environ Geol* 37:107–113
- Martin M, Janneck E, Kermér R, Patzig A, Reichel S (2015) Recovery of indium from sphalerite ore and flotation tailings by bioleaching and subsequent precipitation processes. *Miner Eng* 75:94–99
- Nengovhela AC, Yibas B, Ogola JS (2006) Characterisation of gold tailings dams of the Witwatersrand Basin with reference to their acid mine drainage potential. *Water SA* 32(4):499–506
- Nordstrom K (2011) Mine waters: acidic to circumneutral. *Elements* 7:393–398
- Novhe NO, Yibas B, Coetzee H, Mashalane T, Atanasova M, Vadapalli VRK, Wolkersdorfer C (2018) Geochemistry and mineralogy of precipitates formed during passive treatment of acid mine drainage in the Ermelo coalfield, South Africa. Proc, IMWA 2018 Conf, pp 171–176
- Padilla R, Aracena A, Ruiz MC (2014) Kinetics of stibnite (Sb_2S_3) oxidation at roasting temperatures. *J Min Metall* 50(2 B): 127–132
- Parbhakar-Fox A, Fox N, Jackson L (2016) Geometallurgical evaluations of mine waste - an example from the Old Tailings Dam, Savage River, Tasmania. In: Proceedings of 3rd AusIMM International Geometallurgy Conference, pp 193–204
- Pires KS, Mendes JJ, Figueiredo VC, Silva FL, Von Krügera FL, Vieira CB, Araújo FGS (2019) Mineralogical characterization of iron ore tailings from the Quadrilatero Ferrífero, Brazil, by electronic quantitative mineralogy. *Mat Res.* <https://doi.org/10.1590/1980-5373-mr-2019-0194>
- Porto CG (2008) A mineralização aurífera do depósito Córrego do Sítio e sua relação com o enxame de diques metamáficos no corpo Cachorro Bravo - Quadrilátero Ferrífero - Minas Gerais. MSc Thesis, Univ Federal de Minas Gerais [in Portuguese]
- Rao GV, Markandeya R, Sharma SK (2016) Recovery of iron values from iron ore slimes of Donimalai tailings dam. *Trans Indian Inst Met* 69:143–150
- Redwan M, Rammlmair D (2012) Understanding micro-environment development in mine tailings using MLA and image analysis. In: Proceedings of 10th International Congress for Applied Mineralogy (ICAM), pp 589–596
- Robben C, Condori P, Pinto A, Machaca R, Takala, (2020) A X-ray transmission based ore sorting at the San Rafael tin mine. *Miner Eng.* <https://doi.org/10.1016/j.minen.g.2019.105870>
- Ruchkys UA, Azevedo DT, Machado MMM (2013) Patrimônio geológico e mineiro do Quadrilátero Ferrífero, Minas Gerais – Caracterização e iniciativas de uso para educação e geoturismo. *Boletim Paranaense de Geociências* [in Portuguese]. Doi: <https://doi.org/10.5380/geo.v70i0..31541>
- Ryan MJ, Kney A, Carley T (2017) A study of selective precipitation techniques used to recover refined iron oxide pigments for the production of paint from a synthetic acid mine drainage solution. *Appl Geochem* 79:27–35
- Sang Y, Li F, Gu Q, Liang C, Chen J (2008) Heavy metal-contaminated groundwater treatment by a novel nanofiber membrane. *Desalination* 223:349–360
- Schorscher HD (1978) Komatiitos na estrutura "Greenstone Belt" Série Rio das Velhas, Quadrilátero Ferrífero, Minas Gerais. *Brasil Congr Bras Geol* 30(1):292–293 [in Portuguese]
- Shi T, Jia S, Chen Y, Wen Y, Du C, Guo H, W Z. (2009) Adsorption of Pb(II), Cr(III), Cu(II), Cd(II) and Ni(II) onto a vanadium mine tailing from aqueous solution. *J Hazard Mater* 169:838–846
- Silva SR, Procópio SO, Queiroz TFN, Dias LE (2004) Caracterização de rejeito de mineração de ouro para avaliação de solubilização de metais pesados e arsénio e revegetação local. *Rev Bras Cienc Solo.* [https://doi.org/10.1590/S0100-06832 00400 01000 18\[inPor tuge se\]](https://doi.org/10.1590/S0100-06832 00400 01000 18[inPor tuge se])
- Singh S, Sukla LB, Goyal SK (2020) Mine waste & the circular economy. *Mater Today Proc* 30(2):332–339
- Skoronski E, Ohrt AC, Cordella RO, Trevisan V, Fernandes M, Miguel TF, Menegaro DA, Dominguini L, Martins PR (2017) Using acid mine drainage to recover a coagulant from water treatment residuals. *Mine Water Environ* 36:495–501
- Souza Junior TF, Moreira EB, Heineck KS (2018) Barragens de rejeito e contenções no Brasil. *Holos* 5:1–39 [in Portuguese]
- Spooren J, Binnemans K, Björkmal M, Bremeresch K, Dams Y, Folens K, González-Moya M, Liesbeth H, Komnitsas K, Kurylak W, Lopez M, Mäkinen J, Onisei S, Oorts K, Peys A, Pietek G, Pontikes Y, Snellings R, Triplana M, Varia J, Willquist K, Yurramendi L, Kinnunen P (2020) Near-zero-waste processing of low-grade, complex primary ores and secondary raw materials in Europe: technology development trends. *Resour Conserv Recy.* <https://doi.org/10.1016/j.resconrec.2020.104919>
- Tayebi-Khorami M, Edraki M, Corder G, Golev A (2019) Re-thinking mining waste through an integrative approach led by circular economy aspirations. *Minerals.* <https://doi.org/10.3390/min90 50286>
- Twardowska I, Allen HE, Kettrup AAF, Lacy WJ (2004) Solid waste: assessment, monitoring and remediation. Elsevier, UK, pp 319–394
- Valente T, Grande JA, De La Torre ML (2016) Extracting value resources from acid mine drainages and mine wastes in the Iberian Pyrite Belt. In: Drebendstedt C, Paul M (Eds), In: Proceedings of Mining Meets Water – Conflicts and Solutions, pp 1339–1340
- Von Ketelhodt L (2009) Viability of optical sorting of gold waste rock dumps. Proc, World Gold Conf, pp 271–27.

scientific reports

Geochemistry and mineralogy of auriferous tailings deposits and their potential for reuse in Nova Lima Region, Brazil

Mariana Lemos ^{1,2}✉, Teresa Valente ¹, Paula Marinho Reis ¹, Rita Fonseca ³, João Paulo Pantaleão ², Fernanda Guabiroba ², José Gregorio Filho ², Marcus Magalhães ², Bruno Afonseca ², Antonio Roberto Silva ² & Itamar Delbem ⁴

Since the mid-nineteenth century, gold ores, mainly hosted in sulfides, have been processed at metallurgical plants located in Nova Lima, Brazil. The generated wastes have been accumulated over the years in tailings dams or in piles. These materials represent wasted from old circuits, as well as from plants still in production. In this study, geochemical, mineralogical, 3D modelling, and metallurgical analyses wastes were carried out to evaluate potential reuse of these wastes. The performed characterization detected residues of very fine grain size containing sulfides and oxides. The wastes show high grades of Au hosted in different minerals. In addition to Au, samples contain S, Fe, Zn, Pb, Sc, Si, and As. The 3D modelling for spatial definition of Au was performed using ordinary kriging with dimensional variograms. The results indicated the occurrence of Au enrichment zones and allowed to reveal the most attractive tailing deposits in terms of Au content. Metallurgical tests showed recovery of 70% of Au and suggested other potential reuse of the wastes, such as aggregates for the civil construction sector and recovery of other metals. The present work highlights the importance of an integrative characterization within the scope of the circular economy and the value of tailings in the production chain of the mineral sector.

In Brazil, the mining sector is one of the most economically and socially important. This sector currently represents between 3 and 5% of the Gross Domestic Product (GDP). The importance of this economic sector goes back to the seventeenth century, at the beginning of the first gold cycle¹. In the mid-eighteenth century, Brazil produced approximately half of the world's gold, attracting the immigration of around 400,000 Portuguese, mainly to the Nova Lima region, Minas Gerais.

Currently, this sector moves others, such as construction, automotive and aerospace industries, among others, through the supply of raw materials². Although its importance is relevant and strategic for the economy, the generation of abundant tailings materials remains an obstacle to sustainable development. The total inventory of mining wastes in the State of Minas Gerais exceeds 500 million t ons^{3,4}. The main infrastructures used for the deposition of these wastes are dams and mine dumps that exceed 500 registered occurrences in the state, with at least 15 referring to gold mining⁵. Dams and mine dumps represent risks to the environment and the population, as demonstrated by tragedies of dam collapses in Brumadinho and Mariana regions, both in Minas Gerais, Brazil⁶. The generation of mining waste associated with possible interruptions in supply and limited replacement, and therefore interruptions in the supply of critical

substances, can generate negatives for all parties directly and indirectly involved, with generation of socioeconomic impacts globally⁷. However, these wastes may be regarded as mineral deposits with grades and physical characteristics different from the exploited primary ore^{8,9}. Often, mine wastes have interesting concentrations of substances that are currently critical for technological society. This criticality led the EU to create the Critical Raw Materials list¹⁰. This list includes key elements with economic importance and supply risk. In addition, materials with continuous use and high demand are also highlighted, such as Au¹¹. Thus, the need for detailed and in-depth studies on these types of waste is indisputable.

Different approaches have been explored by researchers around the world to address the problem of solid mining tailings generation. There are some paths that aim to balance the exposure of tailings in balance with the environmental, social and economic sectors. These include reuse of waste with its recycling and reprocessing in various ways, leading to proactive waste management. These models aim to add new value to tailings by identifying the proper destination of potentially hazardous materials¹².

Studies using a combination of characterization techniques are the starting point to add value and increased knowledge to these wastes¹³. The integration of analytical techniques such as specific chemical analysis for solids, mineralogical and particle size distribution, and density determination, can be found in a number of publications^{6,13–19} (demonstrating that this characterization stage is critical to evaluating and understanding the waste deposits).

The use of mathematical and geostatistical tools, common in the numerical definition of mineral deposits, is also of great value in defining the sampling grid, modeling the distribution of grades, tonnage and contaminants dispersion patterns of tailings²⁰. Different case studies using mathematical techniques are reported in the literature [e.g., ^{13,17,21–23}]. In general, they combine waste characterization and statistical tools to obtain models for the valorization potential while attaining a better understanding of the environmental impacts of the mine dumps.

With such evolutions in the characterization stage, market and technology changes, these wastes can thus provide an alternative to primary exploitation, contributing to the sustainable development of the mining sector and the region. A reuse study based on statistical variables and waste characterization is an important step in the valuation and knowledge of the economic potential of these secondary deposits. This phase covers the processing of any form and types of waste, passing through waste from solid to gaseous phases^{24,25}. Various types of proposals can be described in this stage. The reuse of base elements from solutions of acidic drainage in abandoned mining waste deposits^{26–32}, the recovery of metals from dam water, and the reuse of solid tailings with recovery of valuable and critical elements for society^{33–37} are some examples of these approaches. Regarding the tailings deposits resulting from the treatment of Au ores^{38,39} proposed different methodologies for recovering this element from secondary sources. The combination of geochemical and mineralogical characterization techniques with hydrometallurgy, pyrometallurgy and even biological agents seems to be effective for Au recovery from tailings deposits.

In addition to these reviews and methodologies, the state-of-the-art shows success in recovering gold from mining tailings through different procedures^{6,34,40–42}. Nevertheless, dams and tailings deposits have environmental impact due the potentially hazardous substances they contain⁴³. In other words, the economic potential of the huge volume of wastes and the high environmental impact and risk to human health are two opposing and challenging components that justify the interest and the opportunity of the present study.

The present work, therefore, combines the characterization stage with statistical modeling to identify the potential for the valorization of tailings from Au processing in the Nova Lima region-MG, Brazil. The developed methodology is applied in five different deposits in varying stages of use, deposition methods and origin of the tailings. The main aims are (1) to present a characterization of the solid tailings; (2) making

comparisons between the different deposits; (3) investigate chemical associations and spatial patterns distribution of the metal contents to assess the potential for metallurgical recovery, especially Au, in the tailings. This work demonstrates the importance of the characterization and processing stages for correct waste management, avoiding socioenvironmental impacts and tragedies. Also, it highlights the need to rethinking tailings as potential new products, which further contribute to the sustainable development of the mining sector.

Local setting

The study areas are in the Quadrilátero Ferrífero (QF), which contains present among the largest deposits of gold and iron in Brazil (Fig. 1a)⁴⁴. Two main tectonostratigraphic domains of Archean and Proterozoic ages, define the QF province: granitic–gneissic terrains, a greenstone belt-like sequence (Rio das Velhas Supergroup) and a supracrustal sequence of chemical and clastic sedimentary rocks (Minas Supergroup) (Almeida, 1967). The first domain, which contains the Rio das Velhas Greenstone Belt, includes the most important gold-bearing region in Brazil^{45,46}. The reserves represent 4.5% (936 t) of Au ore worldwide. The deposits are structurally associated and controlled by hydrothermal alteration. In addition, they are hosted in tholeiitic mafic volcanic rocks, banded iron formations, komatiites, metavolcanoclastic shales and phyllites and terrestrial clastic sequences, metamorphosed from greenschist to amphibolite facies^{47–49}.

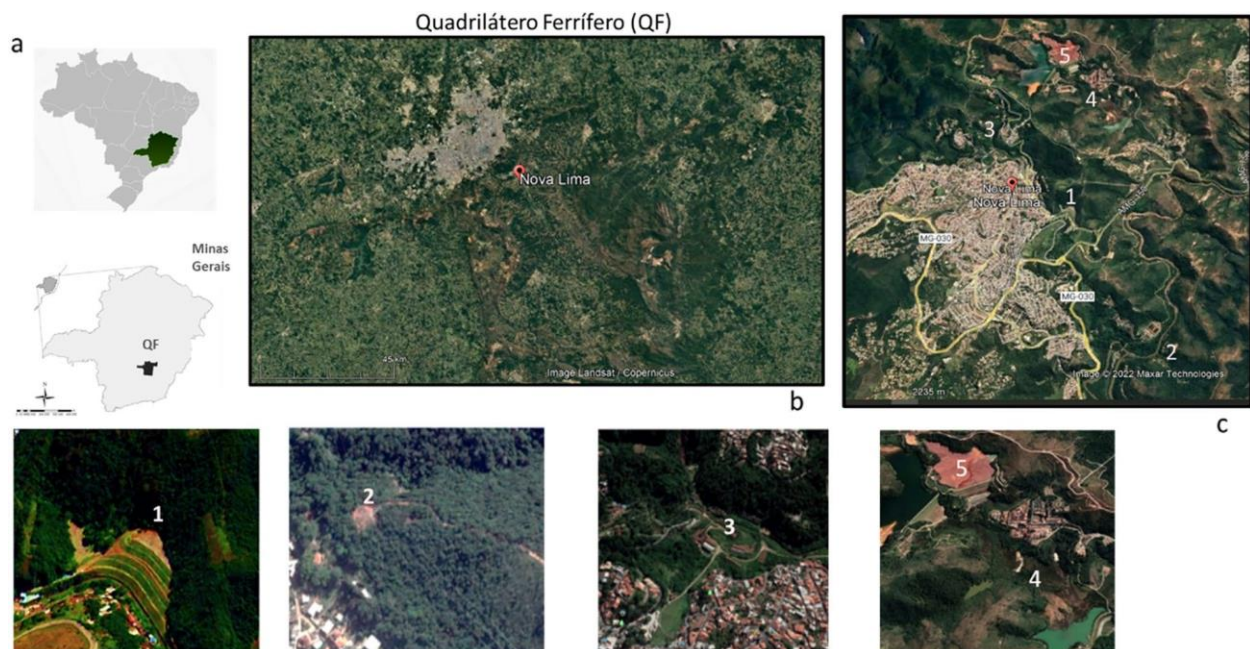


(Figura 5.21) **Figure 1.** Location of the QF (a), Nova Lima Region and the location in the QF (b), and the illustration location of the tailings deposit 1 to deposit 5. Google earth Pro V 7.3.6.9345 (64-bit). Image date 6/22/2022 19° 59' 05.66" S and 43° 50' 49.070" W. The dams and mine dumps in this region are located between the cities of Nova Lima and Raposos, 25 km from its capital, Belo Horizonte, Minas Gerais, Brazil (c).

The mines in the Nova Lima region (Fig. 1b) are orogenic gold mineral deposits, as well as others present in the QF, including Morro Velho, São Bento, Raposos, Juca Vieira and Cuiabá, directly related to the evolution of the Rio das Velhas greenstone belt (ca. 2.75 Ga) and its banded iron formations (BIF)^{50,51}. The mineralization is a sulfide-enriched BIF. The presence of pyrite (\pm arsenical) associated with arsenopyrite

indicates gold mineralization. In addition, gold is also associated with quartz veins and ranges from weakly to strongly refractory ore.

According to the Koppen classification (humid subtropical climate), the region has a warm and temperate climate. Precipitation is higher in December, with an average of 302 mm and August is the driest month. January is the hottest month of the year and June the coldest, with an average temperature of 17.6 °C⁵².

Deposits 1, 2 and 3 (Fig. 1c) received numerous types of rejects from old gold plants in the region. Unlike deposits 4 and 5, these are over 80 years old deposits that are not currently used. Deposits 1 and 3 are represented by piles, while deposit 2 consists of a dam. For these deposits, it is estimated that the oldest waste from twentieth century may represent gold extraction processes prior to the use of cyanide, which hinders describing the extraction process accurately⁵³. Table 1 presents a tentative historical description of the beneficiation processes that have occurred in the oldest deposits, contents of gold (Au), sulfur (S) and arsenic (As), as well as the recovery of Au.

At deposit 3 (Fig. 1c—the first plant operating in the city of Nova Lima), tailings from gravimetric recovery (50% Au recovery), cyanide leaching, and Zn precipitation processes have been deposited since the nineteenth century. The wastes in deposits 1 and 2 underwent flotation processes in addition to gravimetry, flotation, cyanide leaching and precipitation using Zn (Table 1).

(Tabela 5.11) **Table 1.** Forms of Au extraction, mass estimates and concentrations of Au, As, and S for deposits 1, 2, and 3 (modified from⁵³).

Area	Operation year	Au recovery (%)	Metallurgical methodology	Tonnage (kT)	Au (mg/kg)	As (%)	S (%)
1	1930–1945	90	Gravity + flotation + CN + Zn precipitation	500	4.93	8.07	9.06
2	1960–1980	93	Gravity + flotation + CN + Zn precipitation	240	1.83	3.7	7.63
3	1834–1930	50–80	Gravity + CN + Zn precipitation	315	4.06	8.87	6.61

The Nova Lima plant has been processing sulfide gold ores, no-refractory, for over 30 years. The materials processed at the plant used to be subdivided into two distinct circuits. The old circuit, named as Raposos (Fig. 2a), has achieved 90% Au recovery and the workflow are represented grinding, gravity concentration, conventional leaching and CIP (carbon in leaching), elution, and electro-recovery. This metallurgic plant operated until 1998 with the decommissioning of the Raposos underground mine^{9,53,54}. Waste from this circuit was deposited in tailings dam 4 (Fig. 1c).

In the current workflow at the Nova Lima plant, the Au is extracted from the sulfide concentrates through roasting and further leaching with cyanide (Fig. 2b). The tailings are deposited at the dam labelled as 5 (Fig. 1c). The content of Au feed from current mines varies from 5 ppm to 1, depending on each mine¹The tailings dams 4 and 5 are downstream, monitored and declared safe according to the national mining agency⁵.

Materials and methods

Study design. The flowchart presented in Fig. 3 illustrates the different stages of this study.

Sampling. The sampling campaign was carried out during winter and early spring (May–September 2020) when weather conditions vary greatly. Normally, during these months weather conditions are dry and slightly humid. The temperatures ranging from 15 to 25 °C⁵². Depending on the type of deposit, the sampling techniques included percussion, direct push and diamond drilling methods, up to a maximum of 20 m depth, totaling 1342 m of samples. The methods used, the average depth and the drilling mesh varied according to the sampled deposit. Additional information on the sampling procedures is provided as supplementary material (Fig. S1a,b, Table S1).

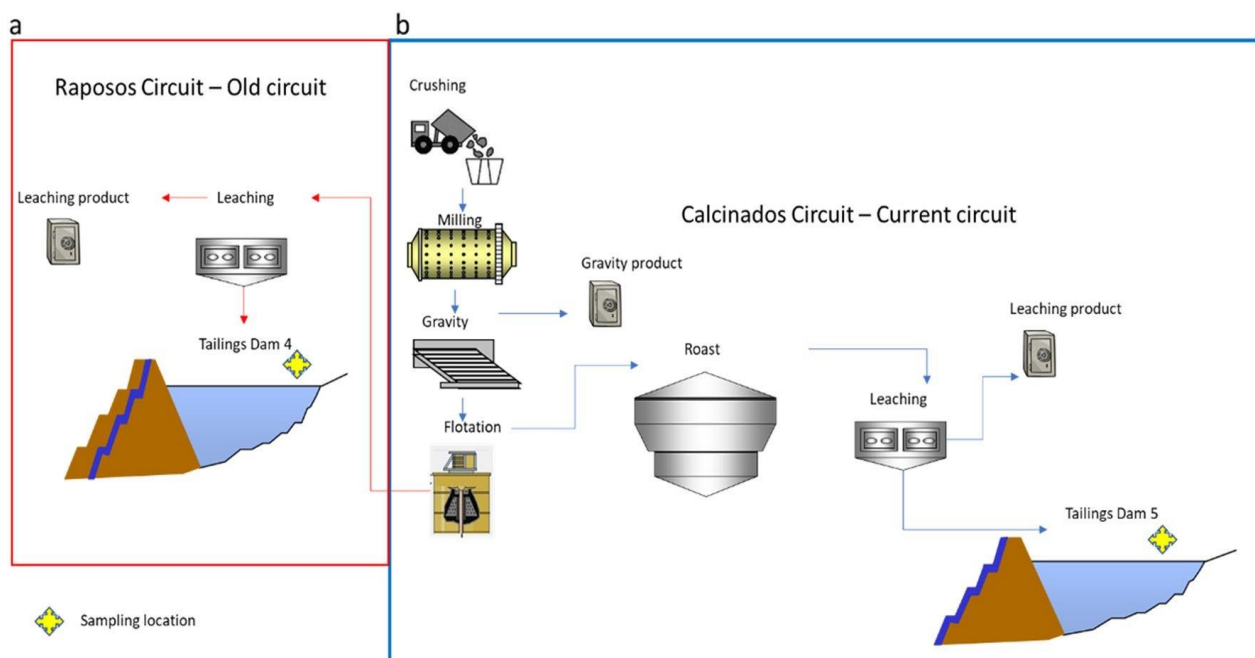


(Figura 5.22) **Figure 2.** Schematic flowchart of the process that fed the Au extraction dams 4—old circuit (a—red line) and 5—current circuit (b—blue line) of the Nova Lima Metallurgical Plant.

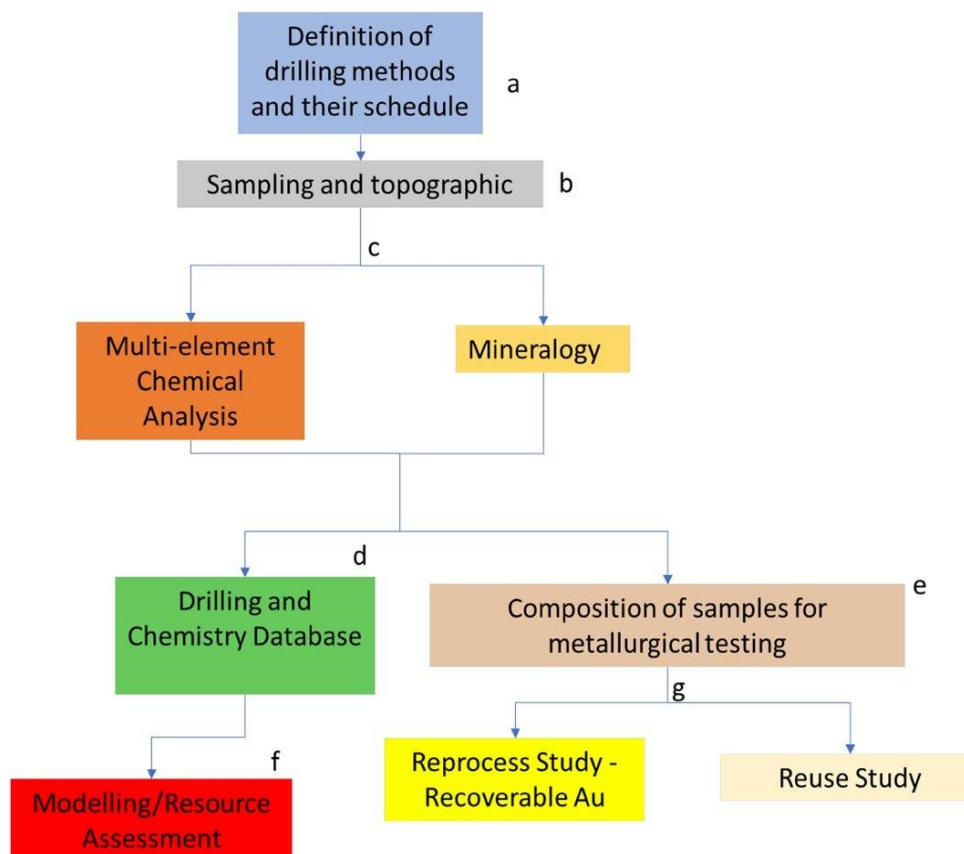


(Figura 5.23) **Figure 3.** Methodology applied to study tailings from deposits 1 to 5. (a) Step of defining the collection methodology for each deposit, (b) sampling of deposits and survey of the exact position of each sampled point, (c) stage of collecting information on the about chemistry and mineralogy of the samples, (d) assembly of a database containing survey and characteristics of each sample, (e) 3D modelling and geostatistical analysis of information obtained from sampling, (f) composition of samples after 3D modeling for metallurgical tests e, (g) study of the potential extraction of Au and reuse of the tailings in its entirety.

1586 samples were collected at 1 m intervals in depth and the position of the samples (hole starting point) were surveyed for exact control of the position of the cores. The samples densities were obtained from those with 100% recovery inside the sampling cylinder of known volume. After weighting, the density was calculated and added to the database².

All samples were transferred to polypropylene bags and kept at a 5 °C until chemical analysis.

Analytical procedures.

Chemical analysis. Before chemical analysis, all samples were homogenized and ground to a 2 mm size fraction, quartered and a quarter was ground to a – 37 µm particle size. The coarser fraction was stored for mineralogical analysis and metallurgical tests.

The main chemical analyzes were obtained with inductively coupled plasma mass spectrometry (ICP-MS, PerkinElmer SCIEX, Waltham, Massachusetts, USA). Before analysis, the samples were submitted to acid digestion (nitric acid, hydrogen peroxide, and hydrochloric acid) in the laboratory of AngloGold Ashanti and SGS in Brazil (complementary table S1). Sulfur (S) and carbon (C) concentrations were obtained by infrared detection (LECO, St Joseph, Michigan, USA, detection limit 0.01%). In addition, all Au analyzes were performed by atomic absorption spectroscopy (AAS, Varian, Palo Alto, California, USA—detection limit 0.05 mg/kg) using the fire assay method. All data were processed and validated using the LogasTM-Reflex-64.v 7.2.1 software.

For all analyses, duplicates, blanks and standard reference materials (Si81 from Rocklabs) were included. All controls were obtained within the necessary references and ensured the quality and accuracy of the analyses.

Mineralogy. The – 2 mm particle size fraction was used for mineralogical analyses. About 80% of the samples were used in the mineralogical study due to the good recoveries obtained in the sampling. The high number of samples allowed a good representativity of the tailings and enabled identifying variations in and between deposits.

The mineralogy of the samples was obtained through scanning electron microscopy (Scanning Electron Microscopy—SEM-FEI quanta 200) coupled with an energy dispersive spectrometer (EDS) and mineral liberation analyzer software (MLA-FEI). Before the analysis, the samples were prepared in polished section and described under an optical microscope (Leica DM4500 P LED). To produce the MLA equipment database, the main phases were analyzed using a Jeol JXA 8900RL WDS/EDX microprobe. The spectra obtained by wavelength scanning (WDS) entered the MLA software for calibration and subsequent automated analysis. During automated analysis of the obtained data, two modes were used: grain based X-ray mapping (GXMAP) to collect modal information and sparse phase release (SPLDZ) to collect information related to Au-bearing minerals⁵⁵.

Dataview v 3.1.4.686 software was used to process the MLA data as it enables to analyze quantitative mineralogical data obtained through the MLA measurement software. Pixel data is combined with the chemical composition and density of the identified minerals, allowing various analysis such as modal mineralogy⁵⁶.

Gold metallurgical tests. Estimation of the Au extraction potential in the deposits under study was based on the previous geochemical and mineralogical characterization of the samples. Then, samples representing the most enriched zones of the modeled deposits were submitted to two different leaching procedures to define this Au extraction potential.

Within the scope of this work, two protocols were developed for Au extraction in samples ground at 74 µm. The first involved calcination and leaching steps and the second consisted of direct leaching. These two protocols, based on the work of³⁹, adapted according to the sample's mineralogy. According to these authors, finely disseminated gold associations in quartz-sulfide, sulfides of non-ferrous metals, and oxide minerals as hydrogoethite, are major challenges for the industry due to the complexity of extraction. For this type of gold association two types of metallurgical processes are suggested: flotation + calcination + cyanidation and calcination + cyanidation. Therefore, two similar procedures were proposed for the samples of the five study areas (supplementary Fig S2).

Modelling. Once the database was complete, geostatistical tools were applied to analyze the distribution of elements of economic interest and the contaminants. All models are 3D block model with discretization cell of 5 m × 5 m × 1 m^{13,23,57}.

The analysis comprised the assessment of sampling errors, namely sample recovery efficiency, removal of outliers to avoid overestimation of the models (capping), a statistical summary, estimation, and validation. The topography of the deposits was used to define the boundaries of the area to be modelled (Fig. S3). Topographic data used for 3D modeling were obtained using the total station method. The initial position (0 m depth) of all samples was also obtained by this method. The use of surface topography in modeling is important as it influences the calculations of the volume of deposited or stacked material, in addition to being a necessary tool for physical stability in future operations^{11,13}. The volumes were defined by the topography limit and the density of the samples (see “Sampling”). Density data was interpolated by block kriging, and each block presented its density value. In this way, we could calculate the model volume. The method was

used for all tailings deposits. All data were processed using leapfrog v2021.1 software and datamine studio RM. Principal component analysis (PCA) was performed on 19 geochemical variables to define the primary element associations. This approach put in evidence mineralogical variations within the study areas, important for the interpretation of the source materials and deposition processes of each structure. PCA is a widely used statistical technique to reduce the spatiality of the dataset, decreasing the number of variables by transforming variables that are highly correlated, preserving data variability whenever possible. The transformed variables, referring to the principal components, are a linear function of those of the original data set^{13,58,59}. All analyzes were performed in the software logastm-Reflex-64.v7.2.1.

To define the spatial patterns of variation of Au concentrations in the tailings deposits, geochemical maps were obtained through ordinary kriging^{13,21,22,60,61} for the previously defined volumes. The identification of Au spatial patterns was critical to identify areas of high contents. The omnidirectional variogram calculated for the geochemical variables was used to obtain the models of spatial variability⁶². The use of variograms with omnidirectional ellipsoid are due to the existent uncertainty in the location of feed sources in the dams and tailings dumps. Based on the model of spatial continuity it was possible to obtain the distribution of Au concentrations for each area.

Results and discussion

Mineralogy. A detailed mineralogical characterization of the wastes was performed to obtain the base knowledge necessary to develop extraction procedures suitable to achieve the recoveries that guarantee economic viability. This characterization is of uppermost importance for the proposed aims since the mineralogical phases occurring in the wastes differ from those in the primary ore. Table 2 presents the results of the tailings' mineralogical characterization deposits under study.

(Tabela 5.12) **Table 2.** Means values of the modal mineralogy of the deposits 1 (**N = 130), 2 (N = 207), 3 (N = 400), 4 (N = 229) and 5 (N = 193). *Au particles accounting; **N number of samples.

Minerals	Ideal formula	1 (wt%)	2 (wt%)	3 (wt%)	4 (wt%)	5 (wt%)
Quartz	SiO ₂	36.65	31.57	37.83	55.8	15.6
Feldspar group						
Albite	NaAlSi ₃ O ₈	2.81	5.33	7.56	0.37	1.5
Anorthite	CaAl ₂ Si ₂ O ₈	0.010	–	0.030	0.010	0.053
K-feldspar	KAlSi ₃ O ₈	1.22	0.120	0.730	0.390	–
Phyllosilicates						
Muscovite group	KAl ₃ Si ₃ O ₁₀ (OH)1.9F0.1	27.0	9.08	32.7	112.0	17.1
Oxides						
Fe oxide/hydroxide	Fe ₂ O ₃ /FeOOH	8.95	–	9.06	8.86	56.8
Rutile	TiO ₂	0.560	0.190	0.600	0.490	0.599
Carbonates						
Ankerite	Ca(Fe,Mg,Mn)(CO ₃)O ₂	0.850	16.8	1.49	11.2	1.00
Siderite	FeCO ₃	8.94	2.92	0.010	7.25	–
Calcite	CaCO ₃	–	0.020	0.230	2.25	0.200
Sulfates						
Gypsum	CaSO ₄ 2H ₂ O	–	–	–	0.030	7.00
Sulfides						
Pyrite	Fe ₂ S ₂	0.220	0.310	0.060	0.500	0.002
Pyrrhotite	Fe ₂ +0.95S	4.70	0.060	0.148	0.790	0.004

Arsenopyrite	Fe^{3+}AsS	1.71	0.520	0.022	0.240	0.056
Chalcopyrite	$\text{CaMg}(\text{CO}_3)_2$	0.210	0.010	—	—	—
Gersdorffite	NiAsS	—	0.020	—	—	0.010
Covellite	CuS	0.010	—	—	0.070	0.100
Sphalerite	ZnS	—	—	—	0.010	—
Au minerals*						
Native Au	Au > 80%, Ag, Cu, Hg	60	45	2	364	526
Electrum	Au = 80%, Ag = 20%	5	8	1	10	42

In general, the gangue minerals are similar between the studied deposits, except for dam 5, the dam receiving wastes resulting from calcination and leaching procedures used in the Nova Lima facilities. However, statistically significant differences were observed between deposits 1 and 3, the first mainly composed by carbonates such as ankerite and siderite, and the later dominated by minerals from the feldspar group. The primary silicate is quartz containing Au inclusions, mainly in dams 4 and 3 (Fig. 4).

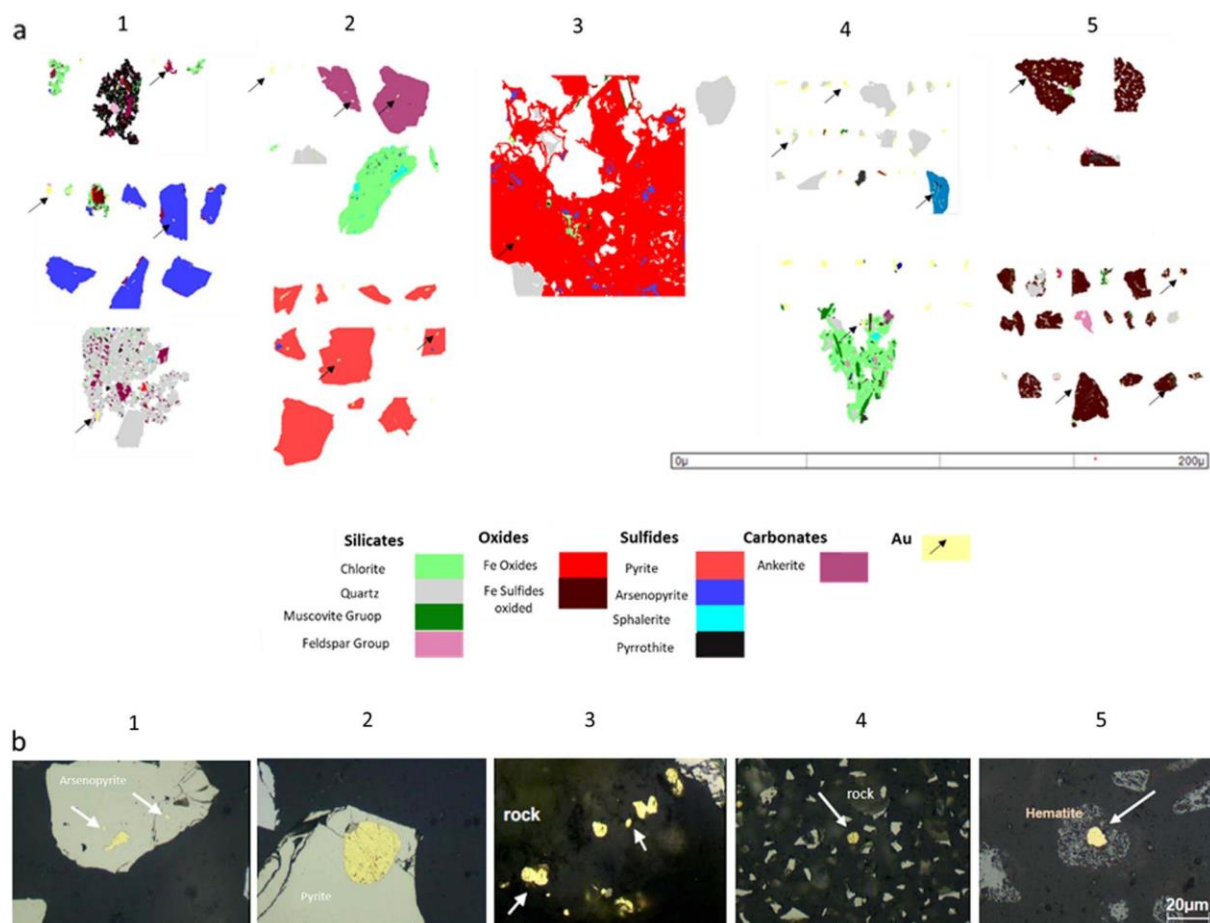


(Figura 5.24) **Figure 4.** (a) False color electron images of Au-bearing particles (yellow and black arrows): Deposit 1—Gold enclosed in pyrrhotite (black), chlorite (green), arsenopyrite (blue) and quartz (gray). Deposit 2: Free and enclosed gold particles in ankerite (purple), chlorite, quartz, and pyrite (dark pink). Deposit 3: Relics of arsenopyrite and gold particles enclosed in iron oxide (red). Deposit 4: Free gold particles and associated in quartz, chlorite, and Deposit 5: Gold particles enclosed in iron oxide and silicates (pink and gray). (b) Microphotographs of coarse gold particles associations (reflected light and parallel Nicols) in arsenopyrite (deposit 1), pyrite (deposit 2), rock minerals as quartz, chlorite, muscovite (deposits 3 and 4) and Hematite (deposit 5).

The primary sulfides and their association with Au express the distinctive mineralogical features between deposits 1, 2, 3, and 4. Pyrrhotite, pyrite, and arsenopyrite are abundant, and their ratios vary between deposits. While pyrrhotite/arsenopyrite are frequently observed in samples from deposit 1, pyrite/arsenopyrite are found in deposit 2. Although in considerably lower amounts relatively to deposit 1, the main sulfide mineral found in deposits 3 and 4 is pyrrhotite. In the sulfides of deposits 1 and 2, Au phases occur as inclusions (Fig. 4b1,b2). The differences in sulfide mineralogy in these deposits may indicate (1) the different sources, that is, wastes originated from mines having distinctive mineral assemblages; (2) different ore processing methods, since dam 4 received flotation wastes (Fig. 2), while the others received wastes from gravimetric concentration and leaching; (3) differences in the kinetics of flotation and leaching processes, since historically the concentration and types of reagents used focused exclusively on the concentration of pyrite, rendering higher concentrations of pyrrhotite in the wastes; (4) different forms of waste storage, since deposits 2 and 4 are dams and deposits 1 and 3 correspond to waste piles. Dam 5 shows a different mineralogical composition, having more than 50% of Fe oxides with small Au inclusions (Fig. 4b5). The presence of high content of oxides in the tailings is due to the different ore processing used in the metallurgical plants that include a roaster to extract Au^{9,54}. Comparing with the other deposits, deposit 5 presents the greatest degree of mineralogical transformation between the source and the place of storage. All concentrated sulfides underwent high temperature transformations and were thus calcined, explaining why these Fe oxides are enriched in As, Cu, Ni, and Ag, besides Au (Fig. S4). The presence of gypsum was also observed, probably formed by the addition of reagents such as lime during the calcination process. The other deposits, characteristically, comprise more common minerals because they receive wastes from less aggressive processes such as flotation, gravimetry, and leaching.

In addition to the distinctive mineral associations, the composition of Au grains varies between the deposits. Native Au occurs in all deposits; electrum is more common in dams 4 and 5. In deposits 1 and 2, Au is mainly associated with the sulfides while in deposits 3 and 4 the precious metal occurs in quartz and other silicates, as well as carbonates. In dam 5, Au is mainly associated with iron oxides. These results represent the different sources and treatment processes that originated the wastes deposited in these structures.

Chemistry. To evaluated differences in the chemistry of the tailings, concentration of 19 chemical elements were analyzed distance in samples collected at one meter along the core. Table 3 shows a statistical summary for the chemical results obtained for the solid wastes.

In general, the 19 chemical variables present dissimilar distributions that are expressed by the variable skewness coefficients, as can be observed in Table 3. Heavily skewed distributions are expected due to the presence of outlier values (supplementary Fig. S5). Asymmetric distributions represent mixtures of populations, and can be defined due to multiple and different sources or processes⁶³. The data presented in Table 3 show that mean Fe concentration, in addition to Cu, Zn, Ag, Pb, and Ni, are higher in deposit 5. This can be explained by the presence of Fe oxides containing these elements (Table 2; Fig. S4). Here, the C concentrations are lower than those of the other deposits.

Deposits 1, 4, and 5 are marked by the highest average of S, Al, and Ca. Sulfur concentrations can be explained by the presence of sulfides, while Al is related to the presence of aluminum silicates such as muscovite and chlorite (Table 3). Deposits 3 and 2 are depleted in S and Ag. The Sc content is relevant for deposit 2 and should be further investigated in future work.

(Tabela 5.13) **Table 3.** Statistical summary of chemical variables of tails deposits 1 to 5. *LOD* below detection limit.

Variable	Deposit	N	Mean	S.D	Min	Q1	Median	Q3	Max	Skew
Ag (mg/kg)	1	266	LOD	LOD	LOD	LOD	LOD	LOD	LOD	LOD
	2	162	0.516	0.199	0.230	0.330	0.460	0.690	0.900	0.320
	3	615	0.658	2.21	0.250	0.250	0.250	0.250	13.8	6.03

RESULTADOS E DISCUSSÕES

Scientific Reports | (2023) 13:4339

<https://doi.org/10.1038/s41598-023-31133-6>

	4	286	1.51	0.134	1.50	1.50	1.50	1.50	3.00	11.1
	5	230	7.27	3.31	1.00	6.00	8.00	9.00	15.0	-0.530
Al (%)	1	266	5.24	2.71	0.410	3.12	5.57	7.46	9.70	-0.340
	2	162	2.94	6.03	0.100	0.460	0.660	3.30	26.3	3.60
	3	615	1.07	0.536	0.233	0.541	1.09	1.53	2.00	0.070
	4	286	3.26	2.17	1.33	2.03	2.50	3.42	11.0	2.12
	5	230	2.92	1.07	0.780	2.28	2.75	3.40	8.46	1.82
As (%)	1	266	0.532	0.322	0.120	0.240	0.470	0.834	1.00	0.280
	2	162	0.634	0.416	0.100	0.200	0.600	0.910	1.35	0.460
	3	615	0.009	0.109	0.100	0.100	1.99	0.0006	1.99	14.8
	4	286	0.550	0.205	0.123	0.417	0.557	0.674	1.00	0.250
	5	230	0.868	0.137	0.281	0.804	0.886	1.00	1.00	-1.47
Au (mg/kg)	1	266	0.695	0.606	0.115	0.250	0.415	1.05	2.54	1.14
	2	162	1.28	0.819	0.250	0.630	1.16	1.73	3.30	0.940
	3	615	0.362	0.245	0.100	0.150	0.300	0.500	1.19	1.26
	4	286	0.961	0.718	0.100	0.595	0.772	1.19	8.71	5.56
	5	230	2.40	1.06	0.127	1.93	2.35	2.57	9.45	3.70
C (%)	1	266	1.08	1.28	0.100	0.300	0.410	1.40	4.37	1.62
	2	162	2.56	1.76	0.100	0.430	2.45	4.30	4.95	-0.070
	3	615	2.68	0.124	2.52	2.62	2.70	2.69	3.30	3.70
	4	286	3.60	1.17	0.130	3.48	3.82	4.10	12.1	0.140
	5	230	0.230	0.222	0.100	0.120	0.140	0.180	0.900	2.21
Ca (%)	1	266	0.720	0.919	0.100	0.200	0.400	0.770	4.82	3.15
	2	162	1.35	1.61	0.100	0.170	0.490	3.27	4.46	0.930
	3	615	0.563	0.656	0.132	0.234	0.437	0.677	4.19	4.79
	4	286	4.045	1.86	0.150	3.76	4.26	4.46	16.0	3.03
	5	230	2.70	0.656	0.160	2.36	2.61	2.92	5.75	0.460
Cu %	1	266	0.344	0.249	0.100	0.152	0.230	0.492	0.900	1.06
	2	162	0.487	0.250	0.110	0.200	0.500	0.700	0.800	-0.380
	3	615	0.464	0.271	0.100	0.188	0.432	0.670	0.980	0.410
	4	286	0.267	0.184	0.100	0.172	0.213	0.260	0.990	2.31
	5	230	0.550	0.365	0.111	0.129	0.683	0.890	0.998	-0.180
Fe (%)	1	266	8.88	5.44	1.48	3.47	7.77	15.0	15.0	0.010
	2	162	8.54	3.24	1.24	6.20	8.80	9.95	14.2	-0.220
	3	615	0.003	0.006	0.005	0.005	0.080	0.005	0.080	5.95
	4	286	12.6	3.22	1.00	12.5	13.6	15.0	15.0	-2.02
	5	230	8.02	13.4	4.00	4.00	4.00	4.00	67.0	3.33
Mg (%)	1	266	1.08	1.28	0.100	0.305	0.550	1.38	4.80	1.76
	2	162	1.90	1.07	0.300	0.900	2.12	2.76	3.35	-0.270
	3	615	0.641	0.558	0.129	0.283	0.538	0.844	3.22	2.96
	4	286	2.201	0.918	0.130	1.58	2.49	2.84	3.90	-0.610
	5	230	0.597	0.1435	0.170	0.515	0.600	0.700	0.930	-0.370
Mn (%)	1	266	0.385	0.269	0.100	0.140	0.300	0.600	0.900	0.610
	2	162	0.331	0.170	0.100	0.184	0.322	0.415	0.733	0.840
	3	615	0.418	0.278	0.111	0.160	0.381	0.649	0.940	0.570
	4	286	0.295	0.068	0.100	0.280	0.300	0.320	0.800	1.92
	5	230	0.434	0.370	0.100	0.100	0.130	0.900	0.900	0.300
Na (%)	1	266	0.642	0.491	0.100	0.245	0.430	0.960	1.81	0.850
	2	162	0.698	0.421	0.110	0.430	0.600	0.900	1.90	1.33

Ni (mg/kg)	3	615	0.201	0.144	0.100	0.132	0.158	0.230	0.921	3.93
	4	286	0.609	0.273	0.120	0.340	0.680	0.8300	1.6	- 0.120
	5	230	0.233	0.100	0.100	0.175	0.220	0.260	0.900	3.20
	1	266	76.4	57.3	1.00	36.5	61.0	112	298	1.26
	2	162	193	109	23.0	157	168	233	547	1.75
P (%)	3	615	61.6	52.0	0.500	34.0	48.3	85.6	271	2.14
	4	286	80.2	50.1	1.00	54.0	81.0	99.0	243	0.670
	5	230	425	199	3.00	326	497	559	744	- 0.890
	1	266	0.333	0.142	0.100	0.200	0.300	0.400	0.800	0.550
	2	162	0.397	0.145	0.250	0.330	0.380	0.410	0.950	3.30
Pb (mg/kg)	3	615	0.350	0.180	0.132	0.230	0.291	0.396	0.876	1.66
	4	286	0.360	0.0978	0.100	0.300	0.300	0.400	0.800	1.96
	5	230	0.459	0.073	0.300	0.400	0.500	0.500	0.700	0.680
	1	266	29.9	92.6	1.00	9.00	14.0	21.5	749	7.57
	2	162	148	146	7.00	22.1	92.6	297	429	0.670
Sc (mg/kg)	3	615	26.7	90.1	1.50	3.90	10.5	16.6	564	6.04
	4	286	41.3	23.6	1.00	27.3	42.5	56.0	124	0.170
	5	230	197	106	2.00	142	231	267	383	- 0.600
	1	266	8.25	6.20	1.00	2.50	7.00	10.0	27.0	1.17
	2	162	14.4	7.27	1.50	9.40	13.1	17.7	28.4	0.180
Ti (%)	3	615	4.18	1.58	1.60	4.00	4.00	4.00	13.4	5.49
	4	286	8.26	5.200	1.00	6.00	7.00	9.00	26.0	1.99
	5	230	7.74	4.16	1.00	6.00	8.00	11.0	22.0	- 0.010
	1	266	0.262	0.185	0.100	0.155	0.200	0.295	0.800	2.13
	2	162	0.459	0.299	0.110	0.180	0.510	0.750	0.970	0.230
Zn (mg/kg)	3	615	0.417	0.261	0.100	0.185	0.372	0.628	0.917	0.480
	4	286	0.498	0.185	0.100	0.400	0.500	0.600	0.900	- 0.460
	5	230	0.538	0.186	0.100	0.400	0.500	0.700	0.900	- 0.280
	1	266	25.2	80.6	1.00	31.0	58.0	112	199	0.670
	2	162	11.4	34.7	6.00	46.0	94.0	127	167	- 0.080
	3	615	11.3	42.2	2.20	30.6	53.6	123	368	2.03
	4	286	162	311	1.00	43.0	86.0	148	3419	7.21
	5	230	1872	1796	18	499	2778	3641	6187	- 0.080

Average Au concentrations range, in general, from 0.1 to 2 mg/kg (Table 3). The highest average was found in deposit 5, followed by deposits 4 and 1. The tailings from area 3 show the lowest average concentration, indicating that tailings with lower Au content were accumulated in this deposit. This result is supported by the mineralogical study, which indicated a larger number of Au grains in samples from deposit 5 than deposit 3.

Although As is one of the main contaminants, it can also be an element of economic interest¹⁰. In these deposits, the geochemical pattern of As is similar to that of Au, and the element is more abundant in deposits 5, 4, and 1. From Fig. 5 and Table 3, the relationship of this element with Au can be explained by the associations found for the Au phases, most commonly with As-Fe containing sulfides in deposits 1 and 4.

The Mn contents are higher in deposit 4, probably due to the presence of carbonates⁵⁴. Although this element is not as hazardous as As, Mn levels must be taken into account in the context of contamination⁶⁴.

The PCA performed for the dataset resulting from the chemical analysis of the tailings collected from the different deposits shows the geometrical relationships between the geochemical variables. About 50% of the variability in the data is explained by the two first principal components (Fig. 5). PCA analysis has

identified three distinct groups of geochemical variables. The first comprises elements such as Pb, Ni, Au, Ag, Zn, and Cu. The second group encloses S, Ca, C, and Mg. Comparing these results with those of the mineralogy (Table 2) and geochemistry (Table 3), it is likely that variables in the first group represent the deposit 5 while variables in group 2 represent deposits 1, 3, and 4 (Fig. 5). The Sc-Al association possibly indicates deposit 2, which presents the most elevated Sc concentrations (Table 3).

Therefore, the distinctive geochemical patterns clearly indicate different characteristics for deposits 2 and 5 and common features for deposits 1, 3, and 4 (Fig. 5, Fig. S6). Such detailed information is essential to assess the metallurgical potential for reuse and the impacts associated with the disposal of these tailings^{6,9}.

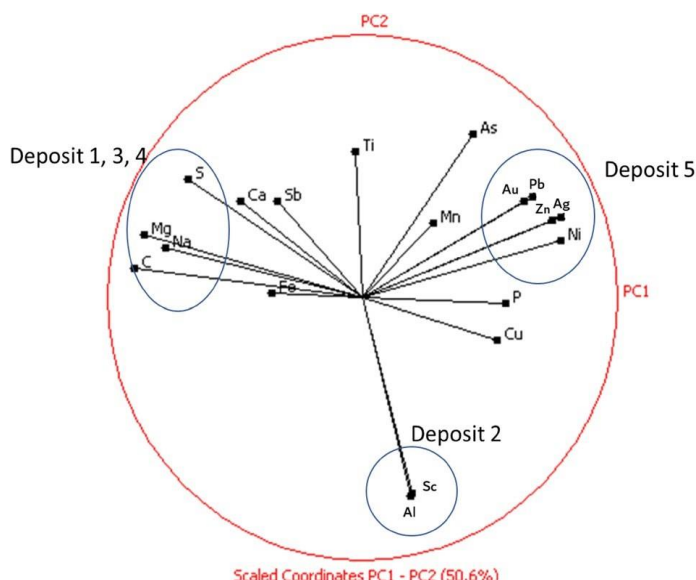


(Figura 5.25) **Figure 5.** Variables projections on the first factorial plane (PC1/PC2). This plane accounts for about 50% of the total explained variance of the dataset. The blue circles highlight the clusters obtained by the PCA analysis.

3D modelling of Au contents. Besides to the mineralogical and geochemical characteristics of the deposits, the size and shape of the mineral masses are also important factors to consider when assessing the potential for the valorization of the wastes. Therefore, for the Au concentrations, a 3D spatial continuity model was defined for the five deposits considering the heterogeneity study of each one individually. For each deposit, a variogram was built that considers the individuality of the spatial continuity of the distribution of the Au concentration. 3D maps obtained by ordinary kriging are presented in Fig. 6. In these maps, the concentration intervals correspond to the minimum, the quartiles, and the maximum value of the kriged blocks. From the maps, it is possible to identify the distributions of Au concentrations within the deposit and target enrichment areas that can be used in feasibility analysis and reserves estimations.

Figure 7 shows histograms with Au distribution in the blocks of the 3D model of deposits 1–5. Table 4 shows the mean estimated concentrations of Au, as well as the tonnages and ounces for the five deposits under study.

For deposit 1, the ounces obtained by this modeling represent 14 Moz (Table 4). Enrichment areas with Au grades above 1 mg/kg are observed in the northwest portion of the area. Concentrations above 1 mg/kg also occur in blocks from 15 m deep forward (Fig. 6). The blocks show an average concentration close to 1 mg/kg (Fig. 7), indicating potentially interesting values for the waste volume under study.

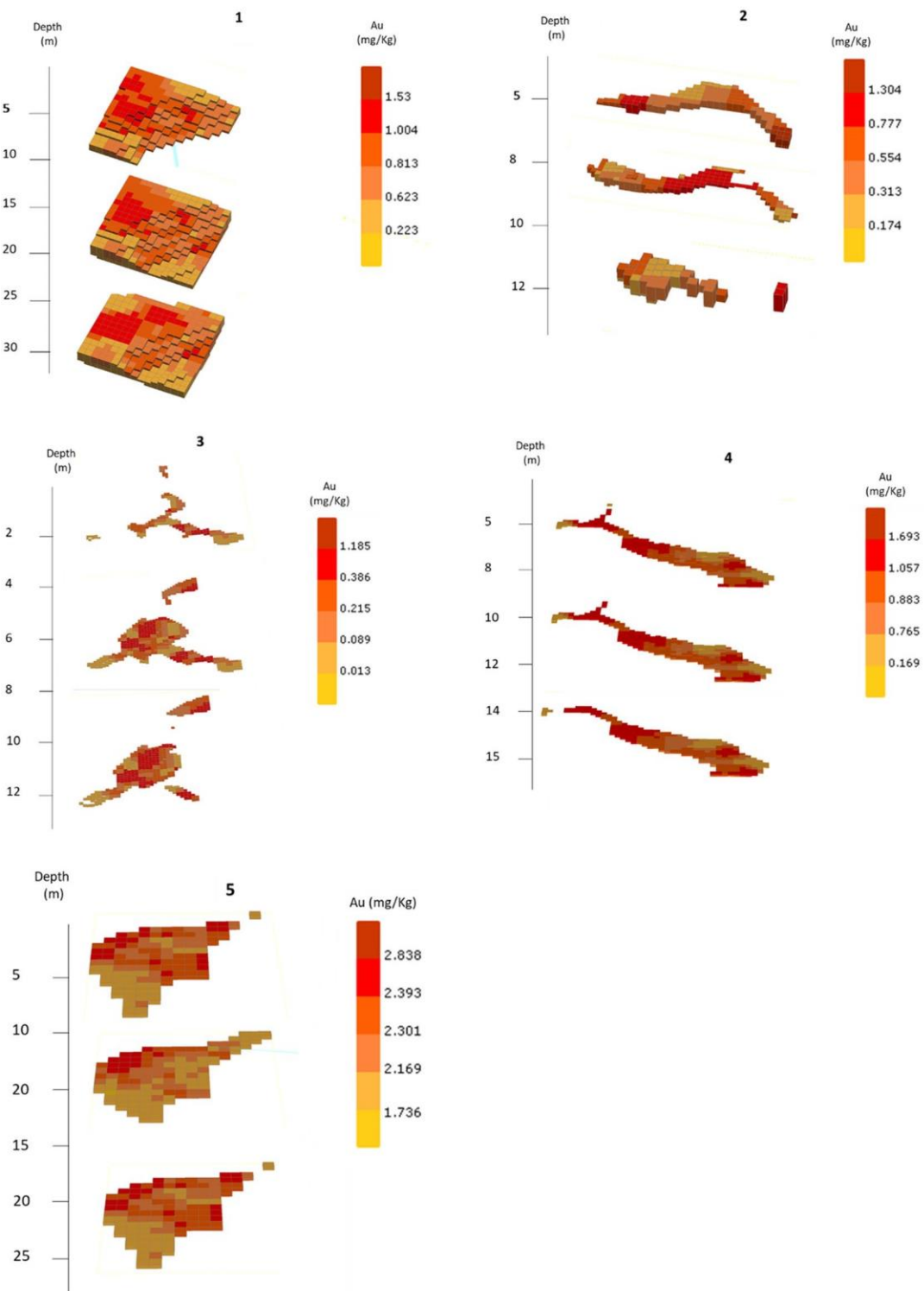


(Figura 5.26) **Figure 6.** Spatial distribution of Au grades from 3D model by elevation and deposits 1 to 5.

In deposit 2, it is observed a limited continuity in Au contents with depth. Small enrichment zones occur at the east boundaries of the deposit for the first 5 m depth and in the center for the next 10 m (Fig. 6). The highest frequency obtained for these blocks is 0.5 mg/kg (Fig. 7), although several blocks have

contents above 1 mg/kg, which are regarded as enrichment areas. Nevertheless, the amount of Au contained in this deposit is relatively low, represented only by 0.179 Moz (Table 4).

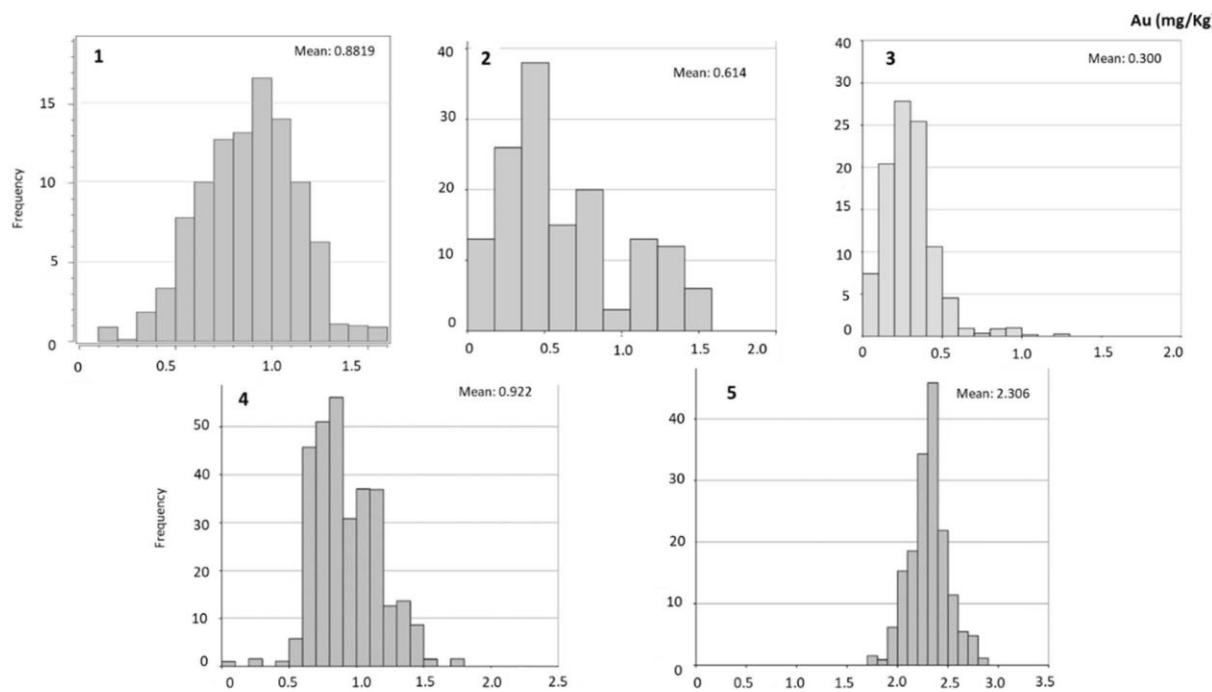


(Figura 5.27) **Figure 7.** Distribution of Au contents in the block from 3D model for deposits 1 to 5.

Deposit 3, a stockpile, is less attractive, as the enrichment zones show limited spatial continuity. The random vertical and lateral distribution of these relatively high Au-content areas decreases the potential for valuation of these wastes. The histogram of Fig. 7 also shows most blocks having concentrations below 0.5 mg/kg. Therefore, the Au contained in this deposit is very low (Table 4).

(Tabela 5.14) **Table 4.** Estimation resources of Au for deposit 1 to 5.

Structure	Tonnes (Mt)	Au (mg/kg)	Onces (Moz)
1	501	0.88	14
2	7	0.61	0.179
3	413	0.30	4
4	3350	0.92	100
5	2048	2.30	150

In the deposit 4, high content blocks (Au concentrations equal to 0.8 mg/kg and 1.0 mg/kg) show considerable spatial continuity with depth (Figs. 6, 7). Low grades are observed at the northeast boundaries, but in terms of representation and continuity may be considered negligible since the Au content is 100 Moz (Table 4).

In deposit 5, the Au concentrations increase in the last 40 m depth (Figs. 6, 7). This deposit has the higher Au concentration, reaching 150 Moz (Table 4).

Therefore, based on the estimates, Au contents range from 0.3 to 2 mg/kg. The highest grades (average = 2.30 mg/kg) are obtained for deposit 5. Tailings 3 presents the lowest Au grade, with an average estimate of 0.30 mg/kg. Deposits 1 and 4 show average Au grades that are similar and range from 0.88 to 0.92 mg/kg. Finally, estimated value for deposit 2 is 0.61 mg/kg for the mean Au content.

The results suggest that the deposits 4 and 5 have a high potential for Au recovery and reuse compared to other mines around the world that are described in many research^{11,53,65}. Deposits 3 and 2 show lower potential for valuation, as the estimates indicate low metal contents and smaller volumes.

It is important to note that, in addition to Au contents, a range of other factors influence the potential for valuation. The efficiency of metallurgical Au recovery, available technologies, metal price, OPEX/CAPEX costs, and socio-economic situation of the region, are among the most important constraints¹³.

Au metallurgical tests. According to the results of the 3D models (Table 4), the distribution of Au showed, in general, a potential for extracting this element. Therefore, new information is necessary, namely on the recovery efficiency, to properly assess this potential. Thus, two extraction procedures (Supplementary Fig. S2) were developed based on the mineralogical and geochemical characteristics described earlier for the different tailings.

To test the two procedures, composite samples were obtained from the enrichment zones identified in the 3D models (Fig. 6). In the first procedure, the samples were ground at 74 µm, calcined at 700 °C, and leached with cyanide (concentration 2000 mg/kg) and lime (concentration 2090 mg/kg). In procedure 2, the samples were leached in the same conditions as in scenario 1, but without calcination stage.

The Au recovery (%) obtained for each deposit are presented in Table 5. The results indicated that Au recovery potentials vary with the procedure used and between deposits (Table 5). The recoveries obtained for deposit 5 are low, especially with procedure 1.

(Tabela 5.15) **Table 5.** Summary of results of metallurgical tests for reuse of Au.

Deposit	Feed grade (mg/kg)	Au mineralogical association	Procedure 1 (calcine + leach- in 74 µm %Au recovery)	Procedure 2 (leach in 74 µm-% Au recovery)
1	1.16	Au in sulfides and quartz	78.5	64.0
2	1.05	Au in sulfides and quartz	77.7	24.1
3	0.60	Au in sulfides and quartz	53.4	93.0
4	0.87	Au in sulfides and quartz	79.7	50.7
5	2.40	Au in Fe oxides	0.600	32.2

Deposits 1, 2, and 4 showed better results when submitted to calcination followed by leaching (procedure 1). In these deposits, Au is associated with sulfides such as arsenopyrite, pyrite, and pyrrhotite, and the calcination effectively liberate the enclosed Au-particles^{9,39}. In addition, an important amount of Au associated with quartz was partially stripped in the leaching stage of procedure 1.

Although dam 5 has better estimated Au grades (Table 4), it was challenging to extract Au using the proposed procedures. Based in mineralogy data, the previous calcination processes produced secondary mineral phases that are extremely resistant, and the Au inclusions are tightly bound to the iron oxides (Fig. 4, Fig. S4). The results indicate that when the wastes underwent calcination, a second calcination stage decreases the efficiency of the extraction.

More than 90% of Au were recovered from deposit 3 samples when subjected to procedure 2 (74 µm leaching), which indicates a high potential to leach Au associated to silicate minerals by the acid solutions. However, as referred, technological challenges are foreseen for the recovery of deposit 5, the one with the highest content. This fact is probably due to the form of occurrence of Au in the Fe oxides (Fig. 4). Gold is extremely fine-grained and is entrapped in the pores of the Fe-oxides formed during the calcination stage of the metallurgical treatment of the Au-ores. Therefore, the mineralogical and textural features of the mine wastes are critical factors for recovery.

Nevertheless, the extraction of these wastes seems feasible and has the potential for valuation. However, together with other variables, it must be carefully evaluated when deciding the destination of these deposits.

Potential for generating other products. There is a need to generate and disseminate new technologies, especially the so-called clean and sustainable technologies. These must respond to the great challenges of the mining sector, such as minimizing environmental impact and maximizing social satisfaction^{66,67}. Although this work has focused on the recovery of Au, the potential for other applications and use of these tailings should be considered. Therefore, for the five deposits under study, other valuation potentials are also suggested. Important for this evaluation were the mineralogy (Table 2) and the geochemical patterns previously identified (Fig. 6). Table S2 shows other proposals for the potential valuation of these tailings.

In general, some method of separation, e.g. triboelectrostatic⁶⁸, is efficient to concentrate and liberate sulfides for better extraction of Au. Based on the described mineralogy, the developed methodologies for Au extraction may potentially be used to generate other valuable resources such as vapor generated energy, iron, and gypsum. Furthermore, silicate minerals could form a dry sand for use in construction. In some cases, such as deposits 5 and 4, Fe oxides can also be concentrated by magnetic separation.

In addition, other potential resources can also be investigated. This may be the case of As and Sb, which can be tested to generate a new product, thereby decreasing the potential for contamination. The vitrification of As and Sb has great potential for application in these types of materials³⁷.

Also, studies of the use of these materials as rock meal and fertilizers can be of great interest due to the K and Al concentrations⁶⁹.

Conclusions

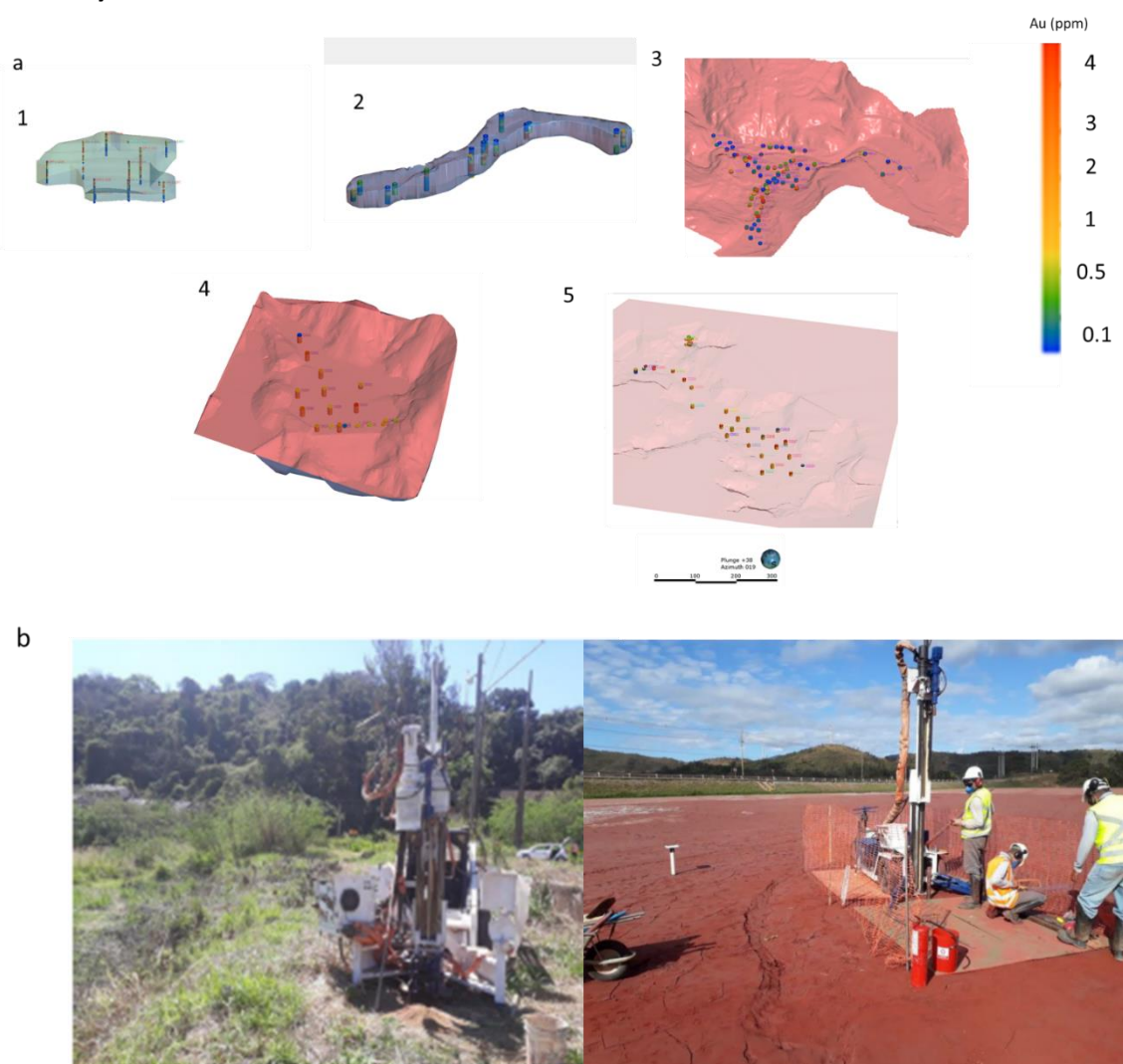
In this work, gold mining tailings were studied in order to identify their value through the use of characterization and geostatistical tools. The use of these tools identified Au as a valuable element and generated motivation for paths that avoid undesirable disposal of waste and large-scale environmental impacts. The result of the characterization and modeling showed that Au is the most interesting metal in terms of resources with concentration like low-grade mines currently in operation. Interesting Au enrichment zones were identified in the deposits 1–5 through 3D models. Deposits 4 and 5 are more appealing since they present higher Au concentrations and more homogeneous spatial distributions. In general, wastes discarded in dams show higher valuation potential than waste piles, mainly to the higher lateral and vertical continuity of the Au-contents.

The metallurgical tests show good recoveries for Au. Deposits 1, 2 and 4 presented above 70% for procedure 1, while the au from samples from deposit 3 was better extracted in procedure 2. Even with higher levels of Au, deposit 5 showed low extraction potential, demonstrating a challenge technology for the reuse of Au from this deposit.

Furthermore, in addition to Au, some elements like As, Sc, Mg, Ti, and Si that are in the list of critical elements of the EU, may have potential economic value, indicating the need for future works.

In the present study, through the combination of statistical, mineralogical and geochemical tools, it was possible to assess the potential for valuation of the mining wastes. This study, thus, adds new knowledge contributing to the sustainable development of the mineral sector, towards a future where waste becomes a product and that the generation of zero tailings becomes a reality in this sector.

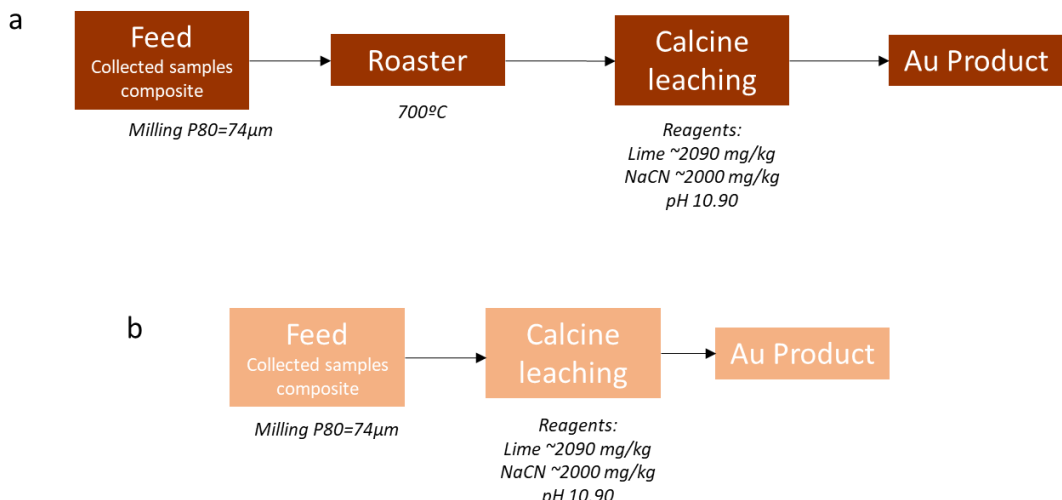
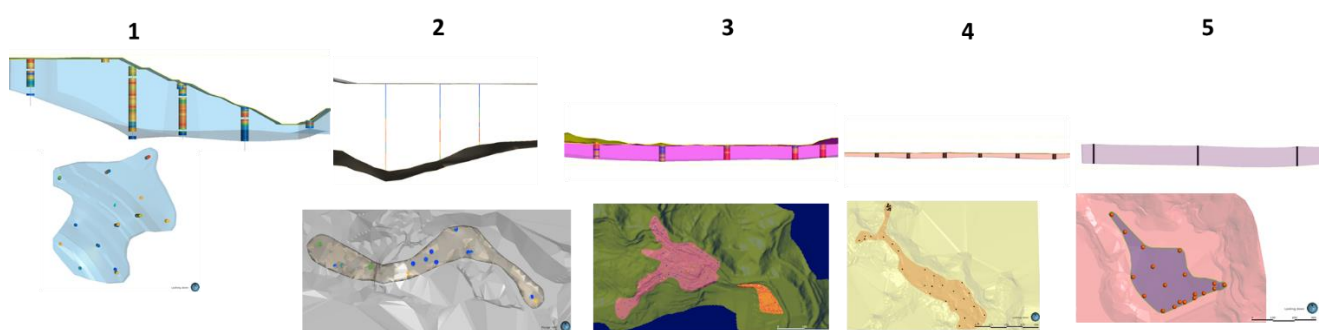
Supplementary material



(Figura 5.28) **Fig S1.** **a.** Collection points of structures 1 to 5 and **b.** Instrument images and collections in dry deposits (above) and dam (below).

(Tabela 5.16) **Table S 1.** Sampling Method by Tailings Deposit

Area	Sampling Method	Depth (~m)	Samples Numbers	Analysis
1	Percussion+Diamond Probing	15.88	266	ICP, Fire Assay, PSD, Mineralogy and Metallurgical Tests
2	Percussion Probing	4.43	162	
3	Direct push	4.0	615	
4	Direct push	6.70	286	
5	Direct push	12.50	257	

(Figura 5.29) **Fig S2.** Workflow of Au Metallurgical Procedure 1 (a) and 2 (b)(Figura 5.30) **Fig S3.** Topography limits of 3D modeled by areas 1 to 5

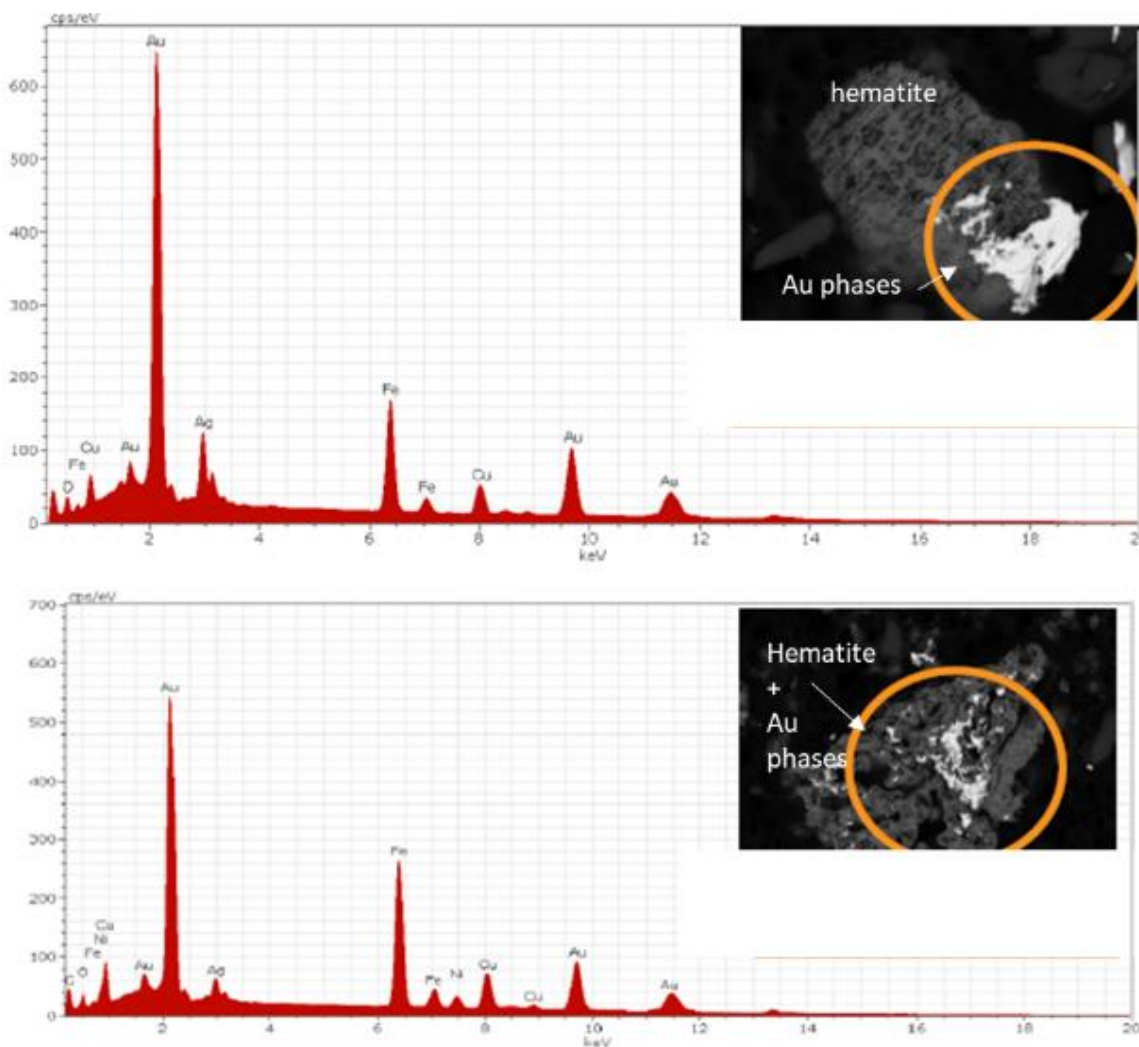


(Figura 5.31) **Fig S4.** EDS spectra of Fe oxides and Au phases containing elements such as Cu, Ni, Ag, As from deposit 5.

RESULTADOS E DISCUSSÕES

Scientific Reports | (2023) 13:4339

<https://doi.org/10.1038/s41598-023-31133-6>

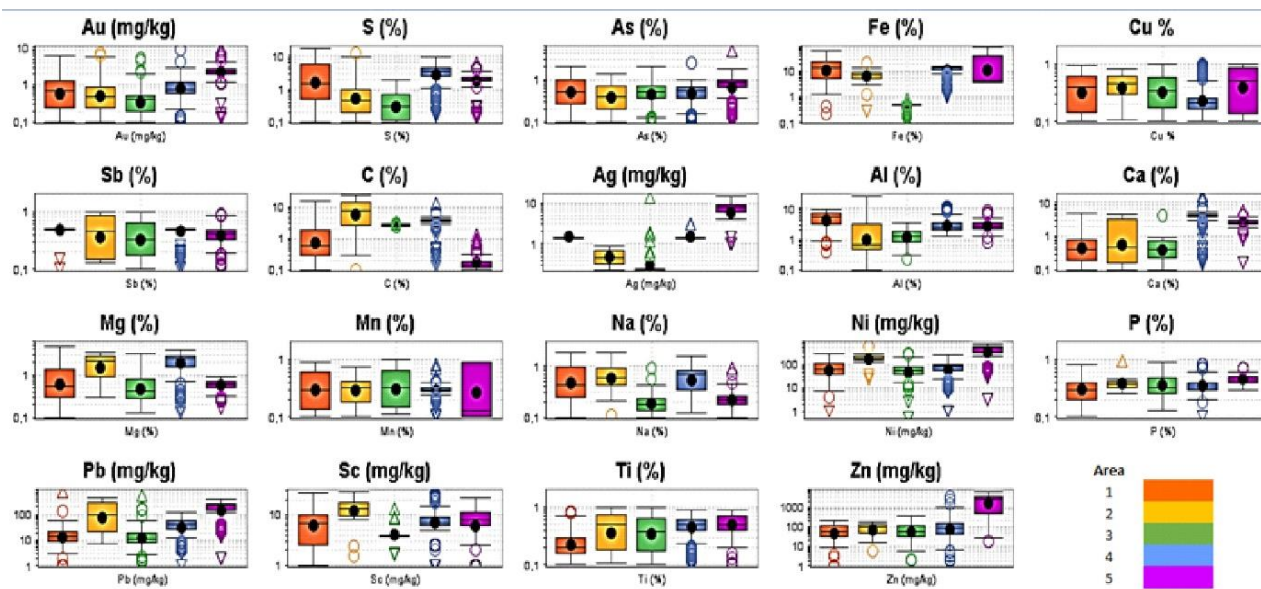


(Figura 5.32) **Fig S5.** Box plots for 19 elements-based on dataset collected.

(Tabela 5.17) **Table S2.** Summary of the main potential uses of the studied samples.

Struture	Product	Au recovery	Reuse potential 1	Reuse potential 2	Reuse potential 3
1	Tailings pile	78.5	As vitrification	sand, filler, cement	-
2	Tailings Dam	77.7	As vitrification Sr recovery	sand, filler, cement	plaster
3	Tailings pile	93.0	As vitrification	sand, filler, cement	-
4	Tailings Dam	79.7	As vitrification	sand, filler, cement	Fertilizers, rock meals
5	Tailings Dam	32.2	As vitrification Fe recovery	-	Fertilizers, rock meals

Data availability

The datasets used and/or analysed during the current study available from the corresponding author on reasonable request.

Received: 15 December 2022; Accepted: 7 March 2023

Published online: 16 March 2023

References

1. Fernandes, C. Mineração no Brasil Colonial. <https://brasilescoia.uol.com.br/historiab/mineracao-no-brasil-colonial.htm> (2022).
2. Souza Júnior, T. F., Moreira, E. B. & Heineck, K. S. Barragens de rejeito e contenções no Brasil. *Holos* 5, 1–39 (2018).
3. FEAM. Fundação Estadual do Meio Ambiente. <http://www.feam.br/> (2022).

RESULTADOS E DISCUSSÕES

Scientific Reports | (2023) 13:4339

<https://doi.org/10.1038/s41598-023-31133-6>

4. Vinaud, L. U P. Barragens de rejeito de mineração em Minas Gerais: Lista de verificação e aspectos técnicos, legais e ambientais. https://www.engmi.nas.araxa.cefet.mg.br/wpcotent/uploads/sites/170/2020/02/TCC_Laura_Vinaud.pdf (2019).
5. ANM. <https://www.gov.br/anm/pt-br> (2022).
6. Lemos, M. G. *et al.* Geoenvironmental study of gold mining tailings in a circular economy context: Santa Barbara, Minas Gerais, Brazil. *Mine Water Environ.* **40**, 257–269. <https://doi.org/10.1007/s10230-021-00754-6> (2021).
7. Gaustad, G., Krystofik, M., Bustamante, M. & Badami, K. Circular economy strategies for mitigating critical material supply issues. *Resour. Conserv. Recycl.* **135**, 24–33. <https://doi.org/10.1016/j.resconrec.2017.08.002> (2018).
8. Campomar, M. C. Do uso de estudo de caso em pesquisas para dissertações e teses em administração. *Rev. Admin. RAUSP* **26**(3), 95–97 (1991).
9. Lemos, M. *et al.* Mineralogical and geochemical characterization of gold mining tailings and their potential to generate acid mine drainage (Minas Gerais, Brazil). *Minerals* **11**, 1–16. <https://doi.org/10.3390/min11010039> (2021).
10. European Commission. Communication from the commission to the European parliament, the council, the European economic and social committee and the committee of the regions. Critical Raw Mater. Resilience: Charting a Path towards. https://doi.org/10.1007/978-3-030-40268-6_9 (2020).
11. Parviaainen, A., Soto, F. & Caraballo, M. A. Revalorization of Haveri Au–Cu mine tailings (SW Finland) for potential reprocessing. *J. Geochem. Explor.* <https://doi.org/10.1016/j.gexplo.2020.106614> (2020).
12. Edraki, M. *et al.* Designing mine tailings for better environmental, social and economic outcomes: A review of alternative approaches. *J. Clean. Prod.* **84**, 411–420. <https://doi.org/10.1016/j.jclepro.2014.04.079> (2014).
13. González-Díaz, E. *et al.* Geochemical, mineralogical and geostatistical modelling of an IOCG tailings deposit (El Buitre, Chile): Implications for environmental safety and economic potential. *J. Geochem. Explor.* <https://doi.org/10.1016/j.gexplo.2022.106997> (2022).
14. Martin, C. J., Al, T. A. & Cabri, L. J. Surface analysis of particles in mine tailings by time-of-flight laser-ionization mass spectrometry (TOF-LIMS). *Environ. Geol.* **32**, 107–113. <https://doi.org/10.1007/s00254-0050-199> (1997).
15. Silva, S. R., Procópio, S. O., Queiroz, T. F. N. & Dias, L. E. Characterization of gold mine tailing to evaluate the arsenic and heavy metal solubility and local revegetation. *Rev. Brasil. Cie. Solo* **28**, 189–196. <https://doi.org/10.1590/s0100-06832004000100018> (2004).
16. Shi, T. *et al.* Adsorption of Pb(II), Cr(III), Cu(II), Cd(II) and Ni(II) onto a vanadium mine tailing from aqueous solution. *J. Hazard. Mater.* **169**, 838–846. <https://doi.org/10.1016/j.jhazmat.2009.04.020> (2009).
17. Parbhakar-Fox, A., Fox, N. J. L. Geometallurgical evaluations of mine waste - an example from the Old Tailings Dam, Savage River, Tasmania. In Proceedings of 3rd AusIMM International Geometallurgy Conference, 193–204 (2016).
18. Novhe, N. O., Yibas, B., Coetzee, H., Mashalane, T., Atanasova, M. Geochemistry and Mineralogy of Precipitates Formed During Passive Treatment of Acid Mine Drainage in the Ermelo Coaleld, South Africa. 11th ICARD/IMWA/MWD Conference: Risk to Opportunity 171–176 (2018).
19. Guanira, K. *et al.* Methodological approach for mineralogical characterization of tailings from a Cu(Au, Ag) skarn type deposit using QEMSCAN (Quantitative Evaluation of Minerals by Scanning Electron Microscopy). *J. Geochem. Explor.* **209**, 106439. <https://doi.org/10.1016/j.gexplo.2019.106439> (2020).
20. Reis, A. P., Sousa, A. J., Ferreira da Silva, E., Patinha, C. & Fonseca, E. C. Combining multiple correspondence analysis with factorial kriging analysis for geochemical mapping of the gold–silver deposit at Marrancos (Portugal). *Appl. Geochem.* **19**(4), 623–631. <https://doi.org/10.1016/j.apgeochem.2003.09.003> (2004).
21. Ansh-sam, M., Binczyk, T., Dobek, C., Guo, C., Mimura, W. A Geostatistical Study to Quantify Uncertainty in Tailings Fines Content as a Function of Data Spacing AND Workflow and Software Guide for Constructing a Three Dimensional Geostatistical Model of a Tailings Deposit for the Purpose of Conducting a Geostatistical Resampling Study. <https://cosia.ca/sites/default/files/attachments/Tailings/Geostatistical/Study/-/Imperial.pdf> (2015).
22. Medina Tripodi, E. E., Gamboa Rueda, J. A., Aguirre Céspedes, C., Delgado Vega, J. & Collao Gómez, C. Characterization and geostatistical modelling of contaminantes and added value metals from an abandoned Cu–Au tailing dam in Taltal (Chile). *J. South Am. Earth Sci.* **93**, 183–202. <https://doi.org/10.1016/j.jsames.2019.05.001> (2019).
23. Wilson, R., Toro, N., Naranjo, O., Emery, X. & Navarra, A. Integration of geostatistical modeling into discrete event simulation for development of tailings dam retreatment applications. *Miner. Eng.* **164**, 106814. <https://doi.org/10.1016/j.mineeng.2021.1.06814> (2021).
24. Spooren, J. *et al.* Near-zero-waste processing of low-grade, complex primary ores and secondary raw materials in Europe: Technology development trends. *Resour. Conserv. Recycl.* **160**, 104919. <https://doi.org/10.1016/j.resconrec.2020.104919> (2020).
25. Singh, S., Sukla, L. B. & Goyal, S. K. Mine waste and circular economy. *Mater. Today Proc.* **30**, 332–339. <https://doi.org/10.1016/j.matpr.2020.01.616> (2020).
26. Akinwekomu, V. *et al.* Beneficiation of acid mine drainage (AMD): A viable option for the synthesis of goethite, hematite, magnetite, and gypsum—gearing towards a circular economy concept. *Miner. Eng.* **148**, 106204. <https://doi.org/10.1016/j.mineeng.2020.106204> (2020).
27. Antunes, M., Fernandes, R., Pinheiro, A., Valente, T., N. S. Potential of reuse and environmental behavior of ochre-precipitates from passive mine treatment. In *IMWA Proceedings*, pp. 205–208 (2010).
28. Macías, F., Pérez-López, R., Caraballo, M. A., Cánovas, C. R. & Nieto, J. M. Management strategies and valorization for waste sludge from active treatment of extremely metal-polluted acid mine drainage: A contribution for sustainable mining. *J. Clean. Prod.* **141**, 1057–1066. <https://doi.org/10.1016/j.jclepro.2016.09.181> (2017).
29. Rezaie, B. & Anderson, A. Sustainable resolutions for environmental threat of the acid mine drainage. *Sci. Total Environ.* **717**, 137211. <https://doi.org/10.1016/j.scitenv.2020.137211> (2020).
30. Ryan, M. J., Kney, A. D. & Carley, T. L. A study of selective precipitation techniques used to recover refined iron oxide pigments for the production of paint from a synthetic acid mine drainage solution. *Appl. Geochem.* **79**, 27–35. <https://doi.org/10.1016/j.apgeochem.2017.01.019> (2017).
31. de Silva, R. A. *et al.* Optimizing the selective precipitation of iron to produce yellow pigment from acid mine drainage. *Miner. Eng.* **135**, 111–117. <https://doi.org/10.1016/j.mineeng.2019.02.040> (2019).
32. Valente, T., Grande, J. A. D.L.T.M. Extracting value resources from acid mine drainages and mine wastes in the Iberian Pyrite Belt. In *Mining Meets Water—Conflicts and Solutions*, pp. 1339–1340 (2016).
33. Chen, T., Lei, C., Yan, B. & Xiao, X. Metal recovery from the copper sulfide tailing with leaching and fractional precipitation technology. *Hydrometallurgy* **147–148**, 178–182. <https://doi.org/10.1016/j.hydromet.2014.05.018> (2014).
34. Dehghani, A., Mostad-Rahimi, M., Mojtabahedzadeh, S. H. & Gharibi, K. K. Recovery of gold from the mouteh gold mine tailings dam. *J. South Afr. Inst. Min. Metall.* **109**, 417–421 (2009).
35. Falagán, C., Grail, B. M. & Johnson, D. B. New approaches for extracting and recovering metals from mine tailings. *Miner. Eng.* **106**, 71–78. <https://doi.org/10.1016/j.mineeng.2016.10.008> (2017).
36. Martin, M., Janneck, E., Kermér, R. & Patzig, A. R. S. Recovery of indium from sphalerite ore and flotation tailings by bioleaching and subsequent precipitation processes. *Miner. Eng.* **75**, 94–99 (2015).
37. Technologies, D.S. Method for vitrification of arsenic and antimony. US9981295B2. <https://patents.google.com/patent/US9981295B2/en> (2006).
38. Syed, S. Recovery of gold from secondary sources—a review. *Hydrometallurgy* **115–116**, 30–51. <https://doi.org/10.1016/j.hydromet.2011.12.012> (2012).
39. Samadov, A. U. & Nosirov, N. I. Overview of the concepts of gold recovery from stale tailings of a gold recovery plant. *J. Adv. Res. Stabil.* **2**, 3–8 (2022).

40. De Andrade Lima, L. R. P., Bernardez, L. A. & Barbosa, L. A. D. Characterization and treatment of artisanal gold mine tailings. *J. Hazard. Mater.* **150**, 747–753. <https://doi.org/10.1016/j.jhazmat.2007.05.028> (2008).
41. Liu, B., Zhang, Z., Li, L. & Wang, Y. Recovery of gold and iron from the cyanide tailings by magnetic roasting. *Xiyou Jinshu Cailiao Yu Gongcheng Rare Metal Mater. Eng.* **42**(9), 1805–1809. [https://doi.org/10.1016/s1875-5372\(14\)60009-6](https://doi.org/10.1016/s1875-5372(14)60009-6) (2013).
42. Li, H. *et al.* Investigation on the recovery of gold and silver from cyanide tailings using chlorination roasting process. *J. Alloys Compd.* **763**, 241–249. <https://doi.org/10.1016/j.jallcom.2018.05.298> (2018).
43. Acheampong, M. A., Meulepas, R. J. W. & Lens, P. N. Removal of heavy metals and cyanide from gold mine wastewater. *J. Chem. Technol. Biot.* **85**, 590–619 (2010).
44. Porto, C.G. A mineralização aurífera do depósito Córrego do Sítio e sua relação com o enxame de diques metamáficos no corpo Cachorro Bravo-Quadrilátero Ferrífero-Minas Gerais. Univ Federal de Minas Gerais (2008).
45. Goldfarb, R. Orogenic gold and geologic time: A global synthesis. *Ore Geol. Rev.* **18**, 1–75 (2001).
46. Lobato, L. M., Ribeiro-Rodrigues, L. C. & Vieira, F. W. R. Brazil's premier gold province. Part II: Geology and genesis of gold deposits in the Archean Rio das Velhas greenstone belt, Quadrilátero Ferrífero. *Miner. Depos.* **36**, 249–277 (2001).
47. Almeida, F. F. M. Estruturas do Pré-Cambriano Inferior Brasileiro. In: 29º Congresso Brasileiro de Geologia, pp. 335–342 (1976).
48. Schorscher, H. D. Polimetamorfismo do Pré-Cambriano na região de Itabira, Minas Gerais. In: 29º Congresso Brasileiro de Geologia. Sociedade Brasileira de Geologia, pp. 194–195 (1976).
49. Schorscher, H.D. Komatiitos na estrutura "Greenstone Belt" Série Rio das Velhas, Quadrilátero Ferrífero, Minas Gerais, Brasil. In: Congr. Bras. Geol., 30. pp. 292–293 (1978).
50. Martins, B. S. *et al.* The Archean BIF-hosted Lamego gold deposit, Rio das Velhas greenstone belt, Quadrilátero Ferrífero: Evidence for Cambrian structural modification of an Archean orogenic gold deposit. *Ore Geol. Rev.* **72**, 963–988 (2016).
51. Ribeiro-Rodrigues, L. C., Oliveira, C. G. & Friedrich, G. The Archean BIF-hosted Cuiabá Gold deposit. *Ore Geol. Rev.* **32**, 543–570 (2007).
52. IBGE, 2022. Instituto Brasileiro de Geografia e Estatística. <https://www.ibge.gov.br/>.
53. AGA, 2016. AngloGold Ashanti AngloGold Ashanti recommendations.
54. Moura W, 2005. Especiação de cianeto para redução do consumo no circuito de lixiviação de calcinado da usina do Queiróz.
55. Bachmann, K., Frenzel, M., Krause, J. & Gutzmer, J. Advanced identification and quantification of in-bearing minerals by scanning electron microscope-based image analysis. *Microsc. Microanal.* **23**(3), 527–537. <https://doi.org/10.1017/S1431927617000460> (2017).
56. Fandrich, R., Gu, Y., Burrows, D. & Moeller, K. Modern SEM-based mineral liberation analysis. *Int. J. Miner. Process.* **84**, 310–320. <https://doi.org/10.1016/j.minpro.2006.07.018> (2007).
57. Soto, F. *et al.* Transitive kriging for modeling tailings deposits: A case study in southwest Finland. *J. Clean. Prod.* **374**, 133857. <https://doi.org/10.1016/j.jclepro.2022.133857> (2022).
58. Jolliffe, I. T. Cadima Principal component analysis: A review and recent developments. *Philos. Trans. R. Soc. A* **374**, 20150202. <https://doi.org/10.1098/rsta.2015.0202> (2016).
59. Marinho Reis, A. P. *et al.* Lead and zinc concentrations in household dust and toenails of the residents (Estarreja, Portugal): A source-pathway-fate model. *Environ. Sci. Process Impacts* **20**(9), 1210–1224. <https://doi.org/10.1039/c8em00211h> (2018).
60. Journel, A. Geostatistics : Models and tools for the earth sciences. *Math. Geol.* **18**, 119–140 (1986).
61. Reis, A. P. *et al.* Metal fractionation of cadmium, lead and arsenic of geogenic origin in topsoils from the Marrancos gold mineralisation, northern Portugal. *Environ. Geochem. Health* **34**, 229–241. <https://doi.org/10.1007/s10653-011-9433-z> (2012).
62. Reis, A. P. *et al.* Geochemical associations and their spatial patterns of variation in soil data from the Marrancos gold–tungsten deposit: A pilot analysis. *Geochem. Explor. Environ. Anal.* **9**, 319–340. <https://doi.org/10.1144/1467-7873/09-1> (2009).
63. Zhao, X. *et al.* Origin of skewed frequency distribution of regional geochemical data from stream sediments and a data processing method. *J. Geochem. Explor.* <https://doi.org/10.1016/j.gexplo.2018.07.007> (2018).
64. CONAMA. Resolução nº 396, de 03 de abril de 2008. Dispõe sobre a Classificação e Diretrizes Ambientais para o Enquadramento das águas Subter-râneas e dá outras Providências (2008).
65. Calvo, G., Mudd, G., Valero, A. & Valero, A. Decreasing ore grades in global metallic mining: A theoretical issue or a global reality?. *Resources* **5**(4), 36. <https://doi.org/10.3390/resourcres5040036> (2016).
66. Nader, B., de Tomi, G. & Passos, A. O. Indicadores-chave de desempenho e a gestão integrada da mineração. *Rev. Escol. Minas* **65**, 537–542. <https://doi.org/10.1590/S0370-44672012000400015> (2012).
67. Passos, A. O. Proposta de Modelo para o Desenvolvimento de Projetos Minerais Sustentáveis no Brasil 110 (2015).
68. Yang, X. *et al.* Triboelectric properties of ilmenite and quartz minerals and investigation of triboelectric separation of ilmenite ore. *Int. J. Min. Sci. Technol.* **28**, 223–230. <https://doi.org/10.1016/j.ijmst.2018.01.003> (2018).
69. Kaźmierczak, U., Blachowski, J., Górnjak-Zimroz, J. & Wirth, H. Quantitative and qualitative research on the waste from the mining of rock raw materials in Lower Silesia. *Minerals* <https://doi.org/10.3390/min8090375> (2018).

Acknowledgements

We thank our colleagues from the ICT, microscopy center from Universidade Federal de Minas Gerais (CMUFMG), and AngloGold Ashanti who provided insight and expertise that greatly assisted the research. We also thanks to FCT—Fundação para a Ciência and Tecnologia through projects UIDB/04683/2020, UIDP/04683/2020 and Nano-MINENV 029259 (PTDC/CTA-AMB/29259/2017). The authors are grateful to the anonymous reviewers and to the editor for their valuable contributions to improving the manuscript.

Author contributions

M.L., T.V., P.R. and R.F. wrote the main manuscript text. M.L., J.P., J.G.F., M.M. and F.G. supported by providing information, metallurgic tests and data analysis. M.L., B.A. and A.S. analysis and execution of dam models. M.L. and I.D. carried out the mineralogical analyzes and data analysis.

Competing interests

The authors declare no competing interests.

Additional information

Supplementary Information The online version contains supplementary material available at <https://doi.org/10.1038/s41598-023-31133-6>.

Correspondence and requests for materials should be addressed to M.L.

Reprints and permissions information is available at www.nature.com/reprints.

Publisher's note Springer Nature remains neutral with regard to jurisdictional claims in published maps and institutional affiliations.

Open



Access This article is licensed under a Creative Commons Attribution 4.0 International

License, which permits use, sharing, adaptation, distribution and reproduction in any medium or format, as long as you give appropriate credit to the original author(s) and the source, provide a link to the Creative Commons licence, and indicate if changes were made. The images or other third party material in this article are included in the article's Creative Commons licence, unless indicated otherwise in a credit line to the material. If material is not included in the article's Creative Commons licence and your intended use is not permitted by statutory regulation or exceeds the permitted use, you will need to obtain permission directly from the copyright holder. To view a copy of this licence, visit <http://creativecommons.org/licenses/by/4.0/>.

© The Author(s) 2023

5.1.3. O estudo de reuso e reprocessamento

Os estudos de reuso e reprocessamento dos resíduos sólidos são o tema que finaliza o item

5.1.1. Os resultados dos ensaios metalúrgicos descritos na metodologia (capítulo 4) são apresentados e debatidos no artigo *Adding Value to Mine Waste through Recovery Au, Sb, and As: The Case of Auriferous Tailings in the Iron Quadrangle, Brazil* publicado na revista *Minerals*. Neste documento são apresentados resultados detalhados das rotas para reprocessamento de Au, e dois ensaios para reaproveitamento de Sb e As, incluído a tentativa de encontrar produtos que os mantenham em forma estáveis e, além disso, uma rota sustentável para obtenção de outros produtos usando processamento a seco. A seguir, são apresentados os resultados e discutidos.



Article

Adding Value to Mine Waste through Recovery Au, Sb, and As: The Case of Auriferous Tailings in the Iron Quadrangle, Brazil

Mariana Gazire Lemos ^{2,2,*}, Teresa Maria Valente ¹, Amélia Paula Marinho Reis ¹, Rita Maria Ferreira

Fonseca ³, Fernanda Guabiroba ², José Gregorio da Mata Filho ², Marcus Felix Magalhães ², Itamar

Daniel Delbem ⁴ and Giovana Rebelo Diório ⁵

¹ Institute of Earth Sciences, Pole of University of Minho, Universidade do Minho, Campus de Gualtar, 4710-057 Braga, Portugal; teresav@dct.uminho.pt (T.M.V.); pmarinho@dct.uminho.pt (A.P.M.R.)

² Anglogold Ashanti, Mining & Technical, COO International, Nova Lima 34000-000, Brazil

³ Institute of Earth Sciences, Pole of University of Évora, University of Évora, 7000-345 Évora, Portugal; rfonseca@uevora.pt

⁴ Microscopy Center, Universidade Federal de Minas Gerais, Belo Horizonte 31270-013, Brazil; danieldelbem@gmail.com

⁵ Laboratory on Basin Analysis, Universidade Federal do Paraná, Curitiba 81532-980, Brazil;

g.rebelo.d@gmail.com

* Correspondence: id8548@alunos.uminho.pt



Citation: Lemos, M.G.; Valente, T.M.; Marinho Reis, A.P.; Ferreira Fonseca, R.M.; Guabiroba, F.; da Mata Filho, J.G.; Magalhães, M.F.; Delbem, I.D.; Rebelo Diório, G. Adding Value to Mine Waste through Recovery Au, Sb, and As: The Case of Auriferous Tailings in the Iron Quadrangle, Brazil. *Minerals* **2023**, *13*, 863. <https://doi.org/10.3390/min13070863>

Academic Editor: Wentao Hu

Received: 23 May 2023

Revised: 19 June 2023

Accepted: 23 June 2023

Published: 26 June 2023



Copyright: © 2023 by the authors. Licensee MDPI, Basel, Switzerland. This article is an open access article distributed under the terms and conditions of the Creative Commons Attribution (CC BY) license (<https://creativecommons.org/licenses/by/4.0/>).

Abstract: From the colonial era to modern times, gold mining has played a crucial role in shaping Brazil's economy, culture, and landscape, particularly in the Iron Quadrangle region. Therefore, resulting waste has accumulated in tailings structures, either from deactivated circuits or plants still in production. The present study reveals the potential assessed based on a set of metallurgical tests, assuming specific scenarios depending on the occurrence modes of interesting economic elements. For Au, calcination, leaching, and flotation are promising techniques to recover this element. Tests indicated that toxic elements such as Sb and As could be effectively reused in the form of glass. The generation of other products from dry cleaning techniques was not effective but promising since there was an enrichment of elements with Au, Fe, Al, and K in specific fractions.

Keywords: tailings properties; circular economy; metallurgical tests; Au recovery; As recovery; Sb recovery

1. Introduction

Socio-political changes and population growth are crucial factors for the exploration of new mineral assets [1,2]. The United Nations (UN) projects a continuous increase in global population, reaching 9 billion by 2030 and 10 billion by 2050, with a corresponding rise in urban areas [3]. Urbanization and population density are strongly linked to the consumption of metals and minerals, and this sector influences others by supplying raw materials to several industries [4]. As a result, the mineral industry has become the world's largest waste producer, generating ca. 65 billion tons/year, of which 14 billion consist mostly of fine (<150 µm) particles [5].

An important noble metal is gold (Au), widely used in jewelry manufacturing and as a monetary reserve. South Africa holds 40% of the world's gold reserves, while Brazil contributes approximately 2% [6,7].

Brazil's minable Au reserves amount to nearly two thousand tons. During the extraction and processing of gold-bearing rocks, various processes such as crushing, grinding, gravimetry, flotation, and cyanidation are employed [6]. However, due to the low ore concentration in host rocks, mining operations generate significant amounts of tailings [8]. In Brazil, the Au mining industry produces approximately 600 million tons of tailings annually, and this figure is projected to reach almost 1 billion tons by 2030 [9].

There are other problems associated with current mining methods. Metals are often linked to contamination, which poses risks to ecosystems and human health. It is crucial to understand toxicities, percolation processes, and human absorption mechanisms to enhance research on their environmental impacts and ecological risks [10]. For instance, elements like arsenic (As) and metals such as zinc (Zn), lead (Pb), nickel (Ni), and antimony (Sb) are commonly found in association with Au waste, presenting a high potential for contamination [11–14]. Moreover, the geopolitical context and the monopoly of strategic commodities in specific countries, along with events such as Russia–Ukraine conflict and the COVID-19 pandemic, directly affect raw materials supply chains. Recent assessments have identified 87 individual raw materials, most found in mining waste, as critical due to these factors [15,16]. Finally, environmental disasters related to waste and tailing, including recent ones in Brazil, further highlight the significance of these issues [13].

With market and technological advances, tailings can serve as an alternative to primary exploitation. Thus, in line with sustainable development objectives and other circular economy goals, it is crucial to investigate the reuse of mining tailing worldwide [6,16]. This can be achieved through the application of innovative new technologies to extract value from low-grade “ores” or by repurposing tailings for various uses [1,12,17–19]. However, each situation is unique, and ongoing research and analysis are necessary to explore these opportunities further.

The potential for Au recovery from various types of tailings has been extensively investigated. Flotation and cyanidation tests are the primary methods employed to reprocess such material, sometimes involving additional stages such as regrinding, roasting, and cyanidation of flotation concentrates. In certain studies [20], Au dissolution and recovery rates ranged from 87.8% to 98.4% in sulfide-containing Au tailings. Advances in processing technology, coupled with the residual Au content found in aged cyanidation tailings, offer opportunities for developing recovery routes for Au present in these wastes [21]. Reprocessing gold mine tailings has proven to be economically viable and beneficial, particularly when integrated into existing facilities to compensate for raw ore shortages and operational losses [22]. Some plants currently incorporate Au tailings reprocessing into their production chains, such as the Elikhulu tailings re-treatment plant (Southern Africa), which processes 1.2 Mt of historic tailings per year from three existing slime dams [23] and

Paracatu mine (Brazil) in which 10 million tons of hydrometallurgy tailings containing 1 mg Au/kg are reprocessed [24]. Furthermore, health-hazard elements, which occur alongside Au, can also possess industrial value [11–14]. Moreover, state-of-the-art research indicates that gangue minerals found in tailings have significant potential for application in civil construction and even as fertilizers, depending on properties such as granulometry and chemical composition [25–29].

Hence, the vast volumes of waste generated by mining and mineral processing, combined with geopolitical contexts, significant environmental impacts, and risks to human health, justify the importance of adding value to tailings. In light of these challenges, this study was conducted in the region of Santa Barbara and Nova Lima cities (Brazil), encompassing four active and inactive Au tailings dams, as well as three piles and tailings from depleted mines. The objective of this article is to evaluate the potential for value addition to the waste in this area and explore options for its reuse, not solely limited to the recovery of valuable elements such as Au, Sb, and As. For recoveries of these elements, this paper will go through steps of characterization, extraction of elements by flotation, leaching, calcination, and even the use of vitrification techniques. In addition, a study attempting to reuse other elements was performed using dry concentration (recovery using

triboelectrostatic stages). The applications of the generated products can be directly used in the metallurgical industries, such as the production of gold bars, in the textile industry, in the production of plastics, and in sectors such as fertilizers and building materials. In addition, reuse can be an important tool for the resolution of environmental liabilities and pollution control, such as the neutralization of toxic elements like As.

2. Study Area

The seven tailing structures investigated in this study are located in the main Brazilian mineral province known as Iron Quadrangle (IQ; Figure 1). Among these structures, five are situated in Nova Lima, while the remaining two are found in Santa Barbara, in Minas Gerais, Brazil. Both cities have a long-standing history of Au mining, dating back to the 19th century, and continue to be significant Au production regions in Brazil. These metallogenic Au deposits are hosted within the Rio das Velhas Greenstone Belt, which is recognized as the biggest Au district in Brazil [30,31].

Santa Bárbara dam and tailing piles are situated in the northern part of the IQ, in Santa Bárbara city, ca. 110 km away from Belo Horizonte, the capital of Minas Gerais state. These waste deposits have been accumulating since 1986, receiving the tailings generated from Au underground mines and processed at metallurgical plants. The tailings at this site originated from different sources and exhibited distinct characteristics: (a) oxidized tailing piles resulting from the heap leach plant that receives ore extracted from open pit mines (CDS1; Figure 2a); and (b) tailing dams from flotation and leaching plant, fed by fresh ores from underground mining operations (CDS2; Figure 2b).

The Nova Lima mines encompass both inactive and active operations, with a significant presence of tailings from deposits that have been exploited since the previous century. Waste from local mines has been accumulating since 1834, and the estimated Au reserves in the area currently amount to ca. 107 tons [35]. The main structures are the (1) Isolamento tailings deposit (ISO); (2) Bicalho inactive mine dam (BIC); (3) deposits at the Mina Velha (MV) plant; and (4) active and inactive dams at Queiroz metallurgical plant (CA and CO) (Figure 2).

These dams and tailing deposits are in the northern part of the IQ, from near the cities of Nova Lima and Raposos, ca. 25 km away from Belo Horizonte (Figure 1). Within ISO, BIC, and MV, a wide variety of waste materials from historical Au plants have been deposited. The presence of waste from the previous century suggests that these tailings may originate from Au extraction processes that predate the use of cyanide. Unfortunately, due to the lack of historical archives, accurately describing the extraction processes becomes challenging; however, it is believed that wastes predominantly result from gravimetric processes [35].

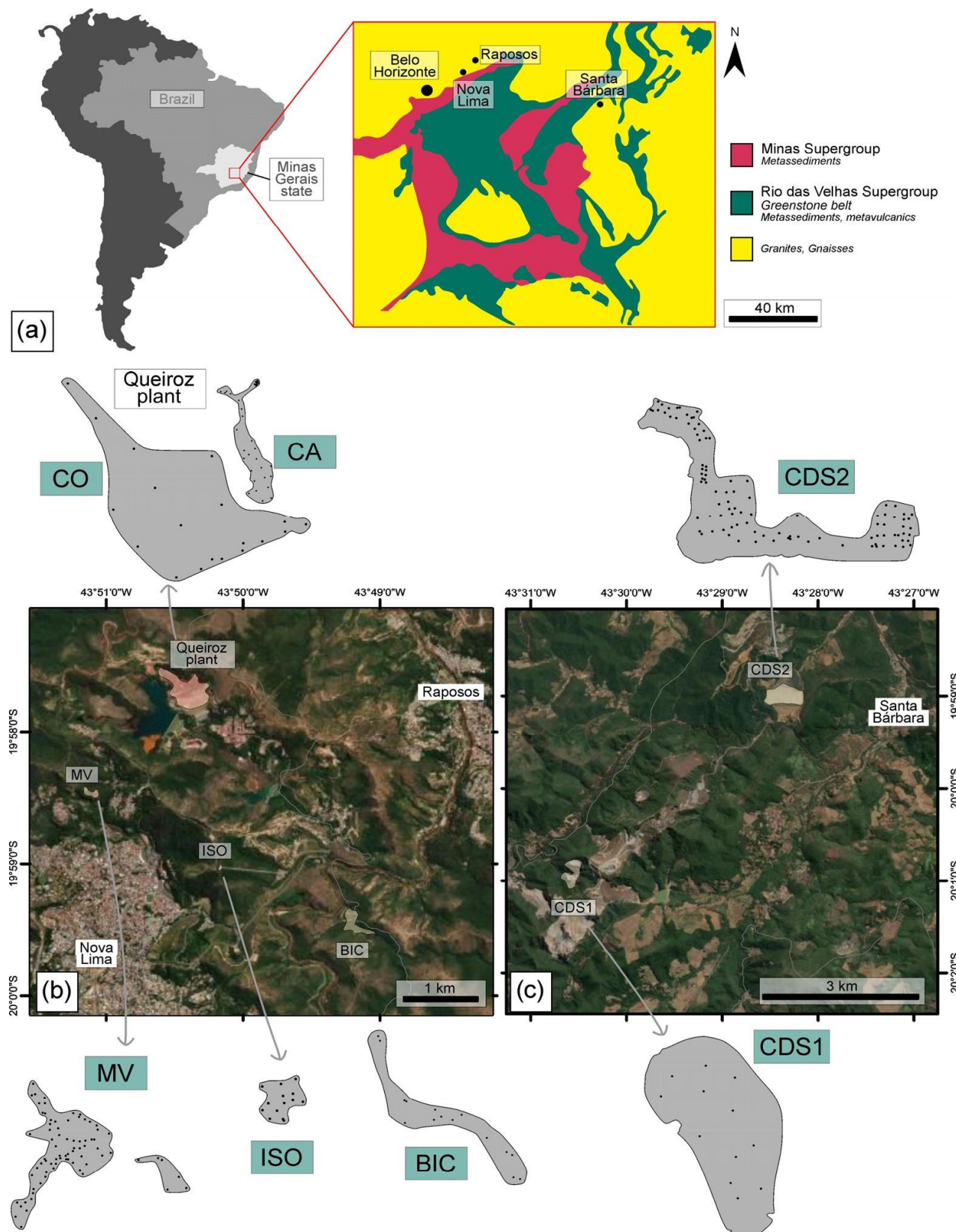


(Figura 5.33) **Figure 1.** (a) Location of the studied sites within the IQ, as shown in the modified schematic map from [32]. Dams and tailing piles in (b) Nova Lima (MV, ISO, and BIC) and (c) Santa Barbara (CDS1, CDS2), along with the sampling locations (black dots).

In contrast, the Queiroz plant has been processing Fe sulfide with Au ores for over thirty years. The materials treated at the factory are divided into two distinct circuits. The Raposos circuit (Figure 2c) primarily treats non-refractory sulfide ore from Raposos mines. This circuit achieves an Au recovery rate of 90% through various treatment stages, including milling, gravity separation, conventional leaching, CIP (carbon leaching) process, elution, and electro-recovery. The resulting tailings from this circuit are deposited in the Cocoruto (CO) tailings basin. However, the Raposos circuit and the associated metallurgical process stage were deactivated in 1998, along with the Raposos mine [13,33,35]. Currently, the Queiroz plant circuit treats refractory Au, which requires an additional calcination step after milling and flotation (Figure 2d). Following calcination, Au is recovered through leaching, CIP (leaching carbon), elution, and electro-recovery [13,33,35,36]. The resulting tailings are then deposited in the calcined dam (CA).

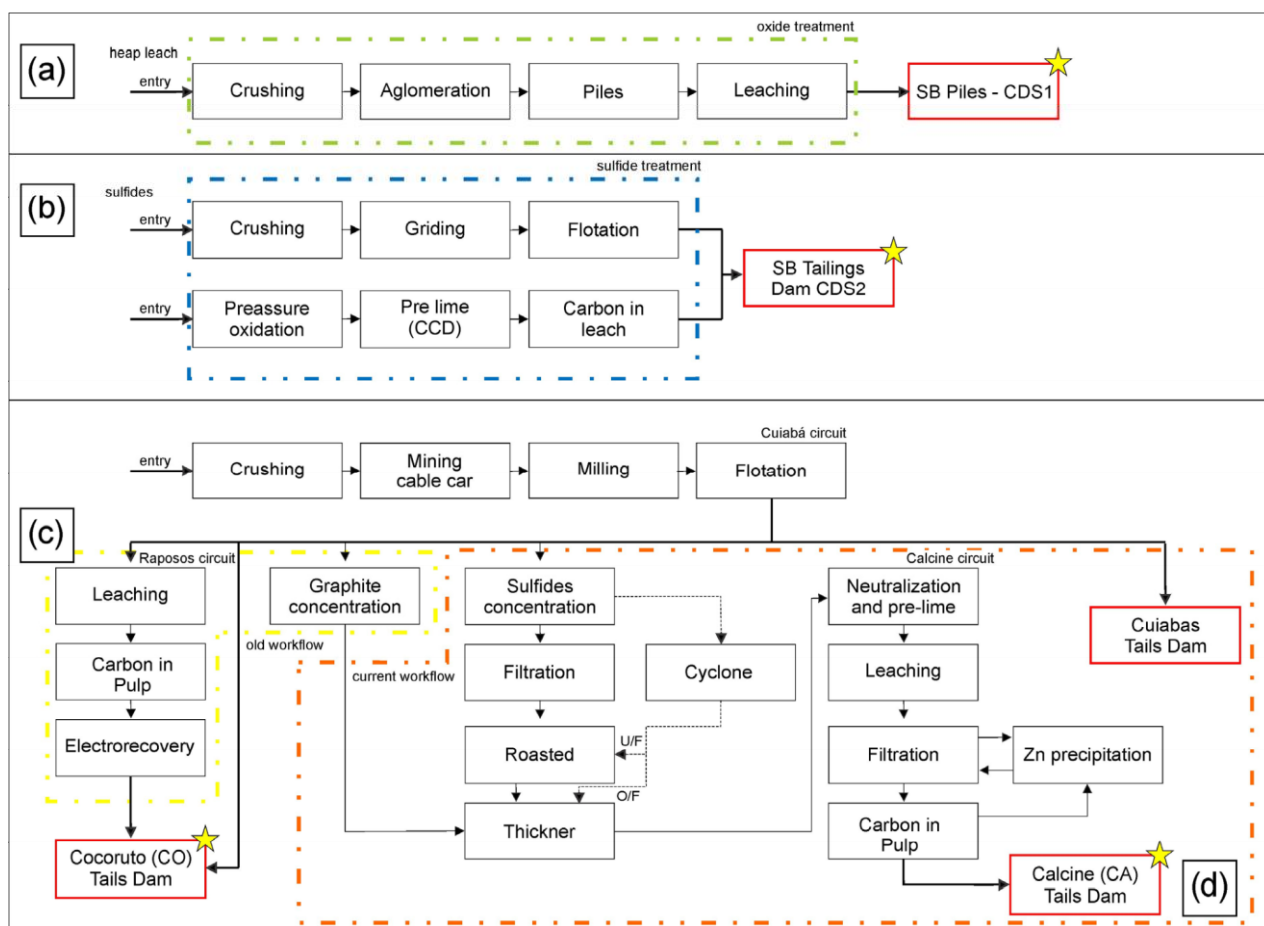


(Figura 5.34) **Figure 2.** Waste generation flowchart for (a) CDS1, (b) CDS2, and Queiroz plant—(c) CO (Cocoruto) and (d) CA (Calcine) samples. Sample locations are marked with a yellow star. Modified from [33,34].

3. Methodology

3.1. Characterization of Tailing Samples

3.1.1. Sampling

The sampling stage was conducted during late winter and early spring in southeastern Brazil (Figure 1). Samples were obtained through drilling at varying depths, depending on the specific structure being assessed. Subsequently, individual samples were combined to create composite samples, which represented each tailings structure for the recovery/reuse tests.

3.1.2. Sample Composition

Multielement analysis to assess the reuse of the composite samples and metallurgical test products was conducted using inductively coupled plasma mass spectrometry (ICPMS, PerkinElmer SCIEX, Waltham, MA, USA). Prior to analysis, acid digestion (nitric acid, hydrogen peroxide, and hydrochloric acid) was performed at the laboratory of AngloGold Ashanti and SGS Geosol in Brazil. Sulfur (S) and carbon (C) concentrations were evaluated using infrared (IR) analysis (LECO, St Joseph, MI, USA, with a detection limit of 0.01%). Au analysis was carried out using atomic absorption spectroscopy with the fire test method.

(AAS, Varian, Palo Alto, CA, USA, with a detection limit of 0.05 mg/kg). To ensure the quality and accuracy of the analyses, duplicates, blanks, and standard reference materials (Si81 from Rocklabs) were included.

3.1.3. Particle Size Distribution

The particle size distribution (PSD) was obtained using the MasterSizer 3000 equipment (Malvern Instruments Ltd., Worcestershire, UK). Laser diffraction was employed for this analysis, and composite samples were used. The PSD results were categorized as follows: <2 µm for mud fraction, 2–20 µm for fine silt, 20–63 µm for coarse silt, and 63–2000 µm for the sand fraction.

3.1.4. Mineralogy

Composite samples were submitted to a mineralogical study employing various techniques, including optical microscopy, X-ray diffraction (XRD), and scanning electron microscopy (SEM—Field Electron and Ion Company—FEI), conducted at the Universidade Federal de Minas Gerais (Belo Horizonte, Brazil) and University of Minho (Braga, Portugal). The mineralogical composition was determined using XRD analysis with an X'pert

Pro-MPD diffractometer (Philips PW 1710, APD), using CuK α radiation, and equipped with an automatic divergence slit and graphite monochromator. The diffractograms were obtained from <2 mm powders fraction, covering a range of 3 to 65° 2θ with a 2θ step size of 0.02° and a counting time of 1.25 s [36]. In addition, fifty thin polished sections by structure were analyzed using a Leica optical microscope and a FEI electron microscope, Quanta 600 FEG, high vacuum mode, coupled to the automated analyzer software (MLA-GXMAP and SPL-DZ mode), and the EDS Esprit Bruker microanalysis system (20 Kve).

3.2. Assessment of Potential Recovery/Reuse

In the initial stage, a multivariate statistical analysis utilizing the clustering method was conducted, combining complete linkage and Euclidean distance [37]. Physical-chemical parameters of the samples were employed for this analysis. A dendrogram was generated, which revealed distinct groupings based on specific characteristics and established a potential reuse matrix for these wastes. Four main parameters were identified for the analysis of the observed groups: (1) Evaluation of the main mineralogy and its grouping based on potential reuse; (2) identification of contaminants with a high level of critical risk and contamination; (3) analysis of particles size; and (4) assessment of Au content. This analysis allowed for a more targeted approach in selecting samples for laboratory tests based on their potential for reuse.

Composite samples were then created to represent each group aiming to encompass the maximum variation range for each element with reuse potential. The tables below present the variations observed in the tested samples, ensuring that all values fall within the range identified for each composite group.

3.2.1. Gold Extraction

Various laboratory-scale scenarios were carried out to evaluate the potential recovery of Au [34,38], considering the specific characteristics of each structure. Therefore, three different setups were conducted, involving grinding, leaching, calcination, and, in the case of CDS2, flotation (refer to Figure S1). In addition,

these setups were designed to be easily adaptable and applicable to metallurgical plants in the region should a viable and efficient reuse scenario arise.

In the first scenario, samples were ground to a particle size of 74 µm, with 80% of the particles falling within this range, after a liberation-by-size analysis for sulfides and gold particles. The calcination step was disregarded, and the samples were directly subjected to leaching. For Au extraction, bottle roll tests were performed using a leaching solution containing 2000 mg/kg of cyanide (NaCN) and 4000 mg/kg of lime (CaO), with a solid-to-liquid ratio of 50%.

In the second test, specifically designed for the waste characteristics in the CDS2 area, the sample underwent grinding to the particle size of 74 µm using a ball mill, followed by pre-concentration via flotation. This flotation step involved two phases (rougher and cleaner), with the addition of 150 mg/kg of CuSO₄ for particle activation, 30 mg/kg of collectors (xanthate and Sodium Diphosphate—INT214), and 60 mg/kg of mibcol foaming agent. The latter was also added during the milling step. The resulting concentrate was calcined in a muffle at 700 °C to facilitate access to the gold included in the sulfide particles and subsequently leached in a bottle with a solid-to-liquid ratio of 50%, using a leaching solution containing 2000 mg/kg of NaCN and 4000 mg/kg of CaO. The rougher and cleaner tailings were combined and subjected to leaching under the same conditions as the concentrate.

The third setup involved grinding the material to a particle size of 74 µm using ball mills, followed by calcination in a muffle at 700 °C. For Au extraction, the calcinated material was placed in bottles containing a solution with 40% solids, comprising 2000 mg/kg of NaCN and 6000 mg/kg of CaO. The extraction process occurred over 24 h, divided into two stages with a pre-airing period of 2 h. The residues from this stage will be submitted to tests for recovery of As and Sb and new products.

3.2.2. Recovery and Stabilization of Arsenic and Antimony

A protocol based on the methodology described by [12] was employed for samples with potential Sb extraction due to defined similarities in characteristics. The objective of the test was to recover Sb and As thermally by volatilizing and collecting them downstream as oxide by-products. Waste samples underwent two tests in a quartz rotary and horizontal klin, with a final temperature of 850 °C, lasting for 6 h, and with a gas mixture of 20% CO and 80% N₂ (Procedure 4). The second test (Procedure 5) was conducted in two phases, reaching a final temperature of 930 °C, and lasting for 16 h, with 3% O₂ and 97% N₂ (Figure S2a).

Regarding the sample with potential As stabilization and reuse, the protocol outlined in the DST-s GlassLock™ patent process [11] was followed. This process involved mixing the tailing samples with silica, hematite, and sodium carbonate, followed by subjecting them to an oven at temperatures ranging from 1000 °C to 1200 °C and atmospheric pressure for two hours. This treatment resulted in a glass product containing stable forms of oxides, including As and Sb (Procedure 6—Figure S2b).

3.2.3. Recovery of Gangue Minerals

The utilization of triboelectrostatic separation has demonstrated promising results in producing by-products from Au tailings [39]. Additionally, selective grinding and pneumatic concentration techniques are also considered favorable for this type of material, as they are dry-cleaning processes with minimal environmental impacts [40]. The objective of selective grinding and pneumatic separation is to pulverize minerals with a hardness of less than five on the Mohs scale and separate the fraction smaller than 8 µm for concentration. Thus, these methods enable the generation of multiple products from a single source [41–43].

Therefore, after prioritizing samples, the chosen method for assessing the potential generation of alternative products involved: (1) grinding in a pendular mill with hot gas at 450 °C; (2) pneumatic separation into three granulometric fractions (fine, less than 8 µm; intermediate, 30–8 µm; and coarse, greater than 30 µm); and (3) triboelectrostatic concentration of the fine fraction (Figure S3).

Consequently, three potential products were generated and analyzed to investigate their potential use in civil industries and as fertilizer, among other applications.

4. Results and Discussion

4.1. Main Properties of Tailing Materials

4.1.1. Chemical Composition

Table 1 provides a summary of the chemical results for potential valuable elements in each structure. Au is present in all the characterized samples, with the highest concentrations observed in CA samples and the lowest in the MV Group. Anomalous values for other elements are also observed when comparing the sample groups. This detailed information is crucial for subsequent stages, such as the study of reuse potential and the assessment of the environmental impacts associated with waste disposal [34]. The major and trace elements are presented in Tables S1 and S2.

4.1.2. Grain Size Distribution

Granulometric distribution is a crucial parameter for determining the reuse potential and appropriate destination for these materials. As they have already undergone previous grinding and size reduction stages, their particle size distribution presents challenges and complexities for reuse studies [44,45].

Figure 3 illustrates the particle size distribution (PSD) of the samples. In general, 80% of the particles fall within the range of 2–63 µm, classifying them as silty. The samples from the CDS2 structure are coarser, while CA samples contain a higher proportion of clay particles.

(Tabela 5.18) **Table 1.** Statistical summary of potential value elements for the structures' tailings samples.

Structure	N ¹	Element	Mean	SD ²	Min ³	Max ⁴	N ¹	Element	Mean	SD ²	Min ³	Max ⁴
BIC	162		0.441	0.211	0.07	0.79	162		0.59	1.17	0.025	7.26
CDS1	175		1.54	0.449	1.5	7	175		0.363	0.235	0.025	2.17
CDS2	293		1.52	0.237	1.5	4	293		0.742	0.937	0.24	12.7
CO	282	Ag (mg/Kg)	1.51	0.134	1.5	3	282	Au (mg/Kg)	0.911	0.715	0.003	8.71
MV	615		0.515	1.66	0.25	13.8	615		0.126	0.353	0.001	5.17
ISO	266		1.37	0.42	0.05	1.5	266		0.649	0.793	0.001	5.99
CA	230		8.49	2.29	0.05	15	230		2.39	1.08	0.001	9.45
BIC	111		337	156	144	628	70		163	148	7	429
CDS1	150		283	58.1	166	490	150		51.6	18.1	4	100
CDS2	293	Cr	198	38.8	118	323	111		69.6	28.2	16	171
CO	282	(mg/kg)	142	50.3	40	423	248	Pb (mg/kg)	46	22.4	4	124
MV	615		137	126	13.3	650	293		30.9	71.9	2.03	564
ISO	251		102	79.3	0.1	311	133		30	89.1	0.1	749
CA	230		98.3	36.9	0.1	308	218		241	64.4	0.1	383

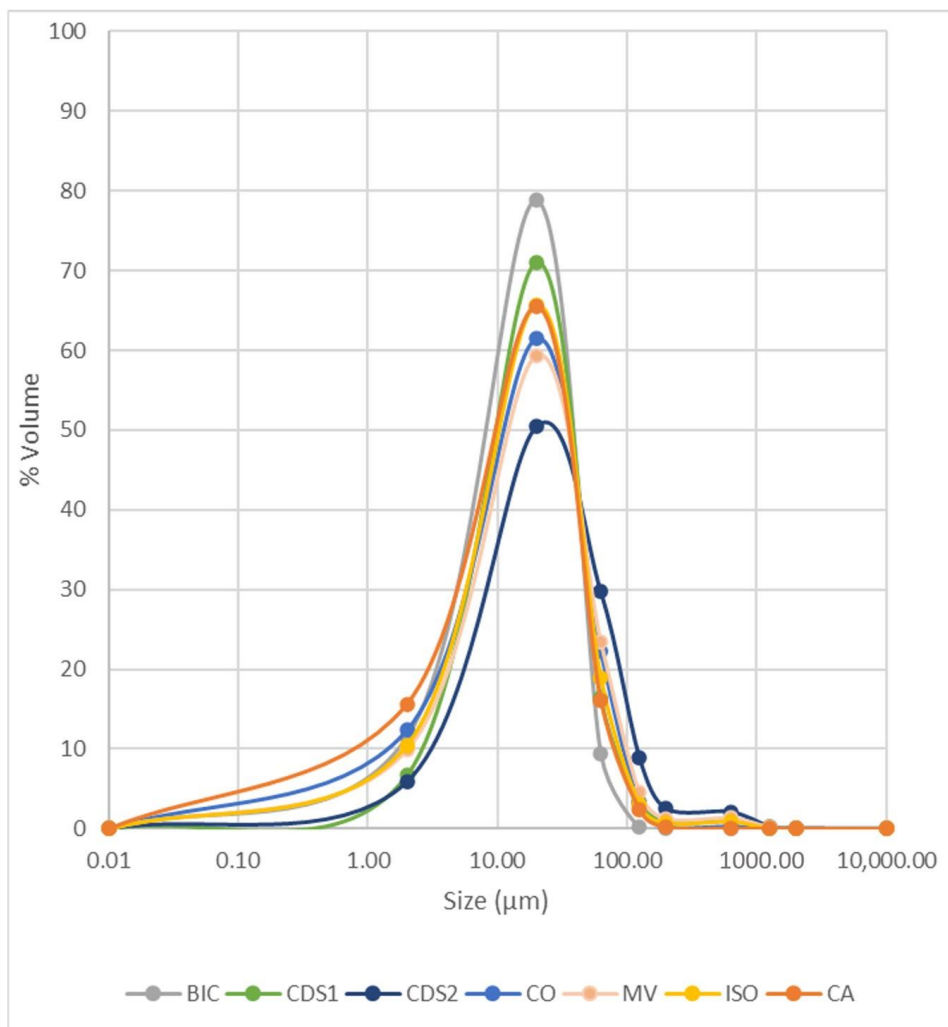
RESULTADOS E DISCUSSÕES

Minerals 2023, 13, 863.

<https://doi.org/10.3390/min13070863>

BIC	111	0.914	0.351	0.49	1.85	111		0.179	0.338	0.001	2.18	
CDS1	150	1.68	0.733	1.5	7	150		0.122	0.403	0.001	5.00	
CDS2	291	1.5	0.0	1.5	1.5	291		0.093	0.095	0.001	0.657	
CO	282	Mo (mg/kg)	2.12	2.55	1.5	23	282	As (%)	0.223	6.01	0.001	58.8
MV	321	2.17	3.06	0.5	11.6	321		0.595	5.97	0.001	87.5	
ISO	266	1.37	0.42	0.05	1.5	266		0.717	0.945	0.001	5.7	
CA	230	7.2	1.78	0.05	10	230		0.725	0.466	0.001	4.80	
BIC	162	54.5	35	19.3	137	162		0	0	0	0.002	
CDS1	175	93.4	39.2	18	273	175		0.013	0.01	0.001	0.056	
CDS2	293	21.4	6.22	4	42	293		0.104	0.184	0.001	0.988	
CO	282	Co (mg/kg)	19.6	11.7	4	76	282	Sb (%)	0.003	0	0.003	0.003
MV	615	34.6	46.2	5.53	361	615		0.001	0	0.001	0.001	
ISO	266	33.1	34.1	0.10	214	266		0.002	0	0.002	0.002	
CA	230	132	35.8	0.10	195	230		0.004	0.008	0.001	0.059	
BIC	163	0.148	0.056	0.03	0.24	111		0.005	0.009	0.001	0.06	
CDS1	51.6	1.5	0	1.5	1.5	150		0.007	0.001	0.001	0.012	
CDS2	69.6	1.5	0	1.5	1.5	293		0.01	0.008	0.001	0.04	
CO	46	Cd (mg/kg)	1.52	0.277	1.5	5	282	Cu (%)	0.019	0.018	0.001	0.266
MV	30.9	0.285	0.259	0.05	0.95	615		0.001	0	0.001	0.001	
ISO	30	1.34	0.461	0.05	1.5	251		0.04	0.046	0.001	0.17	
CA	241	1	0.866	0.05	1.5	230		0.086	0.029	0.001	0.16	

¹ N = number of samples; ² SD = standard deviation; ³ Min—minimum; and ⁴ Max—maximum.

(Figura 5.35) **Figure 3.** Particle size distribution of waste samples.

This information is valuable for guiding and designing reuse tests, such as civil construction aggregates, which requires larger particle sizes. Typically, products within the sand fraction, e.g., [45], are discarded at this stage of characterization. However, alternative possibilities will be explored, considering other characterization parameters outlined in Section 4.2.

4.1.3. Mineralogical Composition

Tables 2 and S3 present the mineralogy of Au tailing samples from the IQ.

With the exception of CA samples, the quartz content in the tailings is generally greater than 30%, with CO samples having the highest levels (>50%). Silicates belonging to the Muscovite Group are also present, particularly in samples from the ISO, CDS1, and MV structures. Additionally, well-preserved carbonates such as Ankerite and Siderite were identified in CO and BIC samples.

Relic sulfides are observed in all structures, indicating the potential for acid mine drainage. Therefore, the recovery and reuse of metals from these sulfides can also serve as an environmentally sound alternative [13,46]. The main sources of S, particularly in CO, ISO, and BIC structures, are Pyrite, Arsenopyrite, and Pyrrhotite. In CDS2, the presence of Berthierite also contributes to the presence of Sb.

(Tabela 5.19) **Table 2.** Mineralogy of Au tailing samples from the IQ. Analyses are a result of the combination of SEM, optical microscopy, and XRD.

Mineral	Chemical Composition (Ideal Formula)	BIC (Wt%)	CDS1 (Wt%)	CDS2 (Wt%)	CO (Wt%)	MV (Wt%)	ISO (Wt%)	CA (Wt%)
Quartz	SiO ₂	31.57	34.18	35.6	55.8	37.83	36.65	15.6
Feldspar Group	NaAlSi ₃ O ₈	5.33	0.07	1.11	0.37	7.56	2.81	1.5
Albite								
Anorthite	CaAl ₂ Si ₂ O ₈	-	0.07	0.053	0.01	0.03	0.01	0.053
K feldspar	KAlSi ₃ O ₈	0.12	1.18	1.27	0.39	0.73	1.22	-
Phyllosilicates	KMg _{2.5} Fe _{2+0.5} AlSi ₃ O ₁₀ (OH) _{1.75} F _{0.25}	0.11	1.74	1.26	0.16	2.55	0.52	1
Biotite								
Muscovite	KAl ₃ Si ₃ O ₁₀ (OH) _{1.9} F _{0.1}	6.53	38.46	29	5.69	28.85	20.58	12.8
Chlorite	(Mg,Fe) ₃ (Si,Al) ₄ O ₁₀ (OH) ₂ ·(Mg,Fe) ₃ (OH) ₆	2.44	3.34	5.01	6.12	1.28	5.83	3.3
Oxides	Fe ₂ O ₃	-	17.09	0.378	8.86	9.06	8.95	56.8
Hematite								
Fe antimoniate	FeSb(As)O	-	0.07	0.806	-	-	-	-
Rutile/Anathase	TiO ₂	0.19	0.29	0.599	0.49	0.60	0.56	0.599
Carbonates	Ca(Fe, Mg, Mn)(CO ₃)O ₂	16.84	0.02	9	11.2	1.49	0.85	1
Ankerite								
Siderite	FeCO ₃	2.92	0.17	7.2	7.25	0.01	8.94	-
Calcite	CaCO ₃	0.02	0.05	5.4	2.25	0.23	-	0.2
Sulfates	KFe(SO ₄) ₂ (OH) ₆ and (H ₃ O)Fe(SO ₄) ₂ (OH) ₆	-	-	1.00	-	-	-	-
Jarosite (Sb)								
Gypsum	CaSO ₄ ·2H ₂ O	-	-	2.00	0.03	-	-	7.00
Sulfides	Total	9.92	0.03	0.36	1.61	0.23	6.85	0.17
Pyrite	Fe ₂₊ S ₂	5.31	0.03	0.08	0.5	0.06	0.22	0.002
Pyrrhotite	Fe ₂₊ 0.95S	2.06	-	0.041	0.79	0.148	4.7	0.004
Arsenopyrite	Fe ³⁺ AsS	2.52	-	0.056	0.24	0.022	1.71	0.056
Berthierite	FeS ₂ S ₄	-	-	0.141	-	-	-	-
Chalcopyrite	CuFeS ₂	0.01	-	0.028	-	-	0.21	-
Gesdorffite	NiAsS	0.02	-	-	-	-	-	0.01
Covellite	CuS	-	-	-	0.07	-	0.01	0.1
Sphalerite	ZnS	-	-	0.009	0.01	-	-	-
Au Minerals *								
Au Content (mg/kg)		0.59	0.363	0.742	0.911	0.126	0.649	2.39
Native Au	Au > 80%, Ag, Cu, Hg, Fe, Ni	45	20	158	364	2	60	526
Electrum	Au = 80%, Ag = 20%	8	5	6	10	1	5	42

* Au number particles.

XRD and SEM analyses reveal that Hematite is the main mineral composition of CA and CDS1 samples. This occurrence is attributed to both metallurgical processes and natural oxidation, as the material fed into the CDS1 metallurgical treatment plant consists of oxidized Au ores (Figure 2a).

Sulfates such as Gypsum were also in CA and CDS2 samples, mainly due to treatment steps where lime was used for pH neutralization. Another noteworthy finding in CDS2 samples is the presence of Jarosite, which contains Sb and serves as an indicator of sulfides oxidation, including Berthierite, during the pressure oxidation step (Figure 4b).

The geochemical study indicates that CA samples have higher concentrations of metals and metalloids, such as As, Cu, Pb, Zn, and Fe. Table 2 shows the dominance of Hematite, but SEM-EDS analysis suggests that these elements were somehow adsorbed in Hematite itself during the metallurgical oxidation process (Figure 4a). S is also present in Hematite, and Fe oxides with As concentration above 40% were rarely detected by EDS.

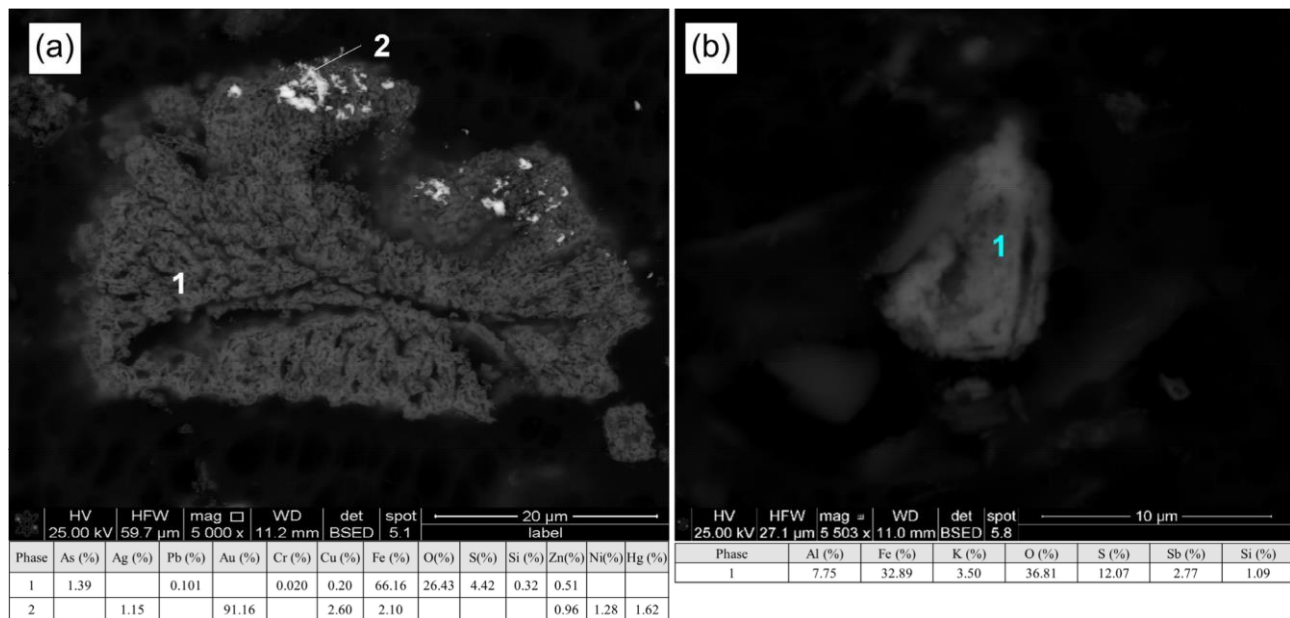


(Figura 5.36) **Figure 4.** Electronic microscopy images of two phases of CA samples. (a) Hematite with As, Pb, S, Cu, and Zn, and (b) Jarosite with Sb.

For this study, the distribution of main minerals according to sample grain size was also assessed. If there is a predominance of a mineral carrying an element of interest for reuse or decontamination within a specific preferred granulometric range, it can guide selective separations or pre-merger possibilities [40,47–50].

Table 3 presents the key mineralogical differences between particle sizes above and below 6 μm.

(Tabela 5.20) **Table 3.** Mineralogy (in two size fractions) by tailing structures. Mineral abbreviations after [51].

Sample	Size Fraction	Mass (%)	Minerals (wt%) *															
			Py	Fe hox/ox	Po	Apy	Qz	Ank	Cal	Ab	Sd	Ms Group	Chl Group	Kfs	Rt	Gp	Ap	Jrs (Sb)
BIC	>6 μm	88.5	0.001	-	11.2	5.30	66.4	-	-	5.90	0.0	-	7.50	2.57	1.18	-	-	-
	<6 μm	15.0	5.94	-	-	-	0.023	2.45	-	0.012	25.8	59.3	6.53	-	-	-	-	-
CDS1	>6 μm	93.3	0.013	21.5	0.033	0.013	43.0	0.023	0.063	0.089	0.213	25.8	7.33	1.48	0.360	-	-	0.078
	<6 μm	6.67	0.027	8.77	1.25	0.019	25.5	0.016	0.068	0.164	0.750	50.4	0.387	2.72	0.973	-	-	8.97
CDS2	>6 μm	94	0.094	-	0.183	0.128	81.4	-	-	2.53	-	10.2	-	2.83	1.32	-	0.459	0.432
	<6 μm	6	-	-	-	-	0.274	18.8	-	0.013	15.0	51.1	10.4	0.080	0.050	4.17	0	0.061
CO	>6 μm	87.6	-	-	0.822	0.402	93.1	-	-	0.613	-	0.602	2.68	0.637	0.805	-	0.335	-
	<6 μm	12.4	2.69	-	0.031	-	0.695	38.2	-	0.014	24.7	18.2	15.4	0.033	0.032	-	-	-
MV	>6 μm	90.1	0.170	10.3	0.063	0.025	43.4	1.70	-	8.64	0.013	32.8	1.47	0.787	0.680	-	-	-
	>6 μm	90.1	0.170	10.3	0.063	0.025	43.4	1.70	-	8.64	0.013	32.8	1.47	0.787	0.680	-	-	-
ISO	>6 μm	89.5	0.00	16.5	-	3.20	68.7	-	-	5.19	0.0	-	3.20	2.27	1.03	-	-	-
	<6 μm	10.5	11.8	0.488	0.552	0.016	0.295	2.13	-	0.121	22.5	51.7	10.4	0.034	0.036	-	-	-
CA	>6 μm	84.4	-	76.1	-	-	20.4	-	-	1.78	-	0.905	-	-	0.768	-	-	-
	<6 μm	15.0	-	8.37	-	-	3.59	3.68	0.736	0.833	-	44.7	12.1	-	0.180	25.8	-	-

* Py = Pyrite; Fe hox/ox = Fe Hydroxide/Oxide; Po = Pyrrhotite; Apy = Arsenopyrite; Qz = Quartz; Ank = Ankerite; Cal = Calcite; Ab = Albite; Sd = Siderite; Ms = Muscovite; Chl = Chlorite; Kfs = K-Feldspar; Rt = Rutile; Gp = Gypsum; Ap = Apatite; Jrs = Jarosite; and Fe ant = Fe Antimoniate.

In support of the reuse tests, the main observations were as follows:

- There is a predominance of 24 common minerals among the structures, with Quartz, Iron Oxides, Muscovite, Ankerite, Chlorite, Siderite, and Albite being the main ones;
- Depending on the structure, Quartz is commonly found in fractions above 6 μm and can be a potential product for applications in, e.g., civil construction. Previous research [52] suggests that tailings should have a SiO_2 concentration above 15% and a maximum size of less than 1 mm to be used as an aggregate. The inclusion of tailings as fine aggregate in concrete has been shown to increase compressive strength. It is generally recommended to substitute no more than 30% of the fine aggregates with tailings to maintain durability. Additionally, the solidification of metals within the tailings can be beneficial, and the clinker can be produced using the tailings;
- Minerals from the Muscovite and Chlorite Groups are the most commonly found in fractions below 6 μm and can be utilized in products such as fertilizers and rock meal. Research [52] identified important specifications for these types of products, including the presence of Ca and Mg as carbonates, high alkalinity, good availability of P, average availability of K, and the presence of micronutrients such as Zn, B, Cu, Fe, and Mn;
- The distribution of sulfides, if present, varies depending on each structure. Generally, they are found in finer fractions at BIC, CDS1, MV, and ISO, while coarser fractions contain sulfides in other structures. These sulfides may indicate the presence of noble metals such as Au, particularly because they are derived from this metal treatment process;
- CDS2 samples contain minerals and Sb compounds in finer fractions;
- CA samples are rich in Fe Oxides in fractions coarser than 6 μm .
- Consequently, this analysis allows for the identification of different potential products that can be derived from a single source.

In addition to the previously described potentials identified through granulometry and mineralogy, it is noteworthy that Au particles are present in all samples from different structures. SEM analysis reveals that Au is present in its native form, with low associations of Fe, Ni, Pb, and Hg, as well as in the form of an electrum. In the CO, BIC, ISO, and CDS2 structures, Au is associated and enclosed within sulfides (Figures 5a–d and S4) alongside Quartz. Furthermore, in the CDS2 sample, Au is also observed in association with Jarosite

(Figure 5d). In the MV and CDS1 structures (Figures 5e,f and S4), fine Au particles are found to be associated with Quartz and Muscovite, while in the CA structure, the main association is identified as fine Au particles within Hematite pores (Figures 5g and S4).

4.2. Tests for Potential Recovery/Reuse

Physical-chemical data, including mineralogy, chemistry, and PSD, from each tailing structure were used for multivariate analysis to cluster observations. The objective was to assess similarities among characteristics and determine the potential for grouping to facilitate and guide the reuse tests.

The dendrogram (Figure 6) reveals the presence of five groups, as CDS2, CA, and ISO samples exhibit distinctive characteristics with similarities to the remaining samples below 66%. The key variables influencing these groupings were the concentrations of Au, S, Sb, Fe, As, and types of sulfides. Table S4 provides the parameter values obtained from the centroid of each group, thus showcasing their unique identities.

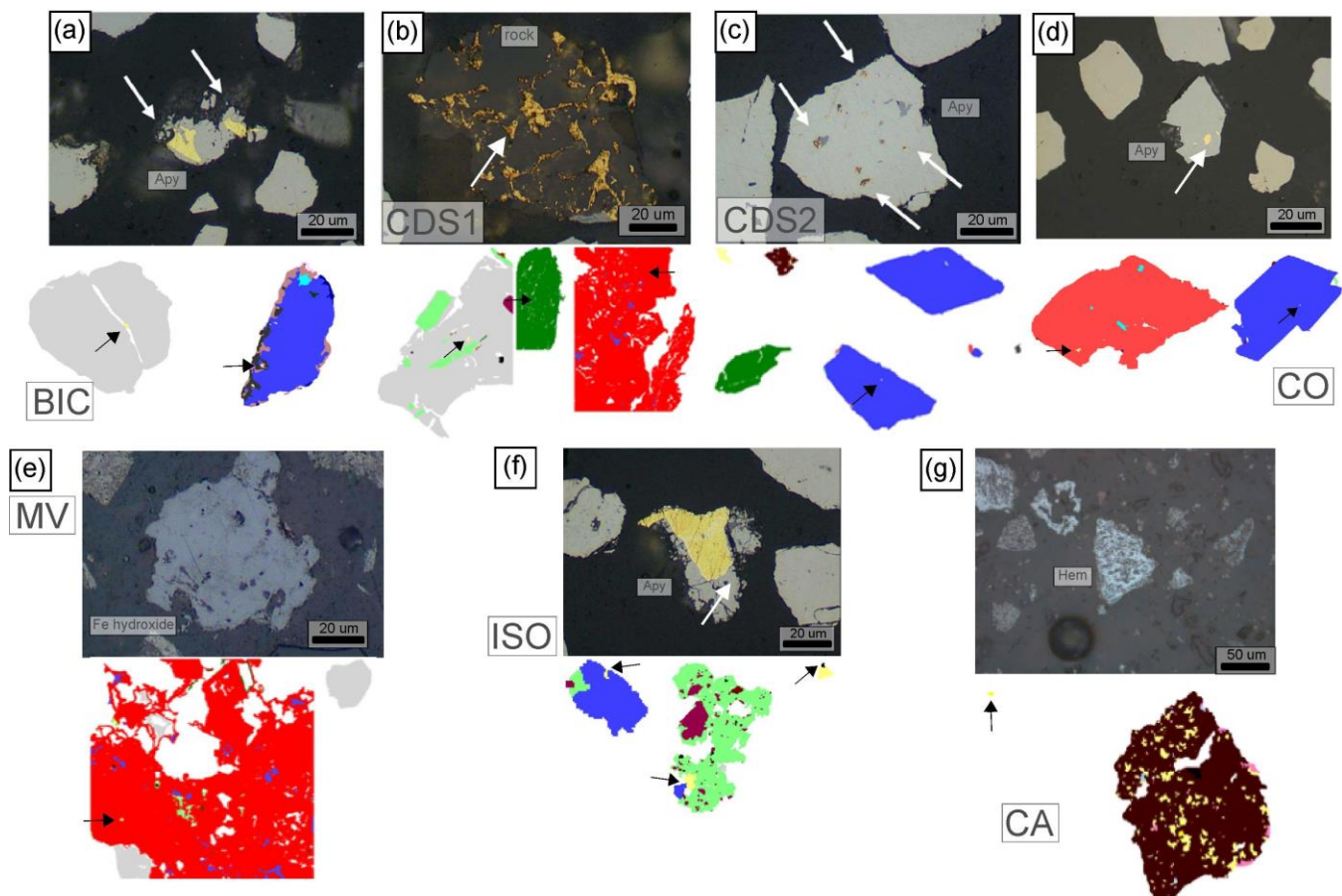


(Figura 5.37) **Figure 5.** False color electron images and microphotographs (reflected light and parallel Nicols) illustrate the presence of Au-bearing particles (indicated by yellow and black/white arrows) and Fe Hydroxide. Mineral abbreviations follow [51]. (a) BIC—enclosed Au particles in Quartz (gray) and Arsenopyrite. (b) CDS1—Au particles enclosed in rock minerals (Quartz and Muscovite) and Fe Hydroxide. (c) CDS2—Free Au particles and Muscovite (dark green) along with Arsenopyrite. (d) CO—Au particles enclosed in Pyrite (orange) and Arsenopyrite (blue). (e) MV—fine Au particles enclosed in Fe Hydroxide (red). (f) ISO—Au particles enclosed in Arsenopyrite and rock minerals (Chlorite—light green). (g) CA—free Au particles and Au particles within porous Hematite (brown).

Based on this multivariate analysis, a matrix was constructed to identify the potential for reuse (Table 4). The matrix is divided into three categories: high (H), medium (M), and low (L), determined by the composition and occurrence modes of elements such as Sb, Fe, As, and, of course, Au.

Considering the relevant potential of Au across all Groups, an assessment was conducted to evaluate its overall recovery potential. For the recovery tests targeting Sb, samples from Group 2 (CDS2) were used, with additional attempts to recover As. To explore the utilization of Fe and potentially generate other products, samples representing Group 5 were selected. Lastly, to determine the potential for generating alternative products (as indicated in Table 4), samples representing Groups 1 and 4 were chosen.

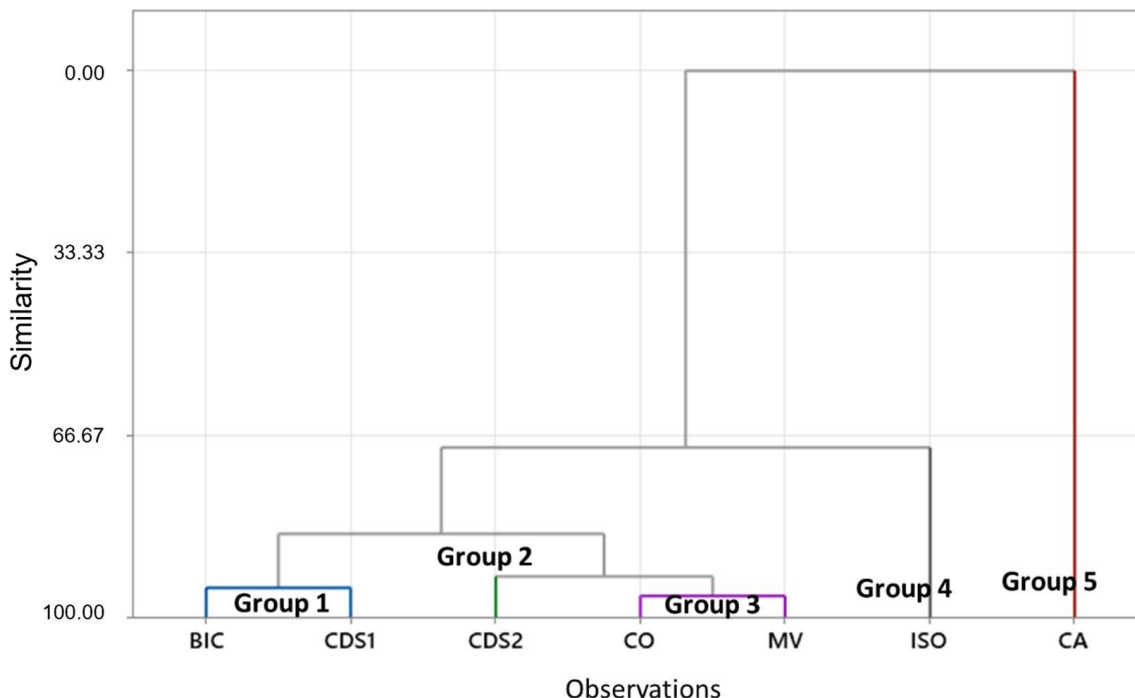


(Figura 5.38) **Figure 6.** Dendrogram (generated using complete linkage and Euclidean distance), which illustrates the grouping of tailings samples for the purpose of guiding reuse tests. Group 1: BIC and CDS1 samples. Group 3: CO and MV samples. The remaining groups (2, 4, and 5) did not exhibit sufficient similarity within the 100% to 70% range and therefore were not grouped.

(Tabela 5.21) **Table 4.** Potential recovery of metals, metalloids, and other products based on chemical, textural, and mineralogical characteristics.

Group	Samples	Au Recovery	As Recovery	Sb Recovery	Fe Recovery	Others *
Group 1	BIC + CDS1	H	L	L	L	H
Group 2	CDS2	H	M	H	L	H
Group 3	CO + MV	H	L	L	L	H
Group 4	ISO	H	H	L	M	H
Group 5	CA	H	H	L	H	L

* K and Si enrichment.

4.2.1. Au Recovery

Table 5 presents the recovery results obtained from the tests conducted in three different scenarios for each Group. Samples from Group 5 were exclusively tested using Procedures 1 and 3, as they did not exhibit characteristics that warranted concentration through the flotation stage.

The aggressiveness of the procedures increases from Procedure 1 to Procedure 3. In the roasting step, the aim was to open up the sulfide minerals to gain access to the encapsulated gold.

The obtained results demonstrate a promising potential for Au recovery. Procedure 1 yields better recoveries for Group 3 due to the presence of Au grains attached to sulfides and Quartz (Table 5 and Figure S4). Procedure 2 was more suitable for Group 2 as it contains both sulfide and oxidized sources of Au. In the oxidized samples, Au is attached, while in the sulfide samples, it is enclosed. Therefore, concentrating the sulfides and subjecting them to calcination is crucial for achieving higher recovery rates. However, for the other groups, there are losses in flotation recovery due to sulfide losses during the flotation stage and their

limited oxidation. Procedure 3 results in higher recoveries for Groups 1 and 4 because calcination provides access to locked gold in sulfides, in addition to the pre-existing Au oxide.

(Tabela 5.22) **Table 5.** Summary of metallurgical tests results for Au reuse in each Group of tailing samples. Modified from [38].

Group	Structures	Calculated Feed Grade (mg/kg)	Au Mineralogical Association	Procedure 1*¹	Procedure 2*²	Procedure 3*³
					(% Au recovery)	
1	BIC+CDS1*⁴	0.740		29.5	30.9	77.7
2	CDS2	0.742		49.9	70.7	34.9
3	CO+MV*⁴	0.735	sulfides and Quartz	71.8	59.4	66.4
4	ISO	1.16		64.0	48.2	78.5
5	CA	2.39	Fe Oxides	32.2	-	0.60

*¹ Leach in 74 µm, *² Flotation+Calcine+Leach in 74 µm, *³ Calcine+Leach in 74 µm, *⁴ CDS1 and MV presented amount of gold particles in oxide, as well.

Despite having the highest Au content among all procedures, samples from Group 5 exhibit poor recoveries. This can be attributed to the presence of very fine Au inclusions associated with Hematite (Figure 4a). This association poses a challenge for the treatment and reuse of Au in this cluster.

In general, Table 5 highlights that good levels of recovery are achieved through the same procedures for Groups 1 and 4. This information is significant as it would facilitate the industrial re-treatment of these structures with minimal investment, considering their proximity to metallurgical units that already have the necessary stages in Au production [13,33]. Although the calcination step is not covered, samples from Groups 2 and 3 can also be considered in this potential reuse setup. However, for Group 5, further viability studies are required, as additional stages and technological advancements are necessary.

The residues from this stage will be submitted to tests for recovery of As and Sb and new products. The next items, the residues produced in this item, will be submitted to the recovery of As and Sb (4.2.2) and total reuse (4.2.3).

4.2.2. Arsenic and Antimony Recovery

For the assessment of Sb and As recovery potential in composite samples, Groups 2 and 5 were selected (Table 4). In the case of Group 2, the same procedure described by [12] was employed due to the presence of Sb and As in sulfides and sulfates. For samples in Group 5, the vitrification procedure was followed, mainly due to the high Fe content required for this type of test. The results are summarized in Table 6.

(Tabela 5.23) **Table 6.** Summary of metallurgical tests results for Sb and As recovery for Groups 2 and 5.

Group	Samples	Sb Feed Grade (%)	As Feed Grade (%)	Procedure 4 (1 stage of klin roasting)		Procedure 4 (2 stages of klin roasting)		Procedure 5 (As e Sb vitrification)	
				Sb Recovery (%)	As Recovery (%)	Sb Recovery (%)	As Recovery (%)	Sb Recovery (%)	As Recovery (%)
2	CDS2	0.104	0.010	2.00	1.00	18.7	3.97		
5	CA	0.080	0.776					75.0	93.7

In the tested scenario for Group 2, a low recovery is achieved, consistent with the observations made by [12]. The best setup would involve two stages of calcination, which would result in higher volatilization rates and, consequently, better recovery.

On the other hand, the tests conducted for Group 5 successfully recovered these elements. Most of them are neutralized in the form of glass (Figure 7), making them potential inputs for various applications such as civil construction.



(Figura 5.39) **Figure 7.** Glass formed from GlassRock™ methodology demonstrates the possibility of As and Sb recovery and its use as an industrial product.

These tests provide an opportunity for exploring new paths, not only for the reuse of Group 5 but also for other structures and operational facilities facing challenges in the treatment of waste containing hazardous metals and metalloids such as As and Sb.

4.2.3. Selective Grinding, Pneumatic and Triboelectrostatic Separation—Other Products and Opportunities

For the tests aimed at identifying the potential for generating other products, samples were chosen based on their mineralogical size distribution. Two Groups were chosen: Group 3, which exhibited similarities with Groups 1, 2, and 4, and Group 5, which was the most distinct. The objective of these tests was to assess the possibility of pre-concentration and evaluate the potential for generating multiple products from the same source.

In this stage, the samples underwent selective grinding and pneumatic separation, resulting in two products from each feed: a fine fraction below 6 µm and a coarse fraction above 30 µm (Groups 3 and 5—Figure S5). The intermediate product is further subjected to triboelectrostatic separation, resulting in the generation of two additional products. Table 7 provides an overview of the mass distribution and the chemical quality of these products.

(Tabela 5.24) **Table 7.** Summary of size separation results of Groups 4 and 5.

Group	Samples	Size (µm)	S1 *		S2 **		Products Chemical Quality							
			w (%)	w (%)	Al (%)	As (%)	Au (mg/kg)	Ca (%)	Fe (%)	K (%)	Mg (%)	Na (%)	S (%)	Si (%)
3	CO + MV	>30	69.8	-	3.04	0.036	0.690	3.68	6.95	0.856	1.44	0.190	1.13	30.4
		30–6	23.1	E1	14.6	26.2	0.100	0.260	2.10	9.30	4.00	1.0	0.400	0.900
		<6	7.04	E2	8.56	6.50	0.400	1.19	8.00	17.9	1.00	2.10	0.700	4.10
5	CA	>30	71.5	-	-	1.19	0.062	3.16	0.339	53.0	0.307	0.436	0.107	0.063
		30–6	21.9	E1	7.67	8.50	2.00	1.36	3.40	49.3	1.70	1.70	0.800	0.30
		<6	6.62	E2	14.3	6.50	2.00	2.46	3.40	58.4	0.900	1.00	0.500	0.40

* S1: Selective grinding and pneumatic separation and ** S2: triboelectrostatic separation.

The results presented in Table 7 indicate that there are similar mass distributions in terms of granulometric separations for both Groups. However, chemical enrichment of certain elements is observed in fractions of Group 3. The triboelectrostatic separation process proves to be relatively efficient in concentrating Al and K (probably Muscovite) for fertilizer production (63%), as well as sulfides, Fe, Au, and As (37%). Nevertheless, when evaluating other size fractions ($>30\text{ }\mu\text{m}$ and $<6\text{ }\mu\text{m}$), it can be observed that the previous steps are not as effective as expected.

Regarding Group 5, the triboelectrostatic separation process does not yield satisfactory results. However, enrichment of Fe and Au in coarse fractions ($>30\text{ }\mu\text{m}$) and relative depletion of Si can be observed. However, there are also limitations in achieving good separation rates in the preceding steps.

These observations can be explained by the mineralogical complexity of the samples, which compromised the efficiency of the tests. Further reassessment and identification of improvements are needed, as some elements show enrichment in specific fractions. However, in these initial tests, no generation of by-products from a single source has yet been identified. This does not invalidate the potential of these samples but rather highlights the challenges involved in transforming them into multiple products solely through physical separations. For the use of this technique and the production of new products, further studies are needed.

5. Conclusions

This study explores various possibilities to add value to different Au mining tailings in the Iron Quadrangle region. The waste materials were characterized and distinguished for concentration tests targeting different elements, with Au being the most promising element for recovery. Calcination, leaching, and flotation techniques showed promise for recovering Au, particularly in samples from the CDS mine. The results obtained from these techniques were comparable to successful Au mines in Brazil and South Africa.

On the other hand, the tests demonstrated that toxic elements such as Sb and As could be effectively reused in the form of glass, thereby adding value and offering a solution for the disposal of hazardous waste. Although the generation of other products using dry cleaning techniques was not highly effective, it showed promise due to the enrichment of elements such as Au, Fe, Al, and K in specific fractions.

The information obtained from this study can be further optimized, and economic analyzes need to be conducted for each value-adding technique. Future research should explore different methods and equipment to identify further opportunities for improvement and value addition through modifications or additional setups.

Supplementary Materials: The following supporting information can be downloaded at: <https://www.mdpi.com/article/10.3390/min13070863/s1>.

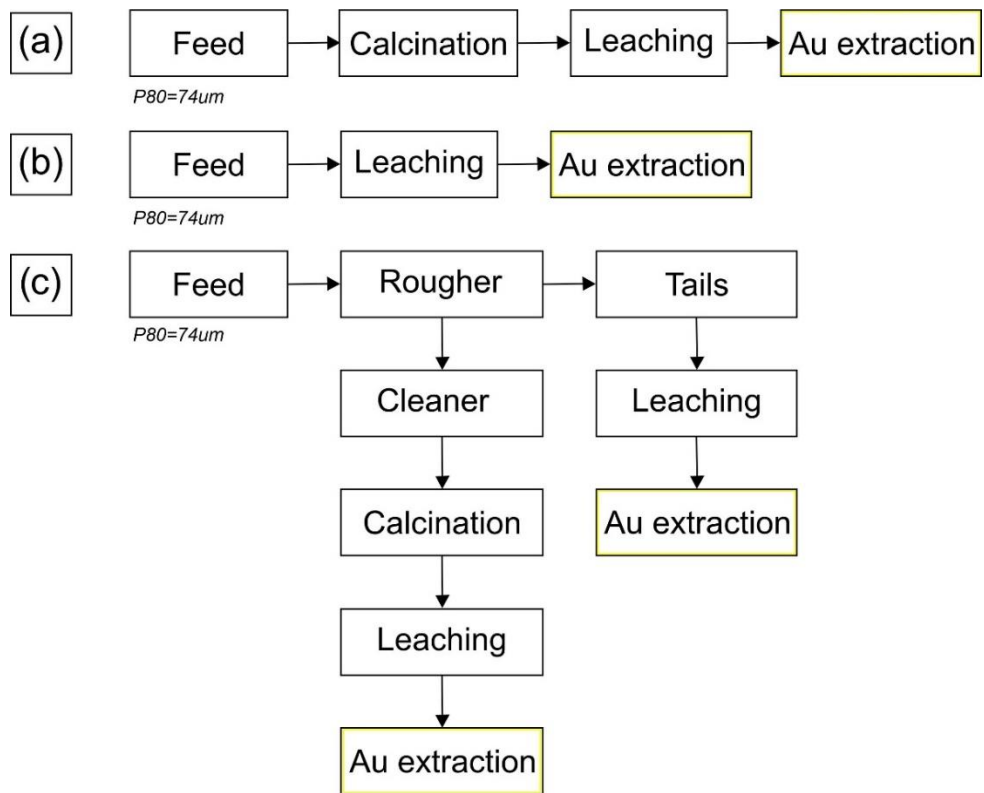


(Figura 5.40) **Figure S1.** Au extraction potential in (a) Calcination + Leaching, (b) Direct Leaching and (c) Flotation+Calcination+Leaching, modified from [34].

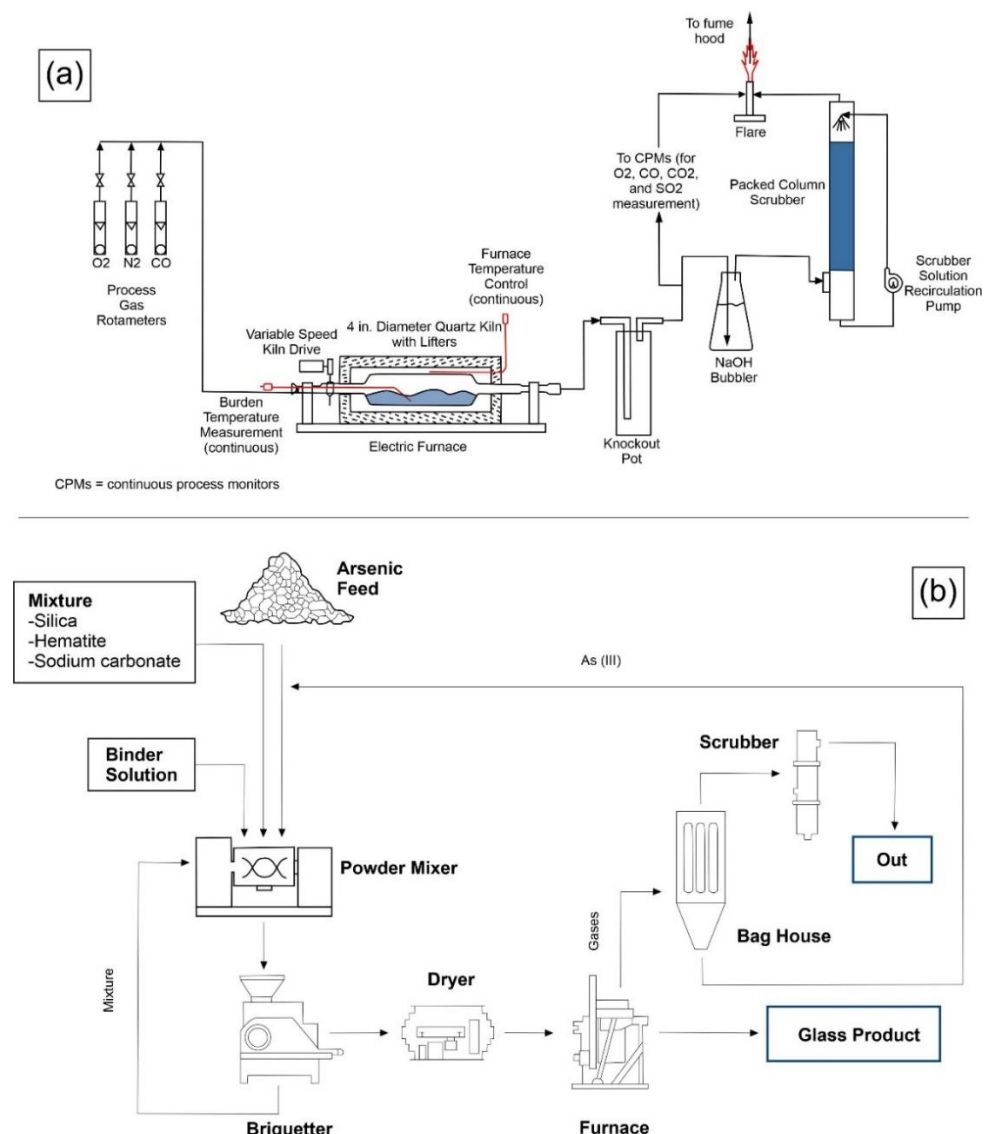


(Figura 5.41) **Figure S2.** Sb and As extraction potential in (a) rotative klin and (b) GlassLock™, modified from [11, 35].

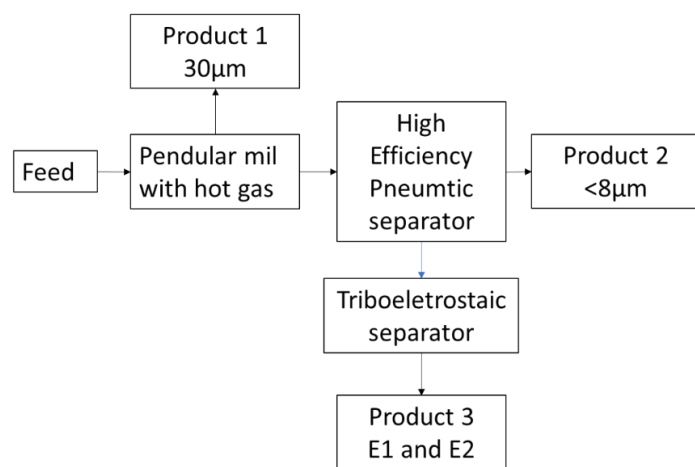


(Figura 5.42) **Figure S3.** Test flowchart for generation of three potential input-generating products in the civil, fertilizer and other industries.

RESULTADOS E DISCUSSÕES

Minerals 2023, 13, 863.

<https://doi.org/10.3390/min13070863>

(Tabela 5.25) **Table S1.** Statistical summary of major elements for the structures' tailings samples.

Structure	N ¹	Element	Mean	SD ²	Min ³	Max ⁴	N ¹	Element	Mean	SD ²	Min ³	Max ⁴	N ¹	Element	Mean	SD ²	Min ³	Max ⁴	
BIC	162		1.32	0.4	0.8	2.1	Sn (mg/kg)	162		1.2	1.64	0.03	4.46	111		1.9	1.07	0.3	3.35
CDS1	175		10	0	10	10		175		0.379	0.923	0.005	10.8	150		0.229	0.349	0.005	3.99
CDS2	293		10	0	10	10		293		3.02	0.613	2.16	6.89	291		1.98	0.264	1.07	2.44
CO	282		10	0	10	10		282	Ca (%)	3.99	1.88	0.02	16	282	Mg (%)	2.15	0.879	0.13	3.36
MV	615		10.7	4.25	10	40.4		615		0.244	0.527	0.023	4.19	321		0.394	0.497	0.007	3.22
ISO	266		9.16	2.8	0	10		266		0.519	0.946	0	4.82	266		0.885	1.21	0	4.23
CA	230		9.93	0.864	0	10		230		2.63	0.686	0	5.75	230		0.593	0.151	0	0.93
BIC	162		0.805	1.69	0	11.8	162		1.53	0.563	0.83	2.82	162		478	221	190	1080	
CDS1	150		0.017	0.014	0.005	0.14	150		2.2	0.561	0.005	2.81	150		381	92.6	21	672	
CDS2	293		0.785	0.378	0.005	3.93	293		1.7	0.332	0.57	2.3	293		259	47.9	95	350	
CO	282	S (%)	3.47	1.93	0.02	9.47	282	K (%)	0.617	0.587	0.19	3	282	Ba (mg/kg)	129	156	35	844	
MV	321		0.11	0.206	0	1.98	321		0.072	0.081	0.007	0.401	321		83.6	68.7	3.93	310	
ISO	181		3.45	4.5	0	17.7	181		0.953	0.682	0	2.49	181		1091	1238	0	5065	
CA	230		1.97	0.704	0	6.33	230		0.912	0.37	0	2.71	230		93.8	39.3	0	339	
BIC	111		5.31	4.2	0	21.4	111		0.231	0.1437	0.032	0.494	162		0.116	0.061	0.051	0.262	
CDS1	150		6.86	1.7	4.28	14.3	150		0.188	0.14	0.05	1.55	150		0.174	0.224	0.04	1.06	
CDS2	293		4.12	2.2	0.86	16.4	293		0.097	0.009	0.08	0.12	257		0.135	0.032	0.07	0.21	
CO	282	Fe (%)	12.42	2.9	2.42	15	282	Mn (%)	0.281	0.067	0.01	0.42	286	Ti (%)	0.069	0.037	0.02	0.23	
MV	321		0.007	0.007	0	0.08	321		0.094	0.098	0.004	0.65	615		0.019	0.02023	0.001	0.097	
ISO	266		17.29	15.4	0	65.6	266		0.163	0.172	0	0.62	266		0.143	0.1	0	0.44	
CA	230		42.49	8.91	0	83.3	230		0.097	0.021	0	0.17	230		0.058	0.022	0	0.16	
BIC	70		9.24	6.71	0.1	30.5	70		0.04	0.015	0.025	0.095	162		54.5	35	19.3	137	
CDS1	150		0.293	0.109	0.05	0.98	150		0.035	0.011	0.02	0.12	150		93.4	39.2	18	273	
CDS2	111		2.06	0.281	1.29	3.09	111		0.033	0.004	0.03	0.04	257		21.4	6.22	4	42	
CO	248	C (%)	3.55	1.14	0.13	12.1	248	P (%)	0.037	0.014	0.02	0.18	286	Co (mg/kg)	19.6	11.7	4	76	
MV	293		2.66	0.071	2.44	3.03	293		0.04	0.021	0.009	0.142	615		34.6	46.2	5.53	361	
ISO	133		1.27	2.13	0	15.6	133		0.035	0.022	0	0.11	266		33.1	34.1	0	214	
CA	218		0.157	0.113	0	1.29	218		0.046	0.008	0	0.07	230		132	35.8	0	195	

¹N = number of samples; ²SD = standard deviation; ³Min – Minimum; ⁴Max – Maximum

(Tabela 5.26) **Table S2.** Statistical summary of trace elements for the structures' tailings samples.

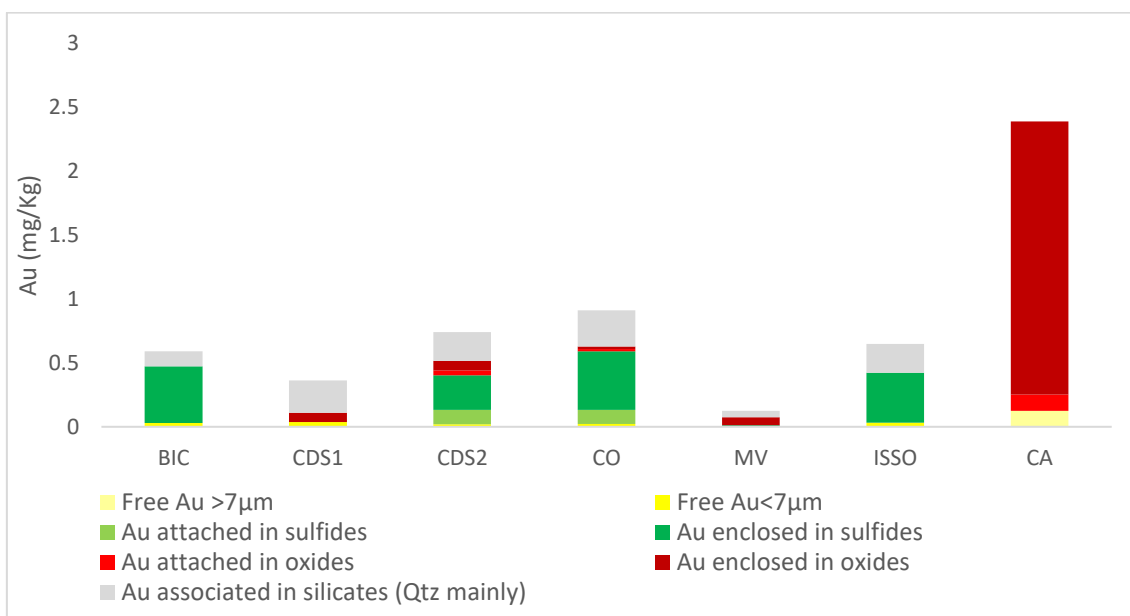
Structure	N ¹	Element	Mean	SD ²	Min ³	Max ⁴	N ¹	Element	Mean	SD ²	Min ³	Max ⁴	N ¹	Element	Mean	SD ²	Min ³	Max ⁴	
BIC	162		17.6	7.31	11.1	40.7	La (mg/kg)	162		27.2	25.9	7.9	113	162		116	89.7	11	236
CDS1	175		36.7	15	10	81		150		29.9	9.42	11	61	150		97.8	42.2	1.5	393
CDS2	293		14.5	5.78	10	35		293		23.5	5.73	5	34	293		137	36.2	101	386
CO	282		13.8	32.6	10	489		282	Li (mg/kg)	6.34	4.37	1.5	21	282	Sr (mg/kg)	83.2	100	12	1040
MV	615		17	13.6	10	79.1		321		8.54	14.8	1.5	88	321		20.4	22.4	10	117
ISO	266		17.9	20.4	0	124	181		26.4	21.7	0	79	181		166	152	0	531	
CA	230		10.4	2.46	0	22	230		1.69	1.33	0	15	230		94.8	29.2	0	222	
BIC	162		11.2	4.9	1.9	20.5	111		1.11	0.516	0.5	2	111		6.94	2.46	4.7	14.6	
CDS1	150		10.1	0.898	10	21	150		10	0	10	10	150		7.69	2.3	3	27	
CDS2	257		19.5	32.1	10	172	293		10	0	10	10	293		6.01	0.745	4	9	
CO	286	W (mg/kg)	48	20.5	10	105	282	Se (mg/kg)	11	10.9	10	158	282	Y (mg/kg)	5.09	6.47	3	96	
MV	615		11.9	12.9	10	114	615		0.05	0	0.05	0.05	615		10.8	16.1	1.5	86	
ISO	266		131	334	0	1854	251		9.16	2.8	0	10	251		6.52	4.31	0	21	
CA	230		8.75	3.54	0	10	230		9.93	0.864	0	10	230		4.96	1.32	0	8	

¹N = number of samples; ²SD = standard deviation; ³Min – Minimum; ⁴Max – Maximum

(Tabela 5.27) **Table S3.** Mineralogical composition by XRD of < 2 mm fraction. Mineral abbreviations after [51].

SAMPLE	Qz	Fsp	P	Ms	Tlc	Cb	Kfs	Gbs	Gth	Hem	Py	Po	Ank	Sd	Gp	Apy	Au
BIC	30	4	8	43	-	3	8	3	tr								
CDS1	22	4	6	60	-	-	5	-	3	-	-	-	-	-	-	-	-
CDS2	45	2	2	23	-	-	19	1	6	-	-	-	-	-	-	-	2
CO	13	1	1	18	4	9	23	3	2	-	-	-	14	2	-	-	1
MV									n.a.								
ISO	12	-	7	5	-	1	5	-	-	-	7	12	30	16	-	5	-
CA	8	-	4	2	-	-	-	-	-	73	-	-	-	-	13	-	-

*Qz = Quartz; *Fsp = Feldspar; *Ms = Muscovite; Tlc = Talc; Cb = Carbonate Mineral; Kfs = K-Feldspar; Gbs = Gibbsite; Gth = Goethite; Hem = Hematite; Py = Pyrite; Po = Pyrrhotite; Ank = Ankerite; Sd = Siderite; Gp = Gypsum; Apy = Arsenopyrite; Au = Gold; tr = trace; n.a. = not analyzed

(Figura 5.43) **Figure S4.** Gold deportion chart by structure complementing Figure 5 of this study.

(Tabela 5.28) **Table S4.** Parameters of each group's centroids, which defined grouping by observations.

Variable	cluster1	cluster2	cluster3	cluster4	cluster5	Global Centroid
Au (ppm)	0,476	2,39	0,742	0,518	0,65	0,824
S (%)	0,411	1,97	0,785	1,790	3,45	1,515
As (%)	0,150	0,72	0,093	0,412	0,72	0,380
Fe (%)	6,085	42,49	4,120	6,213	17,29	12,642
Cu %	0,006	0,09	0,010	0,009	0,04	0,024
Sb (%)	0,006	0,00	0,104	0,001	0,00	0,017
C (%)	4,766	0,16	2,060	3,105	1,27	2,747
Ag (ppm)	0,991	8,49	1,520	1,012	1,37	2,198
Al (%)	5,700	2,87	5,700	2,265	4,75	4,179
Ba (ppm)	429,500	93,80	259,000	106,300	1091,00	359,343
Be (ppm)	1,400	1,49	1,500	1,019	1,37	1,314
Bi (ppm)	5,149	9,93	10,000	5,730	9,16	7,264
Ca (%)	0,789	2,63	3,020	2,117	0,52	1,712
Co (ppm)	73,950	132,00	21,400	27,100	33,10	55,514
Cr (ppm)	310,000	98,30	198,000	139,500	102,00	185,329
K (%)	1,865	0,91	1,700	0,344	0,95	1,141
La (ppm)	27,150	10,40	14,500	15,400	17,90	18,271
Li (ppm)	28,550	1,69	23,500	7,440	26,40	17,653
Mg (%)	1,065	0,59	1,980	1,272	0,89	1,162
Mn (%)	0,210	0,10	0,097	0,188	0,16	0,164
Mo (ppm)	1,297	7,20	1,500	2,145	1,37	2,422
Ni (ppm)	223,500	494,00	129,000	86,850	83,50	189,600
P (%)	0,038	0,05	0,033	0,038	0,04	0,038
Pb (ppm)	107,300	241,00	69,600	38,450	30,00	90,300
Sc (ppm)	19,050	9,30	15,900	6,570	8,31	12,107
Se (ppm)	5,555	9,93	10,000	5,525	9,16	7,321
Sn (ppm)	5,660	9,93	10,000	10,350	9,16	8,730
Sr (ppm)	106,900	94,80	137,000	51,800	166,00	102,171
Th (ppm)	7,090	9,93	10,000	10,000	9,16	9,039
Ti (%)	0,145	0,06	0,135	0,044	0,14	0,102
U (ppm)	5,610	9,93	10,000	10,000	9,16	8,616
V (ppm)	126,500	58,10	87,200	48,950	63,00	79,886
W (ppm)	10,650	8,75	19,500	29,950	131,00	34,350
Y (ppm)	7,315	4,96	6,010	7,945	6,52	6,859
Zn (ppm)	109,200	3213,00	113,000	145,550	94,30	561,400
Zr (ppm)	90,200	16,00	78,100	16,800	51,00	51,300
Mud	9,082	15,62	5,834	11,113	10,48	10,331
Fine Silt	74,935	65,50	50,498	60,365	65,61	64,601
Coarse Silt	12,975	16,14	29,755	22,848	19,01	19,507
Very fina Sand	1,812	2,43	8,923	3,861	3,10	3,685
Fine Sand	0,517	0,23	2,508	0,790	0,74	0,869
Medium Sand	0,600	0,02	2,088	0,835	0,94	0,845
Coarse Sand	0,076	0,03	0,303	0,147	0,10	0,125
Very Coarse Sand	0,004	0,03	0,046	0,026	0,02	0,022
Pyrite	2,670	0,00	0,080	0,280	0,22	0,886
Quartz	32,875	15,60	35,600	46,815	36,65	35,319

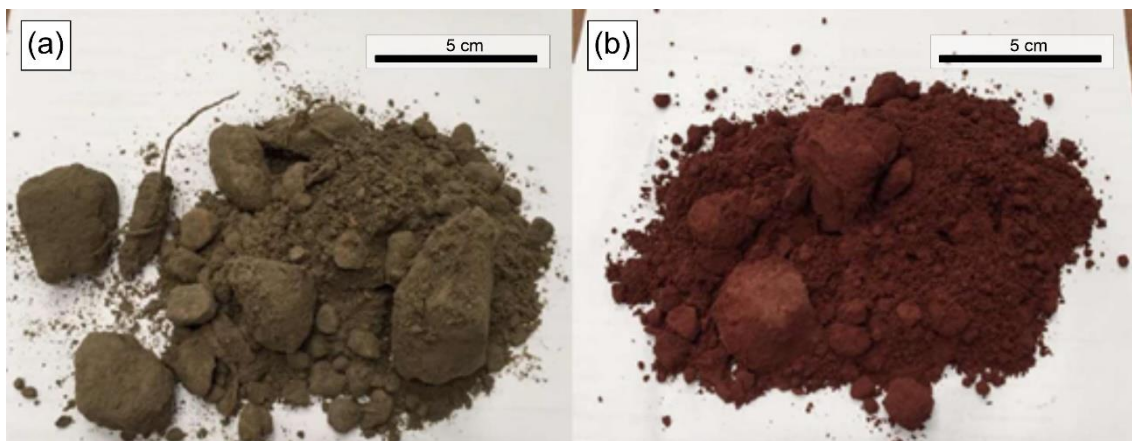


(Figura 5.44) Figure S5. Image of tested samples in the selective grinding test, pneumatic and triboelectrostatic separation from **(a)** Group 4 and **(b)** Group 5.

Author Contributions: Conceptualization, M.G.L., T.M.V., A.P.M.R., R.M.F.F., F.G., J.G.d.M.F. and M.F.M.; methodology, M.G.L., T.M.V., A.P.M.R., R.M.F.F., F.G., J.G.d.M.F. and M.F.M.; software, M.G.L. and I.D.D.; validation, M.G.L., T.M.V., A.P.M.R., R.M.F.F., F.G., J.G.d.M.F., M.F.M. and I.D.D.; formal analysis, M.G.L., T.M.V., A.P.M.R., R.M.F.F., F.G., J.G.d.M.F., M.F.M. and I.D.D.; investigation, M.G.L., T.M.V., A.P.M.R., R.M.F.F., F.G., J.G.d.M.F., M.F.M. and I.D.D.; resources, M.G.L., T.M.V., A.P.M.R., R.M.F.F., F.G., J.G.d.M.F. and M.F.M.; data curation, M.G.L., T.M.V., A.P.M.R. and R.M.F.F.; writing – original draft preparation, M.G.L.; writing – review and editing, M.G.L., T.M.V., A.P.M.R., R.M.F.F. and G.R.D.; visualization, M.G.L., T.M.V., A.P.M.R., R.M.F.F. and G.R.D.; supervision, M.G.L., T.M.V., A.P.M.R. and R.M.F.F.; project administration, M.G.L., T.M.V., A.P.M.R., R.M.F.F., F.G., J.G.d.M.F. and M.F.M.; funding acquisition, M.G.L., T.M.V., A.P.M.R., R.M.F.F., F.G., J.G.d.M.F. and M.F.M. All authors have read and agreed to the published version of the manuscript.

Funding: This research was funded by Fundação para a Ciência and Tecnologia (FCT) through projects UIDB/04683/2020, UIDP/04683/2020, and Nano-MINENV 029259 (PTDC/CTA-AMB/29259/2017).

Data Availability Statement: The data presented in this study are available upon request from the corresponding author. The data are not publicly available due to high amounts of data.

Acknowledgments: We thank our colleagues from the Instituto de Ciências da Terra (ICT), the Microscopy Center from Universidade Federal de Minas Gerais (CM-UFMG), and from AngloGold Ashanti, who provided insights and expertise that greatly assisted this research; Fundação para a Ciência and Tecnologia (FCT) for financial aid; and MSc Alexandre Orlandi and Jean Philippe Mai for laboratory support and reuse tests of other elements such as As, Sb, Fe, and K. The authors are deeply grateful for the support of all expert reviewers.

Conflicts of Interest: The authors declare no conflict of interest.

References

1. Gomes, A.C.F. Estudo de Aproveitamento de Rejeito de Mineração. Master's Thesis, Universidade Federal de Minas Gerais, Belo Horizonte, Brazil, February 2017.
2. Gorakhki, M.H.; Bareither, C.A. Sustainable reuse of mine tailings and waste rock as water-balance covers. *Minerals* **2017**, *7*, 128. [[CrossRef](#)]
3. Circular Economy of Metals and Responsible Mining. Available online: <https://blogs.egu.eu/network/gfgd/2018/04/24/circular-economy-of-metals-and-responsible-mining/> (accessed on 1 April 2023).
4. Mineração no Brasil Colonial. Available online: <https://brasilescola.uol.com.br/historiab/mineracao-no-brasil-colonial.htm> (accessed on 10 April 2023).

5. Jones, H.; Boger, D.V. Sustainability and waste management in the resource industries. *Ind. Eng. Chem. Res.* **2012**, *51*, 10057–10065. [[CrossRef](#)]
6. Silva, A.P.M.; Viana, J.P.; Cavalcante, A.L.B. *Diagnóstico dos Resíduos Sólidos da Atividade de Mineração de Substâncias Não Energéticas*; Instituto de Pesquisa Econômica Aplicada: Brasília, Brazil, 2012; 46p.
7. Shafiee, S.; Topal, E. An overview of global gold market and gold price forecasting. *Resour. Policy* **2010**, *35*, 178–189. [[CrossRef](#)]
8. Moraes, S.L.; Motta, F.G.; Massola, C.P.; Saccoccio, E.M.; Júnior, M.C. Rejeitos de mineração: Um olhar do cenário brasileiro-Parte I: Cadeia produtiva. In *Anais dos Seminários de Redução, Minério de Ferro e Aglomeração, Proceedings of the 18º Simpósio de Mineração, São Paulo, Brasil, 2–6 Editora Blucher Octomber 2017*; Institute for Technological Research: São Paulo, Brazil, 2017. [[CrossRef](#)]
9. ANM. Available online: <https://www.gov.br/anm/pt-br> (accessed on 12 April 2023).
10. Mesquita, P.P.D.; Carvalho, P.S.L.; Ogando, L.D. Desenvolvimento e inovação em mineração e metais. *BNDES Set.* **2021**, *43*, 325–361.
11. Lalancette, J.M.; Lemieux, D.; Nasrallah, K.; Curiel, G.G.; Barbaroux, R. Method for Vitrification of Arsenic And Antimony. U.S. Patent 9981295 B2, 29 May 2015. Available online: <https://patents.google.com/patent/US9981295B2/en> (accessed on 1 January 2020).
12. Lemos, M.G.; Valente, T.M.F.; Marinho Reis, A.P.; Fonseca, R.; Dumont, J.M.; Ferreira, G.M.M.; Delbem, I.D. Geoenvironmental study of gold mining tailings in a circular economy context: Santa Barbara, Minas Gerais, Brazil. *Mine Water Environ.* **2021**, *40*, 257–269. [[CrossRef](#)]
13. Lemos, M.; Valente, T.; Marinho Reis, P.; Fonseca, R.; Delbem, I.; Ventura, J.; Magalhães, M. Mineralogical and geochemical characterization of gold mining tailings and their potential to generate acid mine drainage (Minas Gerais, Brazil). *Minerals* **2021**, *11*, 39. [[CrossRef](#)]
14. Parviainen, A.; Soto, F.; Caraballo, M.A. Revalorization of Haveri Au-Cu mine tailings (SW Finland) for potential reprocessing. *J. Geochem. Explor.* **2020**, *218*, 106614. [[CrossRef](#)]
15. Study on the Critical Raw Materials for the EU 2023—Final Report. Available online: https://single-market-economy.ec.europa.eu/publications/study-critical-raw-materials-eu-2023-final-report_en (accessed on 14 June 2023).
16. European Commission. *Communication from the Commission to the European Parliament, the Council, the European Economic and Social Committee and the Committee of the Regions: Critical Raw Materials Resilience: Charting a Path Towards Greater Security and Sustainability*, 474 Final; European Commission: Brussels, Belgium, 2020; 28p.
17. Antunes, M.; Fernandes, R.; Pinheiro, A.; Valente, T.M.F.; Nascimento, S. Potential of reuse and environmental behavior of ochre-precipitates from passive mine treatment. In *IMWA 2010 Proceedings, Proceedings of the International Mine Water Association Symposium—Mine Water and Innovative Thinking, Sydney, Canada, 5–9 September 2010*; Wolkersdorfer, C., Freund, A., Eds.; Wolkersdorfer & Freund: Aachen, Germany; pp. 205–208.
18. Nwaila, G.T.; Ghorbani, Y.; Zhang, S.E.; Frimmel, H.E.; Tolmay, L.C.; Rose, D.H.; Nwaila, P.C.; Bourdeau, J.E. Valorisation of mine waste-Part I: Characteristics of, and sampling methodology for, consolidated mineralised tailings by using Witwatersrand gold mines (South Africa) as an example. *J. Environ. Manag.* **2021**, *295*, 113013. [[CrossRef](#)]
19. Sibanda, L.K.; Broadhurst, J.L. Exploring an alternative approach to mine waste management in the South African gold sector of the article. In *Proceedings of the 11th ICARD|IMWA|MWD Conference—“Risk to Opportunity”*, Pretoria, South Africa, 10–14 September 2018; Wolkersdorfer, C., Sartz, L., Weber, A., Burgess, J., Tremblay, G., Eds.; pp. 1130–1135.
20. Dehghani, A.; Ostad-Rahimi, M.; Mojtabahedzadeh, S.H.; Gharibi, K.K. Recovery of gold from the Mouteh Gold Mine tailings dam. *J. South. Afr. Inst. Min. Metall.* **2009**, *109*, 417–421.
21. Cairncross, K.H.; Tadie, M. Life cycle assessment as a design consideration for process development for value recovery from gold mine tailings. *Miner. Eng.* **2022**, *183*, 107588. [[CrossRef](#)]
22. Muir, A.; Mitchell, J.; Flatman, S.R.; Sabbagh, C. A practical guide to re-treatment of gold processing residues. *Miner. Eng.* **2005**, *18*, 811–824. [[CrossRef](#)]
23. PanAfrican Resources Mineral Resources and Mineral Reserves Report for the Year Ended 30 June 2018. Available online: <https://www.miningnewsfeed.com/reports/annual/Pan-African-Resources-MRMR-report-2018.pdf> (accessed on 12 April 2023).
24. Monte, M.B.M.; Grisol, S.; Duque, T.F.M.B.; Fenelon, P.A.; Junior, G.G.O. Flotação seletiva para o reprocessamento de rejeitos provenientes do processo de lixiviação da Kinross Paracatu. *Braz. Appl. Sci. Rev.* **2020**, *4*, 2720–2728. [[CrossRef](#)]

25. Ince, C. Reusing gold-mine tailings in cement mortars: Mechanical properties and socio-economic developments for the LefkeXeros area of Cyprus. *J. Clean. Prod.* **2019**, *238*, 117871. [[CrossRef](#)]
26. Mapinduzi, R.P.; Bujulu, P.; Mwegooha, W.J. Potential for reuse of gold mine tailings as secondary construction materials and Phytoremediation. *Int. J. Environ. Sci.* **2016**, *7*, 49–61. [[CrossRef](#)]
27. Yao, G.; Liu, Q.; Wang, J.; Wu, P.; Lyu, X. Effect of mechanical grinding on pozzolanic activity and hydration properties of siliceous gold ore tailings. *J. Clean. Prod.* **2019**, *217*, 12–21. [[CrossRef](#)]
28. Sánchez-Peña, N.E.; Narváez-Semanate, J.L.; Pabón-Patiño, D.; Fernández-Mera, J.E.; Oliveira, M.L.S.; Boit, K.; Tutikian, B.F.; Crissien, T.J.; Pinto, D.C.; Serrano, I.D.; et al. Chemical and nano-mineralogical study for determining potential uses of legal Colombian gold mine sludge: Experimental evidence. *Chemosphere* **2018**, *191*, 1048–1055. [[CrossRef](#)]
29. Swaroop, G.; Bulbule, K.A.; Parthasarathy, P.; Shivakumar, Y.; Muniswamy, R.; Annamati, R.; Priyanka, D. Application of Gold Ore Tailings (GOT) as a source of micronutrients for the growth of plants. *Int. J. Sci. World* **2013**, *1*, 68–78.
30. Goldfarb, R.J.; Groves, D.I.; Gardoll, S. Orogenic gold and geologic time: A global synthesis. *Ore Geol. Rev.* **2001**, *18*, 1–75. [[CrossRef](#)]
31. Lobato, L.M.; Ribeiro-Rodrigues, L.C.; Vieira, F.W.R. Brazil's premier gold province. Part II: Geology and genesis of gold deposits in the Archean Rio das Velhas greenstone belt, Quadrilátero Ferrífero. *Miner. Depos.* **2001**, *36*, 249–277. [[CrossRef](#)]
32. Roeser, H.M.P.; Roeser, P.A. O Quadrilátero Ferrífero-MG, Brasil: Aspectos sobre sua história, seus recursos minerais e problemas ambientais relacionados. *Geonomos* **2010**, *18*, 33–37. [[CrossRef](#)]
33. Moura, W. Especiação de Cianeto para Redução do Consumo no Circuito de Lixiviação de Calcinado da Usina do Queiróz. Master's Thesis, Universidade Federal de Minas Gerais, Belo Horizonte, Brazil, 2005.
34. Lemos, M.; Valente, T.; Reis, P.; Fonseca, R.; Pantaleão, J.P.; Guabiroba, F.; Filho, J.G.; Magalhães, M.; Delbem, I. Caracterização Mineralógica, Geoquímica e Potencial de Valorização de Resíduos de Mineração de Ouro (Minas Gerais, Brasil). In Proceedings of the XXIX Encontro Nacional de Tratamento de Minérios e Metalurgia Extrativa, Armação dos Búzios, Brazil, 25–28 September 2022.
35. Ashanti, A.G. *AngloGold Ashanti AngloGold Ashanti Recommendations*; AngloGold Ashanti: Johannesburg, South Africa, 2016.
36. Valente, T.M.; Antunes, M.; Sequeira Braga, A.; Prudêncio, M.I.; Marques, R.; Pamplona, J. Mineralogical attenuation for metallic remediation in a passive system for mine water treatment. *Environ. Earth Sci.* **2012**, *66*, 39–54. [[CrossRef](#)]
37. Hastie, T.; Tibshirani, R.; Friedman, J. *The Elements of Statistical Learning: Data Mining, Inference, and Prediction*, 2nd ed.; Springer: New York, NY, USA, 2009; 764p.
38. Lemos, M.; Valente, T.; Reis, P.M.; Fonseca, R.; Pantaleão, J.P.; Guabiroba, F.; Filho, J.G.; Magalhães, M.; Afonseca, B.; Silva, A.R.; et al. Geochemistry and mineralogy of auriferous tailings deposits and their potential for reuse in Nova Lima Region, Brazil. *Sci. Rep.* **2023**, *13*, 4339. [[CrossRef](#)]
39. Cho, H.C.; Oh, W.; Han, O.H.; Kang, H.H.; Lee, J.S. Recovery of valuable materials from gold mine tailings. In *Separation Technologies for Minerals, Coal, and Earth Resources*, 7th ed.; Young, C.A., Luttrell, G.H., Eds.; Society for Mining, Metallurgy, and Exploration: Englewood, NJ, USA, 2012; pp. 277–287.
40. Ferguson, D.N. A basic triboelectric series for heavy minerals from inductive electrostatic separation behaviour. *J. South. Afr. Inst. Min. Metall.* **2010**, *110*, 75–78.
41. Jordan, C.E.; Sullivan, G.V.; Davis, B. *Report of Investigations 8457, Pneumatic concentration of Mica*; US Bureau of Mines Report Investigations: Pittsburgh, PA, USA, 1980; pp. 1–24.
42. Emrullahoglu, O.F.; Kara, M.; Tolun, R.; Celik, M.S. Beneficiation of calcined colemanite tailings. *Powder Technol.* **1993**, *77*, 215–217. [[CrossRef](#)]
43. Yang, J.; Xu, W.; Deng, X.; Li, H.; Ma, S. Research on the Selective Grinding of Zn and Sn in Cassiterite Polymetallic Sulfide Ore. *Minerals* **2022**, *12*, 245. [[CrossRef](#)]
44. Peiravi, M.; Dehghani, F.; Ackah, L.; Baharlouei, A.; Godbold, J.; Liu, J.; Mohanty, M.; Ghosh, T. A review of rare-earth elements extraction with emphasis on non-conventional sources: Coal and coal byproducts, iron ore tailings, apatite, and phosphate byproducts. *Min. Metall. Explor.* **2021**, *38*, 1–26. [[CrossRef](#)]
45. Okereafor, U.; Makhatha, M.; Mekuto, L.; Mavumengwana, V. Gold mine tailings: A potential source of silica sand for glass making. *Minerals* **2020**, *10*, 448. [[CrossRef](#)]

46. Valente, T.; Grande, J.A.; De La Torre, M.L. Extracting value resources from acid mine drainages and mine wastes in the Iberian Pyrite Belt. In Proceedings of the IMWA 2016—Mining Meets Water—Conflicts and Solutions, Leipzig, Germany, 11–15 July 2016; Drebendorf, C., Paul, M., Eds.; Technische Universität Bergakademie: Freiberg, Germany, 2016; pp. 1339–1340.
47. Luckeneder, S.; Giljum, S.; Schaffartzik, A.; Maus, V.; Tost, M. Surge in global metal mining threatens vulnerable ecosystems. *Glob. Environ. Chang.* **2021**, *69*, 102303. [[CrossRef](#)]
48. Marion, C.; Grammatikopoulos, T.; Rudinsky, S.; Langlois, R.; Williams, H.; Chu, P.; Awais, M.; Gauvin, R.; Rowson, N.A.; Waters, K.E. A mineralogical investigation into the pre-concentration of the Nechalacho deposit by gravity separation. *Miner. Eng.* **2018**, *121*, 1–13. [[CrossRef](#)]
49. Yang, X.; Wang, H.; Peng, Z.; Hao, J.; Zhang, G.; Xie, W.; He, Y. Triboelectric properties of ilmenite and quartz minerals and investigation of triboelectric separation of ilmenite ore. *Int. J. Min. Sci. Technol.* **2018**, *28*, 223–230. [[CrossRef](#)]
50. Bada, S.O.; Tao, D.; Honaker, R.Q.; Falcon, L.M.; Falcon, R.M.S. A study of rotary tribo-electrostatic separation of South African fine coal. *Int. J. Coal Prep. Util.* **2010**, *30*, 154–172. [[CrossRef](#)]
51. Whitney, D.L.; Evans, B.W. Abbreviations for names of rock-forming minerals. *Am. Mineral.* **2010**, *95*, 185–187. [[CrossRef](#)]
52. Gou, M.; Zhou, L.; Then, N.W.Y. Utilization of tailings in cement and concrete: A review. *Sci. Eng. Compos. Mater.* **2019**, *26*, 449–464. [[CrossRef](#)]

Disclaimer/Publisher's Note: The statements, opinions and data contained in all publications are solely those of the individual author(s) and contributor(s) and not of MDPI and/or the editor(s). MDPI and/or the editor(s) disclaim responsibility for any injury to people or property resulting from any ideas, methods, instructions or products referred to in the content.

5.1.4. Qualidade, distribuição química e potencial reuso para águas de porosidade

A água é um recurso essencial para a vida humana, fundamentalmente para consumo e irrigação, sendo a sua qualidade um dos fatores preponderantes para a saúde humana, mas também determinante na preservação dos ecossistemas (Gomes et al., 2019). Portanto, no âmbito da identificação e entendimento da distribuição de elementos que afetam a qualidade da água de barragens amostradas, tem-se a publicação na revista *Water*, nomeado por “*Recovery of metals in mining tailing waters - Hydrochemistry and elements distribution in gold metallurgical treatment tailings dams*”. Além de caracterizar estes efluentes também tem por objetivo identificar o potencial de recuperação de alguns elementos estratégicos como Au e Sb, foco sempre presente em todos os trabalhos.



Article

Recovery of metals in mining tailing waters - Hydrochemistry and elements distribution in gold metallurgical treatment tailings dams

Mariana Gazire Lemos^{1,2,*}, Teresa Maria Valente¹, Amélia Paula Marinho Reis¹, Amália Sequeira Braga¹,

Rita Maria Ferreira Fonseca³, Fernanda Guabiroba², José Gregorio da Mata Filho², Marcus Felix

Magalhães², Antonio Roberto Silva², Apolo Pedrosa Bhering¹ and Giovana Rebelo Diório⁴

¹ University of Minho, Institute of Earth Sciences, Pole of University of Minho, Campus de Gualtar, 4710-057 Braga, Portugal

² Anglogold Ashanti, Mining & Technical, COO International, Nova Lima 34000-000, Brazil

³ University of Évora, Institute of Earth Sciences, Pole of University of Évora, 7000-345 Évora, Portugal

⁴ Federal University of Paraná, Laboratory on Basin Analysis, Curitiba 81532-980, Brazil

* Correspondence: id8548@alunos.uminho.pt

Abstract: Recovering metals from mining wastewater is important in minimizing environmental pollution and maximizing resource efficiency. For this, a characterization step and understanding the occurrence of metals and other compounds are essential. The present study focused on waters from different mining dams containing metals such as Au, Cu, Ni, Zn, and sulfates, located in the Iron Quadrangle region, (Brazil). The results indicate the occurrence of waters with low to high metal content in a neutral zone in three tailings dams from the metallurgical treatment of Au. With the aim of assessing the potential reuse of these elements, 3D maps of the distribution, statistical analysis, and the processes governing mobility and partitioning are also described. The high potential for Au recovery, especially, can be detected from the use of methods such as nanofibers with biosorbents being more sustainable and of low operational cost.

Keywords: circular economy; Wastewater; mining tailings, Au recovery, hydrochemistry

1. Introduction

Water is a critical issue in mining works and over the entire mining cycle. In addition, proper management of mine tailings is a global and emergent issue. The solid component of the tailing dams is commonly studied, and there are several works reporting the presence of toxic elements and their impacts [e.g., 1, 2, 3]. Also, the nowadays research is trending toward turning ore-extraction waste into by-products [e.g., 4; 5; 6; 7, 8], in a perspective of circular economy. However, is often overlooked that surface wastewater and groundwater are also present in these structures and can contain several hazardous and risky supplier materials. Hence, these waters need to be monitored and managed to prevent environmental impact.

The characteristics of the tailing's wastewater vary depending on the type of mined ore and mining and metallurgic processes [9]. Generally, these wastewaters contain high levels of suspended solids, including colloidal materials, which can increase concentrations of elements in free form and in different complexes (e.g., sulfates, carbonates, and nitrates) most as potential toxic elements (PTE) [1,3]. Furthermore, contaminants in colloidal phases ($> 20 \mu\text{m}$) and/or in solution have an even greater impact due to their higher reactivity and mobility [10, 11]. Thus, the characterization of wastewater from mining tailings is a complex, but essential issue. Multiple elements can be found in surface water and interstitial water associated with the solid part of tailings, which can be hazardous -e.g., gold (Au), silver (Ag), nickel (Ni), manganese (Mn), iron (Fe), and aluminum (Al)- or even pose risks to the surrounding environment and human health -e.g., mercury (Hg) and arsenic (As). Therefore, treatment processes, including neutralization are usually needed to minimize environmental impacts [12]. Knowledge about environmental impact, risk assessment, and potential reuse of all components of the mining tailings involves a complete characterization of the solids and water fractions. This includes a set of techniques, such as atomic absorption spectrometry (AAS) for trace metal concentration analysis, as well as parameters such as pH, electrical conductivity (EC), turbidity, and suspended solids,

153

associated with X-ray diffraction (XRD) to determine the mineralogy of suspended solids [13,14, 3, 15]. Additionally, understanding the occurrence of elements and associated physicochemical parameters within these water bodies is crucial for volume and distribution identification [16, 17, 18, 19]. Geostatistical and mathematical interpolation techniques such as kriging, cokriging, and inverse distance weighted are commonly used for 3D modeling of groundwater parameters [20, 21, 18]. Thus, the characterization of wastewater from mining tailings is a complex, but essential issue. Also, understanding the hydrochemistry of wastewater mining tailings and the partitioning of elements among colloidal fractions is essential for assessing its reuse potential (22; 3, 23).

To address this issue, governments, and international organizations have implemented several measures to reduce the impact of mining tailings wastewater, such as increasing public awareness [24]. As mining operations become larger and more complex, managing tailings wastewater becomes increasingly critical. Then, reusing this wastewater could be an efficient and cost-effective approach to mitigate the environmental impact of mining while ensuring a reliable water source [25, 26].

Recently, numerous case studies have been conducted worldwide to explore the potential for water reuse from mining tailings, especially as water demand rises and mining's environmental impacts become more evident. Therefore, it becomes crucial to treat and reuse mining tailings wastewater safely and sustainably. Such wastewater can be reused for multiple purposes, including crop irrigation, livestock water supply, and even human consumption [27]. In some cases, artificial wetlands and lakes can be created, providing habitats for diverse flora and fauna [28, 29]. Additionally, these wastewaters can be used for industrial processes like cooling or energy generation [30, 31].

In the case of Au tailings, previous works reported a limited potential for wastewater reuse due to its hazardous nature [9, 32, 33]. Firstly, this wastewater typically contains high concentrations of metal(lloid)s such as copper (Cu), zinc (Zn), lead (Pb), and As, and may also contain organic compounds. Treatment processes such as sedimentation, flocculation, oxidation, and ion exchange are commonly employed to reduce the concentrations of these contaminants, but advanced treatments such as membrane filtration can also be applied to minimize associated risks. Once treated, the wastewater can be reused for various purposes (e.g., agricultural irrigation, industrial cooling water, drinking water), but only after a careful thorough assessment of potential environmental impacts [9; 32; 34; 33; 35].

If Au is present, reuse is particularly challenging, because it is often found in fine particulate form, making it difficult to be separated from other elements. Additionally, Au is highly reactive and can form insoluble complexes with other elements, complicating its recovery. Knowledge about the partitioning of Au among colloidal fractions is essential for evaluating its reuse potential [36, 23].

In the above-described scenario, this study aims to characterize and compare the physicochemical characteristics of water from three gold tailings dams in the Iron Quadrangle, Brazil. The results will provide insights into the distribution of critical elements, serving as a foundation for identifying reuse potential and managing these structures to minimize impacts.

2. Study area

The three studied tailing structures are in the main Brazilian mineral province known as the Iron Quadrangle (IQ - Fig 1). Two tailing dams are situated in the city of Nova Lima, and one in Santa Barbara, Minas Gerais. Historically, both cities have been marked by Au exploitation since the early 19th century and are currently important regions for Au production in Brazil. The gold deposits are hosted in the Rio das Velhas metallogenic Greenstone Belt, which is the most significant gold district in Brazil [37, 38].

The QF region is characterized by a warm and temperate climate. It rains much less in winter than in summer. The climate classification is Cwa according to Köppen and Geiger. The average temperature is 20.4 °C with an annual rainfall of 1551 mm. As the climate is temperate, it is difficult to categorize the seasons [8, 42, 45].

The Santa Barbara tailings dam is in the northern part of the IQ, in Santa Barbara, Minas Gerais, ca. 110 km from Belo Horizonte. Waste from underground gold metallurgical plants has been deposited in this structure since 1986. As the workflow reviewed by [8], the sources of waste for these structures have different origins: a) waste from a flotation plant, and b) waste from the leaching stage, both derived from fresh underground mined ores [39, 40]. According to [41], solid tailings contain minerals such as quartz, muscovite,

biotite, and phases formed during processing stages, such as gypsum, jarosite, and iron antimonate. Arsenic (As) is also found to be associated with phases such as antimony oxide and rarely in arsenopyrite. Chemically, elements such as Fe, Au, antimony (Sb), sulfur (S), As, and Cu are present. Furthermore, the authors also described that the surface waters of this dam were alkaline, with maximum pH values of ≈ 10 , and contained potentially toxic elements such as Sb, As, and Cu. The average water volume of this dam during the sampled period was 1766.25 m^3 [42].

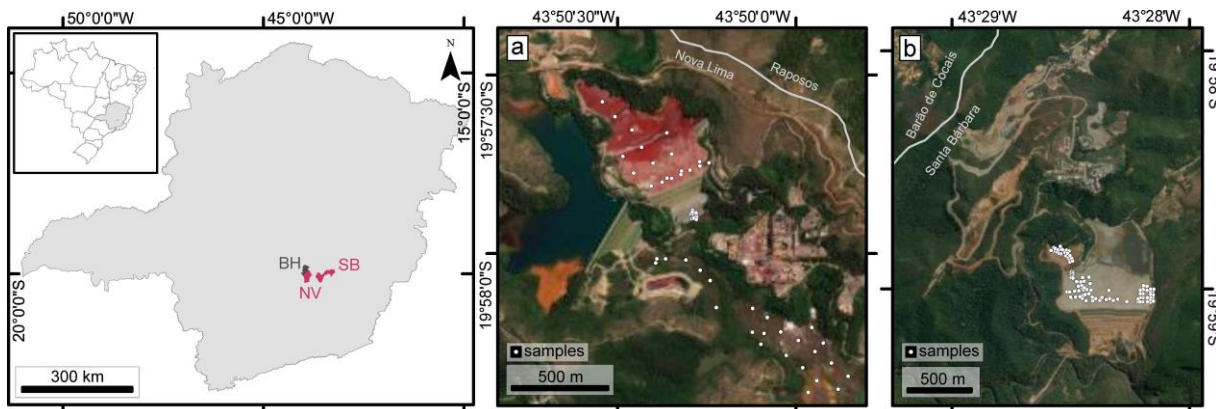


(Figura 5.45) **Figure 1.** Location of the study areas in Minas Gerais State, near Belo Horizonte, Brazil: (a) Nova Lima (NL) dams and deposits; and (b) Santa Barbara (SB) dams and deposits. In both, the sample's locations are highlighted in white.

The Nova Lima dams and tailings deposits are located in the northern part of the IQ, ca. 25 km from the capital Belo Horizonte, Minas Gerais, and are part of the Queiroz metallurgical plant. The Queiroz operation has been treating sulfide Au ores for over thirty years. The materials processed in the plant were divided into two distinct circuits, summarized by [8]. The Raposos circuit treats non-refractory sulfide ore (pyrite, pyrrhotite, and subordinate arsenopyrite) mainly from the Raposos mines. The circuit achieved 90% Au recovery and was divided into grinding, gravity concentration, conventional leaching, carbon-in-leach (CIL), elution, and electrowinning. The tailings generated in this circuit were deposited in the Cocoruto tailings impoundment (CO). This part of the plant was deactivated in 1998 with the closure of the Raposos underground mine [42, 36, 43]. The Cocoruto dam (old circuit) mainly consists of quartz, carbonates, iron oxides, and phyllosilicates such as muscovite and chlorite [36]. Chemically, it contains Fe > calcium (Ca) > magnesium (Mg) > Al > Mn > potassium (K), sodium (Na).

Currently, the Queiroz plant circuit processes refractory Au ore, requiring a calcination step after grinding and flotation. After calcination, Au is recovered through conventional leaching, CIL, elution, and electrowinning [42, 36, 43]. The generated tailings are deposited in the Calcination dam (CA). According to [8], this type of residue undergoes significant mineralogical transformation between the source and the storage location. All concentrated sulfides are subjected to high-temperature transformations and are thus calcined, which explains why these iron oxides are enriched in As, Cu, Ni, Ag, and Au. The presence of gypsum is also observed, likely formed by the addition of reagents such as lime during the calcination process. The water volumes of these dams are $142,000 \text{ m}^3$ for Cocoruto and $23,792 \text{ m}^3$ for Calcinados [42].

3. Methodology

Figure 2 summarized the workflow used in this study.

The sampling campaign was conducted during winter and early spring (May–September 2020). Typically, weather conditions during these months are dry, with temperatures ranging from 15 to 25°C [44].

The samples were collected using direct push drilling methods, with a maximum depth of 20 m, totaling 179 m of samples (Figure 1 and S1). Each sample, representing a 1-meter depth interval, was filtered using $0.20 \mu\text{m}$ syringe filters to represent the groundwater. Aliquots of 50–100 mL were stored in polypropylene bottles, acidified to $\text{pH} < 2$, and maintained in the dark at 5°C for chemical analysis. The solid portion above $0.20 \mu\text{m}$ was placed in plastic bags and sent for chemical analysis. The evaluation of these two fractions is essential for understanding the mobility of elements in groundwater from these structures.

At each sampling site, parameters such as pH, temperature, and EC were measured using methods from the Standard Methods of Water and Wastewater [45].

Wad Cyanide (CN Wad) is a group of cyanide species that are operationally defined and release free cyanide when refluxed under weakly acidic conditions (pH 4.5-6). These parameters are also defined in the Standard Methods of Water and Wastewater [45]. Elements such as Au, As, Fe, cadmium (Cd), Sb, Cu, Mn, Ni, Pb, Zn, Hg, and sulfates were analyzed using inductively coupled plasma mass spectrometry (ICP-MS) for both fractions. Blanks, replicates, and stock solutions were used to assess quality control.

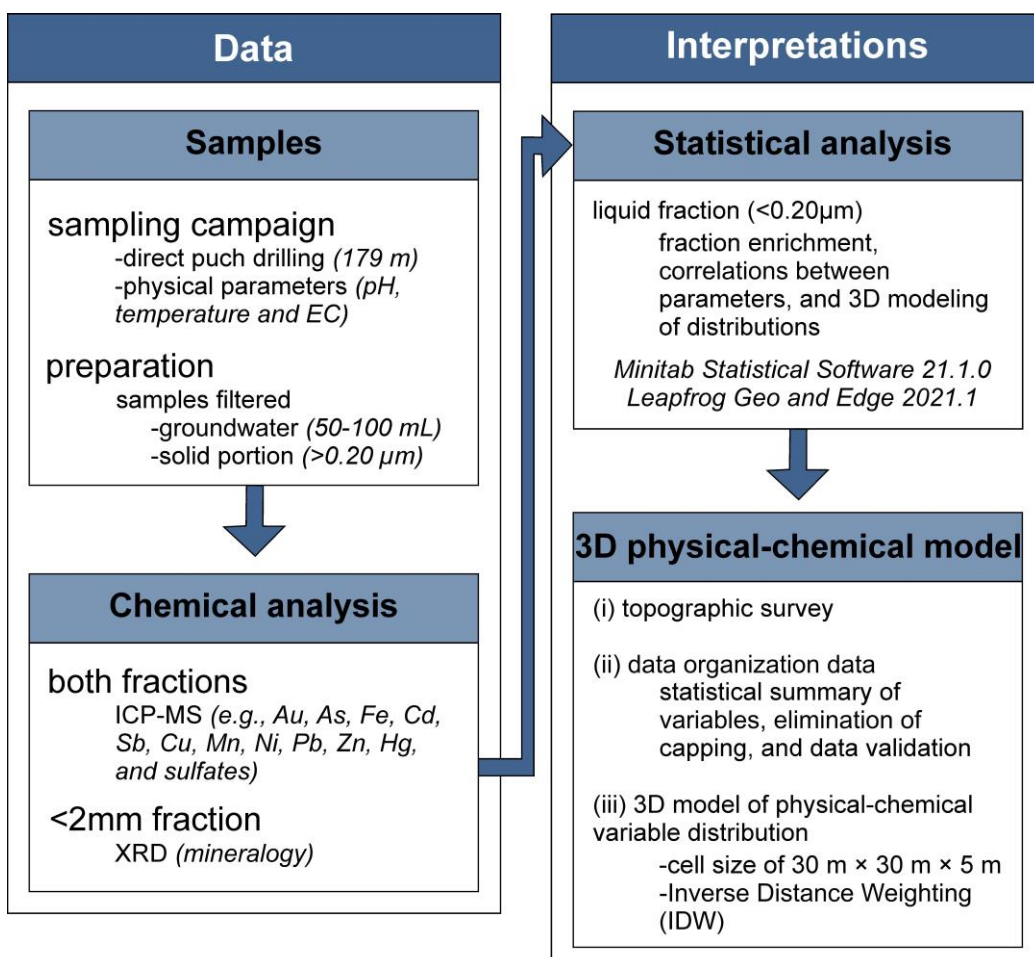


(Figura 5.46) **Figure 2.** Workflow of methodological approach.

To understand possible sources of chemical element distribution in wastewater samples, a mineralogical study was conducted using XRD with a X'pert Pro-MPD diffractometer (Philips PW 1710, APD), using CuK α radiation. The equipment features an automatic divergence slit and graphite monochromator. Diffractograms were obtained from powders of the <2 mm fraction, in the 3 to 65 $^{\circ}$ 2 θ range, with a 2 θ step size of 0.02 $^{\circ}$ and a counting time of 1.25 s.

For interpretation, a statistical analysis such as correlations between parameters, as well as determination of enrichment factors (Efx), and 3D modeling of the distributions of parameters in the liquid fraction (below 0.20 µm) were performed using Minitab Statistical Software version 21.1.0 and Leapfrog Geo and Edge 2021.1.

The enrichment factor can be expressed by calculating Xfraction smaller than 0.20 µm (aqueous phase-Xfraction) compared to the fraction above 0.20 µm (Xsolids). This reflects the ratio between the contents in the aliquots (smaller than 0.20 µm). This factor is particularly relevant when dealing with elements of higher environmental concern [46]. The enrichment factor can be calculated using Eq. (1) [46; 47]:

(Equação 1. Cálculo do fator de enriquecimento.)

$$Efx = X_{\text{fraction}} / X_{\text{solids}} \quad (1)$$

The 3D physical-chemical model was divided into four steps: (i) a topographic survey of the dam and sampled points using a total station, (ii) organization of topographic and physical-chemical data with a statistical summary of variables, elimination of capping, and data validation, and (iii) estimation and construction of the 3D model of physical-chemical variables distribution and validation of the models.

All models are 3D block models with a discretization cell size of $30 \text{ m} \times 30 \text{ m} \times 5 \text{ m}$ [8, 18, 48]. For step 3, a geostatistical tool called Inverse Distance Weighting (IDW) was used, which is one of the widely used interpolation methods in water resources management [49, 50, 18]. The estimation is based on nearby known locations, and the weights assigned to the interpolating points are inversely proportional to their distance from the interpolation point. Therefore, points closer to the interpolation point have higher weights than distant points, and vice versa [18, 20]. In the study areas, a fifth power weight was used to limit the influence of a sample in a distant region and refine the estimation [47].

4. Results and discussions

4.1. Groundwater composition and hydrochemical relationships

The parameters measured in situ, as well as others, serve as the primary indicators of the characteristics of each structure and their distinguishing factors [51].

Tables 1 and 2 provide statistical summaries of the elements and physicochemical parameters (pH and EC) for water samples from the three structures and their interrelationships. Overall, water samples exhibit elevated concentrations of metals, and despite having pH levels close to neutral, attention must be paid to the potential sources of contamination, as certain elements exceed the maximum values according to Brazilian regulations for Class II freshwater [52].

Regarding physicochemical characteristics, it is observed that the waters from the Cocoruto and CDS2 dams exhibit similar pH, ranging from 6 to 8. The sampled waters from the Calcinados dam, however, have a higher alkaline pH, with values above 8. The average EC ranges from $2585 \mu\text{S}/\text{cm}$ to $4402 \mu\text{S}/\text{cm}$. This indicates that EC values are distinct and higher for the Calcinados and CDS2 dams.

In general, this variable (EC) may be directly linked to the sulfate concentrations, which are relatively high for all structures (1270 to 5444 mg/L) and have a Pearson correlation coefficient of 0.4 (Table 2 and Figures S1a, S1b, and S1c). In addition, there is a clear relationship (above 0.5) between pH and EC that can mark zones of mineral-effluent interaction, mainly due to the presence of sulfides and sulfates.

(Tabela 5.29) **Table 1.** Statistical summary of chemical variables of wastewater from CO, CA, and CDS2 tailing deposits.

Structure	pH	EC	CN Wad	Au	Cd	Hg	Mn	Zn	Pb	Cu	Fe	Ni	SO_4^{2-}	As	Sb	Co	
		$\mu\text{S}/\text{cm}$	mg/L	mg/L													
Cocoruto (CO)	Mean	6.90	2585	0.025	0.0250	0.0005	0.001	1.72	0.0125	0.012	0.015	0.9	0.03	1270.8	0.006	0.001	0.0005
	Max	8.67	4036	0.078	0.0250	0.0005	0.001	24.61	0.1000	0.061	0.224	6.1	0.42	5444.5	0.026	0.001	0.0005
	Min	6.08	1390	0.025	0.0250	0.0005	0.001	0.03	0.0100	0.005	0.004	0.1	0.01	33.3	0.005	0.001	0.0005
	SD	0.5867	877	0.0024	0.0000	0.0000	0.000	3.54	0.0133	0.016	0.034	1.2	0.06	892.3	0.004	0.000	0.0000
Calcinado (CA)	Mean	9.07	4402	28.9	0.0280	0.0005	0.001	0.10	0.1018	0.005	1285	0.2	0.39	1989.1	0.005	0.001	0.0005
	Max	10.44	6947	88.0	0.0800	0.0005	0.001	0.62	1.1000	0.028	46523	2.2	9.12	2820.4	0.005	0.001	0.0005
	Min	2.92	2367	6.0	0.0250	0.0005	0.001	0.01	0.0100	0.005	0.0	0.1	0.01	1337.1	0.005	0.001	0.0005
	SD	1.187	1065	14.50	0.0129	0.0000	0.000	0.14	0.2328	0.003	5698.7	0.4	1.32	355.7	0.000	0.000	0.0000
CDS2	Mean	7.32	3808	11.240	0.0408	0.0100	0.001	0.02	0.0104	0.107	19.3	0.1	1.94	2234.7	1.6	4.0	0.0100
	Max	8.03	4460	7.920	0.3000	0.0100	0.001	0.02	0.0159	0.191	20.7	0.4	2.62	3500.0	25.6	23.8	0.0100
	Min	6.66	3455	13.700	0.0250	0.0100	0.001	0.02	0.0050	0.040	14.1	0.0	0.01	1608.0	0.0	0.5	0.0100
	SD	0.3592	229	1.000	0.0519	0.0000	0.000	0.00	0.0040	0.053	1.6	0.1	1.10	687.5	6.2	5.1	0.0000

SD = standard deviation; Min – Minimum; Max – Maximum

The concentrations of metal(loids) are essential indicators for differentiating waters and classifying these structures [3]. According to [51], this differentiation can be expressed using the Ficklin diagram (Figure 3). In the studied structures, Co and Cd showed values close to the detection limits of the method, while the concentrations of Zn, Pb, Ni, and Cu were considerable and varied depending on the evaluated dam.

Sampled waters in Cocomoto are essentially classified as near-neutral low-metal. The waters from CDS2 belong to the near-neutral high-metal zones, while Calcinados exhibited distinct classifications, with 70% of the sampled points falling under near-neutral low-metal zones, and the remaining 30% falling under near-neutral extreme-metal zones. Only one point in Calcinados was classified as high-acid high-metal and will be disregarded.

(Tabela 5.30) **Table 2.** Correlation between the collected parameters for the three dams using Pearson Coefficient. Medium to strongest correlations are highlighted in blue ($r^2 > 0.25$).

	pH	EC μS/cm	Au	Cd	Mn	Zn	Pb	Fe	Cu	Ni	SO ₄ ²⁻	As	Sb
pH	1.00												
EC μS/cm	0.568	1.00											
Au	0.008	0.077	1.00										
Cd	-0.114	0.198	0.319	1.00									
Mn	-0.160	-0.125	-0.041	-0.140	1.00								
Zn	0.315	0.214	-0.035	-0.130	-0.034	1.00							
Pb	-0.122	0.193	0.292	0.903	-0.030	-0.140	1.00						
Fe	-0.114	-0.232	-0.046	-0.191	0.385	-0.026	-0.086	1.00					
Cu	0.275	0.099	-0.020	-0.068	-0.042	-0.021	-0.075	-0.061	1.00				
Ni	0.137	0.160	0.172	0.417	-0.086	-0.063	0.377	-0.134	0.747	1.00			
SO ₄ ²⁻	0.376	0.401	0.066	0.131	0.336	0.042	0.088	-0.175	0.143	0.227	1.00		
As	-0.032	0.013	-0.007	0.263	-0.026	-0.022	0.047	-0.039	-0.013	0.133	0.055	1.00	
Sb	-0.066	0.093	0.334	0.761	-0.091	-0.080	0.389	-0.125	-0.044	0.271	0.154	0.256	1.00

For Calcinados, the differences observed in Figure 3 have a direct relation to the Cu content and are associated with the location within the specific dam. In other words, the points classified as high-metal may be influenced by the discharge of effluents from the plant during a phase of low efficiency, changes in feed sources, or even alterations in the beneficiation process, such as the inclusion of other reagents that may contain this metal [36]. The maps in Figure 4 highlight zones with higher metal contents, especially Cu, Zn, Ni, and sulfates.

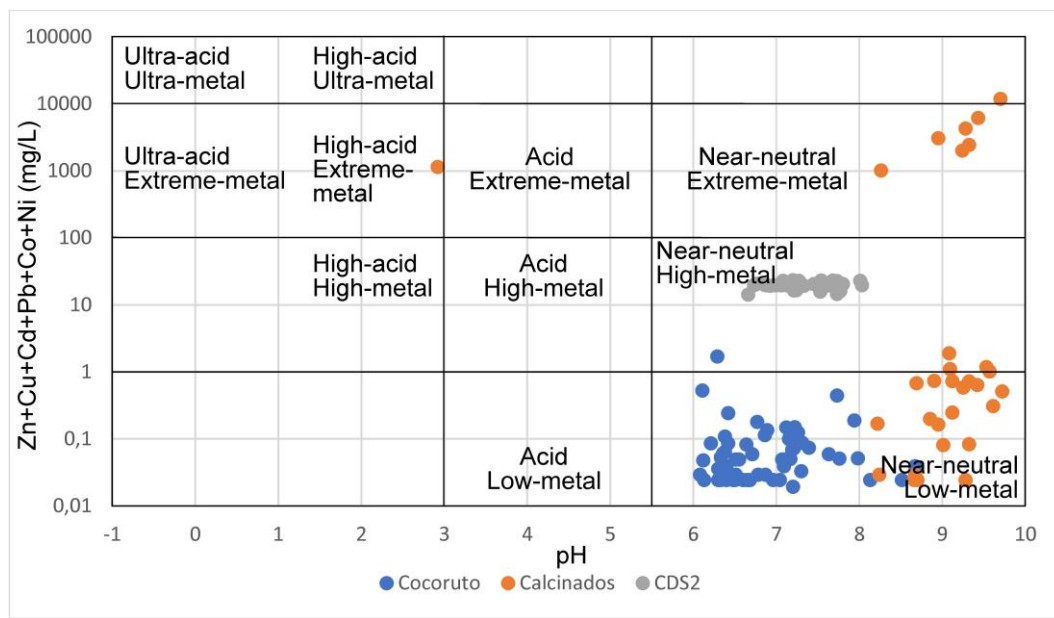
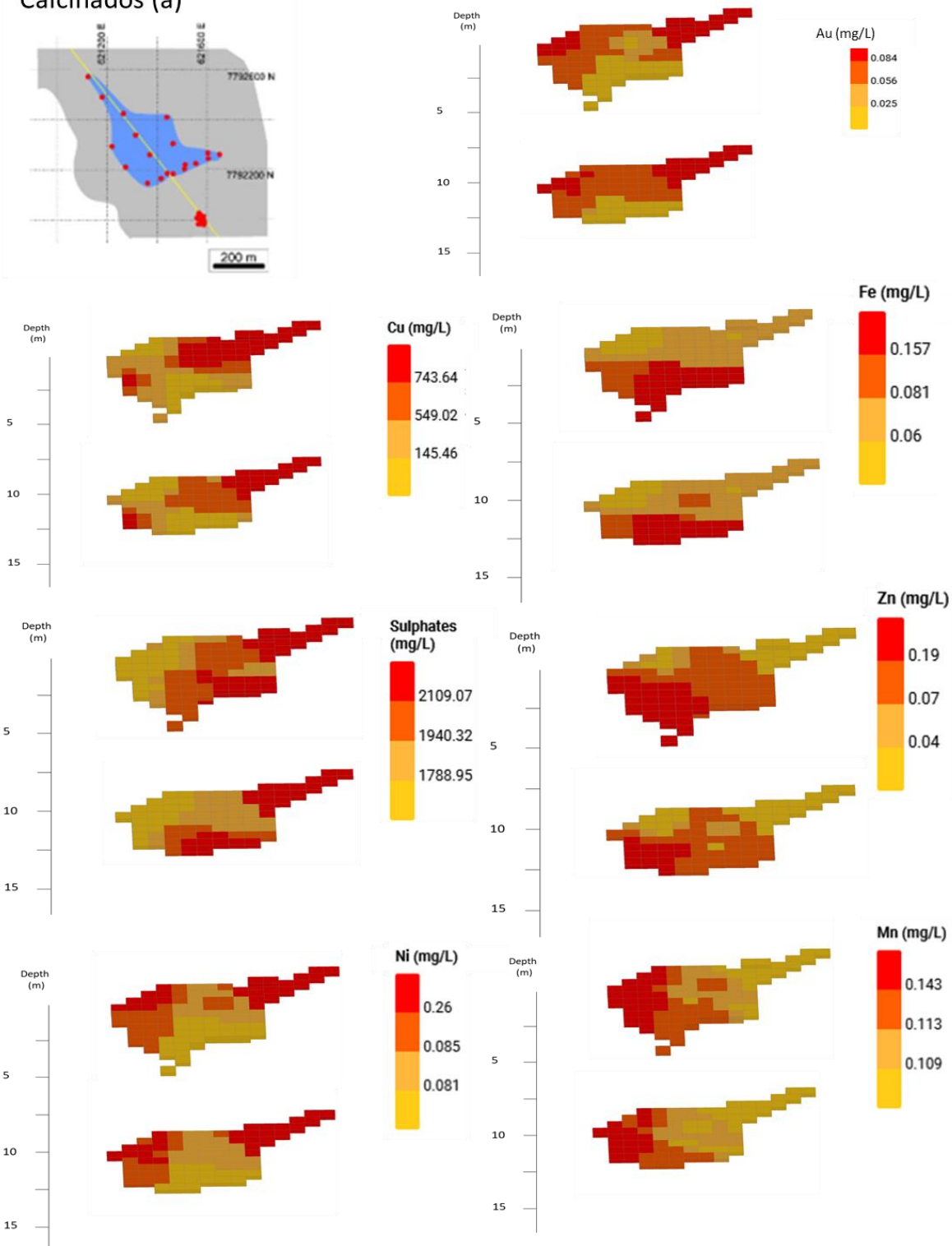


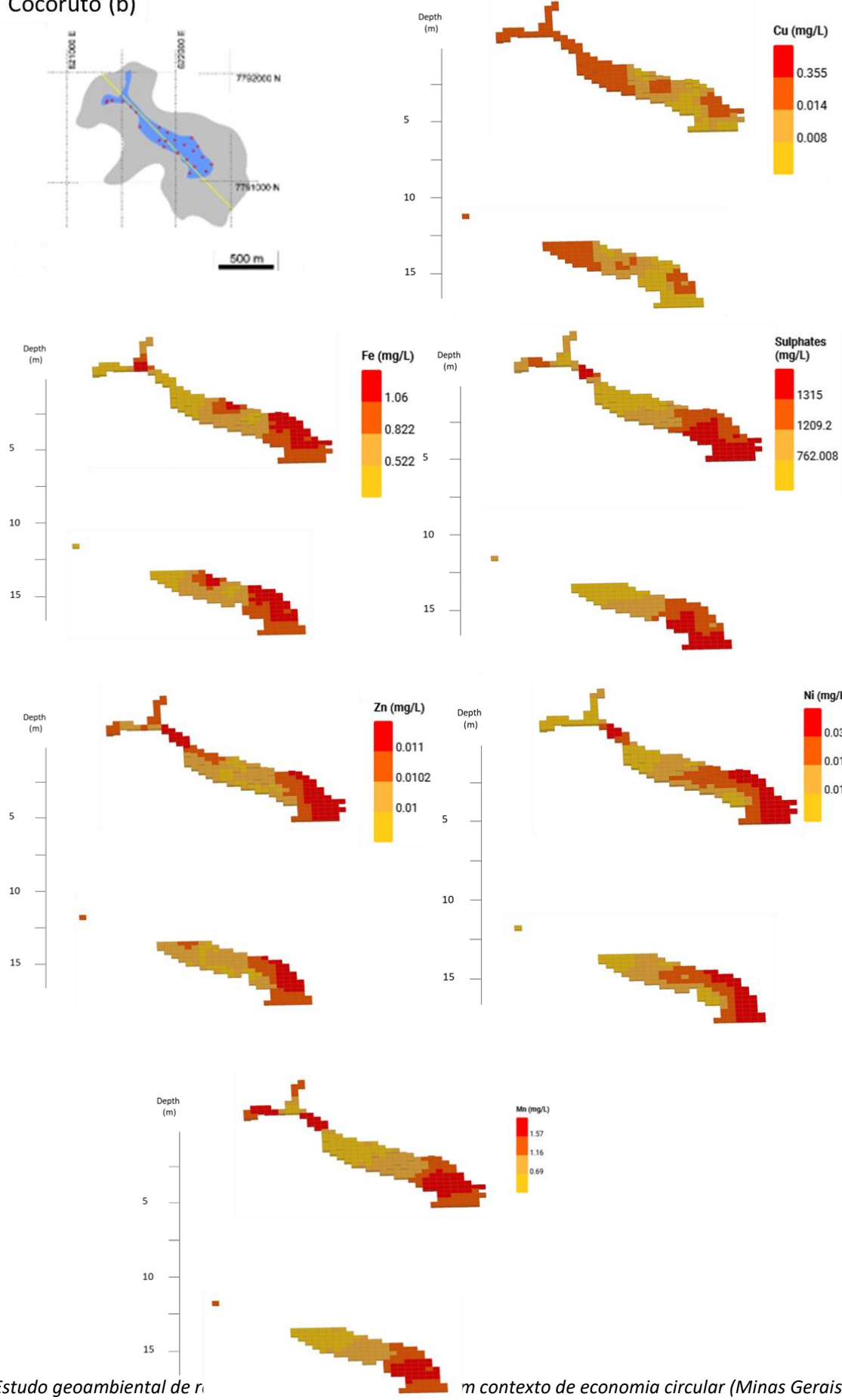
(Figura 5.47) **Figure 3.** Projection of the samples for the three dams according to the Ficklin Diagram.

In Figure 4, it is observed that in the Calcinados dam, spatially, the zones of water with higher concentrations of Cu, Au, Ni, and sulfates are correlated at depths between 0-10 and 10-20 m. This relationship is confirmed by Figure S2 and Table 2. In addition to this relationship, some sulfate-rich zones also show a correlation with Fe. On the other hand, Zn, Mn, and even in some parts Fe indicate enrichment in other portions of the dam (Figure 4, S2a), and their concentration increases in the interstitial waters as depth increases (Figure S3a). The relationship between the concentration of these elements and the depth may be due to the variation of physical parameters such as pH and EC (Figure S3a).

Calcinados-(a)



Cocoruto (b)



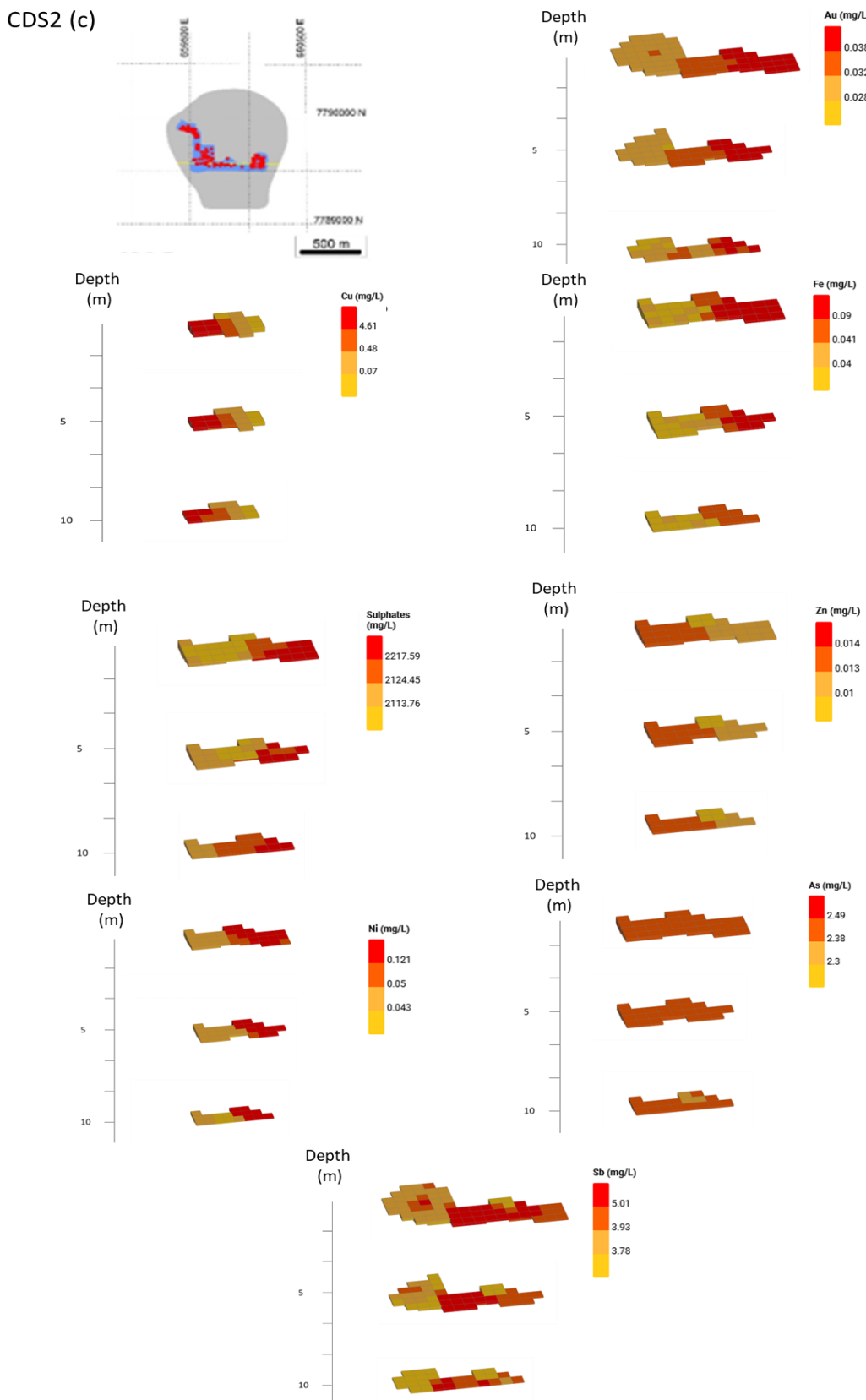


(Figura 5.48) **Figure 4.** 3D distribution of the concentrations of the main elements contained in the water of the three dams. (a) Calcinados, (b) Cocoruto and (c) CDS2.

In the Cocoruto dam, Au concentrations were below the detection limit, and it was not possible to generate a variability map of Au concentrations. Cu shows higher concentrations in the NW portion, up to depths of approximately 15 m, which may be related to the influences of reagents used in the plant (Figure 4) [43]. Zn is also concentrated in this region but in greater proportion in the SE part. Additionally, in Figure S2b, these elements exhibit a high Pearson coefficient, above 0,90. The other elements, although found in smaller zones of high concentration among Cu, have a greater extent in the opposite portion, near the dam spillway, and at lower elevations [42]. There is a clear relationship between Fe, Mn, and sulfates, which is also observed in the Pearson correlation matrix in Figure S2b and Table 2. Regarding variation vs depth, only Fe shows an enrichment relationship at greater depths (Figure S3b). This influence may be due to the treatment of ores rich in this element, especially in banded iron formations, which are rich in Fe-carbonates such as Siderite during the early years of operation of the older mines that supplied the metallurgical circuit [53; 36]. Furthermore, there is a clear variation with respect to decreasing pH and increasing EC in deeper regions of this dam (Figure S3b).

In the CDS2 dam, Mn concentrations did not show variation as they remained below the detection limit. Regarding the highest concentrations within the sampled region, there is a concentration relationship among all elements except for Zn, which contains some enrichment relationship by region and depth only with As (Figure 4 and Figure S2c). A clear positive correlation between sulfate and elements such as As and Fe is observed (Pearson coefficient of Fig S2c). The increase in Au concentration accompanies enrichments mainly with Sb and As (Table 2 and Figure S2c). The difference between these concentrations may be related to changes in ore types and even in the types of reagents used in the processing plant [41]. Moreover, the discharge of the plant effluent is not fixed, and this may also result in spatial differences in the distribution pattern of some soluble elements [42]. Regarding the variation of the elements with the depth of the dam, it is observed that the waters collected in the mid-depth portions (up to 8 m), are in general more enriched than at depth (Fig S3c). This pattern is not verified only for Zn and Fe, which also increase their concentration near 15 m. That is the availability of Fe sulfides and possibly Zn may be relatively high at depth. Furthermore, the environment is more prone to the dissolution of the same elements even at high pH and low EC variation (Figure S3b). This fact can be proven, as the beginning of the feeding of the processing plant in this region started with pyrite, ankerite, siderite, and magnetite-rich bodies with subordinate sphalerite to arsenopyrite and berthierite, which are the source of the current mineralization [39, 41].

4.2. Mineral-water interaction and enrichment factors

The mineral-water interaction analysis uses a set of physicochemical parameters considered relevant by the forms of occurrence, attributed toxicity, and the role they may play in the geochemical evolution of the system under study (Valente, 2004). In addition, the interactions between solids and water are also key to understanding and developing tools for the extraction and even reuse of soluble elements in this type of waters [41].

Figure 5 represents the average enrichment factor (Efx) between the water and the accumulated solids (<0.20 µm) in these dams. The solid waste characteristics are summarized in tables S1 and S2, and described in detail by [8], [36], and [41].

It is generally found that in relation to the solid fraction, the factors are low, but the accumulation of the elements Au, and total S in the effluents cannot be disregarded. In particular, the samples representing the “Cocoruto” are also enriched in Mn (Figure 5b), and the “Calcinados” in Cu, along with that shown by the CDS2 samples, as well (Figure 5a and c). The latter is also more enriched in Pb, Sb, and Ni.

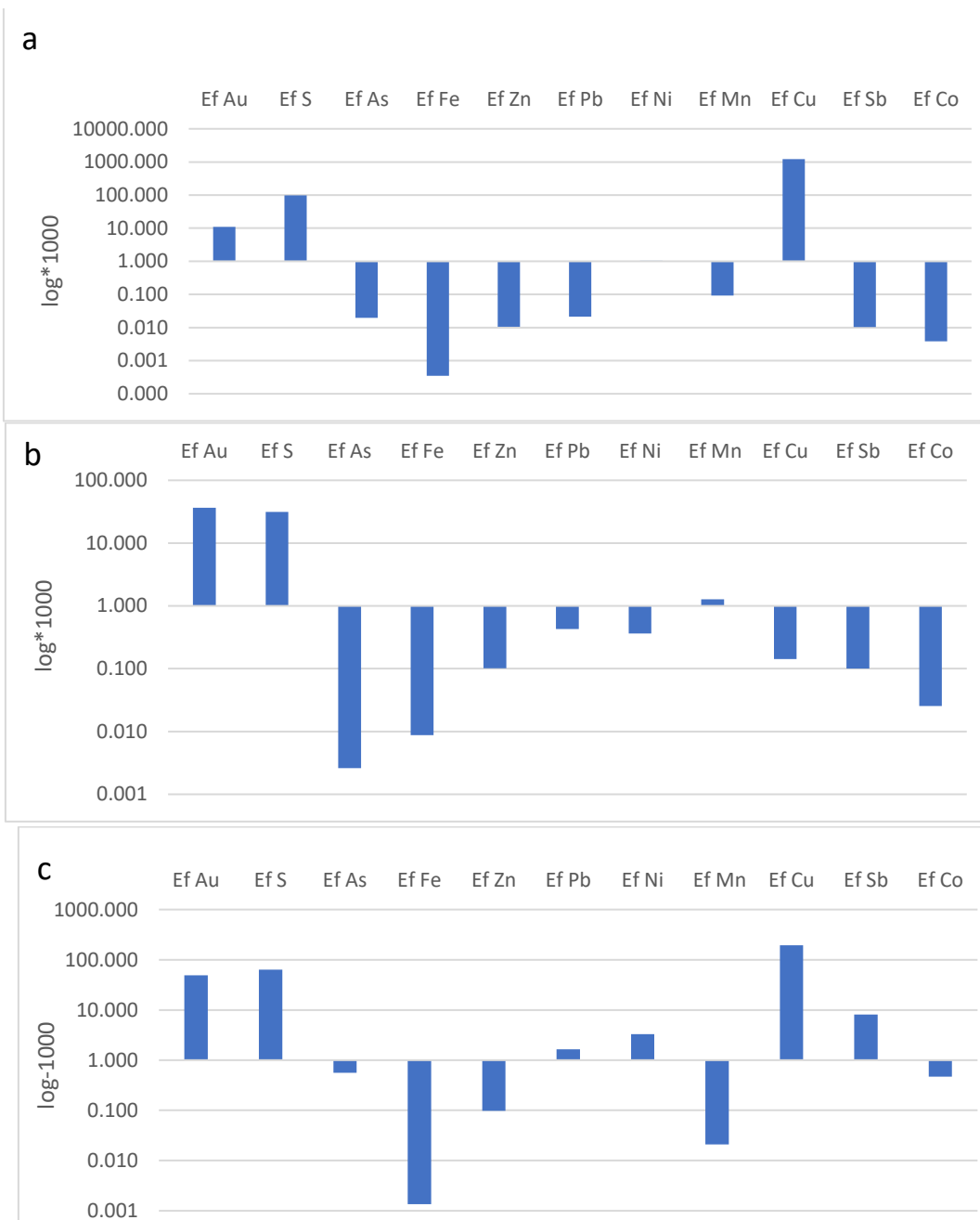
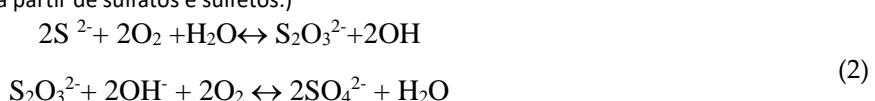


(Figura 5.49) **Figure 5.** Enrichment ratio of the liquid to solid fraction (Ef) in each tailing dam: Calcinados (a), Cocomuto (b) and CDS2 (c).

Considering the mineral-water interaction model, conceived by [54], the chemical composition of these effluents can be explained by two main factors: i) influence of mineral solubility, and ii) influence of surface interaction. Based on item i) and the pH conditions of these dams one can say that the S concentrations originated from sulfides and sulfates (table S1 – Eq 2). Besides these, reagents, such as Cu-sulfate, used in gold processing, may also contribute to this interaction.

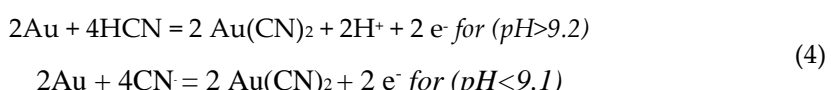
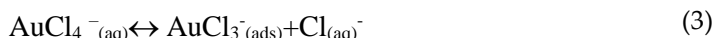
(Equação 2. Origem de S a partir de sulfatos e sulfetos.)



Other metals are also enriched in the three dams as is the case of Au, although it is a complex process with complementary needs and analyses to those presented here. If Au is in an aqueous medium as Au(III) or Au(I) complexed with Cl in the form of AuCl_4^- (Eq 3), for example, there is the possibility of being the result of complexation due to the mechanism of release of Cl ions from some source such as processing reagents (Valente, 2004). Also, the presence of Au in soluble form may be a result of beneficiation steps, since the effluents are discharged into the dam. This fact can be related to the presence of residual CN, according to Table 1, and the high pH conditions (Eq 4) [55].

(Equação 3. Fórmula de associação de Au e Cl em meios aquosos.)

(Equação 4. Influência de CN residual em sistemas com Au, para diferentes situações com alto pH.)



The environment of the three dams can be conducive to such a reaction if the eH is above 1 V or in the natural temperature and pressure conditions [39]. In fact, it is known that, in some cases, the beneficiation of Au ores undergoes oxidation, under pressure and temperature environments conducive to the formation of Au complexes with Cl and CN and, so, it becomes stable in aqueous medium under natural conditions [39]. However, further information needs to be evaluated for the conclusion of these hypotheses. In addition, there may be a large contribution of nano-sized Au, below 2 μm , released or adsorbed on other compounds also nanometric.

In the Cocoruto dam, the Efx factor of the Mn in the effluent, is also interesting and its main source is carbonates (Table S1). The mechanism of Mn ion availability can occur at pH close to 8 if the eH is between -0.2 to 0.4v [56]. The contribution of Mn-containing nanoparticles is also not ruled out.

Regarding the Cu and Ni factors, an Au-like mechanism can occur in these environments. The presence of residual CN in the dams or even during the beneficiation process can provide stable complexes in aqueous media such as $\text{Cu}(\text{CN})_3^{2-}$ and $\text{Ni}(\text{CN})_4$ [39]. The oxidation of sulfides in the tailings can also result in complexes containing Cu and Ni in water, since sulfides containing these elements are present, especially in the CDS2 dam. These sulfides, react with cyanide or other lixiviating agents such as Cl and F, causing reactions and stability of these in aqueous environment [39].

At the CDS2 dam, the influence of Sb in the groundwater samples was also observed. Specifically, in the case of this dam, the sources of the solids are a sulfide called berthierite (Table S1). The presence of this sulfide in an environment of high pH (above 9) and leachable such as CN, provides its stability in the soluble form [39]. Therefore, its presence is probably due to this mechanism.

4.3. Metal concentrations in tailing waters and the key to reuse

From the characteristics discussed above and the understanding of possible mechanisms, a strategy for metal extraction and water reuse in industrial environments is proposed here.

The water contained in these three dams is in active industrial environments. So, besides the possibility of extracting metals and metalloids in high concentrations, water can also be reused in metallurgical plants or even to supply administrative areas of the enterprise.

Therefore, alternatives will be presented that seek extraction in more sustainable ways, such as the use of biosorbents. The work presented by [57] used waters from these dams, characterized in the items above, and aimed to recover Au(III), Cu (II), Ni (II), and other metals using nanofibers of *Bixa orellana Linnaeus* (URU), a typical Brazilian plant with chelating properties. The nanofibers were prepared with polycaprolactone polymer (PCL) together with URU seed powder. The test was performed with pure solution, at pH 2, room temperature (25°C), and contact time of 24 h [58].

The results with water samples from these dams, according to Table 3 adapted from [58], show great potential for extraction in a sustainable way, especially for Au.

(Tabela 5.31) **Table 3:** Recovery results of Au and other metals after contact with nanofiber containing URU (adapted from [57] and [58]).

Element	Mean	Min %	Max	SD
Au(III)	75.898	84.35	58.726	6.043
Cu(II)	2.726	6.647	0.354	1.983
Ni (II)	2.099	4.614	0.045	1.419
Pb(II)	28.488	43.835	21.77	7.029
Zn(II)	4.274	7.09	2.294	1.447
Co (II)	4.299	7.889	1.083	2.252

The obtained results indicate that the PCL nanofibers containing Urucum have the potential to be applied in the recovery of strategic metals for the sustainability of these wastewaters. This approach may present countless possibilities for use, such as in the treatment of effluents and in other technological initiatives that can be developed, also motivated by the low cost. Furthermore, this system suggests the possibility of metal extraction and reuse of two types of resources (metals and water).

5. Conclusions

The present study characterized the wastewater found in three different tailings dams from the metallurgical treatment of Au ores.

Even though they were in the same region, QF, the waters showed to be distinct, with projections varying from neutral with high to low availability of metals according to the Ficklin Diagram classification. However, the concentration of some elements was not discarded, even in samples of low availability. These elements are Au, Ni, Cu, and S (mainly in the form of sulfates).

The distribution of these elements by the three structures and the mechanisms that govern mobility are key issues for their potential recovery. Moreover, in a study with these samples, using nanomembranes with seeds of *Bixa orellana Linnaeus*, a good recovery of these elements, especially Au, was obtained in a specific case with water from the CDS2 dam. The work is an example of recovery and cleaning of these waters in a sustainable way and at a low cost.

Therefore, the present research contributed or the potential reuse of strategic metals for the industry. Moreover, it showed the possibility to obtain water free of toxic elements or below the permitted by environmental regulations, allowing for a more sustainable management of water resources through the use of water from the mining tailings.

Supplementary Materials: The following supporting information can be downloaded at: www.mdpi.com/xxx/s1.

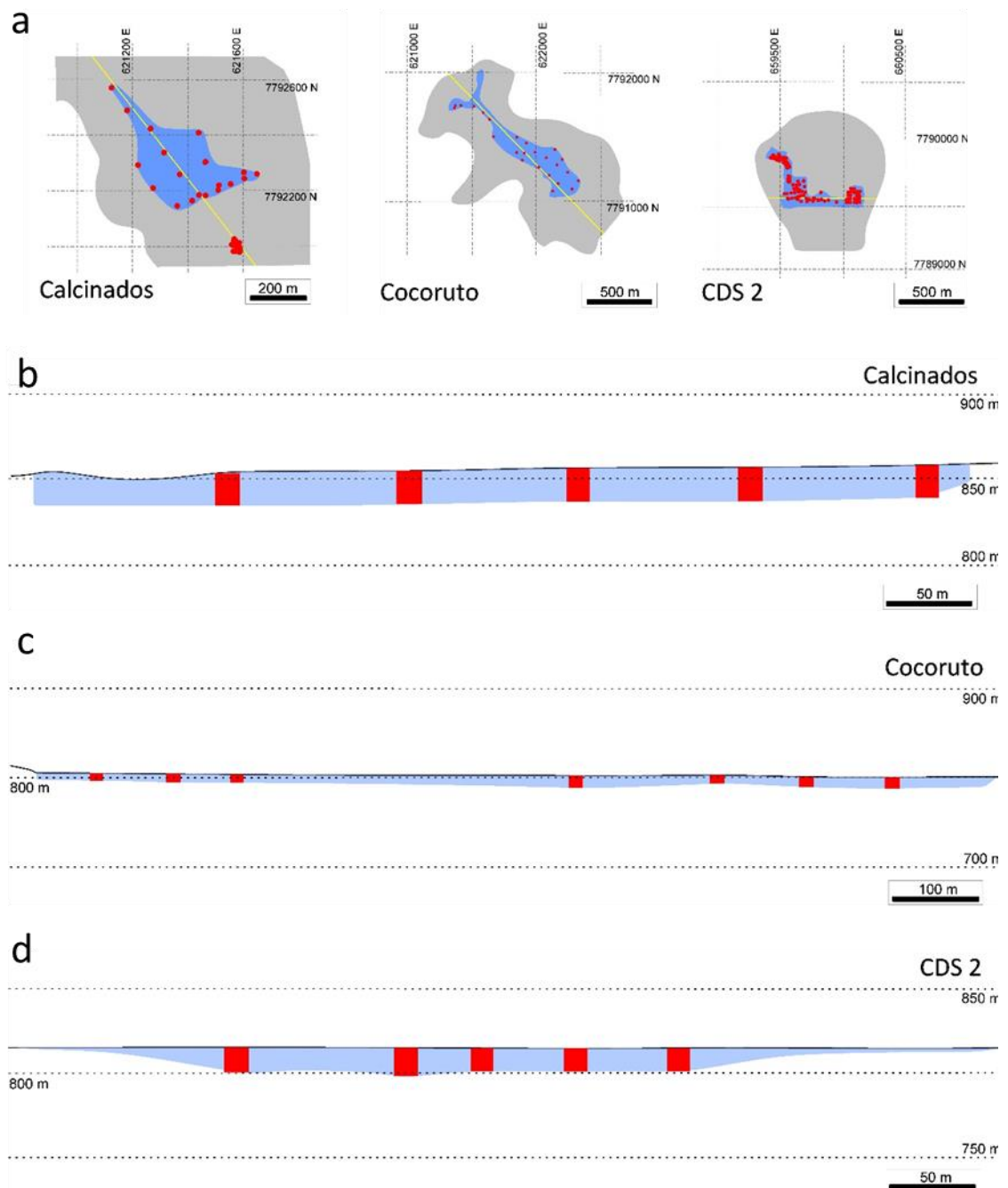


(Figura 5.50) **Figure S1.** (a) Location of sample points in plan and depth for each structure: (b) Calcínados, (c) Cocoruto, and (d) Santa Barbara.

RESULTADOS E DISCUSSÕES

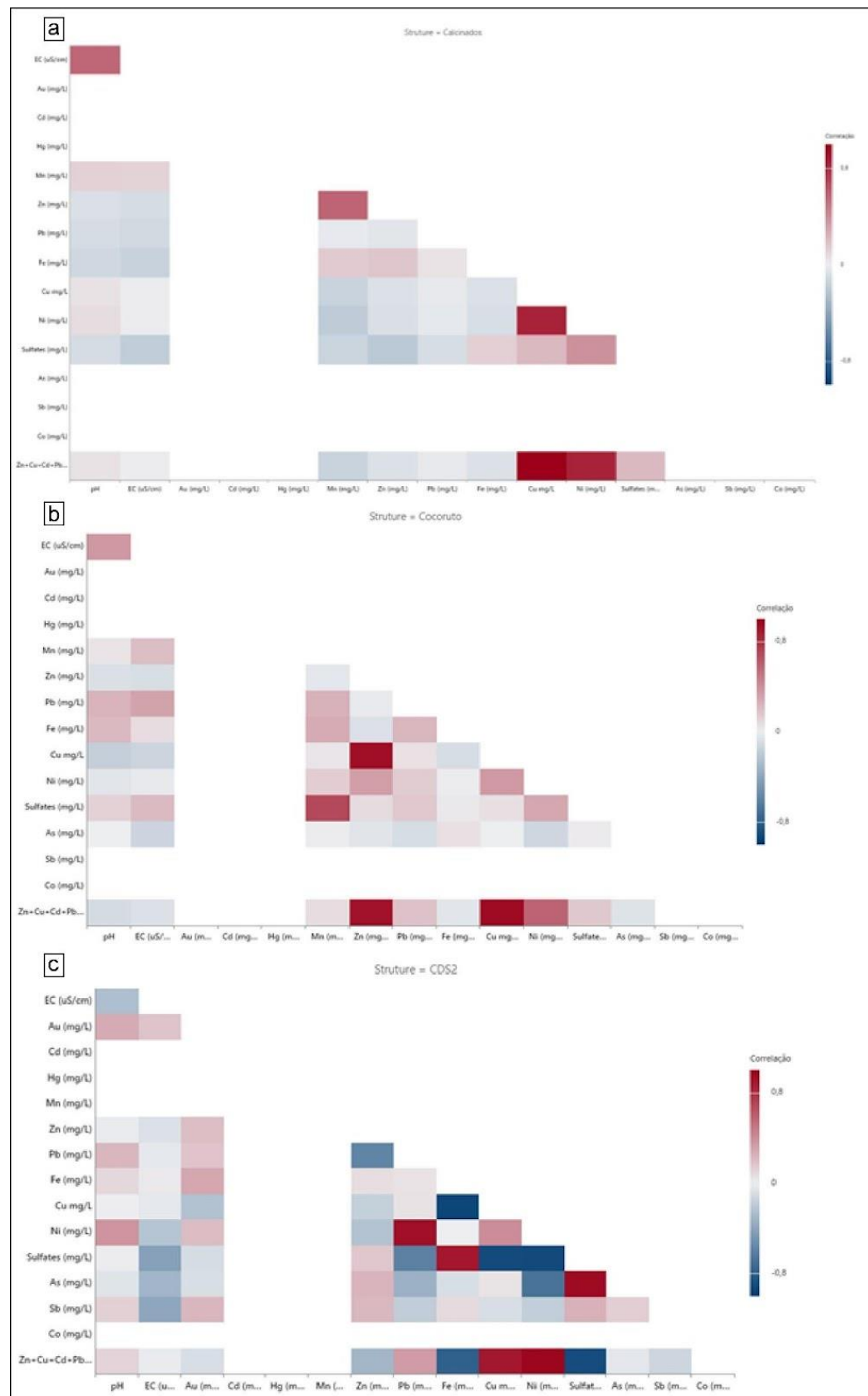


(Figura 5.51) **Figure S2.** Correlogram matrix of physicochemical variables of groundwater by structure: (a) Calcinados, (b) Cocoruto, and (c) CDS2.

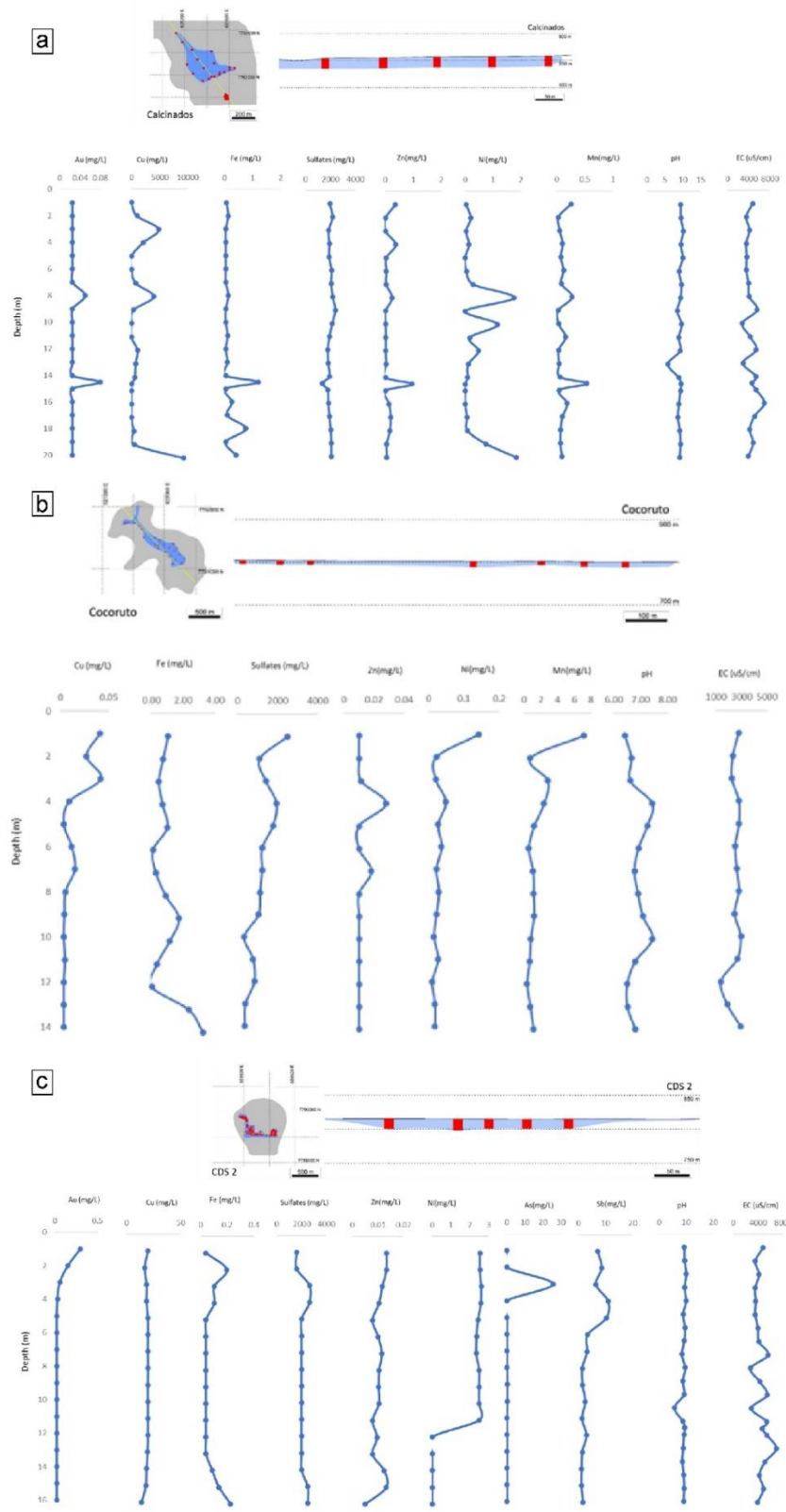


(Figura 5.52) **Figure S3.** Distribuition of elements by depth in struture: (a) Calcinados, (b) Cocoruto, and (c) Santa Barbara.

(Tabela 5.32) **Table S1.** Mineralogy of the solid fraction of the Calcinados, Cocoruto and CDS2 tailings dams – Adapted from Lemos et al. (2023).

Mineral	Chemical composition (Ideal Formula)	CA (Wt%)	CO (Wt%)	CDS2 (Wt%)
Quartz	SiO_2	15.6	55.8	35.6
Feldspar Group				
Albite	$\text{NaAlSi}_3\text{O}_8$	1.5	0.37	1.11
Anorthite	$\text{CaAl}_2\text{Si}_3\text{O}_8$	0.053	0.01	0.053
K feldspar	KAlSi_3O_8	-	0.39	1.27
Phyllosilicates				
Biotite	$\text{KMg}_{2.5}\text{Fe}_{2+0.5}\text{AlSi}_3\text{O}_{10}(\text{OH})_{1.75}\text{F}_{0.25}$	1	0.16	1.26
Muscovite	$\text{KAlSi}_3\text{O}_{10}(\text{OH})_{1.9}\text{F}_{0.1}$	12.8	5.69	29
Chlorite	$(\text{Mg},\text{Fe})_3(\text{Si},\text{Al})_2\text{O}_{10}(\text{OH})_2(\text{Mg},\text{Fe})_3(\text{OH})_6$	3.3	6.12	5.01
Oxides				
Hematite	Fe_2O_3	56.8	8.86	0.378
Fe antimoniate	$\text{FeSb}(\text{As})\text{O}$	-	-	0.806
Rutile/Anathase	TiO_2	0.599	0.49	0.599
Carbonates				
Ankerite	$\text{Ca}(\text{Fe},\text{Mg},\text{Mn})(\text{CO}_3)\text{O}_2$	1	11.2	9
Siderite	FeCO_3	-	7.25	7.2
Calcite	CaCO_3	0.2	2.25	5.4
Sulfates				
Jarosite (Sb)	$\text{KFe}(\text{SO}_4)_2(\text{OH})_6$ & $(\text{H}_2\text{O})\text{Fe}(\text{SO}_4)_2(\text{OH})_6$	-	-	1.00
Gypsum	$\text{CaSO}_4 \cdot 2\text{H}_2\text{O}$	7.00	0.03	2.00
Sulfides	Total	0.17	1.61	0.36
Pyrite	Fe_2S_2	0.002	0.5	0.08
Pyrrhotite	$\text{Fe}^{2+0.96}\text{S}$	0.004	0.79	0.041
Arsenopyrite	Fe^{3+}AsS	0.056	0.24	0.056
Berthierite	FeS_2S_1	-	-	0.141
Chalcopyrite	CuFeS_2	-	-	0.028
Gesdorffite	NiAsS	0.01	-	-
Covellite	CuS	0.1	0.07	-
Sphalerite	ZnS	-	0.01	0.009
Au Minerals*				
Au Content (mg/kg)		2.39	0.911	0.742
Native Au	Au>80%, Ag, Cu, Hg, Fe, Ni	526	364	158
Electrum	Au=80%, Ag=20%	42	10	6

* Au number particles. CA-Calcinados, CO-Cocoruto

(Tabela 5.33) **Table S2.** Statistical summary of the chemistry of the solid fractions of the Calcinados, Cocoruto and CDS2 tailings dams – Adapted from Lemos et al. (2023)

Structure	N ¹	Element	Mean	SD ²	Min ³	Max ⁴	N ¹	Element	Mean	SD ²	Min ³	Max ⁴
Calcinados	230		2.39	1.08	0.001	9.45	230		1.97	0.704	0	6.33
Cocoruto	282	Au (mg/Kg)	0.911	0.715	0.003	8.71	282	S (%)	3.47	1.93	0.02	9.47
CDS2	293		0.742	0.937	0.24	12.7	293		0.785	0.378	0.005	3.93
Calcinados	230		0.725	0.466	0.001	4.80	230		42.49	8.91	0.001	83.3
Cocoruto	282	As (%)	0.223	6.01	0.001	58.8	282	Fe (%)	12.42	2.9	2.42	15
CDS2	293		0.093	0.095	0.001	0.657	293		4.12	2.2	0.86	16.4
Calcinados	230		241	64.4	0.1	383	230		3213	1100	0	6187
Cocoruto	282	Pb (mg/Kg)	46	22.4	4	46	282	Zn (mg/Kg)	187	327	5	3419
CDS2	293		69.6	28.2	16	171	293		113	30.7	75	313
Calcinados	230		494	123	10	744	230		0.097	0.021	0.004	0.17
Cocoruto	282	Ni (mg/Kg)	103	38.7	49	243	282	Mn (%)	0.281	0.067	0.01	0.42
CDS2	293		241	64.4	10	383	293		0.097	0.009	0.08	0.12
Calcinados	230		0.104	0.184	0.001	0.988	230		0.004	0.008	0.001	0.059
Cocoruto	282	Cu (%)	0.019	0.018	0.001	0.266	282	Sb (%)	0.003	0	0.003	0.003
CDS2	293		0.01	0.008	0.001	0.04	293		0.104	0.184	0.001	0.988
Calcinados	230		132	35.8	0.10	195						
Cocoruto	282	Co (mg/Kg)	19.6	11.7	4	76						
CDS2	293		21.4	6.22	4	42						

Author Contributions: M.G.L., T.M.V., A.P.M.R., R.M.F.F., F.G., J.G.d.M.F., and M.F.M.; methodology, M.G.L., T.M.V., A.P.M.R., A.R.S R.M.F.F., F.G., J.G.d.M.F., A.S.B., and M.F.M.; software, M.G.L. and I.D.D.; validation, M.G.L., T.M.V., A.P.M.R., R.M.F.F., F.G., J.G.d.M.F., M.F.M., and I.D.D.; formal analysis, M.G.L., T.M.V., A.P.M.R., R.M.F.F., F.G., J.G.d.M.F., M.F.M., and I.D.D.; investigation, M.G.L., T.M.V., A.P.M.R., R.M.F.F., F.G., J.G.d.M.F., M.F.M., and I.D.D.; resources, M.G.L., T.M.V., A.P.M.R., R.M.F.F., F.G., J.G.d.M.F., and M.F.M.; data curation, M.G.L., T.M.V., A.P.M.R., and R.M.F.F.; writing—original draft preparation, M.G.L., A.P.B; writing—review and editing, M.G.L., T.M.V., A.P.M.R., R.M.F.F., and G.R.D.; visualization, M.G.L., T.M.V., A.P.M.R., R.M.F.F., and G.R.D.; supervision, T.M.V., A.P.M.R., and R.M.F.F.; project administration, M.G.L., T.M.V., A.P.M.R., R.M.F.F., F.G., J.G.d.M.F., and M.F.M.; funding acquisition,

M.G.L., T.M.V., A.P.M.R., R.M.F.F., F.G., J.G.d.M.F., and M.F.M. All authors have read and agreed to the published version of the manuscript.

Funding: This research was funded by Fundação para a Ciência and Tecnologia (FCT) through projects UIDB/04683/2020, UIDP/04683/2020, and Nano-MINENV 029259 (PTDC/CTA-AMB/29259/2017).

Data Availability Statement: The data presented in this study are available upon request from the corresponding author. The data are not publicly available due to high amounts of data.

Acknowledgments: We thank our colleagues from the Instituto de Ciências da Terra (ICT), the Microscopy Center from Universidade Federal de Minas Gerais (CM-UFMG), and from AngloGold Ashanti, who provided insights and expertise that greatly assisted this research; Fundação para a Ciência and Tecnologia (FCT) for financial aid; and Dr Vanessa Soares for laboratory support and reuse tests using nanofibers.

Conflicts of Interest: The authors declare no conflict of interest.

References

1. Lowry. G. V.; Shaw. S.; Kim. C. S.; Rytuba. J. J.; Brown. G. E. Macroscopic and microscopic observations of particle-facilitated mercury transport from New Idria and Sulphur Bank mercury mine tailings. *Environmental Science & Technology* 2004. 38(19). 5101-5111. <https://doi.org/10.1021/es034636c>
2. Ma. J.; Lei. M.; Weng. L.; Li. Y.; Chen. Y.; Islam. M. S.; Zhao. J.; Chen. T. Fractions and colloidal distribution of arsenic associated with iron oxide minerals in lead-zinc mine-contaminated soils: Comparison of tailings and smelter pollution. *Chemosphere* 2019. 227. 614-623. <https://doi.org/10.1016/j.chemosphere.2019.04.030>
3. Moreno. F.; Valente. T. M. F.; Gomes. P.; Fonseca. R.; Costa. M. R.; Costa. A. Partitioning of potentially toxic elements among two colloidal fractions and relevance for their mobility in different water types. In Proceedings of the 16th International Symposium on Water-Rock Interaction (WRI-16) and 13th International Symposium on Applied Isotope Geochemistry (1st IAGC International Conference). Tomsk. Russia. 2019 (21-26 July 2019). <https://doi.org/10.1051/e3sconf/20199809020>
4. Jackson. L. M.; Parbhakar-Fox. A. Mineralogical and geochemical characterization of the Old Tailings Dam. Australia: Evaluating the effectiveness of a water cover for long-term AMD control. *Applied Geochemistry* 2016. 68. 64-78. <https://doi.org/10.1016/j.apgeochem.2016.03.009>
5. Martínez. J.; Hidalgo. M. C.; Rey. J.; Garrido. J.; Kohfahl. C.; Benavente. J.; Rojas. D. A multidisciplinary characterization of a tailings pond in the Linares-La Carolina mining district. Spain. *Journal of Geochemical Exploration* 2016. 162. 62-71. <https://doi.org/10.1016/j.gexplo.2015.12.013>
6. Araujo. F. S.; Taborda-Llano. I.; Nunes. E. B.; Santos. R. M. Recycling and reuse of mine tailings: A review of advancements and their implications. *Geosciences* 2022. 12(9). 319. <https://doi.org/10.3390/geosciences12090319>
7. Cacciuttolo. C.; Cano. D. Environmental Impact Assessment of Mine Tailings Spill Considering Metallurgical Processes of Gold and Copper Mining: Case Studies in the Andean Countries of Chile and Peru. *Water* 2022. 14(19). 3057. <https://doi.org/10.3390/w14193057>.
8. Lemos. M.; Valente. T.; Reis. P. M.; Fonseca. R.; Pantaleão. J. P.; Guabiroba. F.; Filho. J.G.; Magalhães. M.; Afonseca. B.; Silva. A.R.; Delbem. I. Geochemistry and mineralogy of auriferous tailings deposits and their potential for reuse in Nova Lima Region. Brazil. *Scientific Reports* 2023. 13(1). 4339. <https://doi.org/10.1038/s41598-023-31133-6>
9. Acheampong. M. A.; Adiyiah. J.; Ansa. E. D. O. Physico-chemical characteristics of a gold mining tailings dam wastewater. *Journal of Environmental Science and Engineering* 2013. A2(8A). 469-475.
10. Economopoulos. A.P. Assessment of Sources of air, water and soil pollution: a guide to rapid source inventory techniques and their use in formulating environmental control strategies. World Health Organization: Geneva. Switzerland. 1993; 230p.
11. Puls, Robert W., and Robert M. Powell. "Transport of inorganic colloids through natural aquifer material: Implications for contaminant transport." *Environmental Science & Technology* 26.3 (1992): 614-621.
12. Maharajh. D.; Grewar. T.; Neale. J.; van Rooyen. M. Mine Water: A Resource for the Circular Economy in South African Mining Communities. In Proceedings of the Mine Water Solutions. Vancouver. Canada. 349-362 (12-16 June 2018).
13. Stevanović, Zoran, et al. "Mine waste water management in the Bor municipality in order to protect the Bor River water." Waste water—treatment technologies and recent analytical developments. InTech (2013): 41-62.
14. Wastewater Characterization Study. TRC Environmental Corporation. Available online: https://www.ibwc.gov/Files/Characterization_Study_March_2015.pdf (accessed on 06 06 2023)
15. Luc Leroy, M. N., Jacques Richard, M., Mouhamed, A. N., Sifeu, T. K., Reynolds Yvan, A. S., & Said, R. (2020). Physicochemical characterization of mining waste from the Betare-Oya gold area (East Cameroon) and an adsorption test by Sabga smectite (North-West Cameroon). *Scientifica*, 2020.

16. Etteieb, Selma, et al. "Monitoring and analysis of selenium as an emerging contaminant in mining industry: A critical review." *Science of the Total Environment* 698 (2020): 134339.
17. Dippong, Thomas, et al. "Chemical modeling of groundwater quality in the aquifer of Seini town–Someş Plain, Northwestern Romania." *Ecotoxicology and environmental safety* 168 (2019): 88-101.
18. Rostami, Ali Asghar, et al. "Evaluation of geostatistical techniques and their hybrid in modelling of groundwater quality index in the Marand Plain in Iran." *Environmental Science and Pollution Research* 26 (2019): 34993-35009.
19. Rashid, Abdur, et al. "Groundwater Quality, Health Risk Assessment, and Source Distribution of Heavy Metals Contamination around Chromite Mines: Application of GIS, Sustainable Groundwater Management, Geostatistics, PCAMLR, and PMF Receptor Model." *International Journal of Environmental Research and Public Health* 20.3 (2023): 2113.
20. Nas, B. "Geostatistical Approach to Assessment of Spatial Distribution of Groundwater Quality." *Polish Journal of Environmental Studies* 18.6 (2009).
21. Naranjo-Fernández. N.; Guardiola-Albert. C.; Montero-González. E. Applying 3D geostatistical simulation to improve the groundwater management modelling of sedimentary aquifers: The case of Doñana (Southwest Spain). *Water* 2018. 11(1). 39. <https://doi.org/10.3390/w11010039>
22. França. S. C.; Andrade. L. S.; Loayza. P. E.; Trampus. B. C. Water in mining—challenges for reuse. In Proceedings of the 13th International Mine Water Association Congress – Mine Water & Circular Economy. Lappeenranta. Finland. 2017 (25–30 June 2017).
23. Semenkov. I.; Sharapova. A.; Lednev. S.; Yudina. N.; Karpachevskiy. A.; Klink. G.; Koroleva. T. Geochemical partitioning of heavy metals and metalloids in the ecosystems of abandoned mine sites: a case study within the Moscow Brown Coal Basin. *Water* 2022. 14(1). 113. <https://doi.org/10.3390/w14010113>
24. Domingues. A.F.; Boson. P.H.G.; Alípaz. S. Water Resource Management and the Mining Industry; Agência Nacional de Águas. Instituto Brasileiro de Mineração: Brasília. Brazil. 2013; 336p.
25. Dang. H. T.; Tran. H. D.; Tran. N. T.; Tran. A. H.; Sasakawa. M. Potential reuse of coal mine wastewater: a case study in Quang Ninh. Vietnam. In Proceedings of the 37th WEDC International Conference. Hanoi. Vietnam. 2014 (15-19 September 2014)
26. Huertas, E., et al. "Key objectives for water reuse concepts." *Desalination* 218.1-3 (2008): 120-131.
27. Meng. S.; Wen. S.; Han. G.; Wang. X.; Feng. Q. Wastewater treatment in mineral processing of non-ferrous metal resources: a review. *Water* 2022. 14(5). 726. <https://doi.org/10.3390/w14050726>
28. Zhang. C.; Wen. L.; Wang. Y.; Liu. C.; Zhou. Y.; Lei. G. Can constructed wetlands be wildlife refuges? A review of their potential biodiversity conservation value. *Sustainability* 2020. 12(4). 1442. <https://doi.org/10.3390/su12041442>
29. Rajpar. M. N.; Ahmad. S.; Zakaria. M.; Ahmad. A.; Guo. X.; Nabi. G.; Wanghe. K. Artificial wetlands as alternative habitat for a wide range of waterbird species. *Ecological Indicators* 2022. 138. 108855. <https://doi.org/10.1016/j.ecolind.2022.108855>
30. Mohapatra. D. P.; Kirpalani. D. M. Process effluents and mine tailings: sources. effects and management and role of nanotechnology. *Nanotechnology for Environmental Engineering* 2017. 2. 1-12. <https://doi.org/10.1007/s41204-016-0011-6>
31. Araya, Natalia, et al. "Feasibility of re-processing mine tailings to obtain critical raw materials using real options analysis." *Journal of Environmental Management* 284 (2021): 112060.
32. Atlagić, Suzana G., et al. "Recent Patents in Reuse of Metal Mining Tailings and Emerging Potential in Nanotechnology Applications." *Recent Patents on Nanotechnology* 15.3 (2021): 256-269.
- Moreira. V. R.; Lebron. Y. A. R.; Gontijo. D.; Amaral. M. C. S. Membrane distillation and dispersive solvent extraction in a closed-loop process for water, sulfuric acid and copper recycling from gold mining wastewater. *Chemical Engineering Journal* 2022. 435. 133874. <https://doi.org/10.1016/j.cej.2021.133874>
33. Reis. B.G. Toward High Temperature and Low pH Gold Mining Effluent Reclamation by Different Membrane Separation Processes. Doctorate Thesis. Universidade Federal de Minas Gerais. Belo Horizonte. 2018.
34. Urkiaga, A., et al. "Development of analysis tools for social, economic and ecological effects of water reuse." *Desalination* 218.1-3 (2008): 81-91.
35. Lemos. M.; Valente. T.; Reis. P. M.; Fonseca. R.; Delbem. I.; Ventura. J.; Magalhães. M. Mineralogical and geochemical characterization of gold mining tailings and their potential to generate acid mine drainage (Minas Gerais. Brazil). *Minerals* 2020. 11(1). 39. <https://doi.org/10.3390/min11010039>
36. Goldfarb. R. J.; Groves. D. I.; Gardoll. S. Orogenic gold and geologic time: a global synthesis. *Ore Geology Reviews* 2001. 18(1-2). 1-75. [https://doi.org/10.1016/S0169-1368\(01\)00016-6](https://doi.org/10.1016/S0169-1368(01)00016-6)
37. Lobato. L. M.; Ribeiro-Rodrigues. L. C.; Vieira. F. W. R. Brazil's premier gold province. Part II: geology and genesis of gold deposits in the Archean Rio das Velhas greenstone belt. *Quadrilátero Ferrífero. Mineralium Deposita* 2001. 36. 249-277. <https://doi.org/10.1007/s001260100180>

38. Pereira, Márcio Salgado. "Avaliação dos produtos de oxidação e ocorrência do efeito preg-robbing da oxidação sob pressão em autoclave de bancada e industrial para o minério sulfetado da Mina I de Córrego do Sítio, Minas Gerais." (2020).
39. Magalhães. M. F. Utilização de simulação de elementos discretos (DEM) para avaliação de parâmetros da teoria da amostragem Doctorate Thesis. Universidade de São Paulo. São Paulo. 2022.
40. Lemos. M. G.; Valente. T. M. F.; Reis. A. P.M.; Fonseca. R.; Dumont. J. M.; Ferreira. G. M. M.; Delbem. I. D. Geoenvironmental study of gold mining tailings in a circular economy context: Santa Barbara. Minas Gerais. Brazil. Mine Water and the Environment 2021. 40. 257–269. <https://doi.org/10.1007/s10230-021-00754-6>
41. AGA. 2021. AngloGold Ashanti AngloGold Ashanti recommendations.
42. Moura. W. Especiação de Cianeto para Redução do Consumo no Circuito de Lixiviação de Calcinado da Usina do Queiróz. Master Thesis. Universidade Federal de Minas Gerais. Belo Horizonte. 2005
43. IBGE, 2023. Instituto Brasileiro de Geografia e EstatísticaURL <https://www.ibge.gov.br/023>
44. APHA - American Public Health Association (2005) Standard method for examination of water and wastewater, 21st edit. AWWA,WPCF, Washington DC
45. Gomes, P.F. S.S. "Impactos dos processos de drenagem ácida na qualidade ambiental e acumulação potencial de metais estratégicos em barragens localizadas na Faixa Piritosa Ibérica." (2021).
46. Acosta, Jl A., et al. "Distribution of metals in soil particle size fractions and its implication to risk assessment of playgrounds in Murcia City (Spain)." Geoderma 149.1-2 (2009): 101-109.
47. Wilson, R., Toro, N., Naranjo, O., Emery, X. & Navarra, A. Integration of geostatistical modeling into discrete event simulation for development of tailings dam retreatment applications. Miner. Eng. 164, 106814. <https://doi.org/10.1016/j.mineng.2021.106814> (2021).
48. Dinپashoh, Y., et al. "Impact of climate change on potential evapotranspiration (case study: west and NW of Iran)." Theoretical and Applied Climatology 136 (2019): 185-201.
49. Bazar, Seyed Mostafa, Yagob Dinپashoh, and Vijay P. Singh. "Sensitivity analysis of the reference crop evapotranspiration in a humid region." Environmental Science and Pollution Research 26 (2019): 32517-32544.
50. Gomes, Patrícia, et al. "Hydrochemistry of pit lakes in the Portuguese sector of the Iberian Pyrite Belt." E3S Web of Conferences. Vol. 98. EDP Sciences, 2019.
51. CONSELHO NACIONAL DO MEIO AMBIENTE (Brasil). Resolução, nº 357, de 17 de março de 2005. Dispõe sobre a classificação dos corpos de água e diretrizes ambientais para o seu enquadramento, bem como estabelece as condições e padrões de lançamento de efluentes, e dá outras providências, Diário Oficial da União, Brasília, DF, 17 mar. 2005.
52. Junqueira, P. A., et al. "Structural control and hydrothermal alteration at the BIF-hosted Raposos lode-gold deposit, Quadrilátero Ferrífero, Brazil." Ore Geology Reviews 32.3-4 (2007): 629-650.
53. Valente, Teresa Maria Fernandes. "Modelos de caracterização de impacte ambiental para escombeiras reactivas: equilíbrio e evolução de resíduos de actividade extractiva." (2004).
54. Deschamps, Eleonora, et al. "Soil and sediment geochemistry of the iron quadrangle, Brazil the case of arsenic." Journal of soils and sediments 2 (2002): 216-222.
55. Krauskopf, Konrad B. "Separation of manganese from iron in sedimentary processes." Geochimica et Cosmochimica Acta 12.1-2 (1957): 61-84.
56. Soares, V.A.A P. "Recuperação de metais estratégicos au (iii), ag (i), pt (iv) e pd (ii) de barragens de rejeito e lixo eletrônico com o uso de nanotecnologia e urucum visando tecnologias sustentáveis: uma proposta translacional." (2022).
57. Rubén Dario Sinisterra Millan / Roberto Galery / Letícia Malta Costa / Cláudia Carvalhinho Windmoeller / Vanessa Aparecida Alves de Paula Soares / Antônio Gustavo Novais Diniz / Victoria Silva Amador. Processo para tratamento de efluentes e recuperação de metais nobres com uso de sementes de Bixa orellana Linnaeus - BR1020210263202A

Disclaimer/Publisher's Note: The statements, opinions and data contained in all publications are solely those of the individual author(s) and contributor(s) and not of MDPI and/or the editor(s). MDPI and/or the editor(s) disclaim responsibility for any injury to people or property resulting from any ideas, methods, instructions or products referred to in the content.

5.1.5. *Pre feasibility* para o reprocessamento do Au

Baseado em todos os dados coletados, um estudo de análise de sensibilidade e um estudo de pré viabilidade foram desenvolvidos para o reprocessamento de Au da barragem de Cocoruto. A escolha desta barragem como caso de estudo fundamentou-se no volume de rejeitos e teores, além dos potenciais impactos socioeconômicos para população da região.

Portanto, o artigo, *Sensitivity analysis and pre-feasibility of reprocessing Au from a tailings dam in the Iron Quadrangle - The case of Cocoruto Dam, Nova Lima, Minas Gerais*, submetido na revista *REM-International Engineering Journal*, demonstra como o valor do reprocessamento de Au é relevante e o ganho de oportunidades para empreendimento. Um modelo com visão ESG mostra-se ser viável, além de sustentável.

No momento da entrega desta tese, o referido artigo, que se apresenta em seguida, encontra-se em fase de revisão.

Sensitivity analysis and pre-feasibility of reprocessing Au from a tailings dam in the Iron Quadrangle - The case of Cocoruto Dam, Nova Lima, Minas Gerais

Mariana Gazire Lemos, Paulo Henrique da Silva Lack, Teresa Maria Valente, Amélia Paula Marinho Reis, Amália Sequeira Braga, Rita Maria Ferreira Fonseca, Fernanda Guabiroba, José Gregorio da Mata Filho, Marcus Felix Magalhães, Giovana Rebelo Diório.

Abstract: As historical waste has accumulated in dams, the interest in studying the feasibility of reusing mining tailings has increased, yielding environmental and economic benefits. However, since each site has unique characteristics, it is crucial to conduct site-specific assessments. After a previously detailed evaluation of the Cocoruto Dam in Nova Lima, Minas Gerais, this study aims to showcase technical feasibility and financial viability modeling analysis conducted considering three scenarios for potential reuse. Thus, the main objective was to determine the viability and potential benefits of reusing the Au tailings. The employed setups involved grinding, leaching, and calcination, designed to be adaptable and applicable to existing metallurgical plants. Considering the economic potential of Au present in this inactive mine tailing structure (average grade of 0.95 mg/kg and a total resource of 3,350.55 tonnes), multiple factors were analyzed to see the feasibility of Au production using it as a source. Analyzed variables included: cut-off grades and tonnage for each scenario, net present value (NPV) calculated by a discount rate of 8% per year, a general slope angle of 20 degrees, three possible final pits, different annual productions (400,000 t, 800,000 t and 1,000,000 t), and diverse values of Au ounce (\$1300/oz, \$1500/oz, and \$1700/oz). From a financial perspective, for all ounce values and an annual production of 400 tonnes, all scenarios prove profitable, even though other risks and settings should be further evaluated.

Keywords: circular economy; mining tailings; Au recovery; Benefit Function; feasibility

1. Introduction

Historically, tailings have been stored in tailings dams or impoundments, which can pose environmental risks such as water pollution, habitat destruction, and the potential for dam failures (Coffey *et al.*, 2021; Araya *et al.*, 2021; Lemos *et al.*, 2023b), as the recent tragedies in Brumadinho and Mariana, Brazil (Lemos *et al.*, 2021). However, due to containing significant amounts of critical elements in terms of supply and toxicity, there has been increasing interest in finding ways to reuse or reprocess mining tailings to minimize their environmental impact and extract additional value from them (Malli *et al.*, 2015; Lemos *et al.*, 2021).

The feasibility of tailings reuse can vary significantly between mining operations due to site-specific considerations. As they often contain a mixture of fine particles, water, and chemicals used in the extraction process, reprocessing tailings can be challenging. Therefore, conducting a site-specific assessment is crucial to determine the viability and suitability of tailings reuse. When conducting such a multidisciplinary study, several key factors should be considered to ensure a comprehensive evaluation, including ore type, processing methods, tailings characterization, environmental assessment, suitable technologies for reprocessing, local regulations, and economic analysis. Moreover, evaluating market conditions and demand and risk assessments to define a financial model for reprocessing these types of structures with potential profitability are critical issues (Hindle, 2011; Hitch & Dipple, 2012; Pang *et al.*, 2012; Rendu, 2014; Suppes & Heuss-Aßbichler, 2021).

The reuse of mining tailings aligns with the principles of the circular economy, promoting resource efficiency and waste reduction, and contributes to a more sustainable approach to mining by maximizing the utilization of Critical Raw Materials (CRMs) and minimizing environmental impact (European Commission, 2020; Lemos *et al.*, 2023a). Furthermore, broader sustainability benefits, such as reduced reliance on virgin resources, extended mine life, and a lower carbon footprint, should

be considered. However, while reusing mining tailings can yield environmental and economic benefits, it is essential to carefully assess the specific characteristics of the tailings and evaluate the potential risks associated with their reuse. Factors such as hazardous substances, stability considerations, and the long-term environmental impact should be assessed thoroughly before implementing any reuse strategy (Tayebi-Khorami *et al.*, 2019).

So far, a few approaches have been explored (Tayebi-Khorai *et al.*, 2019; Lemos *et al.*, 2021; Araya *et al.*, 2021; Lemos *et al.*, 2023a): (i) Reclamation and rehabilitation, a common practice to reclaim the land disturbed by mining activities, which can involve using tailings as backfill material for underground mine workings or for reshaping and recontouring the landscape; (ii) Tailings reprocessing, in which advances in technology allow to extract additional valuable minerals from tailings, using techniques such as flotation, leaching, and gravity separation to recover metals or minerals that were not effectively extracted during the initial mining process; (iii) Using some types of tailings as construction materials, such as aggregates for concrete, asphalt, or bricks (e.g., tailings with high silica content can be utilized in the production of cement); and (iv) Using some types of tailings as cover material for landfills, providing a protective layer for waste disposal sites. Several historical studies were conducted on the feasibility of reusing mining tailings, and specific studies and outcomes vary depending on multiple local factors (e.g. Zhang *et al.*, 2010; Araya *et al.*, 2021).

For this study, samples from the gold (Au) tailings dam in Nova Lima, Minas Gerais, were processed in a bench-scale metallurgical test to quantify the overall recovery of Au. Subsequently, a technical feasibility and financial modeling analysis was conducted for the entire process, considering three scenarios for potential reuse and the accumulated tonnage available in the tailings storage facility (TSF). Considering these factors and conducting a comprehensive feasibility study is necessary to determine the viability and potential benefits of reusing the Au tailings.

2. Study area

The studied tailing structure is in the northern part of the Iron Quadrangle (IQ), Brazil's main mineral province. These tailings originate from Au mines hosted in the Rio das Velhas metallogenic Greenstone Belt, the country's most important critical Au district (Lobato *et al.*, 2001). The TSF under investigation is Cocomuto (CO) in Nova Lima (Figure 1), Minas Gerais, Brazil. Nova Lima has a rich history of Au mining and played a significant role in the country's Au rush during the colonial period.

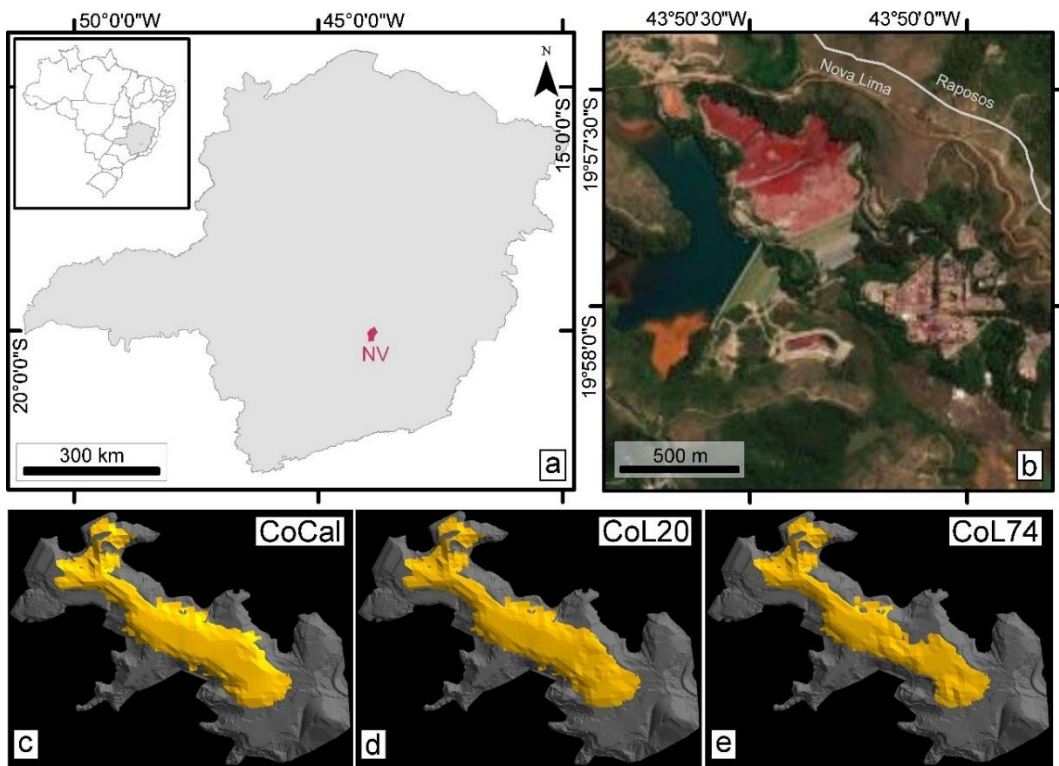


(Figura 5.53) Figure 1. Co dam setting. (a) Location of Nova Lima city in Minas Gerais state. (b) Co dam, near Queiroz plant. (c) Pit designed for CoCal scenario. (d) Pit designed for CoL20 scenario. (e) Pit designed for CoL74 scenario.

The Nova Lima dams, and tailings deposits are associated with the Queiroz metallurgical plant, which has been processing sulfide Au ores for over thirty years. The processed materials are divided into two circuits: one in operation, including a calcination step, and a second one that is no longer active, known as the Raposo circuit (Lemos *et al.*, 2023b). This study deals with the Raposo circuit that treats non-refractory sulfide ore mainly from the Raposo mines, primarily composed of pyrite, pyrrhotite, and subordinate arsenopyrite. However, this circuit, used to supply the CO, was deactivated in 1998 following the closure of this underground mine. The Raposo circuit achieved a 90% Au recovery rate and consisted of grinding, gravity concentration, conventional leaching, carbon-in-leach (CIL), elution, and electrowinning stages (Moura, 2005; Lemos *et al.*, 2020).

Lemos *et al.* (2023a) state that the CO dam contains approximately 3,350 million tons of tailings, with an estimated Au content of ca. 150 million ounces. The CO dam (old circuit) mainly consists of quartz, carbonates, iron oxides, and phyllosilicates such as muscovite and chlorite (Lemos *et al.*, 2020). Chemically, it contains higher levels of iron (Fe) compared to calcium (Ca), magnesium (Mg), aluminum (Al), manganese (Mn), potassium (K), and sodium (Na). Furthermore, in studies such as Lemos *et al.* (2023a) and Lemos *et al.* (2023b), the achieved Au recovery for different scenarios ranged from 70% to 59%, essential for analyzing a financial assessment.

3. Materials and methods

Samples were collected by drilling at a depth of 15 m. Subsequently, individual samples were combined to create composite samples representing the CO tailings structure for the Au recovery/reuse tests. The samples were also used to generate a grade-tonnage model, which is input for the sensitivity analysis (Lemos *et al.*, 2023a). Based on previous results, the final step was undertaken according to the financial viability techniques for the cost-benefit studies. This step provides the attractiveness of the investment and facilitates decision-making.

3.1. Metallurgical testwork

Laboratory-scale experiments were conducted to assess the potential recovery of Au, considering the specific characteristics of each tailings structure (Lemos *et al.*, 2022; Lemos *et al.*, 2023a). Three different setups were employed, involving grinding, leaching, and calcination, all designed to be adaptable and applicable to existing metallurgical plants if a viable and efficient scenario emerges.

In the first scenario (CoL74), samples were ground to a particle size of 74 µm, with 80% of the particles falling within this range, after a liberation-by-size analysis for sulfides and Au particles. The calcination step was disregarded, and the samples were directly subjected to leaching. Bottle roll tests were performed using a leaching solution containing 2000 mg/kg of cyanide (NaCN) and 4000 mg/kg of lime (CaO), with a solid-to-liquid ratio of 50. Another test (CoL20) was conducted with a particle size of 20 µm, following the previously described leaching setup. The third setup (CoCal) involved grinding the material to a particle size of 74 µm using ball mills, followed by calcination in a muffle at 700°C. For Au extraction, the calcinated material was placed in bottles containing a solution with 40% solids, composed of 2000 mg/kg of NaCN and 6000 mg/kg of CaO. The extraction process took over 24 hours, divided into two stages with a pre-airing period of 2 hours.

3.2. Financial analysis

Sensitivity analysis is a decision method employed in a financial-oriented technical study to determine the feasibility or success of a particular project, whether it involves investment, business organization, product launch, or anticipating potential success in a new market (Tomaz, 2013). By developing increasingly complex benefit functions considering the TSF characteristics, it is possible to obtain more precise quantities of tailings that can be reprocessed and utilized more effectively.

Therefore, this step consisted of the following stages: (i) Definition of the input parameters for the CO tailings *in situ*, based on Lemos *et al.* (2023a), using geological resource estimation; and (ii) Incorporation of metallurgical variables as one of the premises in the benefit function (Benefit Function = Revenue – Cost; Peroni *et al.*, 2012) for tailings extraction, along with other relevant variables. Thus, three scenarios were considered and related to the metallurgical tests.

Calculating the net present value (NPV) is a financial evaluation method commonly used in the mining industry to assess the feasibility and profitability of mining projects (Araya *et al.*, 2020). The discounted cash flow (DCF) valuation is a financial model used to assess the worthiness of an investment based on projected future cash flows. It calculates the value of a company by considering its ability to generate cash flows for investors in the future (Fontes *et al.*, 2020). The output of the project analysis is a series of pits, each with its potential for mining under specific economic conditions (Peroni *et al.*, 2012). These pits are optimized for each scenario using the Lerchs-Grossmann algorithm (Lerchs & Grossmann, 1965). Subsequently, optimization of pit designs was performed for each scenario (CoL74, CoL20, and CoCal). Sensitivity analysis was conducted considering different Au prices of \$1300, \$1500, and \$1700, as well as mining time for each scenario. All studies were carried out using the *Deswik Suite v5.1* software.

4. Results and discussions

4.1. Metallurgical testwork

The results obtained demonstrate a promising potential for Au recovery. The recoveries increased from scenarios 1 to 2, meaning that the calcination step was essential for Au extraction. This relationship can be explained by the association between sulfides and Au, as described by Lemos *et al.* (2023a) and Lemos *et al.* (2023b).

(Tabela 5.34) Table 1. Summary of metallurgical test results for Au reuse in CO samples (after Lemos *et al.*, 2023a)

Calculated Feed Grade (mg/kg)	Au Mineralogical Association	CoL74	CoL20	CoCal
		(% Au recovery)		
0.950	sulfides and quartz	50.67	64.13	79.72

This information is important as it would facilitate the industrial reprocessing of these structures with minimal investment, considering their proximity to metallurgical units that already have the necessary stages in Au production (Moura, 2005; Lemos *et al.*, 2023a). These data are one of the main inputs for defining the economic scenarios discussed in the following sections.

4.2. Financial model

The economic assessment consists of two main steps. The first step evaluates the economic potential of Au present in inactive mine tailings as an *in-situ* value. The second step analyzes the feasibility of Au production using mine tailings as a source (Araya *et al.*, 2020).

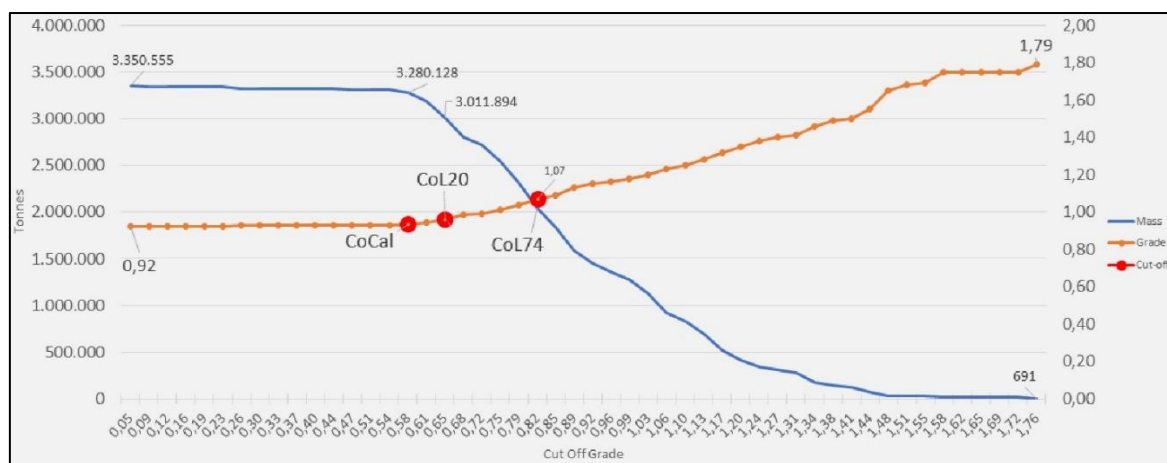
4.2.1. Model and preliminary estimation of resources in the CO dam

An average Au grade of 0.95 and a total resource of 3,350.55 tonnes are the main assumptions for the block model (Table 2). Table 2 summarizes the assumptions obtained from the model and assessment by Lemos *et al.* (2023).

4.2.2. Bases for the Benefit Function

To evaluate the final pits, the same benefit function used in the estimated model by ordinary kriging was employed (Lemos *et al.*, 2023a). For the feasibility analysis, costs and economic parameters expressed in Table 3 were assumed, considering the metallurgical recovery scenarios mentioned: CoL74, CoL20, and CoCal. Figure 2 demonstrates this variation, considering each scenario's cut-off grades and tonnage.

The project's NPV was calculated by applying a discount rate of 8% per year to all developed scenarios. A general slope angle of 20 degrees, equivalent to 36.4% was used.

(Figura 5.54) Figure 2. Cut-of Grade *versus* tonnage for each considered scenario.

(Tabela 5.35) Table 2. Summary statistics of the global resources in the CO dam (after Lemos *et al.*, 2023a).

Block model variables						
Name	Minimum	Maximum	Range	Average	Standard Deviation	Variance
Au (mg/kg)	0.05	1.79	1.74	0.95	0.24	0.06
Density (g/m ³)	1.322	2.043	0.722	1.787	0.140	0.020
Tonnes	1.26	1,082.30	1,081.04	549.18	189.71	35,989.40
Resource	indicated	inferred	measured	-	-	-

(Tabela 5.36) Table 3. Parameters of the reference case for valuation based on the benefit function.

VARIABLE		VALUES	CoCal	CoL20	Col74
Revenue	Revenue from the Block				
Mining cost	Mining and Transportation Costs	R\$ 6.45	R\$ 6.45	R\$ 6.45	
Processing cost	Processing Costs (GFE + PM_*)	R\$ 56.25	R\$ 56.25	R\$ 56.25	
Total cost	Total Cost of the Block				
Benefit	Revenue from the Block - Cost of the Block				
Type	Benefit greater than 0 = ore				
Variable	Description				
Mining cost	Mining and Transportation Costs	R\$ 6.45	R\$ 6.45	R\$ 6.45	
GFE	G&A, Filter, and Dry Tailings Management Costs	R\$ 56.25	R\$ 56.25	R\$ 56.25	
PM_COICAL	Calcined Process and Maintenance Costs	R\$ 51.70			
PM_COL	Leached Process and Maintenance Costs		R\$ 38.43	R\$ 38.43	
USD_RATE	Conversion Rate		R\$ 5.05		
OZ	Dollar per Ounce		\$ 1,500		
RM_COICAL	Calcined Recovery (%)	79.72			
RM_COL20	Leached Recovery 20µm (%)		64.13		
RM_COL74	Leached Recovery 74µm (%)				50.67
CUT-OFF	Minimum Grade for Benefit = 0 (g/t)	0.59	0.65	0.82	

4.2.3. Pit optimization and analysis of simulated scenarios

Three final pits were obtained using the inputs illustrated in Table 3, each with production ranges, as shown in Table 4 and Figure 1. For the CoCal scenario, a sulfur (S) grade limit in the feed was considered restrictive, as the minimum feed grade for this possible treatment route would be 20% (Moura, 2005; Lemos *et al.*, 2020). Therefore, this scenario has only one base possibility.

(Tabela 5.37) Table 4. Variation in annual production for each considered scenario.

Process	Scenario	Annual prod. (t)	Description
CO Calcined	CoCal	65,000	Annual feed limit due to S content
	CoCal-400	400,000	Sensitivity analysis created scenario
CO Leached +20 µm	CoL20	400,000	Base scenario
	CoL20-800	800,000	Sensitivity analysis created scenario
	CoL20-1000	1,000,000	Sensitivity analysis created scenario

CO Leached +75 µm	CoL74	400,000	Base scenario
	CoL74-800	800,000	Sensitivity analysis created scenario

In general, for the base scenario of these pits, annual production of 400,000 t and 800,000 t was considered. Only in the case of CoL20, it was possible to simulate operation with 1,000,000 t annually. Therefore, the first two scenarios presented restrictions regarding the feed grade (CoCal) and mass (CoL74). Figure 3 shows the results for each scenario.

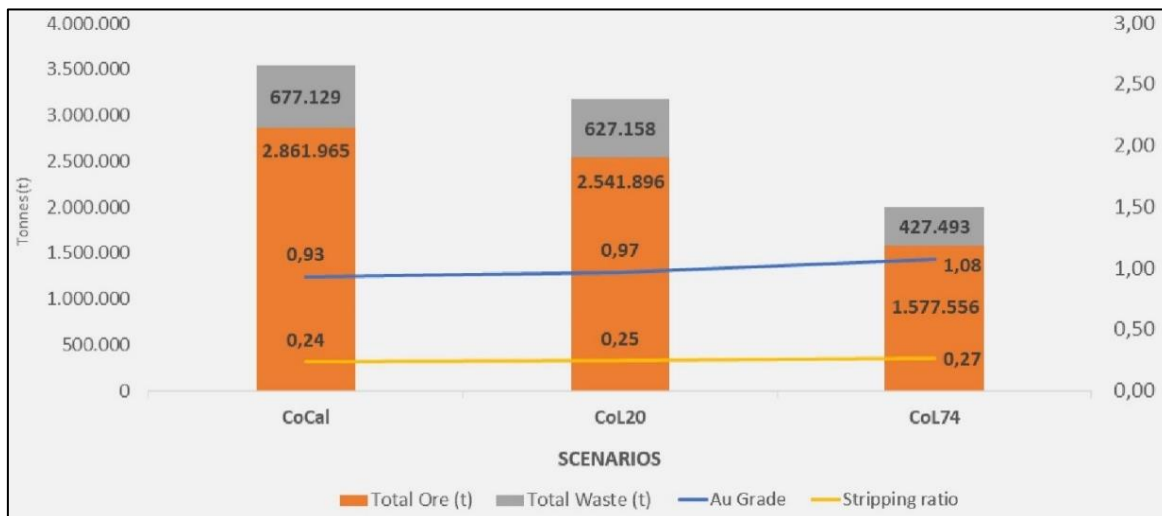


(Figura 5.55) Figure 3. Results of the generated pits for each scenario: CoCal, CoL20, and CoL74.

Considering the base case for each scenario, their production variations (400,000 t/annum, 800,000 t/annum, and 1,000,000 t/annum), and the value of one ounce of Au (31,108 g) at \$1500, it is possible to determine the profit from Au reprocessing in CO. Figure 4 demonstrates that the CoL20 scenario, with an annual production of 800 kt, becomes attractive with potential gains of \$21,093,647 and a production period of up to six years.



(Figura 5.56) Figure 4. Results and mine life for each scenario, considering the base scenario for CoCal (65 kt), CoL20 (400 kt) and CoL74 (400 kt), as well as variations for CoCal (400 kt), CoL20 (800 kt and 1000 kt) and CoL74 (800 kt).

4.2.4. Sensitivity analysis

Figure 5 presents the three scenarios with their respective annual productions but varying the value of the produced ounce and, consequently, the mine life. The considered values are \$1400, \$1500 (base scenario), and \$1700.

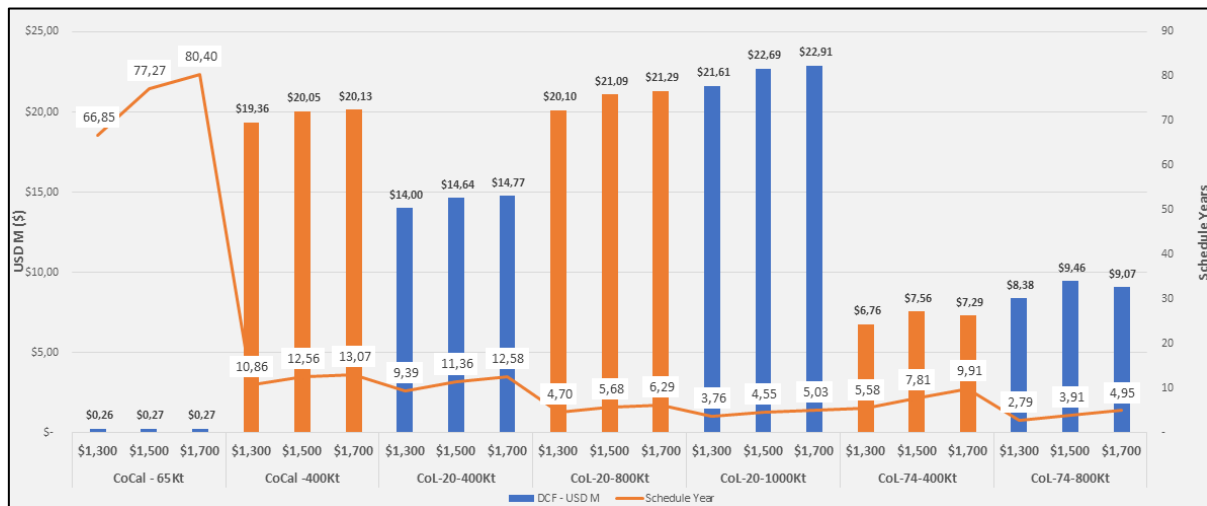


(Figura 5.57) Figure 5. Results and mine life for each scenario considering different ounce values.

The CoCal 65 kt scenario could be more attractive in terms of time and money. This scenario is restrictive due to the high S feed grade for the roaster, exceeding 20%. The others show gains above \$19 million but with a mine life of over ten years. The Col20-800kt and 1,000 kt scenarios are more attractive compared to CoCal 400kt, as they offer a financial return above \$20 million and a relatively shorter mine life. The scenario Col74 is the least attractive compared to the other scenarios.

5. Conclusion

The financial potential of reprocessing one of the Au metallurgical waste dams in the IQ has been demonstrated. From an economic perspective, with cost analyses varying at \$1300/oz, \$1500/oz, and \$1700/oz, and with annual productions of 400 t, all scenarios prove profitable.

Therefore, when comparing the scenarios, CoL20, with annual productions of 800 kt and 1,000 kt, is of interest, with a return above \$20 million. However, it is worth noting that the choice should not be solely based on financial factors, as it involves exploiting old waste accumulation structures near essential river systems. In addition to the parameters presented here, geotechnical and environmental issues should be evaluated for using this resource. Further, environmental impact, mainly on the water resources, and ecological and human health risk assessment should be added to this analysis.

Although this structure is located near industrial complexes that currently process Au ores, investment surveys (CAPEX) are suggested to provide further robustness to the potential analysis presented. The financial study of reusing other elements such as S, As, Ag or even the whole waste is also recommended. This would avoid the generation of additional waste and improve resource utilization.

Acknowledgments

We thank our colleagues from the Instituto de Ciências da Terra (ICT) and from AngloGold Ashanti, who provided insights and expertise that greatly assisted this research; Fundação para a Ciência and Tecnologia (FCT) for financial aid (UIDB/04683/2020 and UIDP/04683/2020).

References

- ARAYA, N., KRASLAWSKI, A., CISTERNAS, L. A. Towards mine tailings valorization: Recovery of critical materials from Chilean mine tailings. *Journal of Cleaner Production*, v. 263, p. 121555, 2020. <https://doi.org/10.1016/j.jclepro.2020.121555>
- ARAYA, N., RAMÍREZ, Y., KRASLAWSKI, A., CISTERNAS, L. A. Feasibility of re-processing mine tailings to obtain critical raw materials using real options analysis. *Journal of Environmental Management*, v. 284, p. 112060, 2021. <https://doi.org/10.1016/j.jenvman.2021.112060>
- COFFEY, J. P., PLUNKETT, J. D., CARNEIRO, A. The benefits of integrating long-term tailings and mine plans. In: 24th International Conference on Paste, Thickened and Filtered Tailings, 2021, Perth. *Annals of Paste 2021*, pp. 165-176. https://doi.org/10.36487/ACG_repo/2115_15
- EUROPEAN COMMISSION. Communication from the Commission to the European Parliament, the Council, the European Economic and Social Committee and the Committee of the Regions: Critical Raw Materials Resilience: Charting a Path Towards Greater Security and Sustainability, 474 Final; European Commission: Brussels, Belgium, 28p, 2020.
- FONTES, M. P., KOPPE, J. C., ALBUQUERQUE, N. Comparison between traditional project appraisal methods and uncertainty analysis applied to mining planning. *REM, International Engineering Journal*, v. 73, p. 261-265, 2020. <https://doi.org/10.1590/0370-44672019730108>
- HINDLE, S. R. Feasibility and sensitivity analysis of integrating mining and mineral carbonation: A case study of the Turnagain Nickel Project. 2011. Master dissertation (Faculty of Graduate Studies, Mining Engineering) - University of British Columbia, Vancouver, 2011.
- HITCH, M., DIPPLE, G. M. Economic feasibility and sensitivity analysis of integrating industrial-scale mineral carbonation into mining operations. *Minerals Engineering*, v. 39, p. 268-275, 2012. <https://doi.org/10.1016/j.mineng.2012.07.007>
- LEMOS, M., VALENTE, T., REIS, P. M., FONSECA, R., DELBEM, I., VENTURA, J., MAGALHÃES, M. Mineralogical and geochemical characterization of gold mining tailings and their potential to generate acid mine drainage (Minas Gerais. Brazil). *Minerals*, v. 11, n. 1, p. 39, 2020. <https://doi.org/10.3390/min11010039>
- LEMOS, M. G., VALENTE, T., MARINHO-REIS, A. P., FONSCECA, R., DUMONT, J. M., FERREIRA, G. M. M., DELBEM, I. D. Geoenvironmental Study of Gold Mining Tailings in a Circular Economy Context: Santa Barbara, Minas Gerais, Brazil. *Mine, Water and the Environment*, v. 40, p. 257–269, 2021. <https://doi.org/10.1007/s10230-021-00754-6>
- LEMOS, M., VALENTE, T., REIS, P., FONSECA, R., PANTALEÃO, J.P., GUABIROBA, F., FILHO, J.G., MAGALHÃES, M., DELBEM, I. Caracterização Mineralógica, Geoquímica e Potencial de Valorização de Resíduos de Mineração de Ouro (Minas Gerais, Brasil). In: XXIX Encontro Nacional de Tratamento de Minérios e Metalurgia Extrativa, 2022. Armação dos Búzios. Anais do XXIX ENTMME, 2022.
- LEMOS, M., VALENTE, T., REIS, P. M., FONSECA, R., PANTALEÃO, J. P., GUABIROBA, F., FILHO, J.G., MAGALHÃES, M., AFONSECA, B., SILVA, A.R., DELBEM, I. Geochemistry and mineralogy of auriferous tailings deposits and their potential for reuse in Nova Lima Region. Brazil. *Scientific Reports*, v. 13, n. 1, p. 4339, 2023a. <https://doi.org/10.1038/s41598-023-31133-6>
- LEMOS, M.G., VALENTE, T.M., REIS, A.P.M., FONSECA, R.M.F., GUABIROBA, F., FILHO, J.G.M., MAGALHÃES, M.F., DELBEM, I.D., DIÓRIO, G.R. Adding Value to Mine Waste through Recovery Au, Sb, and As: The Case of Auriferous Tailings in the Iron Quadrangle, Brazil. *Minerals*, v. 13, p. 863, 2023b. <https://doi.org/10.3390/min13070863>
- LERCHS, H., GROSSMAN, I.F. Optimum design of open-pit mines. *Canadian Institute of Mining Bulletin*, v. 58, n. 33, p. 47-54, 1965.
- LOBATO, L. M., RIBEIRO-RODRIGUES, L. C., VIEIRA, F. W. R. Brazil's premier gold province. Part II: geology and genesis of gold deposits in the Archean Rio das Velhas greenstone belt. *Quadrilátero Ferrífero. Mineralium Deposita*, v. 36, p. 249-277, 2001. <https://doi.org/10.1007/s001260100180>

- MALLI, H., TIMMS, W., BOUZALAKOS, S. Integration of Ultramafic Mine Tailings and Acid Mine Drainage for Carbon Sequestration and Mine Waste Management. *Journal of Research Projects Review*, v. 11, p. 11-19, 2015.
- MOURA, W. Especialização de Cianeto para Redução do Consumo no Circuito de Lixiviação de Calcinado da Usina do Queiróz. 2005. Master thesis - Universidade Federal de Minas Gerais, Belo Horizonte, 2005.
- PANG, Z., O'NEILL, Z., LI, Y., NIU, F. The role of sensitivity analysis in the building performance analysis: A critical review. *Energy and Buildings*, v. 209, p. 109659, 2020. <https://doi.org/10.1016/j.enbuild.2019.109659>
- PERONI, R. D. L., COSTA, J. F. C., KOPPE, J. C. Análise da variabilidade de teores e sua incorporação no planejamento de lavra. *Revista Escola de Minas*, v. 65, p. 263-270, 2012. <https://doi.org/10.1590/S0370-44672012000200016>
- RENDU, J. M. An introduction to cut-off grade estimation. Englewood, Society for Mining, Metallurgy, and Exploration, 2014. 158p.
- SUPPES, R., HEUSS-ABBICHLER, S. Resource potential of mine wastes: A conventional and sustainable perspective on a case study tailings mining project. *Journal of Cleaner Production*, v. 297, p. 126446, 2021. <https://doi.org/10.1016/j.jclepro.2021.126446>
- TAYEBI-KHORAMI, M., EDRAKI, M., CORDER, G., GOLEV, A. Re-Thinking Mining Waste through an Integrative Approach Led by Circular Economy Aspirations. *Minerals*, v. 9, p. 286, 2019. <https://doi.org/10.3390/min9050286>
- TOMÁZ, R.S. Influência da Função Benefício na Geração de Cavas Finais: uma Análise de Sensibilidade. 2013. Undergraduate thesis (Engenharia de Minas) - Universidade Federal de Goiás, Catalão, 2013.
- ZHANG, Q. H., WANG, X. C., XIONG, J. Q., CHEN, R., CAO, B. Application of life cycle assessment for an evaluation of wastewater treatment and reuse project—Case study of Xi'an, China. *Bioresouce technology*, v. 101, n. 5, p. 1421-1425, 2010. <https://doi.org/10.1016/j.biortech.2009.05.071>

5.2. Estruturas Localizadas na Região de Goiás

A pandemia de Covid 19 proporcionou grandes desafios em todos os domínios da Sociedade, pelo que o mesmo se verificou ao nível da pesquisa científica. As restrições impostas e necessárias afetaram a coleta e ensaios com amostras da barragem de Crixás, já que o acesso a elas foi possibilitado apenas em 2022.

Para que esta componente do trabalho e consequentemente os objetivos para a região não fossem desconsiderados, amostras coletadas mais tarde foram submetidas a caracterização química e mineralógica, conforme capítulo 4. Os resultados foram apresentados no último IMWA Congress (IMWA 2022) e serão apresentados a seguir com o título *Geoenvironmental Characterization of Gold Mine Tailings from Minas Gerais and Goiás, Brazil*. A amostra referente a barragem de Crixás foi nomeada como número 8.

No âmbito do reuso, a amostra foi submetida a ensaios para extração de Au por lixiviação em garrafa com 80% das partículas abaixo de 106 µm. Porém, como demonstrado no artigo a seguir, pelas características de associação do Au, os ensaios não foram completamente satisfatórios, uma vez que a recuperação do Au não ultrapassou 20%.

Geoenvironmental Characterization of Gold Mine Tailings from Minas Gerais and Goiás, Brazil

Mariana Lemos^{1,2}, Teresa Valente*¹, Paula Marinho Reis^{1,3}, Rita Fonseca⁴, Itamar

Delbem⁵, José Gregório Filho², Fernanda Guabiroba², João Pantaleão², Marcus Magalhães²

¹Institute of Earth Sciences, Pole of University of Minho, Campus de Gualtar, 4710-057 Braga, Portugal, *teresav@dct.uminho.pt

²Anglogold Ashanti, Mining & Technical, COO International, 34000-000, Nova Lima, Brazil,

³GEOBIOTEC, Departamento de Geociências, Universidade de Aveiro, Campus Universitário de Santiago, 3810-193 Aveiro, Portugal

⁴Institute of Earth Sciences, Pole of University of Évora, University of Évora, 7000 Évora, Portugal ⁵Microscopy Center, Universidade Federal de Minas Gerais, 31270-013, Belo Horizonte, Brasil

Abstract

For more than two centuries, sulfide gold ores have been treated at metallurgical plants located in Nova Lima, Santa Barbara and Crixás. Brazil. In this study, geochemical, mineralogical, and textural properties of tailings from eight tailings deposits were analysed. The samples show high concentration of Au, hosted in different minerals. In addition, samples contain S, Fe, and As. Sulfides, oxides, and sulfates are present, some as preserved relics. This work highlights different geochemistry and mineralogy, dependent on the nature of the tailings. Such information is critical to support long-term decisions about tailings management and circular economy.

Keywords: Environmental geochemistry, Mineralogy, Mining Railings, Brazil.

Introduction

Brazil is a country that has a strong relationship with mining, currently representing between 3 and 5% of GDP. This proximity has been noticed since the end of the 17th century, at the beginning of the first gold cycle. In the mid-18th century, Brazil produced approximately half of the world's gold, attracting the immigration of around 400,000 Portuguese, mainly in the region of Minas Gerais and Goiás (Fig 1).

Currently, this sector moves others through the supply of raw materials, such as the civil construction, automobile, aerospace, and other industries. Although its importance is relevant and strategic for the economy, the generation of waste is also important. The main deposition structures of these wastes are the dams and deposits (mine dumps). However, these structures may constitute mineral deposits with different chemical grades distribution and physical characteristics relatively to the exploited ore. With the evolution and dynamic changes in

the market and technology, these wastes can thus provide an alternative to primary exploitation.

The tailings dams and other deposits resulting from the improvement of ores and/ or Au metallurgical processes constitute waste accumulation infrastructures with two potential valences: focus of environmental impact due to the toxic substances they contain and possible sources of new raw materials.

The present work was carried out in active and non-active tailings dams, as well as depleted mine deposits around the cities of Santa Barbara (SB) and Nova Lima (NL) in Minas Gerais. In addition to these structures, the study also includes the active dam of a project in the city of Crixás (CR), located in the North of the district of Goias.

The study, therefore, meets the concept and objectives of circular economy applied to tailings from gold processing. The main objective is to present an integrated physical, geochemical, and mineralogical characterization of solid tailings to support the detection of potential reuses and avoid possible environmental impacts.



(Figura 5.58) **Figure 1** Location of the main Au dams in Brazil (source: FEAM – State Foundation for the Environment) – Highlight for black dots for the study regions.

Methods

The sampling stage took place during late winter and early spring (late August to late September 2021).

A total of 1560 sediment samples were collected with auger, drilling up to two meters for chemical analysis (at different depths). The distance between samples varied from 13 to 20 meters depending on the sampling area. In table 1 it is possible to verify the names of the studied structures, location, and types of samples.

In the laboratory, chemical analysis was performed by atomic absorption spectroscopy (AAS using AAS280 FS Varian) for the determination of Au, Cu, C, As, Sb, S, Fe. The fire assay was the procedure used to obtain analytical data for Au.

In addition to the geochemical data, polished sections were prepared for mineralogical characterization. The mineralogical study was carried out by means of optical microscopy and scanning electron microscopy (SEM- Field Electron and Ion Company -FEI) at UFMG, Belo Horizonte. The samples were analyzed using a FEI electron microscope, Quanta 600 FEG, high vacuum mode, coupled to the automated analyzer software (MLA – GXMAP and SPL-DZ mode) and to the EDS Espirit Bruker microanalysis system (20 Kve).

Results

Chemical Analysis

In the graph of fig 2, a box plot is presented with the variations and averages of the database surveyed, showing the chemical differences between the studied wastes. Sb is the main differentiator of solid samples from tailings deposits 6 and 7 in relation to other tailings. The Au concentrations are highlighted in structure number 5. The S is relevant for tailings 1, 4, 6, and 8.

In all deposits located in Nova Lima (deposits 1 to 5), higher As concentrations are observed in comparison with the others. The low levels in deposit 6 can be explained by the flotation stages, since all As sources are removed prior to their deposition in the dams (Lemos *et al.*, 2019). The others, 7 and 8, have low levels in the food sources of metallurgical plants (AGA, 2019).

Fe values are lower for tailings in area 3, being, on the other hand, high and variable for the others.

Cu concentrations are higher for deposits 7 and 8, despite deposit 4 having many outliers above the third quartile of the deposit. The C is variable for deposit 2, but on average higher than the other deposits.

(Tabela 5.38) **Table 1** Information about the studied areas, collection methods, depth, number of samples and type of analysis. PSD – Particle size distribution; AAS - Atomic absorption spectroscopy; ICP (MS) – Inductively coupled plasma mass spectrometry.

Area	Tailings Deposit	Sampling Method	Depth (~m)	Samples Numbers	Analysis
NL	1	Percussion+Diamond Probing	16	266	
NL	2	Percussion Probing	4.4 4.0 6.7	162	
NL	3	Direct push	12.5	615	
NL	4	Direct push		286	AAS, ICP (MS),
NL	5	Direct push		257	Fire Assay, PSD,
					Mineralogy
SB	6	Direct push	15	75	
SB	7	Percussion Probing	10	100	
CR	8	Percussion Probing	15	35	

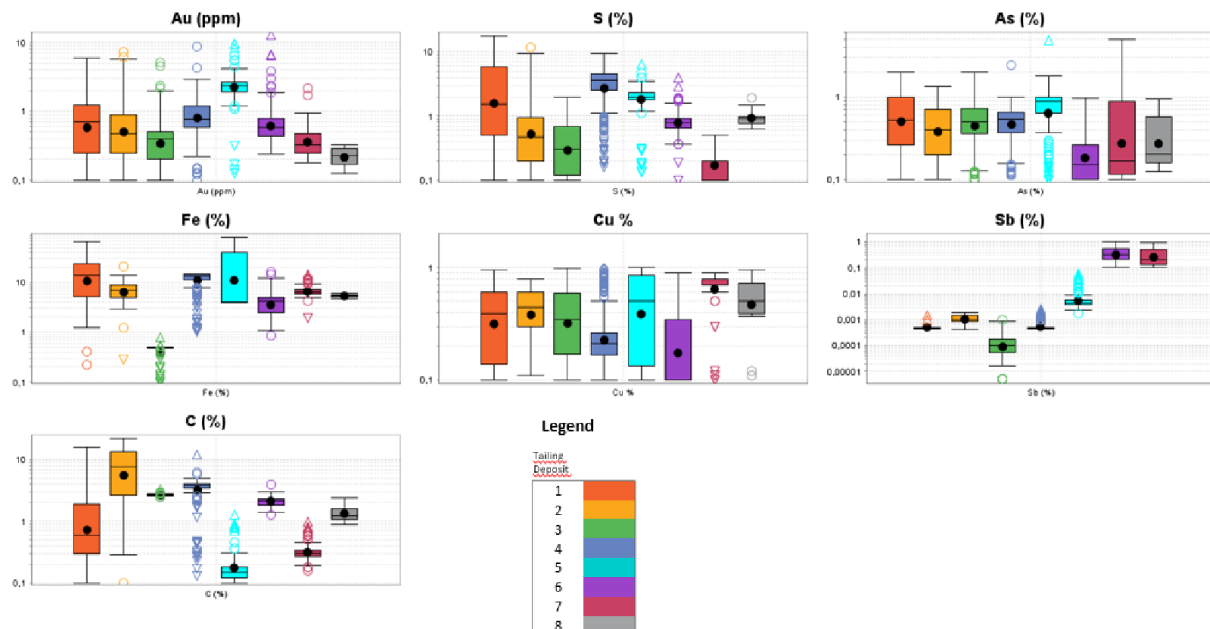


(Figura 5.59) **Figure 2** Box plot graphs demonstrating the variation and differentiation between the tailings of structures 1 to 8 studied for Au (mg/kg), S (%), As (%), Fe (%), Cu (%), Sb (%), and C (%) – Y (Logarithmic scale).

Therefore, in the graph of Fig. 3 it is possible to differentiate the tailings in relation to the seven chemical variables. Three distinct groups are noticed, being 1 represented by points close to the Au axis with most points of deposit 5. Group 2

are, in general, close to the Sb axis with most points of deposits 6 and 7. And a third group, with other deposits between the S, Fe, and C axes (Fig 3).

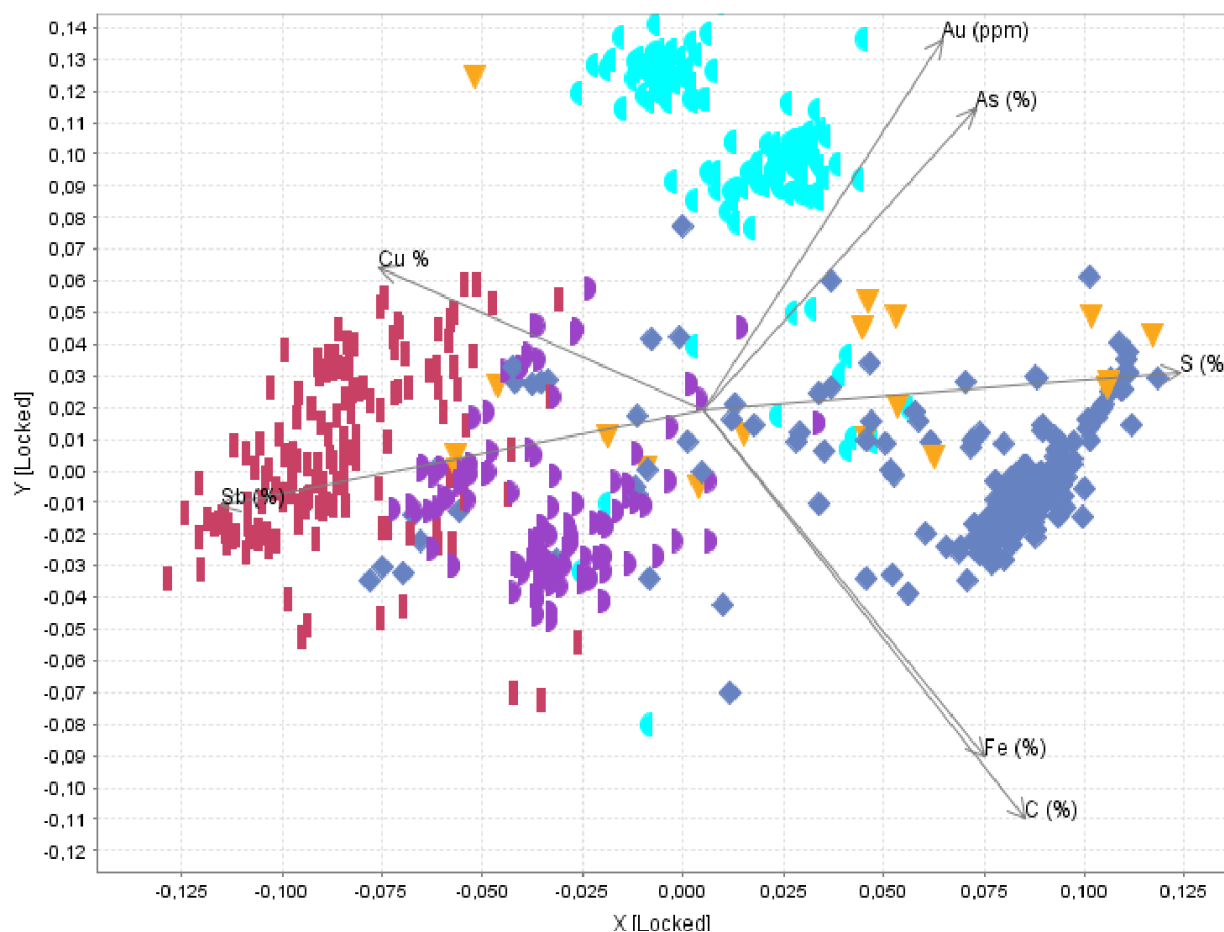


(Figura 5.60) **Figure 3** 3D PCA graphics showing the grouping of chemical results from structures 1 to 8 studied for Au (mg/kg), S (%), As (%), Fe (%), Cu (%), Sb (%), and C (%) – Y (Logarithmic scale).

Mineralogy

Table 2 shows the mineralogy results of the structures under study.

In general, the gangue minerals are similar among the structures already studied (except for dam 5). However, with expressive differences between carbonates of the structure 1, composed of siderite and greater presence of minerals from the feldspar group for samples from 8 and 3. The main silicate is quartz, which is found with inclusions of Au, mainly for deposits 4, 8 and 3 (Fig 4). The differences between the types of sulfides and associations with Au mark the main mineralogical difference between the structures. While berthierite/arsenopyrite is the main source

of S in deposit 6, pyrrhotite/ pyrite/arsenopyrite are abundant in the structures of 4, 1, and 2. In these sulfides, the presence of attached and included Au has also been described (Fig 4).

For dam 6, oxides and jarosite containing high Sb concentration are also observed. This fact also shows that these minerals are distinct from other deposits. The presence of a high content of oxides and jarosite in the rejects of 5 and 6 is due to the transformation steps in a roaster and autoclave for Au extraction in metallurgical plants (Lemos *et al.*, 2019). The other deposits have minerals that are more common among themselves because they receive wastes from the flotation stage, which has a low degree of mineral transformation (Lemos *et al.*, 2019).

(Tabela 5.39) **Table 2** Mineralogy of tailings deposits 1 to 8 obtained by FEI microscopy analysis.

Minerals/compounds	Chemical Formula	1	2	3	4	5	6	7	8
		Wt %	Wt %	Wt %	Wt %	Wt %	Wt %	Wt %	Wt %
	SiO ₂								
	NaAlSi ₃ O ₈								
Quartz	CaAl ₂ Si ₂ O ₈ KAlSi ₃ O ₈	36.65	31.57	7.56	55.8		35.6	34.18	42.83
Albite	KMg _{2.5} Fe ₂ +0.5AlSi ₃ O ₁	2.81	5.33	0.03	0.37	15.6	1.11	0.07	5.44
Anorthite	(OH)	0.01	-	0.73	0.01	1.5	0.053	1.18	0.52
K-feldspar	F								
Biotite	O	1.22	0.12	2.55	0.39	0.053	1.27	1.74	8.30
Smectite	(Si,Al)(Mg,Fe)O(OH)NaH ₂ O	0.52	0.11	1.28	0.16	1	1.26	-	-
Muscovite Group	Chlorite	KAl ₃ Si ₃ O ₁₀ (OH)·1.9F·0.1	-	-	27.57	0.13	1.8	-	38.46
Iron Oxides/Hydroxides	(Mg,Fe) ₃ (Si,Al) ₄ O ₁₀ (OH) ₂ ·(Mg,Fe) ₃	20.58	6.53	1.28	5.56	11	29	3.34	6.13
Fe antimoniate	(OH) ₆	5.83	2.44	9.06		3.3	5.01	0.41	
Rutile	Fe ₂ O ₃ /FeOOH FeSb(As)O	8.95	-	-	6.12	56.8	0.378	17.09	-
Ankerite	TiO ₂	-	-	0.60	8.86	0.599	0.806	0.07	0.16
Siderite	Ca(Fe,Mg,Mn)(CO ₃) ₂	0.56	0.19	1.49	0.49	1	0.599	0.29	6.49
Dolomite	FeCO ₃	0.85	16.84	0.01	11.2	-	9	0.02	0.03
Calcite	CaMg(CO ₃) ₂	8.94	2.92	0.23	7.25	0.2	7.2	0.17	2.10
Jarosite (Sb)	CaCO ₃	-	0.02	-	2.25	-	5.4	0.05	1.60
Gypsum	KFe(SO ₄) ₂ (OH) ₆	-	-	-	-	7	1.00	-	-
Pyrite	& (H ₃ O)Fe(SO ₄) ₂ (OH) ₆	-	-	-	0.03	0.002	2.00	-	-
Pyrrhotite	CaSO ₄ 2H ₂ O	0.22	5.31	0.06	0.5	0.004	0.08	0.03	0.11
Arsenopyrite	Berthierite	Fe ₂ +S ₂	4.7	2.06	0.022	0.79	0.056	0.041	-
Chalcopyrite	Fe ₂ +0.95S	1.71	2.52	-	0.24	0.01	0.056	-	1.803
Gesdorffite	Fe ³⁺ AsS	0.21	0.01	-	-	0.1	0.141	-	-
Covellite	FeSb ₂ S ₄	-	0.02	-	0.07	-	0.028	-	0.05
Sphalerite	CuFe(S) ₂	0.01	45	-	0.01	526	0.009	-	-
Native Gold*	NiAsS CuS	60	8	-	364	42	158	-	-
Electrum*	ZnS	5		2	10		6	20	740
	Au > 80%, Ag, Cu, Hg			1				5	19
	Au = 80%, Ag = 20%								

* Number of Au particles

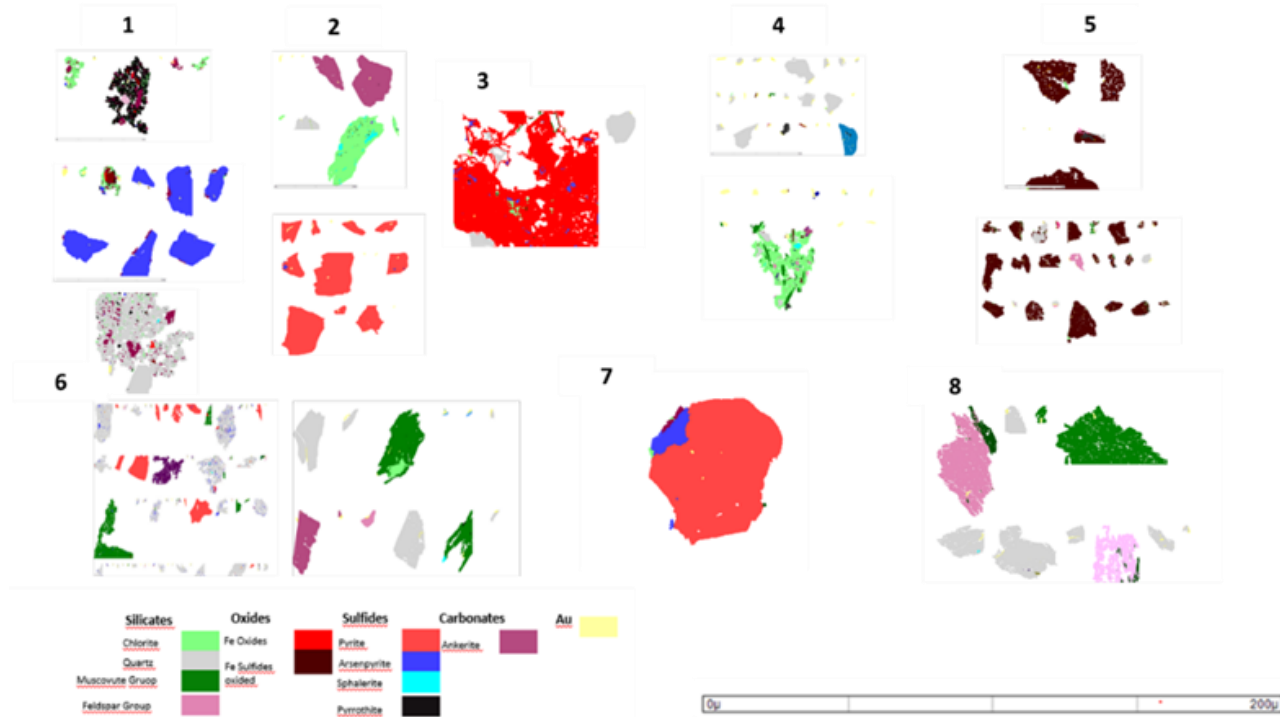


(Figura 5.61) **Figure 4** Electronic image in false color of minerals and Au association of the tailings deposits 1 to 8.

Conclusion

The results showed distinct characteristics between groups of samples from the tailings deposition structures.

Among the seven chemical variables, three distinct groups are identifying, being 1, represented by points close to the Au axis with most points of deposit 5. Group 2 is more close to the Sb axis with most points of deposits 6 and 7. Finally, there is a third group, with other deposits between the S, Fe and C axes.

The sources of S, Cu, and As are represented by sulfides and sulfates, the latter being mainly present in deposits 5 and 6. In the case of deposit 5, it can also be deduced, due to its genesis, that Fe oxides also carry these elements. C contents are related with carbonates, mainly in samples from deposit 2.

Acknowledgment

This work was supported by FCT through projects UIDB/04683/2020 and UIDP/04683/2020, and the Nano-MINENV project 029259 (PTDC/ CTA-AMB/29259/2017), and by AngloGold Ashanti Brasil. Our colleagues at ICT, Centro de Microscopy at Universidade Federal de Minas Gerais (CM-UFGM) and AngloGold Ashanti provide insights and knowledge that greatly aid the research. The authors are also deeply grateful to the anonymous reviewers for their valuable comments and suggestions.

The characterization of tailings solids also revealed the levels and modes of occurrence of elements considered at risk of supply according to the European Commission's list, such as Au, Sb, and As. Jarosite and Fe antimoniate are relevant host phases.

All these chemical and mineralogical relationships demonstrate the need for separate storage and safe management in the handling and disposal of these products.

Even considering that these elements occur in complex forms the high concentrations of Sb, As, and Au demonstrate their potential for reuse. Furthermore, studies should be made to convert these tailings into resources, proving that they could have interesting grades and, thus, aspirations in the context of the circular economy can be validated.

References

- Almeida FFM (1976) Estruturas do Pré-Cambriano Inferior Brasileiro. In: 29º Congresso Brasileiro de Geologia, 1976. Ouro Preto, Resumos SBG: 201-202.
- AngloGold Ashanti (2016) AngloGold Ashanti recommendations. Internal LGU report. Unpublished.
- AngloGold Ashanti (2019) AngloGold Ashanti recommendations. Internal LGU report. Unpublished.
- Goldfarb, R. (2001) Orogenic gold and geologic time: a global synthesis. *Ore Geology Reviews* 18, :1-75
- Lemos, MG, Magalhães MF, Souza TFQ, Pereira MS, Vieira MMS (2019) Geometallurgical analysis for increasing gold recovery – Santa Barbara, MG. In Proceedings World Gold 2019: pp 210–218.
- Lobato LM, Ribeiro-Rodrigues LC, Vieira FWR (2001b) Brazil's premier gold province. Part II: geology and genesis of gold deposits in the Archean Rio das Velhas greenstone belt, Quadrilátero Ferrífero. *Mineralium Deposita* 36:249–277.
- Moura W. Especialização de cianeto para redução do consumo no circuito de lixiviação de calcinado da usina do Queiróz. Dissertação de Mestrado. Dcpm1amento de Engenharia Metalúrgica e de Minas- UFMG- 138p. 2005.
- Porto C.G. (2008). A mineralização aurífera do depósito Córrego do Sítio e sua relação com o enxame de diques metamáficos no corpo CACHORRO BRAVO - Quadrilátero Ferrífero - Minas Gerais. MSc Thesis, Brazil, Universidade Federal de Minas Gerais.

5.3. Os impactos socioeconômicos e potencial dos rejeitos estudados

A tabela 5.40 pretende representar uma matriz com a potencialidade identificada para cada estrutura estudada, com o objetivo de sumarizar as áreas de aplicação e valorizar o resíduo, tornando-o assim um produto com valor econômico para região.

Estrutura	Localização	Produto	Reuso Extração de Au e S (%)	Reuso Outros Elementos	Industria Fertilizantes	Industria Civil
Bicalho	Nova Lima	Resíduo barragem	77.70	As, Sr (vitrificação)		Areia, filler e cimentício Gesso
Isolamento	Nova Lima	Resíduo empilhado	78.50	As (vitrificação)		Areia, filler e cimentício
Cocoruto	Nova Lima	Resíduo barragem	79.72	As (vitrificação)	Fertilizantes – Al e K, Rock Meal - sulfatos	Areia, filler e cimentício
Calcinados	Nova Lima	Resíduo barragem	32.16	Fe, As (vitrificação)	Concentrado de caulinita e base mineral p fertilização	Areia, filler e cimentício
Mina Velha	Nova Lima	Resíduo empilhado	92.95	As (vitrificação)	-	-
CDS1	Santa Bárbara	Resíduo empilhado	34.86	-		Areia, filler e cimentício
CDS2	Santa Bárbara	Resíduo barragem	70	Sb, As (vitrificação)	base mineral p fertilização, sulfatos	Areia, filler e cimentício
Crixás	Críxás	Resíduo barragem	20			Areia, filler e cimentício

Tabela 5.40. Resumo do Mapeamento do potencial de reuso dos resíduos estudados por Região.

Tratando-se de um tema complexo, mas crítico do ponto de vista socioeconómico e ambiental, considera-se a necessidade de uma proposta de modelo de trabalho para possíveis projetos que buscam a valorização dos rejeitos de mineração. Na figura 5.62 apresentam-se os macro estágios que devem ser levados em conta nesta valorização.

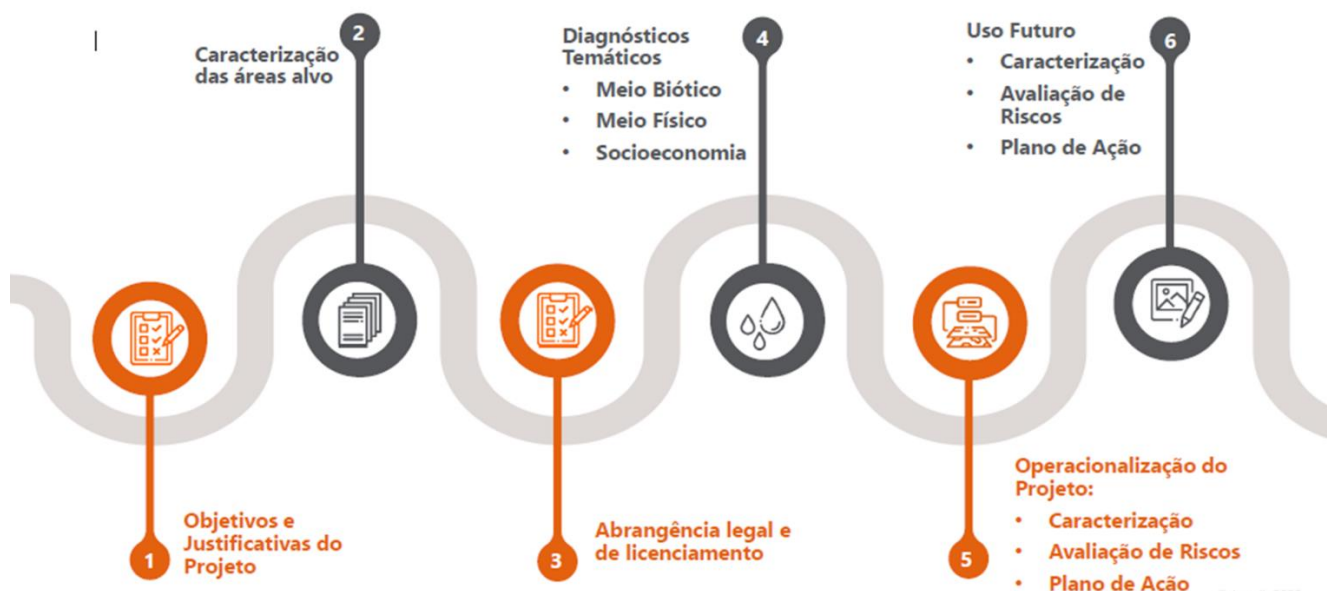


Figura 5.62. Etapas para busca da valorização de resíduos de mineração: uma macroproposta para a indústria da mineração.

Nesse modelo, busca-se:

1. Definição clara e objetiva dos impactos da valorização e transformação em projeto aplicáveis na indústria;
2. Metodologia de caracterização, tal como exposta no capítulo 4, deve ser aplicada em uma segunda etapa com vista à identificação do valor do resíduo;
3. Abrangência das leis para aplicação dos potenciais identificados e promoção do tema na legislação do país de forma clara;
4. Diagnóstico dos impactos do uso do novo recurso como um todo desde a comunidade até meio ambiente (flora, fauna e outros componentes ambientais);
5. Operacionalização do reuso com segurança e incentivos;
6. Uso futuro e aplicação do valor desse recurso na estratégia de negócios de mineração e discussão com os órgãos públicos.

Acredita-se que a aplicação do modelo proposto na Figura 5.62 poderá servir como embrião da mudança de visão e geração de valor em toda a cadeia para empreendimentos mineiros, desde logo no Brasil, mas eventualmente expansível para outros contextos territoriais com lacunas na gestão sustentável dos recursos.

Capítulo 6

Considerações finais

6. Considerações Finais

O estudo de caracterização dos rejeitos no contexto da EC foi desenvolvido com base na integração de diversos métodos e técnicas, provenientes de vários domínios científicos. Foi suportado por abordagens que incluíram desde trabalho laboratorial até à simulação de cenários de extração.

As etapas iniciais do estudo envolveram um extenso trabalho de amostragem, muitas vezes desafiador, em especial pelo contexto de pandemia em que decorreu. A maioria dos depósitos de rejeitos propostos para estudo foram amostrados com técnicas muitas vezes inovadoras, de que foi exemplo os trabalhos realizados na barragem de Cocomuto. Juntamente com essa etapa, levantamentos topográficos foram realizados para localização das amostras e da própria estrutura.

Com intuito de conhecer as características químicas e mineralógica seguiu-se um trabalho essencialmente realizado em laboratório. A parte analítica englobou análises químicas das fases solidas e líquidas (para deposição em barragens), estudos de mineralogia usando técnicas óticas e eletrônicas, ensaios de densidade e granulometria. Desta etapa conclui-se:

1. Os teores de Au são relevantes para maioria dos depósitos, principalmente os localizados na região do QF;
2. Em geral, as formas de associação desse elemento são recuperáveis, porém, alguns depósitos como os casos do “Calcinados” e Crixás, sugerem a necessidade um estudo específico e mais aprofundado para recuperação de Au;
3. Elementos como As, Fe e Sb indicam ser relevantes, quer pela sua toxicidade quer pela forma como é possível proceder à sua estabilização e reutilização;
4. O deposito de Calcinados constitui essencialmente uma acumulação de minérios oxidados de Fe e pode ser aplicado diretamente neste setor mineral;
5. Para os depósitos de Santa Barbara, o Sb mostrou-se um elemento relevante pelos conteúdos e formas de ocorrência. Além disso, se destaca por ser um elemento de risco nomeado pela lista da União Europeia em termos de criticidade e provimento;
6. A caracterização e distribuição de tamanho dos minerais ganga indicam possibilidades de uso em outras áreas da indústria como civil, fertilizantes e pigmentação.

O tratamento de resultados e sua interpretação, mediante a aplicação de métodos geoestatísticos, conduziram à identificação da distribuição dos elementos potenciais, com foco principal no ouro. Estes métodos foram aplicados tanto na fase sólida como na água. Nesta etapa

foram estimados as massas e teores de todas as estruturas localizadas no QF e, muitas delas, mostram-se com teores próximos a recursos hoje lavráveis em todo mundo. As barragens de Calcinados e Cocoruto têm as mais altas tonelagens e maiores teores de Au. Por outro lado, em CDS2 além do Au, foram mapeados elementos críticos como Sb de fácil extração por conter maiores massa em superfície. Assim, desta etapa resultou uma estimativa clara da magnitude dos recursos presentes nestas estruturas, que juntas alcançam mais de 400 mil onças de ouro, além de suas associações potenciais.

Na fase dos ensaios metalúrgicos obteve-se a identificação de rotas e até mesmo suas associações com empreendimentos de tratamento do Au próximos que possam ser um recurso potencial. O trabalho revelou que na maioria das estruturas o material sólido é facilmente recuperado por técnicas tradicionais de recuperação de Au, como lixiviação. Apenas para Calcinados e Crixás os ensaios não foram conclusivos, já que, como se referiu, verifica-se a necessidade de estudos complementares e até mesmo rota mais inovadoras. Porém isso, não invalida o potencial dessas duas áreas.

Ainda nesta fase do estudo, aplicaram-se três técnicas metalúrgicas para recuperação e estabilidade de elementos tóxicos como As e Sb. A vitrificação se mostrou como uma ótima opção para aplicação já que estes elementos se encontram estabilizados e concentrados no produto.

Por fim, constatou-se que rotas a seco com aplicação de técnicas de separação triboeletrostáticas não foram efetivas, mas mostraram ter potencial para geração de diferentes produtos para aplicação em outras áreas como indústria da construção civil. Este tema é bastante controverso já que compete com pedreiras e produtores de areia cujo custo operacional é bem menor. Incentivos governamentais são essenciais para seguir com o tema nesta área da indústria, no sentido da gestão sustentável de recursos geológicos de baixo valor.

O estudo das águas de barragens revelou ausência de drenagem ácida, mas mostrou o interesse de elementos como o Au, Sb e o anião sulfato. Embora sejam classicamente contaminantes do meio aquático, os trabalhos de revisão bibliográfica sugerem a possibilidade de recuperação, que merece ser aprofundada em próximos estudos.

É indiscutível que o reprocessamento de Au é viável. Uma análise econômica e de sensibilidade foi realizada em um estudo de caso para a barragem do Cocoruto. Em um cenário de lixiviação em 20 µm, mostrou-se atrativo com retorno acima de U\$20M, considerando a utilização de um empreendimento próximo à barragem para tratamento.

O estudo, é finalizado com um modelo com etapas a serem seguidas e com integrações socioeconômicas para busca da valorização desses resíduos e inserção como recurso econômico para o país.

O tratamento de resíduos de mineração num contexto de EC deve ser uma estratégia a ser inserida obrigatoriamente nas discussões sobre manejo e gestão de resíduos no âmbito governamental, ajudando a controlar os impactos ambientais, promovendo assim uma gestão sustentável e a visão ESG para empreendimentos mineiros.

Além disso, esta tese abriu caminhos para novas possibilidades de trabalhos futuros como a recuperação de Cu dos rejeitos da estrutura de Crixás, pouco discutida nas publicações, estudos mais concretos do uso dos produtos caracterizados como filler e sua relação com as comunidades próximas das estruturas. Refere-se ainda o interesse de realizar estudos de remoagem para aproveitamento do Au, o uso da biolixiviação para reaproveitamentos de metais e metaloides preciosos e tóxicos. Outro ponto a ser investigado em futuros estudos é o uso de técnicas mais simples como ciclonagem ou peneiramento de alta frequencia para completar a separação triboelectrostática, visando a geração de diversos produtos a partir de uma única alimentação.

Espera-se que esta tese e seus trabalhos publicados possam contribuir a práticas ambientais sociais e de governança corporativa e de investimento que se preocupam com critérios de sustentabilidade – e não apenas com o lucro no mercado financeiro, propondo mudança de paradigma nas relações entre as empresas e seus investidores. As práticas tradicionalmente associadas à sustentabilidade devem ser obrigatórias e previstas em políticas e governanças de um país, como o caso do Brasil, que vive historicamente com mais de 5% do PIB dependente do setor mineral.

Referências bibliográficas

Referências Bibliográficas

- .Leite, T.O.N. (2016). *Modelagem e Simulação do Circuito de Moagem da Mineração Serra Grande.* (Dissertação de Mestrado, Escola Politécnica). Universidade de São Paulo, São Paulo.
- Acheampong, M.A., Meulepas, R.J.W., Lens, P.N.L. (2010) Removal of heavy metals and cyanide from gold mine wastewater. *Journal of Chemical Technology & Biotechnology*, 85(5), 590-613. <https://doi.org/10.1002/jctb.2358>
- Acosta, J. A., Cano, A. F., Arocena, J. M., Debela, F., Martínez-Martínez, S. (2009). Distribution of metals in soil particle size fractions and its implication to risk assessment of playgrounds in Murcia City (Spain). *Geoderma*, 149(1-2), 101-109. <https://doi.org/10.1016/j.geoderma.2008.11.034>
- Akinwekomi, V., Maree, J.P., Masindi, V., Zvinowanda, C., Osman, M.S., Foteinis, S., Mpenyana-Monyatsi, L., Chatzisymeon, E. (2020) Beneficiation of acid mine drainage (AMD): a viable option for the synthesis of goethite, hematite, magnetite, and gypsum – gearing towards a circular economy concept. *Minerals Engineering*, 148, 106204. <https://doi.org/10.1016/j.mineng.2020.106204>
- Alkmin, F.F., Marshak, S. (1998) Transamazonian orogeny in the southern São Francisco craton region, Minas Gerais, Brazil: evidence for paleoproterozoic collision and collapse in the Quadrilátero Ferrífero. *Precambrian Research*, 90(1-2), 29-58. [https://doi.org/10.1016/S0301-9268\(98\)00032-1](https://doi.org/10.1016/S0301-9268(98)00032-1)
- Almeida, F.F.M. (1967). Origem e Evolução da plataforma brasileira. Rio de Janeiro, DNPM.
- Almeida, F.F.M. (1976). Estruturas do Pré-Cambriano Inferior Brasileiro. In *Anais do 29º Congresso Brasileiro de Geologia*, Ouro Preto, Brasil (pp 201–202).
- Altinkaya, P., Liipo, J., Kolehmainen, E., Haapalainen, M., Leikola, M., Lundström, M. (2019). Leaching of trace amounts of metals from flotation tailings in cupric chloride solutions. *Mining, Metallurgy & Exploration*, 36, 335-342. <https://doi.org/10.1007/s42461-018-0015-9>
- American Public Health Association – APHA. (2005). *Standard method for examination of water and wastewater* (21st ed.) Washington, DC, USA: AWWA, WPCF.
- AngloGold Ashanti – AGA. (2016) AngloGold Ashanti recommendations. Internal LGU report.
- AngloGold Ashanti – AGA. (2018) AngloGold Ashanti recommendations. Internal LGU report.
- AngloGold Ashanti – AGA. (2019) AngloGold Ashanti recommendations. Internal LGU report.
- ANM. (2023). Agência Nacional de Mineração. <https://www.gov.br/anm/pt-br>

- Ansah-sam, M., Binczyk, T., Dobek, C., Guo, C., Mimura, W.A. (2015). Geostatistical Study to Quantify Uncertainty in Tailings Fines Content as a Function of Data Spacing AND Workflow and Software Guide for Constructing a Three Dimensional Geostatistical Model of a Tailings Deposit for the Purpose of Conducting a Geostatistical Resampling Study. <https://cosia.ca/sites/default/files/attachments/Tailings%20Geostatistical%20Study%20-%20Imperial.pdf>
- Antunes, M., Fernandes, R., Pinheiro, A., Valente, T., Nascimento, S. (2010). Potential of reuse and environmental behavior of ochre-precipitates from passive mine treatment. In *Proceedings of the IMWA 2010*, Sydney, Canada (pp. 205-208).
- Araújo, T.D., Queiroz, A.A.S.L. (2017) Economia Circular: um breve panorama da produção científica entre 2007 e 2017. In *Anais do XIX Encontro Internacional sobre Gestão Empresarial e Meio Ambiente (ENGEMA)*, São Paulo, Brasil (pp. 1-17).
- Araya, N., Ramírez, Y., Kraslawski, A., Cisternas, L. A. (2021). Feasibility of re-processing mine tailings to obtain critical raw materials using real options analysis. *Journal of Environmental Management*, 284, 112060. <https://doi.org/10.1016/j.jenvman.2021.112060>
- Bailong, L., Zhaojun, Z., Linbo, L., Yujie, W. (2013). Recovery of gold and iron from the cyanide tailings by magnetic roasting. *Rare Metal Materials and Engineering*, 42(9), 1805-1809. [https://doi.org/10.1016/S1875-5372\(14\)60009-6](https://doi.org/10.1016/S1875-5372(14)60009-6)
- Baltazar, O. F., Silva, S. L. (1998). Mapa geológico integrado-texto explicativo em escala 1: 100.000. Projeto Rio das Velhas DNPM/CPRM, Brasília [in Portuguese].
- Baltazar, O.F., Silva, S.L. (1998). Mapa geológico integrado - texto explicativo em escala 1: 100.000. In: *Projeto Rio das Velhas*. DNPM/ CPRM, Brasília.
- Blake, G. R., Hartge, K. H. (1986). Bulk density. In Klute, A. (Ed.). *Methods of Soil Analysis: Part 1 Physical and Mineralogical Methods* (2nd ed., pp. 363–375). Winsconsin, USA: American Society of Agronomy and Soil Science Society of America.
- Brasil. (1967). Decreto-lei nº 227, de 28 de fevereiro de 1967. (Código da Mineração). Câmara dos Deputados. Centro de Documentação e Informação. <https://www2.camara.leg.br/legin/fed/declei/1960-1969/decreto-lei-227-28-fevereiro-1967-376017-publicacaooriginal-1-pe.html>

- Brasil. (1981). Lei nº 6.938 de 31 de agosto de 1981. (Estabelece a Política Nacional do Meio Ambiente). Presidência da República. Casa Civil. Subchefia para Assuntos Jurídicos. https://www.planalto.gov.br/ccivil_03/leis/l6938.htm
- Brasil. (1997). Resolução CONAMA nº 237 de 19 de dezembro de 1997 (Dispõe sobre a revisão e complementação dos procedimentos e critérios utilizados para o licenciamento ambiental). Conselho Nacional do Meio Ambiente. http://conama.mma.gov.br/?option=com_sisconama&task=arquivo.download&id=237
- Brasil. (1998). Lei nº 9.605, de 12 de fevereiro de 1998 (Dispõe sobre as sanções penais e administrativas derivadas de condutas e atividades lesivas ao meio ambiente, e dá outras providências). Presidência da República. Casa Civil. Subchefia para Assuntos Jurídicos https://www.planalto.gov.br/ccivil_03/leis/l9605.htm
- Brasil. (2005). Resolução CONAMA nº 357 de 17 de março de 2005 (Dispõe sobre a classificação dos corpos de água e diretrizes ambientais para o seu enquadramento, bem como estabelece as condições e padrões de lançamento de efluentes, e dá outras providências). Conselho Nacional do Meio Ambiente. <https://www.mpf.mp.br/atuacao-tematica/CCR4/dados-da-atuacao/projetos/qualidade-da-agua/legislacao/resolucoes/resolucao-conama-no-357-de-17-de-marco-de-2005/view#:~:text=Disp%C3%B5e%20sobre%20a%20classifica%C3%A7%C3%A3o%20dos,efluentes%20e%20d%C3%A1%20outras%20provid%C3%A3ncias>.
- Brasil. (2010). Lei nº 12.305 de 2 de agosto de 2010. (Institui a Política Nacional de Resíduos Sólidos). Presidência da República. Casa Civil. Subchefia para Assuntos Jurídicos. http://www.planalto.gov.br/ccivil_03/_ato2007-2010/2010/lei/l12305.htm
- Brasil. (2017). ABNT NBR 13028 (Mineração — Elaboração e apresentação de projeto de barragens para disposição de rejeitos, contenção de sedimentos e reserva de água — Requisitos). Associação Brasileira de Normas Técnicas.
- Cairncross, K. H., Tadie, M. (2022). Life cycle assessment as a design consideration for process development for value recovery from gold mine tailings. *Minerals Engineering*, 183, 107588. <https://doi.org/10.1016/j.mineng.2022.107588>
- Castoldi, M.A.S. (2015). *O distrito aurífero de Crixás-GO: Caracterização do novo corpo de minério Ingá*. (Trabalho de Conclusão de Curso, Instituto de Geociências). Universidade Federal do Rio Grande do Sul, Porto Alegre.

- Castro, F. F. D., Peiter, C. C., Góes, G. S. (2022). Minerais estratégicos e críticos: uma visão internacional e da política mineral brasileira. Brasília, Rio de Janeiro, Brasil: Texto para discussão / Instituto de Pesquisa Econômica Aplicada – IPEA. <http://dx.doi.org/10.38116/td2768>
- Changanane, A.P. (2017). *Estudo dos parâmetros envolvidos na determinação da função benefício na mineração* (Dissertação de Mestrado em Engenharia Mineral, Escola de Minas). Universidade Federal de Ouro Preto, Ouro Preto.
- Chen, T., Lei, C., Yan, B., Xiao, X.M. (2014) Metal recovery from the copper sulfide tailing with leaching and fractional precipitation technology. *Hydrometallurgy*, 147, 178-182. <https://doi.org/10.1016/j.hydromet.2014.05.018>
- Cho, H.C., Oh, W., Han, O.H., Kang, H.H., Lee, J.S. (2012). Recovery of valuable materials from gold mine tailings. In Young, C.A., Luttrell, G.H. (Ed.). *Separation Technologies for Minerals, Coal, and Earth Resources* (7th ed., pp. 277–287). Englewood, NJ, USA: Society for Mining, Metallurgy, and Exploration.
- Comissão da União Europeia. (2023). Communication from the Commission to the European Parliament, the Council, the European Economic and Social Committee and the Committee of the Regions: Critical Raw Materials Resilience: Charting a Path Towards Greater Security and Sustainability, 474 Final; European Commission: Brussels, Belgium.
- Costa, R. R. (1979). *Projeto de mineração*. (1 ed.). Ouro Preto: Universidade Federal de Ouro Preto, Ouro Preto.
- Curi, A. (2014). *Minas a céu-aberto: planejamento de lavra*. Oficina de Textos.
- David, M.E.V. (2006). *Composição isotópica de Pb, Sr e Nd da mineralização de ouro do depósito Córrego do Sítio, Quadrilátero Ferrífero (MG): implicações na modelagem conceitual* (Tese de Mestrado, Instituto de Geociências). Universidade de São Paulo, São Paulo.
- Dehghani, A., Ostad-Rahimi, M., Mojtahezdadeh, S. H., Gharibi, K. K. (2009). Recovery of gold from the Mouteh gold mine tailings dam. *Journal of the Southern African Institute of Mining and Metallurgy*, 109(7), 417-421.
- Dundee Sustainable Technologies. (2006). Method for vitrification of arsenic and antimony. US9981295B2, <https://patents.google.com/patent/US9981295B2/en>
- Ellen MacArthur Foundation. (2023). Circular Economy - UK, USA, Europe, Asia & South America - The Ellen MacArthur Foundation. <https://ellenmacarthurfoundation.org>

- Emrullahoglu, O. F., Kara, M., Tolun, R., Celik, M. S. (1993). Beneficiation of calcined colemanite tailings. *Powder Technology*, 77(2), 215-217. [https://doi.org/10.1016/0032-5910\(93\)80058-I](https://doi.org/10.1016/0032-5910(93)80058-I)
- Falagán, C., Grail, B. M., Johnson, D. B. (2017). New approaches for extracting and recovering metals from mine tailings. *Minerals Engineering*, 106, 71-78. <https://doi.org/10.1016/j.mineng.2016.10.008>
- Fandrich, R., Gu, Y., Burrows, D., Moeller, K. (2007). Modern SEM-based mineral liberation analysis. *International Journal of Mineral Processing*, 84(1-4), 310-320. <https://doi.org/10.1016/j.minpro.2006.07.018>
- Ferguson, D. N. (2010). A basic triboelectric series for heavy minerals from inductive electrostatic separation behaviour. *Journal of the Southern African Institute of Mining and Metallurgy*, 110(2), 75-78.
- Fernandes, C. (2023). Mineração no Brasil Colonial. <https://brasilescola.uol.com.br/historiab/mineracao-no-brasil-colonial.htm>
- Fundação Estadual do Meio Ambiente – FEAM. (2022). Inventário de Barragens. <http://www.feam.br/gestao-de-barragens/inventario-de-barragens>
- Gaustad, G., Krystofik, M., Bustamante, M., & Badami, K. (2018). Circular economy strategies for mitigating critical material supply issues. *Resources, Conservation and Recycling*, 135, 24-33. <http://dx.doi.org/10.1016/j.resconrec.2017.08.002>
- Goldfarb, R. J., Groves, D. I., Gardoll, S. (2001). Orogenic gold and geologic time: a global synthesis. *Ore Geology Reviews*, 18(1-2), 1-75. [https://doi.org/10.1016/S0169-1368\(01\)00016-6](https://doi.org/10.1016/S0169-1368(01)00016-6)
- Gomes, A. C. F., Cordeiro, C. C. M., Santos, R. A. D., Soares, V. R. A., Rocha, S. D. F. (2022). Aplicação de rejeito de mineração em pequena escala de ouro na produção de tijolo de solo-cimento. *Revista Matéria (Rio de Janeiro)*, 27, e13141. <https://doi.org/10.1590/S1517-707620220001.1341>
- Gomes, P., Valente, T., Cordeiro, M., Moreno, F. (2019). Hydrochemistry of pit lakes in the Portuguese sector of the Iberian Pyrite Belt. In *Proceedings of the 16th International Symposium on Water-Rock Interaction (WRI-16) and 13th International Symposium on Applied Isotope Geochemistry (1st IAGC International Conference)*, E3S Web of Conferences. Tomsk Oblast, Rússia: EDP Sciences. (vol. 98, p. 09007). <https://doi.org/10.1051/e3sconf/20199809007>
- González-Díaz, E., García, S., Soto, F., Navarro, F., Townley, B., Caraballo, M. A. (2022). Geochemical, mineralogical and geostatistical modelling of an IOCG tailings deposit (El Buitre, Chile): *Estudo geoambiental de resíduos de mineração de ouro em contexto de economia circular (Minas Gerais e Goiás, Brasil)*

- Implications for environmental safety and economic potential. *Journal of Geochemical Exploration*, 239, 106997. <https://doi.org/10.1016/j.gexplo.2022.106997>
- Grande, J. A., De La Torre, M. L., Andujar, J. M., Valente, T. M. F., Santisteban, M. (2013). Definition of a clean energy system for decontamination of acid mine waters and recovering their metal load. *Mineralogical Magazine (in press)*.
- Guanira, K., Valente, T. M., Ríos, C. A., Castellanos, O. M., Salazar, L., Lattanzi, D., Jaime, P. (2020). Methodological approach for mineralogical characterization of tailings from a Cu (Au, Ag) skarn type deposit using QEMSCAN (Quantitative Evaluation of Minerals by Scanning Electron Microscopy). *Journal of Geochemical Exploration*, 209, 106439. <https://doi.org/10.1016/j.gexplo.2019.106439>
- Guest, R.N., Svoboda, J, Venter, W.J.C. (1988). The use of gravity and magnetic separation to recover copper and lead from Tsumeb flotation tailings. *Journal of the Southern African Institute of Mining and Metallurgy*, 88(1), 21-26.
- Hastie, T.; Tibshirani, R.; Friedman, J. (2009). The Elements of Statistical Learning: Data Mining, Inference, and Prediction, 2nd ed.; Springer: New York, USA.
- Hedin, R. S. (2003). Recovery of marketable iron oxide from mine drainage in the USA. *Land Contamination and Reclamation*, 11(2), 93-98. DOI 10.2462/09670513.802
- Ince, C. (2019). Reusing gold-mine tailings in cement mortars: Mechanical properties and socio-economic developments for the Lefke-Xeros area of Cyprus. *Journal of Cleaner Production*, 238, 117871. <https://doi.org/10.1016/j.jclepro.2019.117871>
- Instituto Brasileiro de Geografia e Estatística – IBGE. (2019). Climatologia. <https://www.ibge.gov.br/geociencias/informacoes-ambientais/climatologia.html>
- Jafari, M., Abdollahzadeh, A. A., Aghababaei, F. (2017) Copper ion recovery from mine water by ion flotation. *Mine Water and the Environment*, 36(2), 323. DOI:10.1007/s10230-016-0408-2
- Jolliffe, I. T., Cadima, J. (2016). Principal component analysis: a review and recent developments. *Philosophical transactions of the royal society A: Mathematical, Physical and Engineering Sciences*, 374(2065), 20150202. <https://doi.org/10.1098/rsta.2015.0202>
- Jordan, C.E.; Sullivan, G.V.; Davis, B. (1980). Report of Investigations 8457, Pneumatic concentration of Mica. Pittsburgh, PA, USA US: Bureau of Mines Report Investigations.
- Jost, H., Fortes, P.T.F.O. (2001). Gold deposits and occurrences of the Crixás Goldfield, central Brazil. *Mineralium Deposita*, 36, 358-376. <https://doi.org/10.1007/s001260100171>

- Journel, A. G. (1986). Geostatistics: models and tools for the earth sciences. *Mathematical Geology*, 18, 119-140. <https://doi.org/10.1007/BF00897658>
- Junior, J.C.O. (2020). Uma Análise da Pandemia do Coronavírus no Brasil sob a Perspectiva do Sistema Político e Constitucional Brasileiro. *Conpedi Law Review*, 6(1), 96 – 117.
- Lalancette, J.M.; Lemieux, D.; Nasrallah, K.; Curiel, G.G.; Barbaroux, R. (2015). Method for Vitrification of Arsenic And Antimony. U.S. Patent 9981295 B2, <https://patents.google.com/patent/US9981295B2/en>
- Lemos, M., Valente, T., Reis, P. M., Fonseca, R., Delbem, I., Ventura, J., Magalhães, M. (2020). Mineralogical and geochemical characterization of gold mining tailings and their potential to generate acid mine drainage (Minas Gerais, Brazil). *Minerals*, 11(1), 39. <https://doi.org/10.3390/min11010039>
- Lemos, M.G., Magalhães, M.F., Souza, T.F.Q., Pereira, M.S., Vieira, M.M.S. (2019). Geometallurgical analysis for increasing gold recovery – Santa Barbara, MG. In *Proceedings of the World Gold 2019*, Perth, Australia (pp. 210–218).
- Lerchs, H., Grossman, I.F. (1965). Optimum design of open-pit mines. *Canadian Institute of Mining Bulletin*, 58(33), 47-54.
- Lobato, L. M., Ribeiro-Rodrigues, L. C., Vieira, F. W. R. (2001). Brazil's premier gold province. Part II: geology and genesis of gold deposits in the Archean Rio das Velhas greenstone belt, Quadrilátero Ferrífero. *Mineralium Deposita*, 36, 249-277. <https://doi.org/10.1007/s001260100180>
- Lottermoser, B. (2007). Mine Wastes: Characterization, Treatment and Environmental Impacts. Springer, Berlin, Heidelberg, New York.
- Magalhães. M. F. (2022). *Utilização de simulação de elementos discretos (DEM) para avaliação de parâmetros da teoria da amostragem*. (Tese de Doutoramento). Universidade de São Paulo, São Paulo.
- Manoucheri, H., Mosser, A., Gaul, F. (2016). Techno-economic aspect of ore sorting - is sorting a missing part in the mining industry - a case study at Sandvik's Mittersill tungsten mine. In *Proceedings of the 28th International Mineral Processing Conference (IMPC)*, Montreal, Canada (pp. 1-11).
- Mapinduzi, R. P., Bujulu, P., Mwegoha, W. J. (2016). Potential for reuse of gold mine tailings as secondary construction materials and Phytoremediation. *International Journal of Environmental Sciences*, 7(1), 49-61. DOI:<http://10.0.23.200/ijes.7005>

- Martin, C. J., Al, T. A., Cabri, L. J. (1997). Surface analysis of particles in mine tailings by time-of-flight laser-ionization mass spectrometry (TOF-LIMS). *Environmental Geology*, 32, 107-113. <https://doi.org/10.1007/s002540050199>
- Martin, M., Janneck, E., Kermer, R., Patzig, A., Reichel, S. (2015). Recovery of indium from sphalerite ore and flotation tailings by bioleaching and subsequent precipitation processes. *Minerals Engineering*, 75, 94-99. <https://doi.org/10.1016/j.mineng.2014.11.015>
- Martins, B.S., Lobato, L.M., Rosière, C.A., Hagemann, S.G., Santos, J.O.S., Villanova, F.L.D.S.P., Silva, R.C.F., Lemos, L.H.A. (2016). The Archean BIF-hosted Lamego gold deposit, Rio das Velhas greenstone belt, Quadrilátero Ferrífero: Evidence for Cambrian structural modification of an Archean orogenic gold deposit. *Ore Geology Reviews*, 72, 963-988. <https://doi.org/10.1016/j.oregeorev.2015.08.025>
- Monte, M.B.M., Grisol, S., Duque, T.F.M.B., Fenelon, P.A., Junior, G.G.O. (2020). Flotação seletiva para o reprocessamento de rejeitos provenientes do processo de lixiviação da Kinross Paracatu. *Brazilian Applied Science Review*, 4(4), 2720-2728. DOI:10.34115/basrv4n4-043
- Moura, W. (2005). *Especiação de cianeto para redução do consumo no circuito de lixiviação de calcinado da usina do Queiróz*. (Dissertação de Mestrado, Departamento de Engenharia Metalúrgica e de Minas). Universidade de Minas Gerais, Belo Horizonte.
- Novhe, N.O., Yibas, B., Coetzee, H., Mashalane, T., Atanasova, M., Vadapalli, V.R.K., Wolkersdorfer, C. (2018). Geochemistry and mineralogy of precipitates formed during passive treatment of acid mine drainage in the Ermelo coalfield, South Africa. In *Proceedings of the 11th ICARD/IMWA/MWD Conference: Risk to Opportunity*, Pretoria, South Africa (pp.171–176).
- ONU. (2023). Objetivos de Desenvolvimento Sustentável | As Nações Unidas no Brasil. <https://brasil.un.org/pt-br/sdgs>
- PanAfrican Resources. (2018). Mineral Resources and Mineral Reserves Report for the Year. <https://www.miningnewsfeed.com/reports/annual/Pan-African-Resources-MRMR-report-2018.pdf>
- Parbhakar-Fox, A., Fox, N., Jackson, L. (2016). Geometallurgical evaluations of mine waste - an example from the Old Tailings Dam, Savage River, Tasmania. In *Proceedings of the 3rd AusIMM International Geometallurgy Conference*, Perth, Australia (pp. 193-204).
- Parviaainen, A., Soto, F., Caraballo, M. A. (2020). Revalorization of Haveri Au-Cu mine tailings (SW Finland) for potential reprocessing. *Journal of Geochemical Exploration*, 218, 106614. <https://doi.org/10.1016/j.gexplo.2020.106614>

- Pires, K. D. S., Mendes, J. J., Figueiredo, V. C., Silva, F. L. D., Krüger, F. L. V., Vieira, C. B., Araújo, F. G. S. (2019). Mineralogical characterization of iron ore tailings from the Quadrilátero Ferrífero, Brazil, by eletronic quantitative mineralogy. *Materials Research*, 22. <https://doi.org/10.1590/1980-5373-MR-2019-0194>
- Porto, C.G. (2008). *A mineralização aurífera do depósito Córrego do Sítio e sua relação com o enxame de diques metamáficos no corpo Cachorro Bravo - Quadrilátero Ferrífero - Minas Gerais.* (Dissertação de Mestrado). Universidade Federal de Minas Gerais, Belo Horizonte.
- Priore, M.D., Venâncio, R. P. (2001). O livro de ouro da história do Brasil. Brasil: Ediouro.
- Rao, G. V., Markandeya, R., Sharma, S. K. (2016). Recovery of iron values from iron ore slimes of Donimalai tailing dam. *Transactions of the Indian Institute of Metals*, 69(1), 143-150. <https://doi.org/10.1007/s12666-015-0809-0>
- Reis, A. P. M., Cave, M., Sousa, A. J., Wragg, J., Rangel, M. J., Oliveira, A. R., Patinha, C., Rocha, F., Orsiere, T., Noack, Y. (2018). Lead and zinc concentrations in household dust and toenails of the residents (Estarreja, Portugal): a source-pathway-fate model. *Environmental Science: Processes & Impacts*, 20(9), 1210-1224. <https://doi.org/10.1039/C8EM00211H>
- Reis, A. P., Silva, E. F., Sousa, A. J., Patinha, C., Martins, E., Guimarães, C., Azevedo, M.R., Nogueira, P. (2009). Geochemical associations and their spatial patterns of variation in soil data from the Marrancos gold–tungsten deposit: a pilot analysis. *Geochemistry: Exploration, Environment, Analysis*, 9(4), 319–340. <https://doi.org/10.1144/1467-7873/09-199>
- Rios, F.J., (2018). Ouro do Brasil: histórias dos caminhos esquecidos : reminiscências dos tempos ancestrais até a corrida do ouro no século XVIII. Belo Horizonte: CDTN.
- Robben, C., Condori, P., Pinto, A., Machaca, R., Takala, A. (2020). X-ray-transmission based ore sorting at the San Rafael tin mine. *Minerals Engineering*, 145, 105870. <https://doi.org/10.1016/j.mineng.2019.105870>
- Rodrigues, C.P., Dias, C.F.S., Malheiros, C. (2022). *Práticas em Circularidade no Setor Mineral* (1 ed.). Brasília: Instituto Brasileiro de Mineração – IBRAM. ISBN: 978-85-61993-14-6
- Rostami, A. A., Isazadeh, M., Shahabi, M., Nozari, H. (2019). Evaluation of geostatistical techniques and their hybrid in modelling of groundwater quality index in the Marand Plain in Iran. *Environmental Science and Pollution Research*, 26, 34993-35009. <https://doi.org/10.1007/s11356-019-06591-z>

- Ruchkys, U.A., Azevedo, D.T., Machado, M.M.M. (2015). Patrimônio ambiental da Serra da Moeda sob a ótica da geodiversidade. In: Baeta A., Piló, H. (Ed.). *Serra da Moeda: patrimônio e história.* (pp. 10-29). Orange Editorial.
- Ryan, M. J., Kney, A. D., Carley, T. L. (2017). A study of selective precipitation techniques used to recover refined iron oxide pigments for the production of paint from a synthetic acid mine drainage solution. *Applied Geochemistry*, 79, 27-35.
<https://doi.org/10.1016/j.apgeochem.2017.01.019>
- Sánchez-Peña, N. E., Narváez-Semanate, J. L., Pabón-Patiño, D., Fernández-Mera, J. E., Oliveira, M. L., da Boit, K., Tutikian, B.F., Crissien, T.J., Pinto, D.C., Serrano, I.D., Ayala, C.I., Duarte, A.L., Ruiz , J.D., Silva, L. F. (2018). Chemical and nano-mineralogical study for determining potential uses of legal Colombian gold mine sludge: Experimental evidence. *Chemosphere*, 191, 1048-1055.
<https://doi.org/10.1016/j.chemosphere.2017.08.127>
- Sang, Y., Li, F., Gu, Q., Liang, C., Chen, J. (2008). Heavy metal-contaminated groundwater treatment by a novel nanofiber membrane. *Desalination*, 223(1-3), 349-360.
<https://doi.org/10.1016/j.desal.2007.01.208>
- Schorscher, H.D. (1976) Polimetamorfismo do Pré-carnbriano na região de Itabira, Minas Gerais, Brasil. In *Anais do XXIX Congresso Brasileiro de Geologia*, Ouro Preto, Brasil (pp.194- 195).
- Schorscher, H.D. (1978). Komatiítos na estrutura "Greenstone Belt" Série Rio das Velhas, Quadrilátero Ferrífero, Minas Gerais, Brasil. In *Anais do 30º Congresso Brasileiro de Geologia*, Recife, Brasil (pp. 292-293).
- Shi, T., Jia, S., Chen, Y., Wen, Y., Du, C., Guo, H., Wang, Z. (2009). Adsorption of Pb(II), Cr(III), Cu(II), Cd(II) and Ni(II) onto a vanadium mine tailing from aqueous solution. *Journal of Hazardous Materials*, 169(1-3), 838-846. <https://doi.org/10.1016/j.jhazmat.2009.04.020>
- Silva, R.A., Secco, M.P., Lermen, R.T., Schneider, I.A.H., Hidalgo, G.E.N., Sampaio, C.H. (2019) Optimizing the selective precipitation of iron to produce yellow pigment from acid mine drainage. *Minerals Engineering*, 135, 111-117. <https://doi.org/10.1016/j.mineng.2019.02.040>
- Silva, S.R., Procópio, S.O., Queiroz, T.F.N., Dias, L.E. (2004) Caracterização de rejeito de mineração de ouro para avaliação de solubilização de metais pesados e arsênio e revegetação local. *Revista Brasileira de Ciência do Solo*, 28, 189-196. <https://doi.org/10.1590/S0100-06832004000100018>
- Singh, S., Sukla, L. B., Goyal, S. K. (2020). Mine waste & circular economy. *Materials Today: Proceedings*, 30, 332-339. <https://doi.org/10.1016/j.matpr.2020.01.616>

- Skoronski, E., Ohrt, A.C., Cordella, R.O., Trevisan, V., Fernandes, M., Miguel, T.F., Menegaro, D.A., Dominguini, L., Martins, P.R. (2017) Using acid mine drainage to recover a coagulant from water treatment residuals. *Mine Water and the Environment*, 36(4), 495-501. <https://doi.org/10.1007/s10230-016-0423-3>
- Soares, V.A.A P. (2022). *Recuperação de metais estratégicos Au (iii), Ag (i), Pt (iv) e Pd (ii) de barragens de rejeito e lixo eletrônico com o uso de nanotecnologia e urucum visando tecnologias sustentáveis: uma proposta translacional* (Defesa de Doutorado, Programa de Pós-Graduação em Inovação Tecnológica). Universidade Federal de Minas Gerais, Belo Horizonte.
- Soto, F., Navarro, F., Díaz, G., Emery, X., Parviainen, A., Egaña, Á. (2022). Transitive kriging for modeling tailings deposits: A case study in southwest Finland. *Journal of Cleaner Production*, 374, 133857. <https://doi.org/10.1016/j.jclepro.2022.133857>
- Spooren, J., Binnemans, K., Björkmal, J., Breemersch, K., Dams, Y., Folens, K., González-Moya, M., Horckmans, L., Komnitsas, K., Kurylak, W., Lopez, M., Mäkinen, J., Onisei, S., Oorts, K., Peys, A., Pietek, G., Pontikes, Y., Snellings, R., Tripiana, M., Varia, J., Willquist, K., Yurramendi, L., Kinnunen, P. (2020) Near-zero-waste processing of low-grade, complex primary ores and secondary raw materials in Europe: technology development trends. *Resources, Conservation and Recycling*, 160, 104919. <https://doi.org/10.1016/j.resconrec.2020.104919>
- Swaroop, G.; Bulbule, K.A.; Parthasarathy, P.; Shivakumar, Y.; Muniswamy, R.; Annamati, R.; Priyanka, D. (2013). Application of Gold Ore Tailings (GOT) as a source of micronutrients for the growth of plants. *International Journal of Scientific World*, 1(3), 68-78.
- Tayebi-Khorami, M., Edraki, M., Corder, G., Golev, A. (2019) Re-thinking mining waste through an integrative approach led by circular economy aspirations. *Minerals*, 9(5), 286. <https://doi.org/10.3390/min9050286>
- Trippodi, E. E. M., Rueda, J. A. G., Céspedes, C. A., Vega, J. D., Gómez, C. C. (2019). Characterization and geostatistical modelling of contaminants and added value metals from an abandoned Cu–Au tailing dam in Taltal (Chile). *Journal of South American Earth Sciences*, 93, 183-202. <https://doi.org/10.1016/j.jsames.2019.05.001>
- UNDP. (2022). Mining and the 17 SDGs: Indicative Priorities. https://m.facebook.com/UNEconomicAnalysis/photos/how-can-mining-contribute-to-the-sustainable-development-goals-htpbbitly1lo429jt/1181013941912018/?locale=zh_CN

- Valente, T.; Grande, J.A., De La Torre, M.L. (2016.) Extracting value resources from acid mine drainages and mine wastes in the Iberian Pyrite Belt. In *Proceedings of the IMWA 2016 – Mining Meets Water – Conflicts and Solutions*, Leipzig, Germany (pp. 1339-1340).
- Von Ketelhodt, L. (2009). Viability of optical sorting of gold waste rock dumps. In *Proceedings of the World Gold 2009 Conference*, Gauteng, South Africa (pp. 271-277).
- Whittig, L. D., Allardice, W. R. (1986). X-Ray Diffraction Techniques. In Klute, A. (Ed.). *Methods of Soil Analysis: Part 1 Physical and Mineralogical Methods* (2nd ed., pp. 331– 362). Winsconsin, USA: American Society of Agronomy and Soil Science Society of America.
- Wilson, R., Toro, N., Naranjo, O., Emery, X., Navarra, A. (2021). Integration of geostatistical modeling into discrete event simulation for development of tailings dam retreatment applications. *Minerals Engineering*, 164, 106814. <https://doi.org/10.1016/j.mineng.2021.106814>
- Yang, J., Xu, W., Deng, X., Li, H., Ma, S. (2022). Research on the Selective Grinding of Zn and Sn in Cassiterite Polymetallic Sulfide Ore. *Minerals*, 12(2), 245. <https://doi.org/10.3390/min12020245>
- Yao, G., Liu, Q., Wang, J., Wu, P., Lyu, X. (2019). Effect of mechanical grinding on pozzolanic activity and hydration properties of siliceous gold ore tailings. *Journal of Cleaner Production*, 217, 12-21. <https://doi.org/10.1016/j.jclepro.2019.01.175>

Anexos

Anexos

Apresenta-se de seguida lista de publicações submetidas, no âmbito desta tese:

i) Artigos submetidos em revisão em revistas indexadas em base de dados internacionais

Recovery of metals in mining tailing waters - Hydrochemistry and elements distribution in gold metallurgical treatment tail-ings dams – revista Water

Sensitivity analysis and pre-feasibility of reprocessing Au from a tailings dam in the Iron Quadrangle - The case of Cocoruto Dam, Nova Lima, Minas Gerais – Revista REM – International Engineering Journal

ii) Publicações em atas de encontros científicos

Lemos, M., Valente, T., Reis, P.M., Fonseca, R., Filho, J.G., D, J.A., Ventura, J., Delben, I. (2021). Characterization of Arsenical Mud from Effluent Treatment of AU Concentration Plants, Minas Gerais – Brazil.

Lemos, M. (2021). Caracterização Mineralógica e Geoquímica de Rejeitos de Mineração de Ouro e Seus Potenciais de Geração de Drenagem Ácida (Minas Gerais, Brasil). (G5). In *Jornadas ICT 2021*.

Lemos, M., Valente, T.M., Reis, P.M., Fonseca, R., Delbem, I., Filho, J.G., Guabiroba, F., Pantaleão, J., Magalhães, M. (2022): Geoenvironmental Characterization of Gold Mine Tailings from Minas Gerais and Goiás, Brazil. In: *Proceedings of the IMWA 2022 – Reconnect*. Pope, J., Wolkersdorfer, C., Rait, R., Trumm, D., Christenson, H., Wolkersdorfer, K (Ed.). Christchurch, New Zealand (pp. 217 – 222).

Lemos, M., Valente, T., Reis, P., Fonseca, R., Pantaleão, J.P., Guabiroba, F., Filho, J.G., Magalhães, M., Delbem, I. (2022). Caracterização Mineralógica, Geoquímica e Potencial de Valorização de Resíduos de Mineração de Ouro (Minas Gerais, Brasil). In: *Anais do XXIX Encontro Nacional de Tratamento de Minérios e Metalurgia Extrativa*. Armação dos Búzios.

Lemos, M. (2022). Caracterização Mineralógica, Geoquímica e Potencial de Valorização de Resíduos de Mineração de Ouro (Minas Gerais, Brasil) (G5). In *Jornadas ICT 2022*.

iii) Comunicações em Painel

Lemos, M., Valente, T., Reis, P.M., Fonseca, R., Filho, J.G., D, J.A., Ventura, J., Delben, I. (2021). Characterization of Arsenical Mud from Effluent Treatment of AU Concentration Plants, Minas Gerais – Brazil.

Lemos, M., Valente, T.M., Reis, P.M., Fonseca, R., Delbem, I., Filho, J.G., Guabiroba, F., Pantaleão, J., Magalhães, M. (2022): Geoenvironmental Characterization of Gold Mine Tailings from Minas Gerais and Goiás, Brazil. In: *Proceedings of the IMWA 2022 – Reconnect*. Pope, J., Wolkersdorfer, C., Rait, R., Trumm, D., Christenson, H., Wolkersdorfer, K (Ed.). Christchurch, New Zealand (pp. 217 – 222).

iv) Comunicações Orais

Lemos, M. (2021). Caracterização Mineralógica e Geoquímica de Rejeitos de Mineração de Ouro e Seus Potenciais de Geração de Drenagem Ácida (Minas Gerais, Brasil). (G5). In *Jornadas ICT 2021*.

Lemos, M., Valente, T., Reis, P., Fonseca, R., Pantaleão, J.P., Guabiroba, F., Filho, J.G., Magalhães, M., Delbem, I. (2022). Caracterização Mineralógica, Geoquímica e Potencial de Valorização de Resíduos de Mineração de Ouro (Minas Gerais, Brasil). In: *Anais do XXIX Encontro Nacional de Tratamento de Minérios e Metalurgia Extrativa*. Armação dos Búzios.

CHARACTERIZATION OF ARSENICAL MUD FROM EFFLUENT TREATMENT OF AU TREATMENT PLANTS, MINAS GERAIS – BRAZIL

Mariana Lemos^{1,2}, Teresa Valente¹, Paula Marinho¹, Rita Fonseca³, José Gregório Filho², José Augusto Dumont², Juliana Ventura², Itamar Delben⁴

¹ Institute of Earth Sciences, Pole of University of Minho, Campus de Guimarães, 4710-057 Braga, Portugal.

² AngloGold Ashanti, Mining & Technical, COO International, 34000-000, Nova Lima, Brazil.

³ Institute of Earth Sciences, Pole of University of Évora, University of Évora, 7000 Évora, Portugal

⁴ Microscopy Center, Universidade Federal de Minas Gerais, 31270-013, Belo Horizonte, Brazil.

Introduction

Arsenic (As) is a common deleterious element in gold (Au) deposits (Jacob-Tatapu 2018). Materials with elevated As concentration are difficult to process without the associated environmental risks. Very few facilities in the world are capable of treating material containing high concentration of As and the main sources are sulfides such as arsenopyrite, commonly associated with Au.

The work was focused on arsenical muds generated from the effluent treatment of an Au concentration plant, located in Nova Lima, Minas Gerais (Fig 1). The ore that feeds the plant comes from mines, located within the Rio das Velhas Greenstone Belt in the Iron Quadrangle region and are mainly composed of sulfides such as pyrite, arsenopyrite, pyrrhotite and rare sulfides, like as gerdosfite, galena, sphalerite (Lobato et al. 2001; Moura 2015; Kresse et al. 2018).

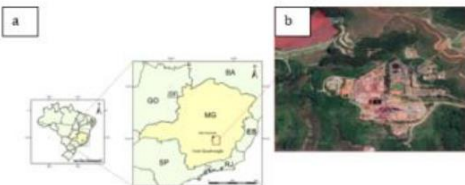


Figure 1 Study area: a. iron quadrangle map location (modified from Ruchkys U.A. 2007) and Nova Lima location and b. Nova Lima Metallurgic plant (SIRGAS2000 – 10-09-2019)

These sulfides are concentrated by flotation, calcined, and subsequently leached to recover Au (Moura 2015). The As, originating from the sulfide concentrated, is volatilized in the form of As trioxide in the roasting stage, absorbed in an aqueous phase in the gas washing towers and finally removed by coprecipitation processes with iron and neutralization with lime. The resulting solid waste (arsenic sludge) is then disposed of in waterproofed ditches (dug into the surface of the land), located in the plant's area of influence (Pantuzzo et al. 2007b).

Therefore, the main objective of the present work is the characterization of this current arsenical mud after neutralization step, mainly the geochemical and mineralogical properties, and identification of the neoformed host phases of As.

Methodology

The sampling campaign was performed over twenty-eight days in September 2019 during the production stage, representing a total of 40 samples after neutralization stage from the active plant.

In the laboratory, parameters as pH of effluent water samples were obtained using methodologies from the Standard Methods of Water and Wastewater (APHA 2005). Water samples were filtered using a 0.45 µm filter (Sigma Aldrich) and subjected to chemical analysis by inductively coupled plasma mass spectrometry (ICP-MS) at Universidade Federal de Minas Gerais (UFMG) water analysis laboratory. Chemical analysis of the solid tailings was performed by atomic absorption spectroscopy (AAS using AAS280 FS Varian). Infrared analysis (LECO) was used to obtain analytical S and C data from the solid. The choice of these elements was based on ore mineralogy and concentrations during production monitoring. All the reagents used were of analytical grade. The mineralogical study was carried out using polished sections analysed by optical microscopy and scanning electron microscopy (SEM, Field Electron and Ion Company, FEI) at UFMG, Belo Horizonte.

Results

This section presents the general properties of the arsenic mud, which in general has particles of fine grain size (P80:15µm).

Geochemistry

The arsenical mud samples are mainly composed of Ca (14.5 - 17.2%), S (13.1 - 13.8%), Fe (6.8 - 8.7%), As (3.6 - 4.2%) and other elements in low concentrations (Tab. 1). The water has low concentrations of Fe (<2.5 mg /L) and As (1.4 - 5.3 mg/L), which is consistent with the neutralization step in the beneficiation plant. For sulfur, the concentration to 1.0 g/L in the solution of the neutralization step is expected as the pH increases because of the lime addition. The consistency of this information is confirmed, therefore, by the concentration of Fe, As and S found in the solid phase already presented.

Table 1 Statistical summary of the major and trace elements - Solid and Water samples; N - number of samples.

	Solid (N=40)	Residual Water (N=10)
Physical Parameters	Average	Average
pH	-	8.0-9.0
Elements		
	%	mg/L
Fe	8.68	<2.50
As	3.58	5.31
S	13.30	436.39
Si	0.36	-
Ca	14.89	491.01
Al	1.50	<2.50
Mg	0.52	16.58
K	0.02	100.73
Zn	0.43	<0.1
C	0.10	-

Mineralogy

The arsenical mud consists essentially of "CSA 1" (38.36% by weight), and "Gypsum Fe" (28.57% by weight). The total percentage of all phases with S (sulfates, "Compounds with S" and "CSA") is 90.63% (Fig 2). Also noteworthy are the low amounts of "Hematite", which make up a total of 1.13% by weight in this sample, as well as Quartz and other silicate phases classified as others. The predominant presence of calcium and sulfur is consistent with the identification of gypsum indicated by electron microscopy (Fig. 4). On the other hand, the occurrence of Fe and As in relevant quantities is associated with the complex phases that contain variable concentrations of As.

Table 2 Statistical summary of mineralogy of Solid samples; N - number of samples.

	Solid (N=40)
Mineral/Composed	Average %
Hematite	1.13
Gypsum (Fe)	28.57
(CSA1 -3%As in composition)	38.36
(CSA2 -13%As in composition)	18.10
(CSA3 -59%As in composition)	11.68
Others	3.03

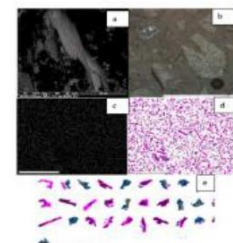


Figure 2 Backscattered electron image of Sulfo Arsenical Compounds in arsenical mud. a) CSA, b) Reflected light image of porous hematite, c) total sample, d) and e) false image of total samples (pink, purple and blue - Gypsum (pink/purple) and CSA (Blue))

Discussion and Conclusion

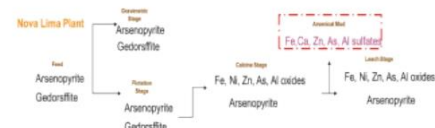


Figure 3 Transformation path of As sources along Nova Lima Au metallurgical plant until reformation of arsenical mud

The samples analyzed underwent several types of "attacks", from breaking the structure by calcination, followed by complementary chemical attacks. This can result in complex phase transformations and, in addition, chemical dissolutions and substitutions in the crystalline structure. As a result, some phases have very complex micro-chemical and textural compositions (Fig 3). In the analyzed samples, these phases with wide compositional variations and made up of several elements as major and minor constituents were generically classified as "Complex Sulfates", "CSA".

From the results of the characterization study, it is possible to propose optimization in the current treatment routes and even propose new alternatives, in addition to initiatives in the reuse of these as a product.

Acknowledgements

We thank our colleagues from ICT, microscopy center from Universidade Federal de Minas Gerais (CM-UFMG), and AngloGold Ashanti who provided insight and expertise that greatly assisted the research. This work was funded by FCT—Fundação para a Ciência e a Tecnologia through projects UIDB/04683/2020 e UIDP/04683/2020 and Nano-MINENV 029259 (PTDC/CTA-AMB/29259/2017, and by AngloGold Ashanti Brazil.



Caracterização Mineralógica e Geoquímica de Rejeitos de Mineração de Ouro e Seus Potenciais de Geração de Drenagem Ácida (Minas Gerais, Brasil)

Mariana Lemos ^{1,2*}, Teresa Valente ¹, Paula Marinho Reis ^{1,3}, Rita Fonseca ⁴, Itamar Delbem ⁵,
Juliana Ventura ² and Marcus Magalhães ²

¹ Institute of Earth Sciences, Pole of University of Minho, Campus de Gualtar, 4710-057 Braga, Portugal, ² Anglogold Ashanti, Mining & Technical, COO International, 34000-000, Nova Lima, Brazil, mglemos@anglogoldashanti.com.br ³ GEOBIOTEC, Departamento de Geociências, Universidade de Aveiro, Campus Universitário de Santiago, 3810-193 Aveiro, Portugal, ⁴ Institute of Earth Sciences, Pole of University of Évora, University of Évora, 7000 Évora, Portugal; ⁵ Microscopy Center, Universidade Federal de Minas Gerais, 31270-013, Belo Horizonte, Brazil,
*mglemos@anglogoldashanti.com

Por mais de 30 anos, os minérios de ouro sulfetados foram tratados em plantas metalúrgicas localizadas em Nova Lima, Minas Gerais, Brasil, e acumulados nas barragens de rejeitos de Cocoruto e Calcinados. Ambos os rejeitos de flotação e lixiviação de um circuito desativado, bem como rejeitos calcinados e lixiviados de uma planta em produção, foram estudados quanto ao seu potencial de drenagem ácida de mina e mobilidade dos elementos químicos. A caracterização detalhada de ambos os tipos de rejeitos indica a presença de material de granulometria fina que hospeda quantidades substanciais de sulfetos que exibem características geoquímicas e mineralógicas distintas. As amostras da planta em produção mostram altos teores de Fe na forma de óxidos, cianeto e sulfatos. Diferentemente, as amostras do circuito antigo apresentam maiores concentrações médias de Al (0,88%), Ca (2,4%), Mg (0,96%) e Mn (0,17%), presentes como silicatos e carbonatos. Essas amostras também mostram relíquias de sulfetos preservados, como pirita e pirrotita. As concentrações de Zn, Cu, Au e As são maiores nos rejeitos do circuito atual, enquanto Cr e Hg se destacam nos rejeitos do circuito desativado. Embora os resultados obtidos mostrem que os resíduos de sulfeto não tendem a gerar drenagem ácida, os testes de lixiviação indicam a possibilidade de mobilização de elementos tóxicos, como As e Mn no circuito antigo, e Sb, As, Fe, Ni no rejeito da planta em processamento. Este trabalho destaca a necessidade de manejo e controle adequados de barragens de rejeito, mesmo em ambientes de drenagem alcalina como o das barragens de Cocoruto e Calcinados. Além disso, um forte conhecimento da dinâmica dos rejeitos em termos de geoquímica e mineralogia seria fundamental para apoiar decisões de longo prazo sobre o gerenciamento e disposição de resíduos.

Palavras chave/ Key words: geoquímica e mineralogia ambiental; rejeitos; mobilidade de elementos tóxicos; drenagem ácida de minas; Minas Gerais — Brasil

Agradecimentos/ Acknowledgments: Agradecemos a todos os colegas da Universidade do Minho e Centro de Microscopia da Universidade de Minas Gerais. Sinceros agradecimento ao apoio da empresa AngloGold Ashanti.



Caracterização Mineralógica, Geoquímica e do Potenciais de Reaproveitamento de Rejeitos de Mineração de Ouro e (Minas Gerais, Brasil)

Mariana Lemos ^{1,2*}, Teresa Valente ¹, Paula Marinho Reis ^{1,3}, Rita Fonseca ⁴, Itamar Delbem ⁵, Fernanda Guabiroba², João Pantaleão² and Marcus Magalhães ²

1 Institute of Earth Sciences, Pole of University of Minho, Campus de Gualtar, 4710-057 Braga, Portugal, 2 Anglogold Ashanti, Mining & Technical, COO International, 34000-000, Nova Lima, Brazil, mglemos@anglogoldashanti.com.br 3 GEOBIOTEC, Departamento de Geociências, Universidade de Aveiro, Campus Universitário de Santiago, 3810-193 Aveiro, Portugal, 4 Institute of Earth Sciences, Pole of University of Évora, University of Évora, 7000 Évora, Portugal; 5Microscopy Center, Universidade Federal de Minas Gerais, 31270-013, Belo Horizonte, Brazil,

*mglemos@anglogoldashanti.com

Por mais de 2 décadas, os minérios de ouro sulfetados foram tratados em plantas metalúrgicas localizadas em Nova Lima e Santa Barbara, Minas Gerais, Brasil. Os rejeitos foram ao longo dos anos acumulados em barragens de rejeitos ou em pilhas. Esses materiais representam rejeitos de flotação e lixiviação de circuitos desativados, bem como rejeitos de plantas ainda em produção. As amostras foram retiradas a partir de sondagem e foram estudados quanto ao seu potencial de reutilização. A caracterização detalhada dos tipos de rejeitos indica a presença de material de granulometria fina que hospeda quantidades substanciais de sulfetos que exibem características geoquímicas e mineralógicas distintas. As amostras mostram altos teores de Au (0.3 a 1.0 pmm) hospedadas em diferentes minerais como sulfetos, quartzo e óxidos de Ferro. Além do Au, as amostras contém maiores concentrações médias de S (0,50 a 0,3%), Fe (30 a 5%) e As (0,17 a 3%). Essas amostras também mostram relíquias de sulfetos preservados, como pirita, bertierita, stinbinita, arsenopirtita e pirrotita. As concentrações de Zn, Cu, são anomolas nas amostras de Nova Limam enquanto o Sb ocorre com teores acima de 0.2% nas amostras de Santa Barbara, representados por sulfetos e óxidos, principalmente. Ensaio metalúrgico para reaproveitamento do Au mostram potencial de recuperação metalúrgica da ordem de 70%, além de potencial reuso em outras áreas como agregados para construção civil e recuperação de outros metais e metaloides como Sb e As. Este trabalho destaca portanto, a importância da caracterização do âmbito da economia circular e o valor do resíduo na cadeia de produção do setor mineral. E Além disso, um forte conhecimento da dinâmica dos rejeitos em termos de geoquímica e mineralogia para apoiar decisões de longo prazo sobre o gerenciamento e disposição de resíduos.

Palavras chave/ Key words: geoquímica e mineralogia ambiental; rejeitos; economia circular; ; Minas Gerais — Brasil

Agradecimentos/ Acknowledgments: Agradecemos a todos os colegas da Universidade do Minho e Centro de Microscopia da Universidade de Minas Gerais. Sinceros agradecimento ao apoio da empresa AngloGold Ashanti.

